Exponential Asymptotics

Multi-level asymptotics of model problems



UNITED KINGDOM · CHINA · MALAYSIA

Fatih Say, MSc

Thesis submitted to the University of Nottingham
for the degree of Doctor of Philosophy

February 2016

Abstract

Exponential asymptotics, which deals with the interpretation of divergent series, is a highly topical field in mathematics. Exponentially small quantities frequently arise in applications, and Poincaré's definition of an asymptotic expansion, unfortunately, fails to emphasise the importance of such small exponentials, as they are hidden behind the algebraic order terms.

In this thesis, we introduce a new method of hyperasymptotic expansion by inspecting resultant remainders of series. We study the method from two different concepts. First, deriving the singularities and the late order terms, where we truncate expansions at the least value and observe if the remainder is exponentially small. Substitution of the truncated remainder into original differential equation generates an inhomogeneous differential equation for the remainders. We expand the remainder as an asymptotic power series, and then the truncation leads to a new remainder which is exponentially smaller whence the related error estimate gets smaller, so that the numerical precision increases. Systematically repeating this process of re-expansions of the truncated remainders derives the exponential improvement in the approximate solution of the expansions and minimises the ignored terms, i.e., error estimate. Second, in establishing the level one error, which is a function of level zero and level one truncation points, we study asymptotic behaviour in terms of the truncation points and allow them to vary. Writing the estimate as a function of the preceding level truncation point and varying the number of the terms decreases the error dramatically. We also discuss the Stokes lines originating from the singularities of the expansion(s) and the switching on and off behaviour of the subdominant exponentials across these lines.

A key result of this thesis is that when the higher levels of the expansions are considered in terms of the truncation points of preceding stages, the error estimate is minimised. This is demonstrated via several differential equations provided in the thesis.

Acknowledgements

Undertaking this project has become one of the most challenging experiences of my life. Without the help and support of certain people and an institution I would not have accomplished it. I would first like to express my gratitude and appreciation to my supervisors Prof. John R. King who introduced me the subject of exponential asymptotics, which I had not heard before, and Dr. Paul Matthews who always has his door open. I am grateful for their invaluable academic support and advice.

I wish to thank my examiners Prof. Christopher Howls, Dr. Stephen Cox and Dr. Richard Tew for reading and providing me useful feedbacks. I would also like to thank to my friends and everyone who has had a role in supporting me in many aspects during my study years.

This work was fully funded by the Turkish Ministry of National Education. I am grateful for their financial support. I could not have completed this study without it. There are no adequate words to express my gratitude to my parents, Mustafa and Elif, my brothers, Muhammed and Murat, and my sisters, Zehra, Dilek and Sukran, for supporting me.

Finally, I am compelled to thank and always be grateful to my brother Murat who was my Physics, Chemistry, Mathematics and Geometry teacher in high school, and I believe he has a right on every word in the thesis. Without his teaching and patience and, his undying presence whenever I needed him, I would not have accomplished what I achieved today. Murat Abi, this thesis is dedicated to you.

Contents

Contents **vii**

Nomenclature **x**

1 Introduction **1**

1.1 Exponential asymptotics 3

1.2 Optimal truncation 5

1.3 Hyperasymptotics 6

1.4 Stokes phenomenon 8

1.5 Overview of the methodology and results 11

1.6 Structure of the thesis 12

1.7 Statement of Originality 16

2 Introductory example of exponential asymptotics **17**

2.1 Introduction 17

2.2 Asymptotic expansion 19

2.3 Optimal truncation and remainder equation 21

2.4 Remainder near $z = 0$ 25

2.5 Remainder analysis and erf function smoothing 28

2.6 Analysing the model problem by residues 32

2.7 Stokes phenomenon 35

2.8 Conclusion 39

3 Stokes phenomenon for first order differential equations 43

3.1 Asymptotic power series 44

3.1.1 Complex ε 46

3.2 Optimal truncation 47

3.3 Stokes structure 49

3.4 First level of hyperasymptotics for general $A(z)$ 56

3.5 Summary 59

4 Exponential integral 61

4.1 Introduction 61

4.2 Asymptotic behaviour of a differential equation and Stokes phenomenon 64

4.3 Zeroth level of hyperasymptotics 65

4.4 Stokes and anti-Stokes lines 70

4.5 First level of hyperasymptotics 71

4.6 Error analysis 80

4.7 Stokes and anti-Stokes lines in first level 89

4.8 Stokes line smoothing 95

4.9 Second level of hyperasymptotics and Stokes lines 98

4.10 Third level of hyperasymptotics and Stokes lines 107

4.11 Comparison and conclusions 112

5 Error function 117

5.1 Introduction 117

5.2 First order differential equation for the error function 119

5.2.1 Zeroth level of hyperasymptotics: superasymptotics 120

5.2.2 Stokes and anti-Stokes lines 123

5.2.3 First level of hyperasymptotics 126

5.2.4 Truncation 131

5.2.5 Stokes and anti-Stokes lines 139

5.3 Second order differential equation for the error function 141

5.3.1 Zeroth level of hyperasymptotics: superasymptotics 144
5.3.2 Truncation 145
5.3.3 First level of hyperasymptotics 146
5.3.4 Truncation 149
5.3.5 Stokes phenomenon 151
5.4 Conclusion and discussion 156

6 Airy function **159**
6.1 Introduction 159
6.2 Airy function expansion 160
6.3 Optimal truncation 164
6.4 Stokes and anti-Stokes lines 165
6.5 First level of hyperasymptotics 166
6.6 Truncation 170
6.7 Error analysis 175
6.7.1 Analysis for $u_1^1(z)$ 175
6.7.2 Analysis for $u_1^2(z)$ 176
6.8 Stokes and anti-Stokes lines 177
6.9 Conclusion 178

7 The confluent hypergeometric function **181**
7.1 Introduction 181
7.2 Rescaled confluent hypergeometric function 184
7.3 Optimal truncation and the WKB approach 189
7.3.1 WKB analysis 190
7.4 Stokes and anti-Stokes lines 194
7.5 Error function near the Stokes line 196
7.6 First level of hyperasymptotics 199
7.6.1 Truncation 202
7.6.2 Error analysis and θ dependence 206

7.6.3 Stokes lines and their form near singularity 213
7.7 Conclusions and comparisons 215

8 Higher-order Stokes phenomenon 219
8.1 Introduction 219
8.2 Model differential equation 220
8.2.1 Asymptotic expansion 222
8.2.2 Truncating optimally and the remainder 225
8.3 Stokes phenomenon 227
8.4 Higher-order Stokes phenomenon 229
8.5 First level of hyperasymptotics 232
8.5.1 Evaluating the remainder 234
8.5.2 WKB approach 240
8.5.3 Stokes and higher-order Stokes phenomenon 242
8.6 Discussion 247

9 Conclusion 251
9.1 Review 252
9.2 Discussion 256
9.3 Further work 257

Bibliography 259

Chapter 1

Introduction

Exponential asymptotics is a subject of asymptotic expansion wherein, as the name suggests, the exponential terms which are hidden behind algebraic order terms in the singular expansion are taken into consideration. Particularly, the subject concerns the importance of exponentially small terms. It mostly is associated with divergent asymptotic series, since the singular perturbation series are usually divergent. By using techniques in exponential asymptotics, mathematicians aim to deal with divergent series. Almost two centuries have passed since Niels H. Abel, in 1828, argued that "Divergent series are the invention of the devil, and it is shameful to base on them any demonstration whatsoever." [1]. Since then, especially in the last two decades, mathematicians have extracted increasing information from divergent series leading to a new subject called Exponential Asymptotics which has wide range of applications and provides the exponential accuracy for asymptotic solutions of the equations.

Computation of exponentially small terms is utilised in a plethora applications including to but not limited to applications in mathematics, mathematical physics [2], plasma physics, engineering, meteorology [1], atmospheric and oceanic science [3], flow in a porous pipe [4], viscous fluid flow [5, 6](p.131), electromagnetic wave theory [2, 5], water waves problems [7], gravity-capillary wave problems [8–12],

analysis and quantum chemistry [13, 14], heteroclinic solutions of differential equations [15], and boundary-value problems [16]. From this wide range of applications a fundamental question arises: Why are these exponentially small terms significant. To express the importance of such small terms, Boyd in [1] inserts that "a mother can regard her baby as insignificant because it is only sixty centimeters long", and he also discusses many applications of these small terms. In fact, exponential asymptotics is important due to the changing behaviour of the subdominant exponential terms-while on one side of some certain rays they become exponentially small, on the other side of these rays they become dominant. Exponential asymptotics is indispensable for shedding light on this changing behaviour as well as localizing exponentially subdominant and dominant terms. For example, upon interpreting these terms, the presence of the gravity and capillary waves and their switching on and off behaviour across Stokes rays (Stokes lines) were discovered [8, 10].

Many important cases exist where exponentially small terms play key roles. Deriving these small order terms of the divergent series by ordinary asymptotics is impractical. Francis Ogilvie was the first person asking about the missing ship waves of his calculations [17–19]. The waves were not able to be observed through regular asymptotics as they were exponentially small. In [13], on the other hand, quantum chemistry with the method of exponential asymptotics is consistent, and the method is used when describing exponential smallness of the molecules in reactions, which govern the reactions. Otherwise, Poincaré's asymptotic method ignores these molecules, and existence of the reaction may be destabilised. The technique of exponential asymptotics (optimal truncation) is applied to determine the radiation coefficient of nonlocal solitary waves. Since such a coefficient is exponentially smaller than the resultant error of the expansion, exponential asymptotics is needed to be applied twice (i.e. hyperasymptotics) in order to determine the radiation coefficient [3, 20]. This newly introduced method is also used to analyse the formation of shocks in waves that appear in partial differential equations [21]. After this subject

was introduced, exponentially small terms are no more negligible in physical sciences as they may affect the existence of problems involving these small terms [2], in which the divergent series has invaluable importance. Because the subject had been used by many different fields in the last few decades, in 1991 NATO and NSF sponsored a workshop on "Asymptotics Beyond All Orders" with the attendance of 50 academics [5].

1.1 Exponential asymptotics

In order to obtain useful information from divergent asymptotics series, the series must be truncated after a finite number of terms. In 1886, the French mathematician Henri Poincaré [22] published the formal definition of an asymptotic expansion; which became widely known as Poincaré's expansion. Assume $\sum_{n=0}^{\infty} a_n(x)x^{-n}$ is an asymptotic power series which could be either convergent or divergent and for each positive integer N

$$f(x) = \sum_{n=0}^{N-1} \frac{a_n(x)}{x^n} + \mathrm{O}\left(x^{-N}\right), \quad \text{as } x \to \infty, \tag{1.1}$$

in an unbounded set S [23](p.42). Then $\sum_{n=0}^{\infty} a_n(x)x^{-n}$, a Poincaré's asymptotic expansion of $f(x)$, may be written as

$$f(x) \sim \sum_{n=0}^{\infty} \frac{a_n(x)}{x^n}, \quad \text{as } x \to \infty. \tag{1.2}$$

An equivalent condition of (1.1) is to write

$$\lim_{x\to\infty} x^N \left\{ f(x) - \sum_{n=0}^{N} \frac{a_n(x)}{x^n} \right\} \to 0, \tag{1.3}$$

where N is a non-negative integer. Truncation of this series at the $(N-1)^{th}$ term generates an approximation with fixed accuracy at $\mathrm{O}\left(x^{-N}\right)$ [1, 24, 25] . However, even though the names look similar, there is a pivotal difference between asymptotic

expansion and exponential asymptotics: in exponential asymptotics exponentially small terms (e.g. $\exp(-1/\varepsilon)$ for sufficiently small ε) that are not calculable by Poincaré expansion [26] come into play. Truncation by this method enables one to find out where and when to truncate expansions. In particular, truncation of divergent series arbitrarily in the sense of Poincaré may generate a good approximation. However if the truncation point is picked any earlier or later, the truncation error may increase due to the additional terms, and therefore his definition unfortunately is not unique. Nevertheless, Poincaré's expansion was not completely useless. Especially in physical sciences, a few terms of the expansion may give the satisfactory results. Because it gives more accurate approximations, it may be regarded that this expansion is extended by exponential asymptotics.

It is difficult to find an exact solution for each singularly perturbed differential equations or sometimes even impossible to find their approximate solution. Therefore, asymptotical interpretation of the differential equations plays a pivotal role. The form of the corresponding series solutions of these differential equations is first decreasing and then diverging to infinity, for instance exponential integral, error function and Airy function. These well-known functions are studied, for instance, by Olde Daalhuis et al. [27] and Dean [28] in detail; in fact, they will also be discussed via hyperasymptotic approximation of this thesis. However, it is possible to have convergent series in exponential asymptotics, but divergent series are comparatively useful as they have to decrease faster [29]. The accuracy of convergent series depends upon the number of the terms: as the number of the terms is increased, the accuracy also increases. However, the accuracy of the divergent series in exponential asymptotics is limited by the optimal truncation point; whereby, increasing the number of the terms after the truncation point is counterproductive, i.e., increases the truncation error.

In summary, exponential asymptotics consists of optimally truncating the divergent

series, whereupon, the resultant remainder turns out to be exponentially small, and then analysing the remainder terms which cannot be extracted by the conventional asymptotics.

1.2 Optimal truncation

The optimal truncation point is the place where the series start growing, or in other words, where the series take their absolute minimum values [1, 3, 15, 20, 28, 30–32]. To be able to find this point, the general representation of the expansion must first be established [12]. At first sight, this may appear easy. However, obtaining the form of the late-order terms is not always straightforward, and may even be impossible at times. That is why, the most crucial part of the interpretation for these divergent series in exponential asymptotics is the determination of the general term and the point of optimal truncation. Optimally truncated series usually occur in the same standard form, which is described by Dingle [24] as factorial-over-a-power, and these series are divergent [24, 33]. This diverging nature of the series in the form of a factorial-over-a-power occurs due to Darboux's theorem, which is discussed in great detail by Dingle in [24, pp. 140], also see [1]. The theorem specifically explains that based on the late-order terms, the asymptotic behaviour of the leading order terms is determined by the closest relevant singularity or singularities in the expansion as the singular points control the whole expression. In fact, we will see throughout the thesis that the tails of the expansions are consistent with the theorem. Hence, the series in exponential asymptotics are divergent whenever the general terms of the series have a singularity or singularities [5, 11, 34, 35]. In 1998, Chapman et al. [30] extended the factorial-over-a-power method, and applied it to the nonlinear ordinary differential equations. It is very important to determine the late-order terms of the expansion; not only in order to obtain the point of optimal truncation but also to receive a more accurate approximation. It is also important to ensure that the expansion is in the expected factorial-over-a-power form. Once the general representation of the

late-order terms is derived, the optimal truncation of the series can be established by equating the ratio of the successive late terms to 1. Alternatively, this point of the divergent series where they take their minimum values can be found by minimising the remainder terms with respect to N [6]. The idea and the technique of optimal truncation point are discussed by Chapman et al. [30] and Adams [31] in more detail.

Exponentially small terms arise because the optimal truncation point has a dependence on x, its presence indeed could be seen after employing the Stirling's formula on the late order terms of the expansion. This process is named superasymptotics (asymptotics beyond all orders) by Berry who was the first person truncating the divergent series optimally (near the least term) in [36]. Upon truncation of the divergent series optimally and ignoring the rest of the terms, he achieved the smallest error with an exponential accuracy. According to Berry and Howls [37] this technique was first studied while analysing the Airy function asymptotically by Stokes [38–40] whose work was ignored or not thoroughly understood by mathematicians for over a century. The method of exponential asymptotics, after it is established, was applied to the error function by Berry [36].

1.3 Hyperasymptotics

In 1991, Berry and Howls published the formal definition of hyperasymptotics to reduce the error of the expansion in which the remainders, which are smaller than the first neglected terms of the expansion, are exponentially small [25, 33, 41, 42]. They defined hyperasymptotics as systematically studying exponentially small remainder leftover of the optimally truncated expansion by repeated reexpansion [43], employing Borel summation of a 'resurgence relation' for the resultant remainder. In [33], they used hyperasymptomatics by employing the exact resurgence relation for integrals with saddles and expressed higher exponential accuracies than that of superasymptotics. Though superasymptotics and hyperasymptotics were introduced

by Berry and Howls, the subject is pioneered by Stokes [38] and Dingle [24] who observed that the Poincaré's definition was not unique. Chapman et al. then applied this method via truncation of the series after the optimum numbers into gravity waves problems to determine exponentially small waves [6, 10, 11], and later on this was developed by Olde Daalhuis et al. in [27].

Hyperasymptotics analyses a remainder equation of the expansion by re-expanding the previous remainder equation. The main consideration behind hyperasymptotics is that each remainder contains a remainder, and upon examination of the remainders, exponentially small terms are added to the expansion, where the precision of the expansion improves exponentially. Superasymptotics can be thought as the zeroth level of the hyperasymptotic expansion, but in both superasymptotics and hyperasymptotics, the remainders are dependent on the truncation point. Because more terms are added in hyperasymptotics, it generates a relatively more accurate approximation than superasymptotics [44]. The hyperasymptotic approach is also known as "beyond asymptotics beyond all orders" since it requires further analysis than superasymptotics [25, 35, 45].

Earlier in the discussions of hyperasymptotics, it was expected that the associated optimal truncation point of the each further level was shorter than the previous level. Berry and Howls also found that the number of the terms of each hyperseries is half the number of the terms of the preceding level [33, 43]. Therefore it was concluded that the hyperasymptotic process has an end, which occurs when the last expansion has only one single term [33]. On the other hand, Olde Daalhuis later on in [45] introduced a new method leading to hyperasymptotic expansion for the confluent hypergeometric functions by using its integral representation. Basically, he found a similar picture to that of Berry and Howls' [33]; at each level of the hyperasymptotics, the remainder is exponentially smaller, and the optimal truncation point increases instead of decreasing [45–47]. Since in each level the approximation

gets better and better, Olde Daalhuis highlighted that there is no limit for the hyperasymptotic expansion [48, 49]. He extended this method of Olde Daalhuis [45] and confirmed this improvement in [47].

In 1937, Airey [50] published the method of 'converging factor', the factor by which the first neglected term must be multiplied to terminate the series to obtain higher accuracy. His interpretation involves truncating the series and discussing the truncated remainder by expressing as a multiplication of the first term neglected. Although this discussion resembles the method of this thesis, it is not identical. In this thesis, the remainder (the divergent part of the series) is rescaled as the product of the first neglected term and a new function, which is similar Airey's converging factor, but this strategy differs from that of Airey since we expand the product function as an asymptotic power series. The form of the series, however, are the same in nature; first deceasing, and then diverging to infinity. However, Airey's technique of discussion applies to alternating series where the general representation is known. He addresses his method, for example for the exponential integral, for the negative values of the argument. Our approach is not restricted to the negative values of the arguments, and, hence does not require to the series to be alternating. We also interpret the remainder and its behaviour in terms of the previous stages truncation points and allow the truncation points to vary as detailed in the thesis. Moreover, in our approach we may go beyond the first level and discuss in detail the higher levels of the hyperasymptotics by doing the successive reexpansion of the remainders.

1.4 Stokes phenomenon

Recent years saw an increasing focus on the method of exponential asymptotics, since it is now widely known that exponentially small terms of the asymptotic series may carry important information which cannot be determined through traditional asymptotic methods. Stokes was the first person who found that the series contains

discontinuous constants which change abruptly as certain lines, known as Stokes lines (rays) [38], are crossed in the complex plane. Berry [51], motivated by the technique of exponential asymptotics through studying the behaviour of the remainder terms, discovered that this abrupt change appears near the Stokes lines. On a Stokes line, exponentially small terms of the expansion are maximally dominated by another term [28, 32, 36, 52]. Berry further demonstrated that this change occurs smoothly via the error function [51] across the Stokes lines. However, Chapman [53] uncovered that this is not a generic property of hyperasymptotics, but it is usually true. The technique of Stokes and Berry was expanded by Olde Daalhuis et al. and Chapman et al. [27, 30]. Stokes phenomenon (i.e. the process of finding the Stokes and anti-Stokes lines [9]) concerns the behaviour of the exponentially small terms when they are switched on and off. As has already been noted, these lines arise when the series are divergent. For example, across Stokes lines, exponential small gravity waves switch on and off [10, 54], and the remainder terms stop oscillating, and its imaginary parts may vanish. This means that the asymptotic solution might miss crucial information about such problems if Poincaré's method is employed.

In order to derive the location of the Stokes and anti-Stokes lines, truncated remainders of the divergent series must be analysed with care. The behaviour of the remainder, specifically the behaviour of the denominator function of the remainder, plays a crucial role for a complete understanding of the behaviour of the expansion, i.e., the Stokes phenomenon. The phenomenon is based on exponential asymptotics that makes the Stokes and anti-Stokes lines visible [55]. In fact, Stokes lines originate from the singularities of the remainder equations [56, 57] at which expansion breaks down. Once these singularities are located, it is possible to determine the Stokes and anti-Stokes lines using each one. Hence, these lines can be located by analysing the denominator function which is called the singulant by Dingle [24, pp. 6-8]. Particularly, Stokes lines occur when the singulant is purely real and positive; whereas, anti-Stokes lines occur when the singulant is purely imaginary, where exponentials

have equal magnitude [34, 43, 56, 58]. Both Stokes and anti-Stokes lines are only meaningful near the singularities of the remainder. According to the other definition given by Dingle [24], the Stokes lines equivalently may occur when the late-order terms have the same phase since the remainder functions stop oscillating when their phases are at Stokes lines [27, 59]. Singularities of the remainder functions dominate the late-order terms which means as the series passes through Stokes lines it goes from subdominant to dominant or dominant to subdominant. This means that the series changes its character, that is the switching on and off, as the Stokes lines are crossed. Hence, based on the sector in the complex plane, exponential terms come into play. Due to the smooth varying of terms, Stokes phenomenon plays a key role, in the subject, and the whole picture in the complex plane should be self-consistent; in other words, one needs to come back to the original solution upon carrying out a complete circuit in the plane.

Subdominant exponential terms obtained by asymptotic expansion are turned on across the Stokes lines emerging from the turning points. Although all singularities and branch cut(s) involved in expansions are taken into account, in some cases an inconsistency, which is the key motivation lying behind the higher-order Stokes lines (HOSL), emerges. Intersection points of the Stokes lines at a regular point may give rise to a new Stokes line, HOSL, for some equations, and for the presence of this phenomenon, two or more asymptotic expansions should be present [39, 56, 57] so that the crossing of the Stokes lines may occur. Whenever Stokes lines cross each other rather than at turning points this phenomenon may be present. Hence, it is termed a Stokes crossing point (SCP) by Howls et al. [39], at which the HOSL may terminate the active Stokes lines [56]. This in turn may influence the presence of the Stokes line itself to switch on or off, for more discussion see [39]. As discussed above, it is anticipated that the usual Stokes lines emerge solely from the singularities, however Howls et al. in [39] and Olde Daalhuis in [60] demonstrated that a new Stokes line might arise by the regular points. Initially, this new line aris-

ing from the crossing point in which two or more Stokes lines cross each other was termed as 'new-Stokes lines' by Berk et al. in [61] who first discussed this issue, which is termed identically by Chapman and Mortimer [62]. However, according to Olde Daalhuis [60], this naming is not appropriate, since these types of crossing points have some similar effects to the turning points, hence he endorsed the term SCP. Even if the divergent series is present in the relevant region, Stokes lines may be inactivated or activated across the HOSL: in one side while they are active, on the other side they may get inactivated. Therefore, it helps to distinguish where the subdominant exponentials are present in the different sectors of the complex plane, which is the main purpose of the Stokes phenomenon as it deals with the appearance and disappearance of the exponential terms. An inability to detect HOSL may lead to erroneous conclusions. For a complete understanding of the Stokes phenomenon, HOSL analysis is required. New Stokes line does not occur from HOSL, as this only may change the activity of the present Stokes lines. As noted previously, one expects to come back to the solution one started with after making a complete circuit around the complex plane.

1.5 Overview of the methodology and results

Figure 1.1 briefly summarises one of the main conclusions of the thesis. Truncating the asymptotic series solution of the exponential integral given in §4 at the optimum number of terms provides the exponentially accurate approximation in superasymptotics shown in red in the figure. Carrying out the process repeatedly in this thesis enables one to have the hyperasymptotic approach results illustrated in the figure, where the red, blue and green dotted lines correspond respectively to the zeroth, first and second levels of hyperasymptotics established by successive optimal truncations. Moreover, by considering the zeroth level truncation point as a free parameter and increasing it, we decreased the error estimate at the first level to a lower value than the optimally truncated error obtained even at the second level; to see this effect,

compare the black and green dots. To be more precise, for example, truncation of the first level expansion only 39 terms after the predicted optimal value of the truncation point provides the equivalent error that can be obtainable in the second level of hyperasymptotics for the chosen values given in the figure; see first black and green dotted lines. Hence, in light of the evidence gathered in this thesis, the hyperasymptotic expansion of this thesis, which we also term as the multi-level asymptotics, is introduced and the error is minimised. Further details of the results of the exponential asymptotics along with the analysis will be provided later on; however, for a detailed explanation of the specific figure, see §4.9.

1.6 Structure of the thesis

In this thesis, we will be using the asymptotic methods as follows. Derivation of an asymptotic series solution of the singular differential equations is the first step:

$$f(x;\varepsilon) \sim \sum_{n=0}^{\infty} a_n(x)\delta_n(\varepsilon) \quad \text{as} \quad \varepsilon \to 0.$$

Substitution of the summation into the original differential equation(s) generates the differential recurrence relation for $a_n(x)$ from which the general term can be generated via either repeated usage of the previous terms or via the factorial-over-a-power method. The latter is employed if it is not directly obtained from the first, since sometimes the formulation of the late order terms could be challenging. When the late-order term is established, the next stage will be truncating the perturbed series whereupon we receive a good approximation. Truncation of such series after N terms yields

$$f(x;\varepsilon) \sim \sum_{n=0}^{N-1} a_n(x)\delta_n(\varepsilon) + R_N(x) \quad \text{as} \quad \varepsilon \to 0,$$

in which the resultant remainder is in $\mathrm{O}(\delta_n(\varepsilon))$, which is the order of the accuracy emerging by Poincaré's method. However, to improve accuracy the technique of

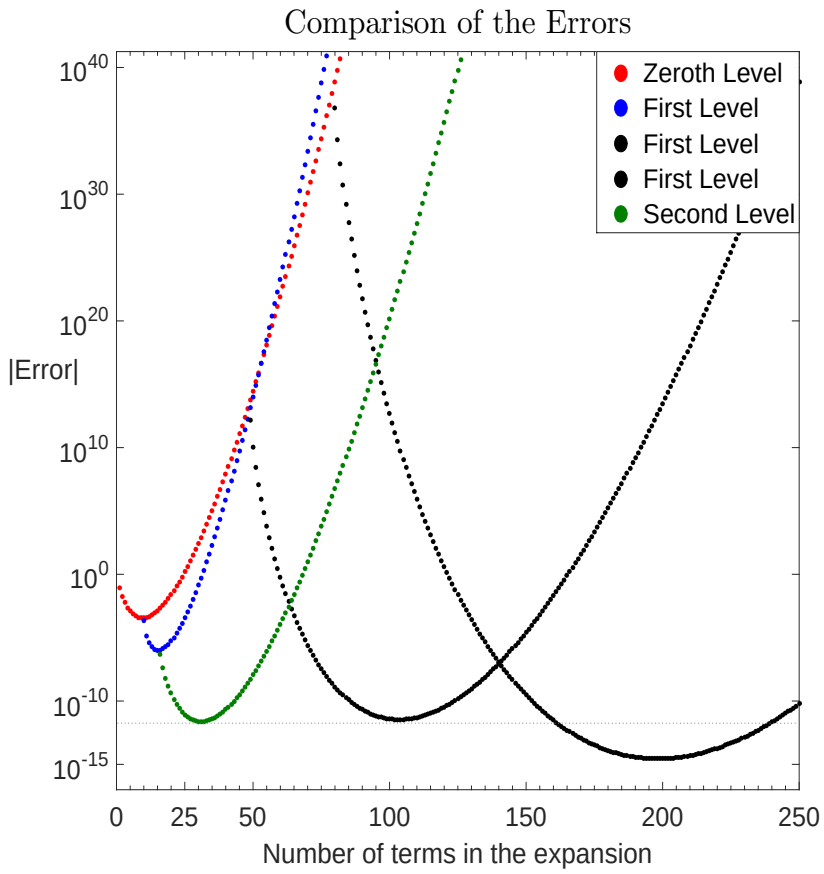


Figure 1.1 Magnitude of the errors, given by (4.12), (4.34) and (4.84), in 3 levels of the expansion where the series are truncated optimally at each level and arbitrarily at the first level for chosen $\varepsilon = 0.1$ with $z = 1/2 + i\sqrt{3}/2$. The figure clearly shows the improvement obtained by the hyperasymptotics, that is, the error decreases at each level. Black dots correspond to the various truncation points of the first level rather than the optimal one.

optimal truncation is required for the divergent series; particularly, if N is the point of optimal truncation, the series takes its least value and the remainder $R_N(x)$ turns out to be exponentially small. Thence, the remainder occurs in the order of optimal truncation whereupon the exponential accuracy arise. In practice, although Poincaré's method is easy to obtain as it may be finalised with a few terms of the expansion, truncation of the series after the least term generates more meaningful results for the divergent series. Inserting the truncated ansatz into the original differential equation(s) produces the inhomogeneous differential equation for $R_N(x)$,

whereby similar analysis can be carried out for the remainder.

We begin this thesis in §2 by addressing an instructive differential equation which demonstrates the features of exponential asymptotics along with the Stokes phenomenon along with the necessary background information which will be needed for this thesis. In fact, the results become transparent upon first observing the behaviour of the leading order term, specifically the singularities, as their location gives birth to the new exponentials. We next truncate the asymptotic series solution of the differential equation after the point it takes its absolute minimum value. Generally, truncation of the series provides the algebraically small error estimate in a small parameter; however, to derive the exponentially small error estimate hidden in a divergent series, we need to perform optimal truncation. The Stokes lines discussion then continues in the chapter as that is expected to have one from each singularity. In doing these, we will observe that the subdominant exponentials are going to switch on and off across the Stokes lines and equal dominance on the anti-Stokes lines. §3 discusses a general first order differential equation which appears in the first level of hyperasymptotics. Therein, we derive the connection formula between the singulant of the expansion and the leading prefactor of the equation, whereby we discuss the differential equation for various prefactors. We also establish the remainder equation of the higher level hyperasymptotics for general singulants for the first order differential equations.

Then, in §4 we employ the method of exponential asymptotics to the exponential integral. First, we find the leading order term from which the singularity of the expansion is identifiable and the recurrence relation by which the full hyperasymptotic expansion is generated. We observe that no new singularities are introduced by this relation. However, having such a recurrence does not always give the possibility of deriving the general term of the expansion in complete form explicitly, so we make use of the factorial-over-a-power method in those cases. In this chapter, hyper-

asymptotic analysis as well as the corresponding Stokes phenomenon for each level will be conducted in 4 levels. Whether or not the error estimate can be improved will be scrutinised in this chapter. At the end of the chapter we address general findings of the hyperasymptotics obtained. In order to demonstrate and support the findings of §4, we study further examples in §§5-7 and apply the general results of hyperasymptotics to them; specifically, the error function arising from both first and second order equations, the Airy function and confluent hypergeometric function. Due to the complexity of studying functions such as the confluent hypergeometric function in §7, we use the WKB theory for differential equations so that we can obtain the explicit approximate solution by exponential terms.

§7 is devoted to investigating the confluent hypergeometric function (CHF) through exponential asymptotics. In comparison with Olver's [63] and Olde Daalhuis's [45] works, we first re-scale the CHF and then employ hyperasymptotics in the sense of §4. As we have already discussed most of the key details in the preceding chapters, like the leading order term analysis, matching asymptotics, recurrence relation, Stokes phenomenon and so on for a singular differential equation, this chapter will repeat the same investigations to verify the outcomes found in the thesis.

In §8, we study the importance of the higher-order Stokes phenomenon via an example addressed in Olde Daalhuis [60]. As well as using the hyperasymptotic expansion techniques used throughout the preceding chapters, we particularly focus on the HOSL and provide a detailed explanation and discussion on the HOSL, where we illustrate the overall results along with the description of the main features in the Stokes phenomenon in a figure. Finally in §9, a summary of the thesis is provided along with the main conclusions obtained in the work.

1.7 Statement of Originality

I hereby declare that, except where specific reference is made to the work of others, the contents of this thesis are original and have not been submitted in whole or in part for consideration for any other degree or qualification in this, or any other university. This thesis is my own work and contains nothing which is the outcome of work done in collaboration with others, except when specified in the text.

Chapter 2

Introductory example of exponential asymptotics

2.1 Introduction

In this chapter, we analyse a singular differential equation by focusing on the method of exponential asymptotics. We will illustrate how the methodology could be used in a differential equation in which it appears. By doing so, some key features of the method and Stokes phenomenon mentioned in the introduction are presented; particularly, these features concern the type of the series, optimal truncation, Stokes and anti-Stokes lines, exponentially small terms and their switching on and off behaviours. In this way, the reader will be familiar with the nature of the exponential asymptotics and its features for the forthcoming chapters. The methods presented in this chapter are discussed in great detail, for example, by Olde Daalhuis et al [27] and Chapman et al [30].

As was mentioned in §1, in exponential asymptotics one is interested in studying the behaviour of series which are in the form of 'first decreasing till reaching its minimum and then diverging to infinity'. In such series, subdominant exponentially small terms, which are invisible by using the method of usual algebraic expansion

alone, will be visible with the application of exponential asymptotics. Berry terms the exponential terms having the biggest magnitude "dominant" and the other exponentials "subdominant" [64]. Although the general term of the expansion could be computed via the usual asymptotics method, it is not possible to observe the exponentially small terms through this method. Therefore, in order to distinguish these small terms, the algebraic series needs to be truncated optimally, which means these terms can only be included in the solution by employing the optimal truncation method, which will be outlined in this chapter. Truncating the series optimally, moreover, enables the error of the expansion to be exponentially small [25]. This whole process and analysing the truncated remainder is termed as superasymptotics, also known as asymptotics beyond all orders, by Berry [25].

Additionally, analysing exponentially small terms will enable us to observe the Stokes and anti-Stokes lines of the equation emerging from the singularities of the asymptotic expansion where it breaks down. Hence, the singularities of the leading term must be derived prior to analysing the expansion near the singularities. As one moves across the Stokes lines, the birth of the subdominant exponential terms will be observed. Upon crossing these lines, exponentially small terms switch on and off, which usually occurs via an error function [36], by the dominant exponential terms. In fact, this switching of the subdominant term affects the behaviour of an asymptotic expansion. By doing this we show, therefore, which exponential terms of the expansion are present in which sectors of the complex plane. This changing behaviour of the expansion is known as the Stokes Phenomenon [51].

In the following model problem we intend to derive an exponentially accurate approximate solution of the differential equation by employing the beyond all orders approach. The equation studied in the present chapter is

$$\varepsilon^2 \frac{d^2y(z)}{dz^2} + y(z) = \frac{1}{1+z^2}, \tag{2.1}$$

in which $0 < \varepsilon \ll 1$. The highest derivative of the equation is a multiple of the small term ε and it contains the singularities $\pm i$ on its right hand side, henceforth denoted by RHS. This singular equation is addressed in this chapter. We hope to minimise the error of its asymptotic expansion by explicitly analysing the turning points of the differential equation.

The outline of the chapter is as follows: We begin in §2.2 analysing the ordinary differential equation (2.1) by conventional asymptotic technique. The first step of the analysis is to expand the series into powers of ε and precisely determine the general term of the expansion from which the singularities of the leading order term will be found. After deriving the tail, the series will be truncated at an optimal order at which the series starts to grow in §2.3. We minimise the remainder function of the truncated expansion by regarding the remainder as a function of the truncation point. By doing this, the exponentially small remainder of the asymptotic expansion will be observed in ε. This stage will provide an illustration of how the remainder depends on the optimal truncation point. The next step is to examine the remainder of the truncated series explicitly by which we will derive the connection between the Stokes lines and the general term of the expansion, i.e., the singularities of the general term from which Stokes lines emerge at the leading order. In §2.6, we will perform a residual calculation of the model problem and address its branch cuts. In §2.7, we first present Stokes as well as anti-Stokes lines, then demonstrate the switching on and off behaviour of the subdominant terms across the Stokes lines by careful consideration of the expansion near the singularities. Finally, we will finalise this chapter with a conclusion.

2.2 Asymptotic expansion

The first step of the technique outlined above is to expand the illustrative differential equation asymptotically by a formal series solution. In this section, let us therefore

begin to study the equation (2.1) with Poincaré's perturbation method expanding $y(z)$ in powers of ε^2 as a regular asymptotic series

$$y(z) \sim \sum_{n=0}^{\infty} \varepsilon^{2n} y_n(z). \tag{2.2}$$

Because this series expression (2.2) must satisfy the differential equation (2.1), it will be formally plugged into the equation (2.1), and we will equate the coefficients of like powers of ε on both sides of the equation. By doing so, the leading-order term and the differential recurrence relation of the expansion in the asymptotic limit will be determined as follows

$$\begin{aligned} y_0(z) &= \frac{1}{1+z^2} && \text{at } \mathrm{O}(1), \\ \frac{d^2 y_{n-1}(z)}{dz^2} + y_n(z) &= 0 && \text{at } \mathrm{O}(\varepsilon^{2n}). \end{aligned} \tag{2.3}$$

It should be pointed out here that the leading-order term $y_0(z)$ of (2.2) contains complex symmetrical singularities at $z = \pm i$. Having derived the leading-order term, we are now in a position to obtain all the terms of the expansion in (2.2) by using the system of the recurrence relation given in (2.3). Taking the second derivative of $y_0(z)$ and plugging into the recurrence relation allow us to determine the first term $y_1(z)$. Carrying out this process repeatedly between $(n-1)^{th}$ term and n^{th} term of the expansion derives the form of the general term of the expansion such that

$$\begin{aligned} y_0(z) &= \frac{1}{1+z^2} = \frac{i}{2}\left(\frac{1}{z+i} - \frac{1}{z-i}\right) && \text{at } \mathrm{O}(\varepsilon^0), \\ y_n(z) &= \frac{i(-1)^n}{2}(2n)!\left(\frac{1}{(z+i)^{2n+1}} - \frac{1}{(z-i)^{2n+1}}\right) && \text{at } \mathrm{O}(\varepsilon^{2n}). \end{aligned}$$

The n^{th} term in the expansion preserves both singularities, and there is no additional singularity created by the recurrence relation. It is worth remarking that, although it is not true in general, for this particular problem, we were able to find the general term $y_n(z)$ exactly for each term in the expansion. Moreover, the term $y_n(z)$

is obtained in the nature of a factorial-over-a-power without the need for using the factorial-over-a-power method. By having established the late-order term of the expansion, an asymptotic solution of $y(z)$ is fully attained, which means the first step of calculation is completed. The expansion is divergent as $\left|\frac{y_{n+1}(z)}{y_n(z)}\right| > 1$ for large n. Furthermore, as the series is in the form of a factorial divided by a power, it must be diverging. In order to obtain more information on the behaviour of the expansion and to observe the importance of the exponentially small terms, the next step is to determine the point at which the series starts changing its direction from decreasing to growing. The expansion (2.2) will be truncated after N terms and then the behaviour of the resultant remainder will be examined in the next section.

2.3 Optimal truncation and remainder equation

The second step is to truncate the expansion (2.2) optimally which will enable us to distinguish exponentially small terms. We begin truncating the series with Berry's technique [65] by writing

$$y(z) = \frac{i}{2}\sum_{n=0}^{N-1} \varepsilon^{2n}(-1)^n(2n)!\left(\frac{1}{(z+i)^{2n+1}} - \frac{1}{(z-i)^{2n+1}}\right) + R_N(z), \tag{2.4}$$

where $R_N(z) = \mathrm{O}(\varepsilon^{2N})$ is the remainder of the expansion. The error of the expansion after truncation is $R_N(z) = y(z) -$ truncated sum. We approximate it by considering the first neglected term as

$$E_N(z) := \frac{i}{2}\varepsilon^{2N}(-1)^N(2N)!\left(\frac{1}{(z+i)^{2N+1}} - \frac{1}{(z-i)^{2N+1}}\right). \tag{2.5}$$

Substituting the truncated expression (2.4) with the remainder into the differential equation (2.1) will provide us a differential equation for the remainder. That is, after taking the first and second derivative of (2.4) and multiplying the second derivative

by ε^2, we find that the remainder, given in (2.4), is a solution of

$$\mathscr{L}\left(R_N(z);\varepsilon\right) = \frac{(2N)!}{2}\varepsilon^{2N}\left(\frac{1}{(1+iz)^{2N+1}} + \frac{1}{(1-iz)^{2N+1}}\right), \tag{2.6}$$

where $\mathscr{L}$ corresponds to the left hand side (LHS) of the equation such that

$$\mathscr{L}\left(R_N(z);\varepsilon\right) = \varepsilon^2 R_N''(z) + R_N(z),$$

in which $\mathscr{L}$ is the same linear operator as in the original equation (2.1). If Stirling's formula is employed for the factorial term of (2.6), the remainder differential equation (2.6) can then be represented in the approximate form for large N

$$\mathscr{L}\left(R_N(z);\varepsilon\right) \sim \sqrt{\pi N}\left(\frac{2N\varepsilon}{e}\right)^{2N}\left[\frac{1}{(1+iz)^{2N+1}} + \frac{1}{(1-iz)^{2N+1}}\right]. \tag{2.7}$$

Due to having identical singularities in the expansion, it is worth commenting briefly that the dominant term of the expansion, in addition to the error, changes depending on a region in the limit $N \to \infty$. Particularly, as there are two singularities in the expansion, as apparent in the summation (2.4), the dominant term changes based on which sector of the complex z-plane we are in. If we are in the the upper-half plane in which z is in the sector $0 < ph(z) < \pi$, $(1+iz)$ term of (2.4) in the square bracket satisfies $|1+iz| < |1-iz|$ if and only if $\Im(z) > 0$; as a consequence, the associated singularity dominates the summation for sufficiently large values of N. Likewise, in the lower-half plane where z in the sector $\pi < ph(z) < 2\pi$, the fraction containing the term $(1-iz)$ leads the series given in (2.2) when N is large enough, so does the RHS of (2.7). These mean that the RHS according to the sector z in is asymptotic to

$$\mathscr{L}\left(R_N(z);\varepsilon\right) \sim \begin{cases} \sqrt{\pi N}\left(\dfrac{2N\varepsilon}{e}\right)^{2N}\dfrac{1}{(1+iz)^{2N+1}} & \text{if } z \in \Im(z) > 0, \\ \sqrt{\pi N}\left(\dfrac{2N\varepsilon}{e}\right)^{2N}\dfrac{1}{(1-iz)^{2N+1}} & \text{if } z \in \Im(z) < 0. \end{cases} \tag{2.8}$$

The next and crucial step of exponential asymptotics is to determine where the point

of optimal truncation occurs. It could be identified by three different ways: either (i) evaluating successive terms of the expansion [31, 62, 66] or (ii) evaluating the residual remainder differential equation [28] by the ratio test for large $n \sim N$, near unity, or (iii) minimising the n^{th} term of the expansion [28], i.e.,

$$\left|\frac{\varepsilon^{2n}y_n(z)}{\varepsilon^{2n-2}y_{n-1}(z)}\right| \sim 1 \quad \text{or} \quad \left|\frac{\mathscr{L}\left(R_n(z);\varepsilon\right)}{\mathscr{L}\left(R_{n-1}(z);\varepsilon\right)}\right| \sim 1 \quad \text{or} \quad \frac{d}{dn}|\varepsilon^{2n}y_n(z)| = 0. \tag{2.9}$$

These imply particularly that the optimal truncation point is a function of z and ε. When deriving the truncation point according to the sector of the complex z-plane we are in, in order to not repeat the same calculations twice for both regions separately, we use one of the above methods without referencing (2.8). By employing the third method of (2.9), we directly verify that the derivative of the general term of the expansion with respect to N is

$$\begin{aligned}\frac{d}{dN}\varepsilon^{2N}y_N(z) = &\sqrt{\frac{\pi}{N}}\left(\frac{2N\varepsilon}{e}\right)^{2N}\left(\frac{1}{(1+iz)^{2N+1}}\right)\left(\frac{1}{2}+2N\ln\left(\frac{2N\varepsilon}{e}\right)+2N-2N\ln(1+iz)\right)\\ &+\sqrt{\frac{\pi}{N}}\left(\frac{2N\varepsilon}{e}\right)^{2N}\left(\frac{1}{(1-iz)^{2N+1}}\right)\left(\frac{1}{2}+2N\ln\left(\frac{2N\varepsilon}{e}\right)+2N-2N\ln(1-iz)\right),\end{aligned}$$

which becomes the following when N is sufficiently large

$$\frac{d}{dN}\varepsilon^{2N}y_N(z) \sim 2\sqrt{\pi N}\left(\frac{2N\varepsilon}{e}\right)^{2N}\left[\left(\frac{\ln\left(\frac{2N\varepsilon}{1+iz}\right)}{(1+iz)^{2N+1}}\right)+\left(\frac{\ln\left(\frac{2N\varepsilon}{1-iz}\right)}{(1-iz)^{2N+1}}\right)\right].$$

It is worth mentioning that the first method of (2.9) derives this point easier in comparison with differentiation. The optimal truncation point occurs differently due to the presence of the singularities at $\pm i$ by the same token as explained earlier regarding the general term of the expansion. To make this point more precise, if we are in the upper half plane, the first term in square brackets provides the optimal truncation point; if in lower half plane, second term provides this point. This explains why the

optimal selection of the truncation point takes place at

$$N(z,\varepsilon) = \begin{cases} \dfrac{|1+iz|}{2\varepsilon} & \text{if } z \in \Im(z) > 0, \\ \dfrac{|1-iz|}{2\varepsilon} & \text{if } z \in \Im(z) < 0. \end{cases} \tag{2.10}$$

The optimal truncation point, in which the error $E_N(z,\varepsilon)$ takes its least value, depends upon the expansion parameter z and ε as discussed in [45, 47]. In order to localise this point N as a function of ε, we could choose $z = 0$ such that

$$\frac{d}{dN}\varepsilon^{2N} y_N(0) \sim 4\sqrt{\pi N}\left(\frac{2N\varepsilon}{e}\right)^{2N} \ln(2N\varepsilon) \quad \text{for large } N, \tag{2.11}$$

which becomes equal to 0 only if $\ln(2N\varepsilon) = 0$. Thence, the optimal truncation of the expansion for $z = 0$ occurs at

$$N = \frac{1}{2\varepsilon}, \tag{2.12}$$

which in fact agrees with setting $z = 0$ in (2.10). To visualise the behaviour of the expansion, which is in the factorial-over-a-power form, and to understand the idea of the point of optimal truncation, the error of the expansion is plotted over N for several values of z in different regions of the complex plane. If the series is optimally truncated at N, it is further to be anticipated that the remainder $R_N(z)$ should be exponentially small. Figure 2.1 represents the curve of the relative error $E_N(z)$ and its typical behaviour which occurs in exponential asymptotics; that is, it first decreases until reaching its minimum value where it begins to grow to infinity. It is straightforward to see from Figure 2.1 that the optimal truncation points are consistent with the results of (2.10) and (2.12).

In the next stage, the remainder of an optimally truncated series will be discussed in more detail. Particularly, employing the optimal truncation points derived in (2.10) will enable us to establish the typical error function occurring in exponential asymp-

totics in the vicinity of the turning points.

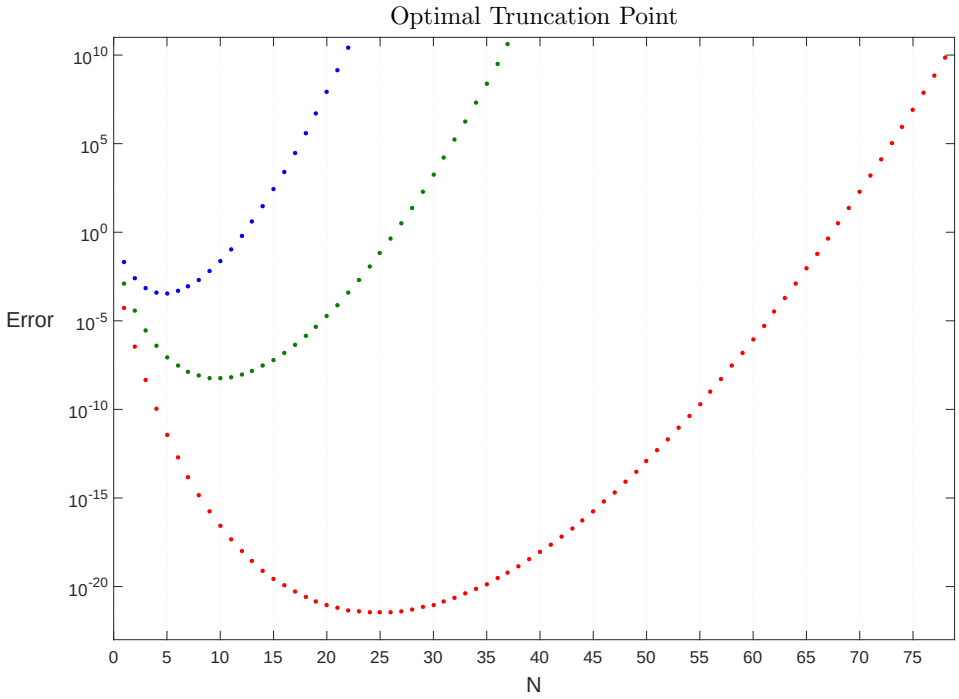


Figure 2.1 Illustrating the truncation error $E_N(z)$ in (2.5) as a function of N. It first decreases, and then diverges to infinity. It takes its minimum value at 5, 10 and 25 for selected values of $z = 0$, $z = -\sqrt{3} - 2i$ and $z = 3 + 5i$ while $\varepsilon = 0.1$ in blue, green and red respectively.

2.4 Remainder near $z = 0$

Before initiating the error analysis near the singularities for sufficiently large N and small ε at the optimal truncation point, we perform a calculation near 0 in which the Stokes lines cross the real axis, since we are most interested in the solution with the real values. This will be addressed in §2.7. Hence, we first re-scale z close to zero which lies on the Stokes line such that

$$z = \delta(\varepsilon)Z, \tag{2.13}$$

where $|\delta(\varepsilon)| \ll 1$, which will be determined shortly, is an unknown function of ε, and Z is $O(1)$. The transformation (2.13) changes (2.7) into

$$\mathscr{L}(R_N(Z);\varepsilon) \approx \sqrt{\pi N}\left(\frac{2N\varepsilon}{e}\right)^{2N}\left(\frac{1}{f(Z)}+\frac{1}{g(Z)}\right), \tag{2.14}$$

where

$$f(Z) = (1+i\delta Z)^{2N+1} \quad \text{and} \quad g(Z) = (1-i\delta Z)^{2N+1}.$$

Based on logarithmic function properties and Taylor series expansion for δ small, these $f(Z)$ and $g(Z)$ can be approximated as

$$f(Z) \approx \exp\left(2Ni\delta Z + N\delta^2 Z^2\right) \quad \text{and} \quad g(Z) \approx \exp\left(-2Ni\delta Z + N\delta^2 Z^2\right),$$

where $N \gg 1$. Substituting these approximate values of $f(Z)$ and $g(Z)$ into the RHS of the remainder differential equation (2.14), we find

$$\mathscr{L}(R_N(z);\varepsilon) \approx \sqrt{\pi N}\left(\frac{2N\varepsilon}{e}\right)^{2N}\frac{1}{\exp(N\delta^2 Z^2)}\left(\frac{1}{\exp(2N\delta Zi)}+\frac{1}{\exp(-2N\delta Zi)}\right), \tag{2.15}$$

which suggests that the right balance in (2.15) should be occurring when $N\delta^2 \sim 1$. Hence, the δ scaling in terms of ε using (2.12) is determined by means of

$$\delta \sim \sqrt{2\varepsilon}.$$

Substitution of this value of δ leads to

$$\mathscr{L}(R_N(Z);\varepsilon) \approx \sqrt{\frac{\pi}{2\varepsilon}}\frac{\exp(-1/\varepsilon)}{\exp(Z^2)}\left[\exp\left(-\sqrt{\frac{2}{\varepsilon}}Zi\right)+\exp\left(\sqrt{\frac{2}{\varepsilon}}Zi\right)\right]. \tag{2.16}$$

Because δ is determined as a function of ε, which defines Z, we can now return to the differential equation (2.16) by back substitution

$$R_N''(z)+\frac{1}{\varepsilon^2}R_N(z) = \frac{A}{\varepsilon^2}\exp\left(-\frac{z^2}{2\varepsilon}\right)\left(\exp\left(-\frac{iz}{\varepsilon}\right)+\exp\left(\frac{iz}{\varepsilon}\right)\right), \tag{2.17}$$

in which we set $A := \sqrt{\pi/2\varepsilon}\exp(-1/\varepsilon)$ for simplicity. In order to interpret the remainder, we first need to solve this differential equation. We use the method of variation of parameters [67] to attain the particular solution of (2.17) as

$$\begin{aligned}(R_N)_p(z) &= \frac{A}{2\varepsilon i}e^{\frac{iz}{\varepsilon}}\int^z e^{-\frac{t^2}{2\varepsilon}}\left(1+e^{-\frac{2it}{\varepsilon}}\right)dt - \frac{A}{2\varepsilon i}e^{-\frac{iz}{\varepsilon}}\int^z e^{-\frac{t^2}{2\varepsilon}}\left(1+e^{\frac{2it}{\varepsilon}}\right)dt \\ &\sim \frac{A}{2\varepsilon i}e^{\frac{iz}{\varepsilon}}\int^z \exp\left(-\frac{t^2}{2\varepsilon}\right)dt - \frac{A}{2\varepsilon i}e^{-\frac{iz}{\varepsilon}}\int^z \exp\left(-\frac{t^2}{2\varepsilon}\right)dt,\end{aligned} \tag{2.18}$$

where the integrals containing $\exp(-2/\varepsilon)$ are neglected due to $\exp(-2/\varepsilon) \ll \exp(-1/\varepsilon)$ from the dominant balance. The particular solution is expressed in terms of the error function

$$(R_N)_p(z) \sim \frac{\pi}{2\varepsilon}\exp\left(-\frac{1}{\varepsilon}\right)\sin\left(\frac{z}{\varepsilon}\right)\operatorname{erf}\left(\frac{z}{\sqrt{2\varepsilon}}\right), \tag{2.19}$$

in which $\operatorname{erf}(z)$ is an error function with the definition of

$$\operatorname{erf}(z) = \frac{2}{\sqrt{\pi}}\int_0^z \exp\left(-t^2\right)dt. \tag{2.20}$$

Herein, it is apparent from $\exp(-1/\varepsilon)$ term of (2.19) that (2.19) is exponentially small in ε as expected. Combining the solution with the homogeneous solution, the general solution of $R_N(z)$ can be written down as

$$R_N(z) \sim C_1\cos\left(\frac{z}{\varepsilon}\right) + \left(C_2 + \frac{\pi}{2\varepsilon}\exp\left(-\frac{1}{\varepsilon}\right)\operatorname{erf}\left(\frac{z}{\sqrt{2\varepsilon}}\right)\right)\sin\left(\frac{z}{\varepsilon}\right). \tag{2.21}$$

If we choose in (2.21) $C_1 = C_2 = 0$ and $\varepsilon = 0.1$, then (2.21) becomes

$$\begin{aligned}R_N(z) \sim& 5\pi\exp(-10)\sin(10z)\operatorname{erf}\left(\frac{z}{\sqrt{0.2}}\right) \\ =& 0.00071314\sin(10z)\operatorname{erf}(2.23607z),\end{aligned} \tag{2.22}$$

which is plotted over z in Figure 2.2, whereby the plot contains an error function smoothing as an envelope function.

Putting (2.21) in (2.6), the truncated series after N terms is

$$y(z) \sim \frac{i}{2}\sum_{n=0}^{N-1} \varepsilon^{2n}(-1)^n(2n)!\left(\frac{1}{(z+i)^{2n+1}} - \frac{1}{(z-i)^{2n+1}}\right) + C_1\cos\left(\frac{z}{\varepsilon}\right) + \left(C_2 + \frac{\pi}{2\varepsilon}\exp\left(-\frac{1}{\varepsilon}\right)\operatorname{erf}\left(\frac{z}{\sqrt{2\varepsilon}}\right)\right)\sin\left(\frac{z}{\varepsilon}\right), \tag{2.23}$$

in which the remainder of superasymptotics is exponentially small for small ε. It has been shown by truncating the series (2.2) that the series is asymptotic to the function $y(z)$ as ε goes to 0 which makes N large. The remainder has been obtained in terms of an error function and $\sin(z)$ function.

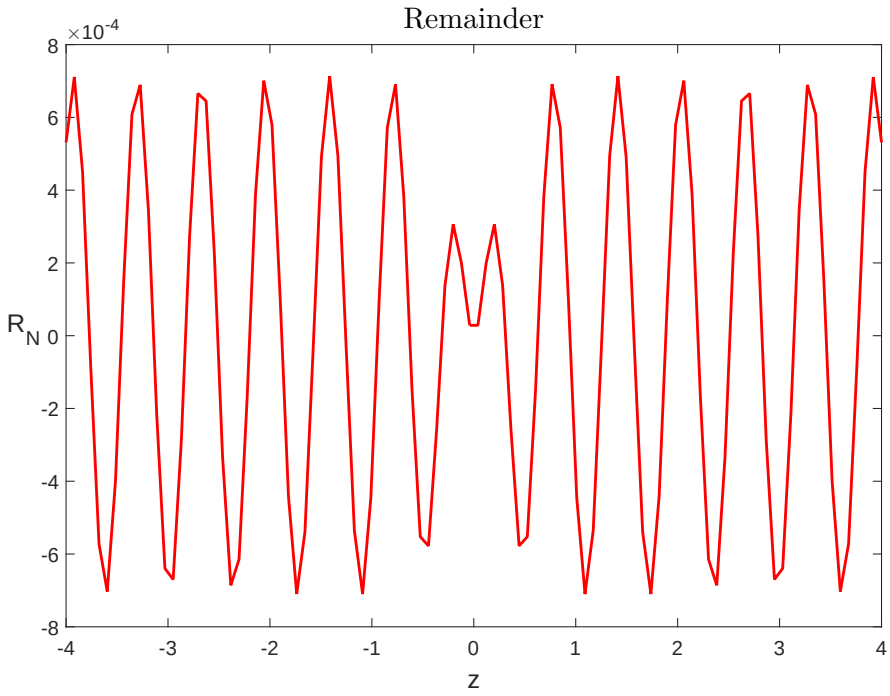


Figure 2.2 A plot of $R_N(z)$ in (2.22) in which C_1 and C_2 are chosen to be 0 and $\varepsilon = 0.1$. Showing the oscillatory behaviour of the remainder.

2.5 Remainder analysis and erf function smoothing

This section is devoted to examining the remainder introduced in (2.4) for a general value of z. To recap from §2.3, suppose that we are in the upper half plane without

loss of generality, then we conduct the error analysis according to $\Im(z) > 0$ throughout this section. Consequently, we focus on the relevant singularity of this region in what follows. This means that the RHS of (2.7) for sufficiently large N is asymptotic to

$$\mathscr{L}\left(R_N(z);\varepsilon\right) \sim \sqrt{\pi N}\left(\frac{2N\varepsilon}{e}\right)^{2N} \frac{1}{(1+iz)^{2N+1}}. \tag{2.24}$$

Note that the similar calculation of this section can be done for $\Im(z) < 0$ by taking into account the singularity of this plane which is symmetrical to the singularity of $\Im(z) > 0$. The homogeneous version of this remainder differential equation (2.24), then, has two solutions

$$R_N(z) \sim \exp\left(\pm\frac{iz}{\varepsilon}\right). \tag{2.25}$$

Motivated by the homogeneous solution, let us introduce function $K(z)$ such that the remainder $R_N(z)$ is

$$R_N(z) = \exp\left(\frac{iz}{\varepsilon}\right) K(z), \tag{2.26}$$

where $K(z)$ will be determined shortly. Substitution of (2.26) into (2.24) produces a differential equation involving only the derivatives of $K(z)$:

$$\varepsilon^2 \exp\left(\frac{iz}{\varepsilon}\right)\frac{d^2K(z)}{dz^2} + 2i\varepsilon\exp\left(\frac{iz}{\varepsilon}\right)\frac{dK(z)}{dz} \sim \sqrt{\pi N}\left(\frac{2N\varepsilon}{e}\right)^{2N}\frac{1}{(1+iz)^{2N+1}}, \tag{2.27}$$

as $\varepsilon \to 0$ and $N \to \infty$. Solving (2.27) will allow us to determine the remainder function by means of an error function. In accordance with the denominator of the RHS of above (2.27), it is convenient to introduce polar coordinates near the singularity in the form of

$$z - i = r\exp(i\theta), \tag{2.28}$$

in which $r = 1$ corresponds to the previous subsection. Making use of polar coordinates (2.28) considering the chain rule as below

$$\frac{d}{dz} = -\frac{ie^{-i\theta}}{r}\frac{d}{d\theta}, \qquad \frac{d^2}{dz^2} = \frac{ie^{-2i\theta}}{r^2}\frac{d}{d\theta} - \frac{e^{-2i\theta}}{r^2}\frac{d^2}{d\theta^2}, \tag{2.29}$$

transforms the differential equation (2.27) into

$$-\varepsilon^2\frac{e^{-2i\theta}}{r^2}\frac{d^2K(r,\theta)}{d\theta^2}+\left(\varepsilon^2\frac{ie^{-2i\theta}}{r^2}+2\varepsilon\frac{e^{-i\theta}}{r}\right)\frac{dK(r,\theta)}{d\theta}\sim\exp\left(\frac{1-ire^{i\theta}}{\varepsilon}\right)\frac{\sqrt{\pi N}\,(2N\varepsilon/e)^{2N}}{(ire^{i\theta})^{2N+1}}. \tag{2.30}$$

Before carrying out the next step of the procedure, we must express the optimal truncation point which soon will be furnished in terms of the polar coordinates explicitly using (2.10) for $\Im(z)>0$, that is

$$N(r,\varepsilon)\sim\frac{r}{2\varepsilon}, \tag{2.31}$$

in which the remainder takes its minimum value. To ensure that N is an integer, we take $N=r/\varepsilon+\alpha$ where $0\leq\alpha<1$, and round N to the closest integer. The behaviour of the remainder in the limit as ε goes to zero and N goes to infinity is important. Therefore, putting this value of N in the remainder equation (2.30) gives

$$-\varepsilon^2\frac{e^{-2i\theta}}{r^2}\frac{d^2K(r,\theta)}{d\theta^2}+\left(\varepsilon^2\frac{ie^{-2i\theta}}{r^2}+2\varepsilon\frac{e^{-i\theta}}{r}\right)\frac{dK(r,\theta)}{d\theta}\sim\frac{\sqrt{2\pi}}{2\sqrt{r\varepsilon}}\frac{\exp\left(-\dfrac{ire^{i\theta}}{\varepsilon}+\dfrac{1-r}{\varepsilon}-2\alpha\right)}{\exp\left(\left(i\theta+i\frac{\pi}{2}\right)\left(\frac{r}{\varepsilon}+2\alpha+1\right)\right)}. \tag{2.32}$$

The RHS is exponentially small and so it is negligible except on the relevant values of θ, i.e., $\pi/2$ in which the RHS takes its maximal value. In fact, Stokes line lies along $\pi/2$. Detailed derivation of this line as well as what happens on it will be discussed in §2.7 with more details. The behaviour of the remainder, however, will be examined in the vicinity of this line in this section. In order to do so, let us rescale θ near $\pi/2$ such that

$$\theta=\frac{\pi}{2}+\delta\widehat{\theta}, \tag{2.33}$$

where the small parameter $\delta\ll1$ which is a function of ε to be derived shortly.

Plugging (2.33) immediately into (2.32) yields

$$\frac{\varepsilon^2\exp(-2i\delta\widehat{\theta})}{r^2\delta^2}\frac{d^2K(r,\widehat{\theta})}{d\widehat{\theta}^2}-\frac{i\varepsilon^2\exp(-2i\delta\widehat{\theta})}{r^2\delta}\frac{dK(r,\widehat{\theta})}{d\widehat{\theta}}-2\frac{i\varepsilon\exp(-i\delta\widehat{\theta})}{r\delta}\frac{dK(r,\widehat{\theta})}{d\widehat{\theta}} \sim \frac{\sqrt{2\pi}}{2\sqrt{r\varepsilon}}\frac{\exp\left(\frac{re^{i\delta\widehat{\theta}}}{\varepsilon}+\frac{1-r}{\varepsilon}-2\alpha\right)}{\exp\left(\left(i\delta\widehat{\theta}+i\pi\right)\left(\frac{r}{\varepsilon}+2\alpha+1\right)\right)}, \quad (2.34)$$

as ε and δ approach zero. After expanding for sufficiently small δ, the RHS of (2.34) becomes

$$\text{RHS of (2.34)} \sim -\frac{i\sqrt{2\pi}}{2\sqrt{r\varepsilon}}\exp\left(-\frac{r\delta^2\widehat{\theta}^2}{2\varepsilon}\right)\exp\left(\frac{1}{\varepsilon}-2\alpha-2i\alpha\delta\widehat{\theta}-i\delta\widehat{\theta}\right). \quad (2.35)$$

Seeking the exact scaling of δ in terms of ε, the exponential term of (2.35) suggests that it should be

$$\delta=\sqrt{2\varepsilon}, \quad (2.36)$$

which is the same as that in the previous section. Upon using (2.36) in (2.34), it is seen that the dominant term of the LHS of (2.34) is the third term. Therefore, after completing the required simplifications, we obtain in leading order that

$$\frac{dK(r,\widehat{\theta})}{d\widehat{\theta}}\sim\frac{i\sqrt{\pi r}}{2\varepsilon}\exp\left(-r\widehat{\theta}^2\right)\exp\left(\frac{1}{\varepsilon}-2\alpha\right). \quad (2.37)$$

Direct integration of (2.37), hence, gives

$$K\left(r,\widehat{\theta}\right)=\frac{i\pi}{4\varepsilon}\exp\left(\frac{1}{\varepsilon}-2\alpha\right)\left(k-\text{erf}\left(\sqrt{r}\widehat{\theta}\right)\right), \quad (2.38)$$

where k is a constant and $\text{erf}(z)$ is the error function. We observe the jump in K emerging when we cross the Stokes line, $\pi/2$, which is obtained as

$$K\left(\frac{\pi}{2}^-\right)-K\left(\frac{\pi}{2}^+\right)=\frac{i\pi}{2\varepsilon}\exp\left(\frac{1}{\varepsilon}-2a\right). \quad (2.39)$$

Thus, determination of $K(r,\theta)$ as well as the jump in the multiplier $K(r,\theta)$ of the remainder $R(r,\theta)$ occurring beyond the Stokes lines is completed via an error function which is typical in exponential asymptotics. In the following sections we undertake the residue calculation of the differential equation and observe the branch points, prior to conducting the Stokes lines analysis.

2.6 Analysing the model problem by residues

In this section, we apply the method of variation of parameters to study (2.1). Once we find the general solution of (2.1), we adopt the residue technique and then evaluate the integrals. Suppose that we return to (2.1) whose homogeneous solution is

$$y_h(z) = C_1 \exp\left(\frac{iz}{\varepsilon}\right) + C_2 \exp\left(-\frac{iz}{\varepsilon}\right).$$

The particular solution of (2.1) calculated by employing the variation of parameters method [67] is

$$y_p(z) = -\frac{\cos\left(\frac{z}{\varepsilon}\right)}{\varepsilon}\int^z \frac{\sin\left(\frac{t}{\varepsilon}\right)}{1+t^2}dt + \frac{\sin\left(\frac{z}{\varepsilon}\right)}{\varepsilon}\int^z \frac{\cos\left(\frac{t}{\varepsilon}\right)}{1+t^2}dt.$$

Then, the general solution becomes

$$\begin{aligned} y_G(z) = C_1\cos\left(\frac{z}{\varepsilon}\right) + C_2\sin\left(\frac{z}{\varepsilon}\right) - \frac{\cos\left(\frac{z}{\varepsilon}\right)}{\varepsilon}\Im\left(\int_{-\infty}^z \frac{\exp\left(\frac{it}{\varepsilon}\right)}{1+t^2}dt\right) \\ + \frac{\sin\left(\frac{z}{\varepsilon}\right)}{\varepsilon}\Re\left(\int_{-\infty}^z \frac{\exp\left(\frac{it}{\varepsilon}\right)}{1+t^2}dt\right). \end{aligned} \tag{2.40}$$

The integrand could be written in terms of the special function exponential integral, which we discuss in §4, as

$$\int_{-\infty}^z \frac{\exp(it/\varepsilon)}{1+t^2}dt = \frac{i\exp(-1/\varepsilon)}{2}\mathrm{Ei}\left(\frac{-1-iz}{\varepsilon}\right) - \frac{i\exp(1/\varepsilon)}{2}\mathrm{Ei}\left(\frac{1-iz}{\varepsilon}\right), \tag{2.41}$$

where the exponential integral $\mathrm{Ei}(z) = \int_{-\infty}^{z} \exp(t)/t\,dt$ as described in [68] is a multi-valued function and has a branch point at the origin. Hence, (2.41) has branch points at $z = \pm i$; whereby, one of the corresponding branch cuts lies above the imaginary axis from $z = i$, while the other lies on the imaginary axis below $z = -i$. We compute (2.40) employing the residue theorem [69], which states that

$$\oint_{\gamma} f(z)dz = 2\pi i \sum_{j=1}^{m} \operatorname*{Res}_{z=z_j} f(z),$$

where $z_1, \ldots, z_m$ are the poles contained inside a closed contour γ, and the contour γ encloses the multiple poles. Herein, $\operatorname*{Res}_{z=z_j} f(z)$ symbolises the residue of $f(z)$ at z_j with the definition of

$$\operatorname*{Res}_{z=z_j} f(z) = \lim_{z \to z_j} (z - z_j) f(z).$$

Consider the contour integral:

$$\oint_{C} \frac{\exp(iz/\varepsilon)}{1+z^2} dz.$$

Herein C is the contour which goes along the real line $-R$ to R and then counter-clockwise on a semicircle of radius R centred on the origin in the upper-half plane returning to $-R$. As the function $\exp(iz/\varepsilon)$ is exponentially small for $R \to \infty$ and the coefficient of iz is $1/\varepsilon > 0$, the contour C is taken in the upper-half plane, see Jordan's Lemma in [70]. Assuming $R > 1$, then, assures that the imaginary part i will be in the curve. Since $\exp(iz/\varepsilon)$ does not have a singularity, we are only going to look at $1 + z^2$ which has singularities at both $z = \pm i$. As we work on the upper-half plane, only the singularity "i" lies in the region enclosed by C. That is, the function has a pole of order 1 at $z = i$. Therefore, the residue at $z_0 = i$ under the light of residue formula [69] is

$$\operatorname*{Res}_{z_0=i} f(z) = \frac{\exp(-1/\varepsilon)}{2i}, \tag{2.42}$$

which using the residue theorem yields

$$\oint_C \frac{\exp(iz/\varepsilon)}{1+z^2}dz = 2\pi i \operatorname*{Res}_{z_0=i} \frac{\exp(iz/\varepsilon)}{1+z^2} = \pi \exp(-1/\varepsilon). \tag{2.43}$$

Separating the contour integral into a line and an arc, then plugging into the left hand side of (2.43) gives

$$\int_{-R}^{R} \frac{\exp(iz/\varepsilon)}{1+z^2}dz + \int_{\gamma} \frac{\exp(iz/\varepsilon)}{1+z^2}dz = \oint_C \frac{\exp(iz/\varepsilon)}{1+z^2}dz = \pi \exp\left(-\frac{1}{\varepsilon}\right), \tag{2.44}$$

where γ is a semicircle whose radius is R on the upper-half plane. Here the second part of the separated integral (2.44) meets zero as R approaches infinity. That is,

$$\lim_{R\to\infty} \int_{-R}^{R} \frac{\exp(iz/\varepsilon)}{1+z^2}dz = \pi \exp\left(-\frac{1}{\varepsilon}\right). \tag{2.45}$$

Using Euler's formula then shows that

$$\int_0^{\infty} \frac{\cos(z/\varepsilon)}{1+z^2}dz = \frac{1}{2}\pi \exp\left(-\frac{1}{\varepsilon}\right) \quad \text{and} \quad \int_{-\infty}^{\infty} \frac{\sin(z/\varepsilon)}{1+z^2}dz = 0. \tag{2.46}$$

Back substitution of these values of (2.46) into (2.40) for large z enables us to derive the general solution of (2.1) by means of

$$y_G(z) = C_1 \cos\left(\frac{z}{\varepsilon}\right) + C_2 \sin\left(\frac{z}{\varepsilon}\right) + \frac{\sin(z/\varepsilon)}{\varepsilon}\pi \exp\left(-\frac{1}{\varepsilon}\right). \tag{2.47}$$

Since error function $|\mathrm{erf}(z)| \approx 1$ for large z, the rightmost term of (2.47) is consistent with the rightmost term of (2.23).

In the next section, the investigation of the Stokes and anti-Stokes lines will be discussed in detail. Crossing the Stokes lines causes subdominant exponentially small terms to appear and disappear smoothly. Therefore, having them located in the complex plane will enable us to demonstrate where these exponential terms are present

in different sectors of the z-plane.

2.7 Stokes phenomenon

Once the singularities of the expansion are located, we expect to find the Stokes lines arising from them. Hence, our goals in this section are firstly to obtain the Stokes and anti-Stokes lines, secondly to demonstrate the existence of the Stokes lines with the aid of an illustration on a figure, and thirdly to show which exponentials are present in which region of the complex plane. To show the existence of the Stokes phenomenon, it is sufficient to identify the exponential terms of the equation (2.1), which are to be determined by the consideration of the singularities. We note although this thesis does not use the Borel plane technique, the key criterion for a Stokes phenomenon to occur is that two singularities in the Borel plane should be lying on the same Riemann sheet, and equivalently they must be adjacent to each other. If these singular points are not adjacent, then they are on the different Riemann sheets; that is, a new asymptotic contribution across the lines this change happens does not occur. Therefore, the Stokes line is inactive. For further discussions, see [39, 71]. On the other hand, more details of determining the Stokes lines can be found in §3.3. Stokes lines appear when the exponential prefactors of the expansion, $\exp(-u_i(z))$, fulfil the following condition [30]

$$\Im(u_i(z)-u_j(z))=0 \quad \text{while} \quad \Re(u_i(z)-u_j(z))>0, \ \text{ for } i,j\in\{1,2,3\}, \tag{2.48}$$

which may equivalently be written as

$$u_i(z)-u_j(z)>0 \qquad \text{for } z\in\mathbb{C}, \ \text{ and } \ \text{for } i,j\in\{1,2,3\}, \tag{2.49}$$

where $i\neq j$. In this problem, $u_{2,3}(z)$ correspond to the powers in the exponential terms of complementary functions, and $u_1(z)$ corresponds to the power in the exponential term of the particular integral. These will be introduced shortly. When the

real part of (2.48) is less than zero it is called an irrelevant Stokes line, since the subdominant exponential can not switch the dominant exponential on. In the terminology of [39], irrelevant Stokes lines are the lines taking a place between the saddles; whence, Stokes lines are active, but irrelevant. Generally, a differential equation of the remainder appears as in (3.12). Likewise, the anti-Stokes lines appear when

$$\Re(u_i(z) - u_j(z)) = 0, \quad \text{for } i, j \in \{1,2,3\}, \tag{2.50}$$

where $i \neq j$. Carrying on, the homogeneous solution of (2.1) is

$$y(z) \sim C_1 \exp\left(\frac{iz}{\varepsilon} - \frac{1}{\varepsilon}\right) + C_2 \exp\left(-\frac{iz}{\varepsilon} - \frac{1}{\varepsilon}\right), \tag{2.51}$$

where C_1 and C_2 are constants. It is important to note that we have $\exp(-1/\varepsilon)$ terms in the solution because the leading order term of the expansion is singular at $-i$ and i. In addition, it is worth mentioning that the solution of (2.1) could be derived by the WKB method [67]. Using the RHS of the differential equation (2.1), all three associated distinct exponential terms are identified by

$$\exp(0), \quad \exp\left(-\frac{i(-z-i)}{\varepsilon}\right) \quad \text{and} \quad \exp\left(-\frac{i(z-i)}{\varepsilon}\right), \tag{2.52}$$

where the related $u_{1,2,3}(z)$ terms are

$$u_1(z) = 0, \quad u_2(z) = \frac{i(-z-i)}{\varepsilon} \quad \text{and} \quad u_3(z) = \frac{i(z-i)}{\varepsilon}. \tag{2.53}$$

It should be emphasised once again that it is crucial to determine which of these exponentials are present in which sectors of the complex plane as they appear and disappear when the active Stokes lines are crossed. Having been able to derive the three exponentials, presence of the Stokes and anti-Stokes lines may now be found by making use of the above definitions. Employing (2.48) first for $u_1(z)$ and $u_2(z)$ terms

$$\Im\left(\frac{i(-z-i)}{\varepsilon}-0\right)=0 \qquad \text{while} \qquad \Re\left(\frac{i(-z-i)}{\varepsilon}-0\right)>0, \tag{2.54}$$

tells us that the Stokes line occurs when

$$x=0 \qquad \text{while} \qquad y>-1, \tag{2.55}$$

where $z=x+iy$. In particular, this means that subdominant $\exp(-u_2(z))$ term may be turned on by $\exp(0)$ when the Stokes line is crossed, and become dominant at the anti-Stokes lines. This changing happens smoothly by the error function as obtained and discussed previously. Similarly, taking (2.50) into account

$$\Re\left(\frac{i(-z-i)}{\varepsilon}-0\right)=0, \tag{2.56}$$

requires that the anti-Stokes line occurs when

$$y=-1. \tag{2.57}$$

Moreover, employing (2.48) for $u_1(z)$ and $u_3(z)$ terms

$$\Im\left(\frac{i(z-i)}{\varepsilon}-0\right)=0 \qquad \text{while} \qquad \Re\left(\frac{i(z-i)}{\varepsilon}-0\right)>0, \tag{2.58}$$

tells us that the relevant Stokes line takes place when

$$x=0 \qquad \text{while} \qquad y<1, \tag{2.59}$$

where $z=x+iy$. That is, $\exp(0)$ turns the $\exp(-u_3(z))$ term on, as the Stokes line is crossed on the complex plane. Likewise, performing (2.50) requires that the anti-Stokes line occurs when

$$y=1. \tag{2.60}$$

Locating the anti-Stokes line shows which exponentials are dominant in which sectors of the complex plane. Subdominant exponential terms grow exponentially up to

anti-Stokes lines then begin decreasing after crossing the lines.

Having verified the conditions of (2.48) and (2.50), the presence of the Stokes and anti-Stokes lines is fully completed. An illustration of these Stokes lines with the contributed exponentials being present or absent are shown in Figure 2.3 which illustrates the overall picture of what happens across these lines. Because there is an overlap between two Stokes lines if both are illustrated together, they are plotted with an offset from $\Re(z) = 0$ to elucidate in one figure.

In Figure 2.3, when we move around the complex z-plane from Sector III toward Sector IV and cross the Stokes line corresponding to red line switch on the exponentially small term $\exp(-u_3(z))$ represented by $\ominus$, where $\ominus$ is singular at $z = i$. Hence, in Sector IV ⓪ and $\ominus$ are present. Moving through Sector I from Sector IV, nothing happens as we have not crossed a Stokes line. While travelling from Sector I to II, there is no inconsistency with having different representations on each side of the branch cut, as the function is discontinuous across the cut. We, therefore, remove the exponential $\ominus$, and so ⓪ is present in Sector II. Similarly, travelling from Sector II to III, nothing gets turned on and off because a Stokes line does not exist. As the travel along the complex plane is completed, we conclude that we return to where we started with ⓪ being present, and end up with the same term. Likewise, similar travel can be done for $\exp(-u_2(z))$ represented by $\oplus$, which is singular at $z = -i$. In that case, regardless of the region we begin, we will come back to where we started due to crossing one Stokes line and one branch cut. To sum up, we observe from Figure 2.3 that the solution has two turning points from which Stokes lines emanate across where a subdominant exponential gets switched on. By these travels, the behaviour of the exponential terms and where they contributed in the complex plane are illustrated in Figure 2.3. We note that in this figure and throughout the thesis, present exponentials of the associated regions are illustrated in the box. In conclusion, having travelled through different sectors, we observe that the exponentially

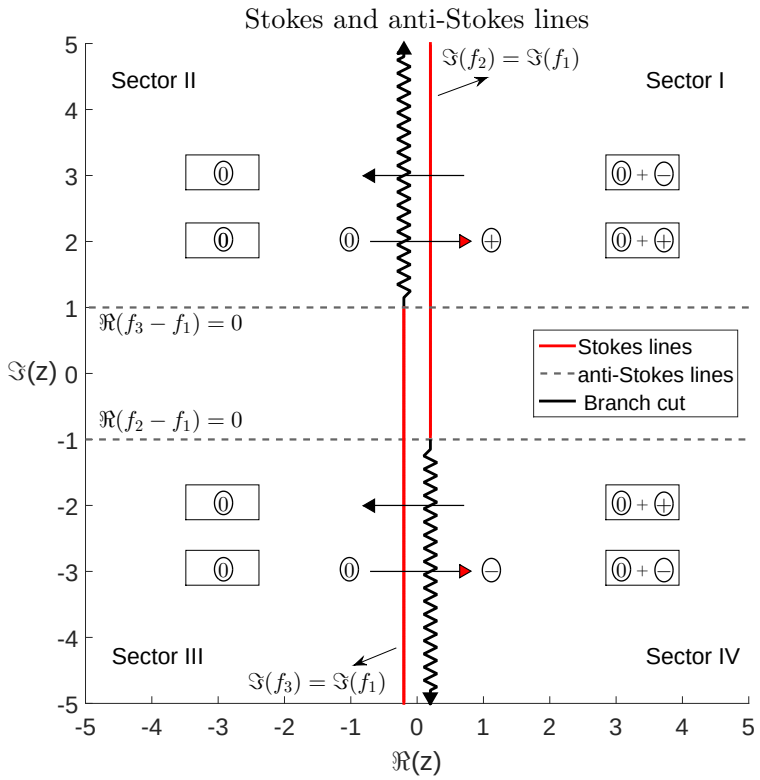


Figure 2.3 Stokes and anti-Stokes lines originating from the singularities $\pm i$ are illustrated, and they are represented by red lines and dashed black lines, respectively. Each exponential terms are allocated ⓞ, ⊕, ⊖ to denote switching on and off, and present exponentials of the associated sectors are shown in the boxes. The exponential on the right hand side of the equation, ⓞ, is present everywhere. Across the Stokes lines, subdominant exponentials are switched on by ⓞ. As the function is discontinuous across the branch cuts represented by the oscillatory lines, one returns to where he started when the travel is completed.

small terms appear and disappear when the Stokes lines are crossed in the complex plane. This switching on and off occurs via error function in the subdominant terms. In fact, this is what Stokes meant by "as it were into a mist" in [72].

2.8 Conclusion

In this chapter, we have studied the asymptotic behaviour of the proposed model problem (2.1) using the method of exponential asymptotics. We summarise the conclusions of this chapter as follows: After deriving the late order term of the expan-

sion, which contained two singularities at $\pm i$, we observed that it is in the form of a factorial-over-a-power, which is a key feature of such systems in exponential asymptotics. In order to study its asymptotic behaviour near the singularities, its series solution has been optimally truncated where the series took its minimum value. We observed that the leading order term of the expansion as well as its asymptotic behaviour changes due to the existence of the singularities in different sectors of the z-plane.

Substituting the truncated series into the differential equation (2.1) has produced a differential equation of the remainder which we have focused on. Since the remainder depends on the optimal truncation point, we have established the exponentially small terms by furnishing this point in the remainder. This result showed that these exponentially small terms cannot be distinguished with Poincaré's asymptotic method. Furthermore, by employing this point, we have minimised the truncation error of the expansion. In other words, the accuracy of the expansion has been improved exponentially by exponential asymptotics. Upon carrying out the process of examination, it has been further deduced that this remainder is exponentially small everywhere except at the Stokes lines.

Investigating the singular points of the differential equation, we have expressed the occurrence of the Stokes and anti-Stokes lines. Having located them, we have considered what happens across these lines. As we travelled along the z-plane, we have observed the switching on and off of the subdominant exponential terms directly each time we crossed the Stokes lines. In fact, the present work has demonstrated that this occurs smoothly via a typical error function. Analysing the remainder differential equation of the expansion in the vicinity of the these singular points has enabled us to obtain this error function. Moreover, we have been able to uncover which exponentials are present in different sectors of the complex plane by keeping track of the contributions from Figure 2.3. Hence, the analysis of present work has

revealed that crossing the active Stokes lines changes the form of the expansion as the subdominant terms appear and disappear in the different regions of the plane.

It is worthwhile to emphasise once more that by investigating the singularities of the presented differential equation, we observed that exponentially small terms are no longer negligible with the technique of exponential asymptotics due to the presence of the singularities. This chapter with the aforementioned results concludes the background information on the exponential asymptotics. This technique of asymptotics beyond all orders with all the arguments taken into account in this chapter will be used throughout the thesis.

Chapter 3

Stokes phenomenon for first order differential equations

The method of exponential asymptotics in this chapter will be considered by analysing a general singularly perturbed differential equation of the first order. Due to its appearance in each level of the hyperasymptotic expansion after the zeroth level for the first order equations, this equation is a special differential equation. Similar to the previous sections, we are interested in its asymptotic behaviour for small ε, and aim to locate the Stokes and anti-Stokes lines of the following equation

$$\varepsilon \frac{dy(z)}{dz} + A(z)y(z) = f(z), \tag{3.1}$$

where $0 < \varepsilon \ll 1$. Through studying this equation, some key features of the hyperasymptotics of this thesis arising from each level will be demonstrated.

The present chapter is organised as follows: The investigation begins with the same structured format as the previous chapter; in detail, we first expand the problem in powers of ε as explained by Hinch in [73] and find the leading order term. Because it is a singular perturbation problem, the series will be divergent and has to be truncated to obtain the minimum error. In order to do so, we first need to find out the general

representation of the late-order terms; hence, the derivation of the general term is our second step in §3.1. We will provide a connection formula between the singulant of the expansion and the pre-factor $A(z)$ function. The optimal truncation point is the point at which the series changes its form from decreasing to increasing. Thus, §3.2 is devoted to truncate the expansion optimally. Substitution of this truncated expansion into the original equation will provide an inhomogeneous equation for the remainder term, which is expected to be exponentially small as indicated by Berry [65]; this will be specifically demonstrated here. In §3.3, we will introduce various choices of $A(z)$ functions. The third step is to inspect the behaviour of the remainder near its singularities, which means that the singulant of the asymptotic expansion in this section will be derived and so the relevant Stokes and anti-Stokes lines based on the pre-factor will be located. Therein, detailed prescriptions which are required for the Stokes phenomenon will be given. In §3.4, we will derive the general first level differential equation of the hyperasymptotics generated by the remainder for general $A(z)$. Finally, the findings of the chapter will be briefly summarised in §3.5.

3.1 Asymptotic power series

In this section, our aim is to express the relationship between the late-order term of the expansion and the pre-factor $A(z)$, by which Stokes and anti-Stokes lines of the equation can be identified. Particularly, deriving this relationship will play a key role in understanding the Stokes structure of the higher levels of hyperasymptotics. Hence, the first step of the investigation of obtaining an accurate approximation is to expand $y(z)$ in powers of ε. Let us suppose the corresponding asymptotic series solution of $y(z)$ in (3.1) is

$$y(z) \sim \sum_{n=0}^{\infty} \varepsilon^n y_n(z). \tag{3.2}$$

Substitution of this solution back into the original differential equation (3.1) and equating like powers of ε generate the leading order equation for $y_0(z)$ at $\mathrm{O}(1)$ and

a recurrence relation for $y_n(z)$ at $\mathrm{O}(\varepsilon^n)$ in the following sense

$$\begin{aligned} A(z)y_0(z) &= f(z), \\ \frac{dy_{n-1}(z)}{dz} + A(z)y_n(z) &= 0 \quad \text{for } n \geq 1. \end{aligned} \tag{3.3}$$

This recurrence relation in (3.3) enables us to compute the general term $y_n(z)$ in terms of $y_0(z)$. Thus, it is important to point out here that zeros of $A(z)$ are the singularities of the leading order term $y_0(z)$, which means they are the singularities of the expansion for all n. Hence, the strength of the singularity or singularities of the expansion increases as n increases. As discussed in the previous chapter, if an asymptotic series solution has a singularity, then the solution is divergent, and this has to be in the factorial-over-a-power nature, which is a generic feature of exponential asymptotics. Therefore, let us assume the late order term takes the form as

$$y_n(z) \sim \frac{\Gamma(n+\gamma)}{u(z)^{n+\gamma}} C \text{ as } n \to \infty, \tag{3.4}$$

in which Γ is the gamma function described in [68, 74], and C is a constant which could be a function of ε and it could be derived by going to the next order of the matching. When we employ this method for example in §4, we will observe that it is indeed a constant. In order to further study the behaviour of the expansion and the Stokes phenomenon, the late order terms has to be generated for large n. Hence, substituting this ansatz into the recurrence relation (3.3) provides us with the following equation after some computations

$$\frac{\Gamma(n+\gamma+1)}{u(z)^{n+\gamma+1}} \left(-u'(z) + A(z)\right) C = 0, \tag{3.5}$$

which requires

$$u'(z) = A(z), \tag{3.6}$$

where prime $'$ represents the derivative d/dz. Due to the relation between $A(z)$ and $y_0(z)$, the integration constant can be derived from the singularities of $y_0(z)$, whilst completing the determination of $u(z)$. Nevertheless, the constant γ in the denominator could be obtained by the repeated use of the recurrence relation from which the degree of the singulant arise, which will be more thoroughly demonstrated later. The link mentioned earlier between the denominator of the expansion and the pre-factor $A(z)$ of (3.1) is finally established; as a consequence, this will be used while locating the Stokes phenomenon of the equation.

3.1.1 Complex ε

This subsection addresses what happens if ε is complex for the equation (3.1). Let us first re-scale

$$\varepsilon = e^{i\theta}\varepsilon_1, \tag{3.7}$$

where ε_1 is real, and $0 < \varepsilon_1 \ll 1$. Substitution of (3.7) into the original differential equation (3.1) gives

$$e^{i\theta}\varepsilon_1 y'(z) + A(z)y(z) = f(z). \tag{3.8}$$

Doing the expansion as $y(z) \sim \sum_{n=0}^{\infty} \varepsilon_1^n y_n(z)$, we match the like powers of ε_1, which yields

$$y_0(z) = \frac{f(z)}{A(z)}, \qquad \text{and} \qquad e^{i\theta} y'_{n-1}(z) + A(z)y_n(z) = 0 \quad \text{for } n \geq 1. \tag{3.9}$$

In order to find the late order terms of the expansion, we employ the 'factorial/power' as in (3.4). In doing this, after some computations, we establish the link between the singulant and the prefactor $A(z)$ as

$$u'(z) = e^{-i\theta}A(z). \tag{3.10}$$

In comparison with (3.6), we express the derivative of the singulant as a multiplication of the prefactor $A(z)$ and $e^{-i\theta}$, as a result of rescaling ε. Hence, the method can be extended to complex ε. We discuss the Stokes phenomenon for complex ε in the Example 3.3.1 of §3.3.

We are interested in determining the general form of the optimal truncation point for this particular equation and then demonstrating whether the remainder is exponentially small. We also study the Stokes and anti-Stokes lines for various $A(z)$ functions in the forthcoming sections.

3.2 Optimal truncation

The next step in the calculation is analysing the equation (3.1) asymptotically by truncating the asymptotic series (3.2) after N terms, that is

$$y(z) = \sum_{n=0}^{N-1} \varepsilon^n y_n(z) + R_N(z), \tag{3.11}$$

where the resultant remainder $R_N(z)$ is of $\mathrm{O}(\varepsilon^N)$. To proceed, substituting the truncated series back into the differential equation (3.1) produces the inhomogeneous remainder differential equation such that

$$\begin{aligned} \varepsilon R_N'(z) + A(z)R_N(z) &= -\varepsilon^N y_{N-1}'(z) \\ &= \varepsilon^N A(z) y_N(z). \end{aligned} \tag{3.12}$$

It is worth commenting that the remainder equation (3.12) has the same form as the original equation (3.1), besides their RHS. The optimal truncation point of the expansion, in its simplest definition, can be found by equating the successive ratio of the RHS of the remainder equation (3.12) in magnitude to one,

$$\left| \frac{\varepsilon^{N+1} A(z) y_{N+1}(z)}{\varepsilon^N A(z) y_N(z)} \right| \sim 1,$$

whereupon it is furnished in the form of "function divided by ε" by

$$N \sim \frac{|u(z)|}{\varepsilon}. \tag{3.13}$$

This means that the minimum number of the terms, N, needed in the expansion depends on ε and z. For any given z, as ε goes to zero, the optimal truncation point increases clearly. Note that α needs to be added to ensure N is an integer,

$$N = \frac{|u(z)|}{\varepsilon} + \alpha, \tag{3.14}$$

where $0 \leq \alpha < 1$. Determination of the optimal truncation point means that the series solution (3.2) does not start to grow until this point. After having derived the truncation point, we find out that the remainder changes its nature from algebraically small as such

$$\mathrm{O}\left(\varepsilon^N\right),$$

to exponentially small. More precisely, employing the truncation point in (3.14) deduces the remainder by means of

$$\begin{aligned} R_N(z) &\sim \varepsilon^N \frac{\Gamma(N+\gamma)}{u(z)^{N+\gamma}} C \\ &\sim \frac{\exp\left(-\left(\dfrac{|u(z)|}{\varepsilon} + \alpha + \gamma - 1\right)\right)}{\sqrt{u(z)}\varepsilon^{\gamma-\frac{1}{2}}} \left(\frac{|u(z)|}{u(z)}\right)^{\frac{|u(z)|}{\varepsilon}+\alpha+\gamma-\frac{1}{2}} \sqrt{2\pi} C. \end{aligned} \tag{3.15}$$

Upon performing Stirling's approximation of gamma function [74], we verify above (3.15) by prefactor $\exp\left(-u(z)/\varepsilon\right)$ that the remainder turns out to be exponentially small as expected. Therefore, examining the truncated remainder equation in its least value enables us to investigate the behaviour of the exponentially small terms. Meanwhile, we further observe that the optimal truncation point obtained in (3.14) occurred exactly the same as in the exponential prefactor of (3.15).

3.3 Stokes structure

In exponential asymptotics, critical points (singularities or turning points) play a key role where Stokes (and anti-Stokes) lines sprout from. Turning point(s) of an asymptotic expansion is a point where the pre-factor $A(z)$ vanishes in which the expansion breaks down since its zeros appear to be the singularities of such an expansion. It could also occur when the RHS of the differential equation has a singularity. For this inhomogeneous equation, the particular integral is the solution which contains an asymptotic expansion. This expansion may generate a Stokes line, and switch on and off the exact homogeneous solution. However, complementary function does not know anything about a particular integral, since there is not a divergent tail from the exact homogeneous solution; therefore, it can not turn the particular integral on. There are several prescriptions for locating these lines:

(i) Stokes lines may be present when $u(z)$ is real and positive, i.e

$$\Im\left(u(z)\right) = 0, \quad \text{and} \quad \Re\left(u(z)\right) > 0,$$

and irrelevant Stokes lines present when $\Re\left(u(z)\right) < 0$ [30, 36, 58, 62],

(ii) Stokes lines occur where the dominant factor of the RHS of the residual equation (3.15) is maximal at $ph(z) = \theta$ [24, 27], [38, pp. 105],

(iii) Stokes lines can be determined by minimising the magnitude of the RHS of (3.15) [6],

(iv) Stokes lines may sometimes be located when the RHS of (3.15) does not depend on α in Olde Daalhuis et al. [27],

(v) Stokes lines arise when the phases of the higher order terms in an expansion are the same [24, 59],

(vi) Anti-Stokes lines arises where $u(z)$ is purely imaginary [36, 57–59], i.e

$$\Re(u(z)) = 0.$$

In this thesis inactive Stokes lines correspond to the irrelevant Stokes lines in which the subdominant exponential can not turn the dominant exponential on. Generally, a differential equation of the remainder appears as in (3.12). In order to examine this type of equation after the zeroth level, we need to rescale the remainder based on its RHS whereupon the RHS becomes 1 in the new equation, which will become apparent in §3.4 and in the later chapters. Therefore, for the following instructive examples, the RHS of (3.1) is set out as $f(z) = 1$. The rest of the chapter discusses the Stokes and anti-Stokes lines of equation (3.1) according to various pre-factor $A(z)$ taking into account of the link derived in (3.6).

Example 3.3.1 *Assume in (3.1) that $A(z)$ is given as $A(z) = z$.*

As indicated earlier, since the Stokes phenomenon of (3.1) is associated with the pre-factor $A(z)$, we begin the determination of the Stokes line of (3.1) for this particular $A(z)$ by first deriving its turning point. The turning point of the expansion (3.2) lies at the origin whereby $A(z) = z$ vanishes for $z = 0$. In order to obtain the singulant $u(z)$ of the late order terms given in (3.4), we perform the formula (3.6). In doing this, after integration, we find

$$u(z) = \frac{z^2}{2} + C_1,$$

in which C_1 is a constant of integration. As explicated above, because $u(z)$ has to vanish at the singular point, it requires C_1 to be zero, whence, the singulant of the late order term is completely derived as

$$u(z) = \frac{z^2}{2}. \tag{3.16}$$

We now have sufficient information to locate the Stokes and anti-Stokes lines. Upon introducing the polar coordinates $z = re^{i\theta}$ and applying them directly into the singulant enable us to write down $u(z)$ in terms of variable θ and r, yielding

$$u(z) = \frac{r^2 \exp(2i\theta)}{2} = \frac{r^2}{2}\left(\cos(2\theta) + i\sin(2\theta)\right). \tag{3.17}$$

Adopting one of the definitions given earlier such as (i) for (3.17) gives that Stokes lines occur whenever θ fulfils the condition

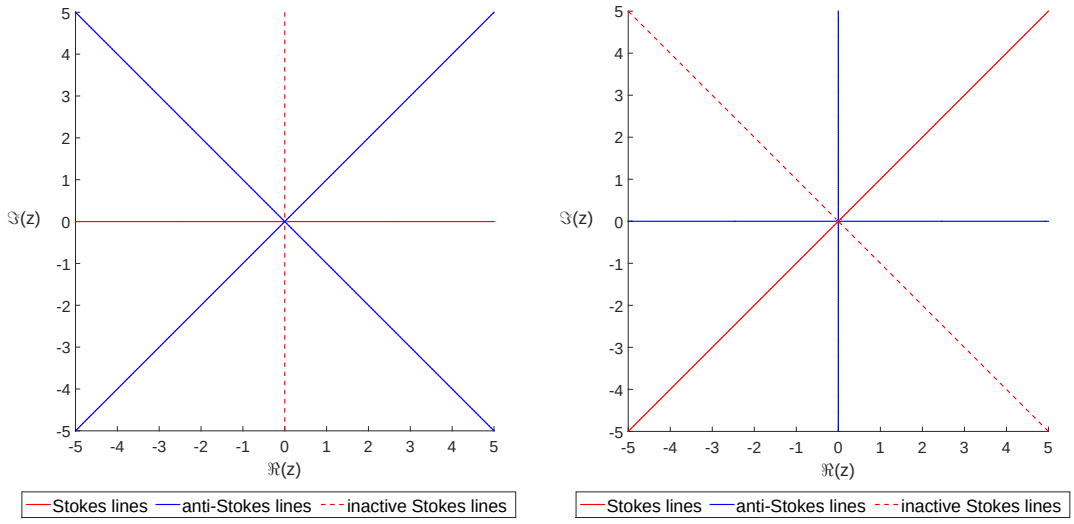
$$\sin(2\theta) = 0 \quad \text{while} \quad \cos(2\theta) > 0. \tag{3.18}$$

Therefore, Stokes lines of the example based upon $A(z)$ present along $\theta = 0$ and π. Inactive Stokes lines lie along $\pi/2$ and $3\pi/2$ in which the RHS of (3.18) is $\cos(2\theta) < 0$. Likewise, the set of points satisfying the condition (vi) is an anti-Stokes line. Considering (3.17) under this condition reads that anti-Stokes lines appear whenever θ satisfies $\cos(2\theta) = 0$. This means they occur along $\theta = \pi/4$, $3\pi/4$, $5\pi/4$ and $7\pi/4$. Both Stokes and anti-Stokes lines are illustrated in Figure 3.1.

Employing the link (3.10) when ε complex, we find the associated singulant for $A(z) = z$ is

$$u(z) = \frac{\exp(-i\theta)z^2}{2}. \tag{3.19}$$

After doing the Stokes lines calculation as above, we do not repeat here for brevity, we find that the associated Stokes lines are rotated as illustrated in the Figure 3.1b, for $\theta = \pi/2$. Hence, the method can be used when ε is complex in this conjecture. On the other hand, it is worth commenting that the solution of the equation (3.1) based on Example 3.3.1, which could be derived by the integration factor method, is from the same family of the error function which is discussed in §5 with more detail.



(a) ε (b) $\varepsilon = -i\varepsilon_1$

Figure 3.1 The red line represents the Stokes lines, and blue lines represent anti-Stokes lines of the equation (3.1) for chosen $A(z) = z$ in Example 3.3.1. When ε complex, Stokes lines picture rotates from Figure 3.1a to Figure 3.1b.

Example 3.3.2 *Suppose in (3.1) that $A(z)$ is given as $A(z) = z^2$.*

In order to give the location of the Stokes and anti-Stokes lines of Example 3.3.2, we can now directly start the investigation by looking at the turning points of the expansion (3.2) for this given $A(z)$. The turning point explicitly occurs at the origin, that is, $A(z) = z^2$ vanishes for $z = 0$. Equation (3.6) implies that the relevant singulant $u(z)$ of the example turns out to be

$$u(z) = \frac{z^3}{3} + C_2,$$

where C_2 is a constant. Since $u(z)$ has to vanish at the singular point, C_2 needs to be zero. Similar to the previous example, applying the polar coordinates into the above singulant produces

$$u(z) = \frac{r^3 \exp(3i\theta)}{3} = \frac{r^3}{3}\left(\cos(3\theta) + i\sin(3\theta)\right), \tag{3.20}$$

where $z = r\exp(i\theta)$. As already discussed, singulant of the expansion presents all the putative Stokes and anti-Stokes lines. Hence, applying the conditions of (i) among the definitions of Stokes lines for (3.20) demonstrates that they appear when

$$\sin(3\theta) = 0 \quad \text{while} \quad \cos(3\theta) > 0.$$

In particular, Stokes lines follow the curve along 0, $2\pi/3$ and $4\pi/3$ whilst the inactive Stokes lines lie along $\pi/3$, π and $5\pi/3$. Likewise, anti-Stokes lines by the condition (vi) may present when θ satisfies $\cos(3\theta) = 0$, which implies they occur along $\pi/6$, $\pi/2$, $5\pi/6$, $7\pi/6$, $3\pi/2$ and $11\pi/6$. Stokes and anti-Stokes lines of this $A(z)$ are shown in Figure 3.2.

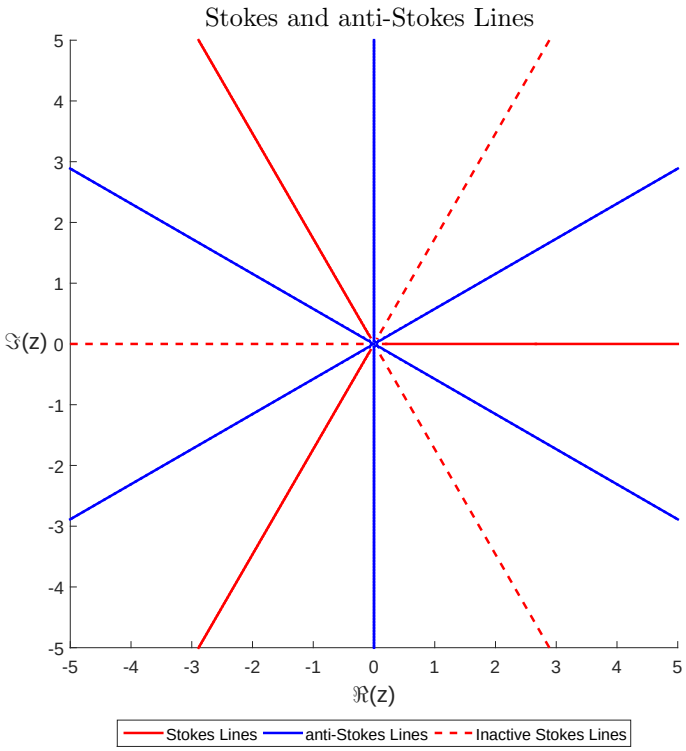


Figure 3.2 Active and inactive Stokes lines of the equation (3.1) are illustrated by the lines in red, while anti-Stokes lines are demonstrated in blue for chosen prefactor $A(z) = z^2$ in Example 3.3.2.

Example 3.3.3 *Assume in (3.1) that $A(z)$ is given as $A(z) = 1 - z^2$.*

We find that the turning points of the expansion (3.2) arise at ± 1 based on the fact that $A(z) = 1 - z^2$ vanishes when $z_{1,2} = \pm 1$. Upon performing the relation (3.6), the relevant singulant for given $A(z)$ is computed as

$$u(z) = z - \frac{z^3}{3} + C_3,$$

in which C_3 is an integration constant. Since $u(z)$ solves the singular points of the expansion, the constant C_3 is obtained as $\pm 2/3$ depending on these points. Substitution completes the derivation by means of

$$u(z) = \begin{cases} z - \dfrac{z^3}{3} + \dfrac{2}{3} & \text{if} \quad z_1 = -1, \\ z - \dfrac{z^3}{3} - \dfrac{2}{3} & \text{if} \quad z_2 = 1. \end{cases} \tag{3.21}$$

As before, we may write out the singulant in terms of the polar coordinates

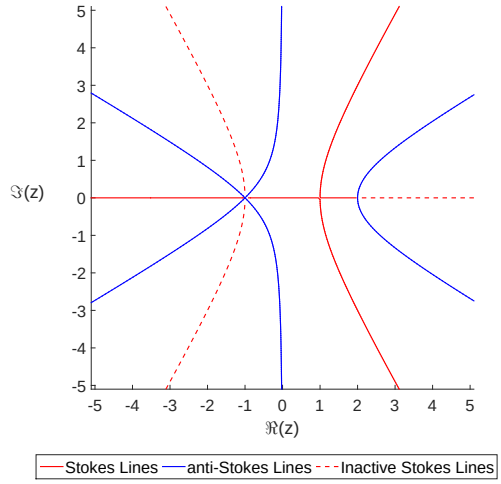
$$\begin{aligned} u(z) &= r\exp(i\theta) - \frac{r^3\exp(3i\theta)}{3} \pm \frac{2}{3} \\ &= r\left(\cos(\theta) - \frac{r^2}{3}\cos(3\theta)\right) \pm \frac{2}{3} + ir\left(\sin(\theta) - \frac{r^2}{3}\sin(3\theta)\right), \end{aligned}$$

where $z = r\exp(i\theta)$. According to the conditions in (i) and in (vi), Stokes and anti-Stokes lines for particular $A(z)$ appear as presented in Figure 3.3a and Figure 3.3b. Their closer view near the relevant singularities occur as in Figure 3.3c and Figure 3.3d. Each singularity of the expansion ± 1 delivers Stokes and anti-Stokes lines.

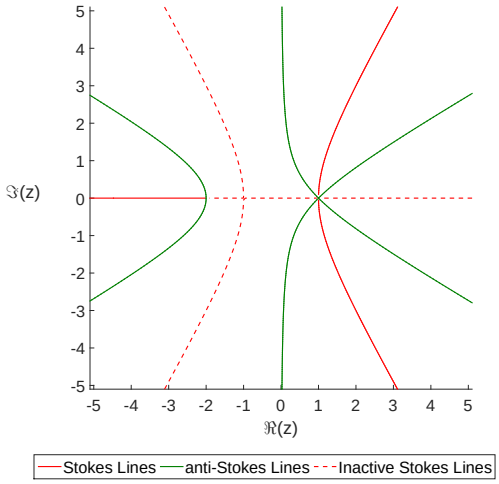
Example 3.3.4 *Suppose in (3.1) that $A(z)$ is given as $A(z) = 1 + z^2$.*

Turning points of the expansion (3.2) for this $A(z)$ are located at $\pm i$ in which $A(z) = 1 + z^2$ vanishes. Using the relationship found in (3.6), we achieve the singulant of this example as

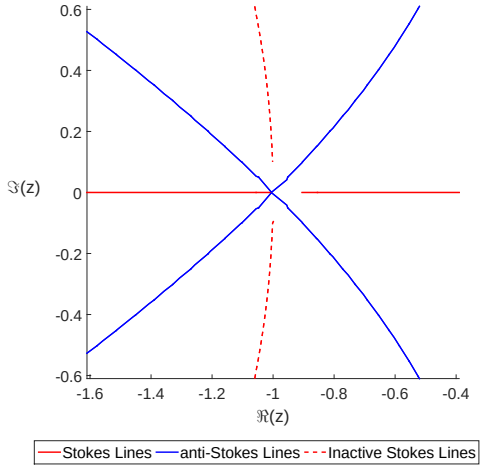
$$u(z) = z + \frac{z^3}{3} + C_4,$$



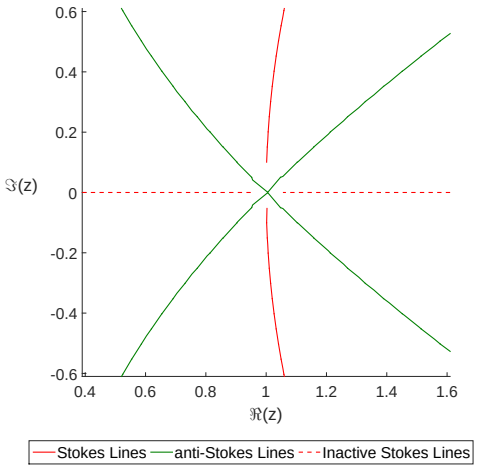
(a) $z = -1$



(b) $z = 1$



(c) $z = -1$



(d) $z = 1$

Figure 3.3 Red lines show Stokes lines of the equation (3.1), blue and green lines show the anti-Stokes lines for the case turning point $z = -1$ and $z = 1$ for $A(z) = 1 - z^2$ in Example 3.3.3, respectively. Figure 3.3c and Figure 3.3d demonstrate the behaviour of the Stokes lines near the turning points. Stokes and anti-Stokes lines of (3.1) behave similar to those in Example 3.3.1.

where C_4 is a constant. Similarly, solving the singulant $u(z)$ subject to singularities $\pm i$ determines the constant C_4 as $\pm 2i/3$. Back substituting these values, we derive the singulant fully as

$$u(z)=\begin{cases} z+\dfrac{z^3}{3}+\dfrac{2i}{3} & \text{if} \quad z_1=-i, \\ z+\dfrac{z^3}{3}-\dfrac{2i}{3} & \text{if} \quad z_2=i. \end{cases} \tag{3.22}$$

The next natural step is to apply the polar coordinates; in doing this, we see that

$$\begin{aligned} u(z) &= r\exp(i\theta)-\frac{r^3\exp(3i\theta)}{3}\pm\frac{2i}{3} \\ &= r\left(\cos(\theta)-\frac{r^2}{3}\cos(3\theta)\right)+ir\left(\sin(\theta)-\frac{r^2}{3}\sin(3\theta)\right)\pm\frac{2i}{3}, \end{aligned}$$

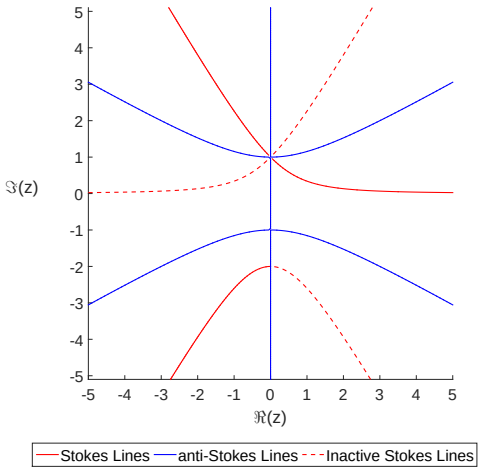
where $z=r\exp(i\theta)$. Based on (i) and (vi), Stokes and anti-Stokes lines are plotted in Figure 3.4. Figure 3.4c and Figure 3.4d delineate a closer view of the lines near the relevant singularities of the example. Moreover, they are plotted together in Figure 3.5 to visually present that they are symmetrical about the x-axis. As the zeroth level of hyperasymptotics is completed, we are now in a position to discuss the first level for general $A(z)$.

3.4 First level of hyperasymptotics for general $A(z)$

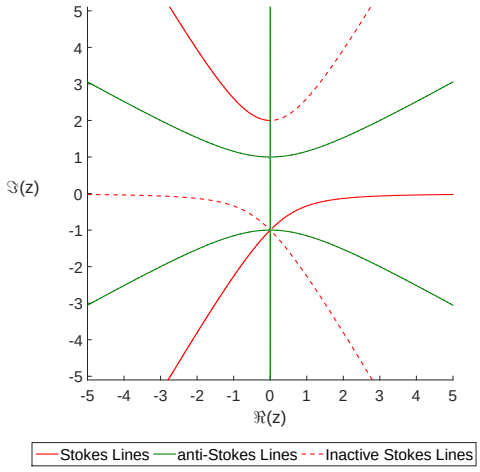
This section aims to establish the inhomogeneous differential equation of the hyperasymptotics in the first level, which we will discuss throughout the thesis, based on the relation obtained in (3.6) for general $A(z)$ generated by the remainder. To do so, our strategy herein, and in every levels of the hyperasymptotics discussed in the thesis, is first to rescale the resultant remainder $R_N(z)$ of level zero according to the RHS of the differential equation (3.12) such that

$$R_N(z)=\varepsilon^N A(z)y_N(z)Q(z), \tag{3.23}$$

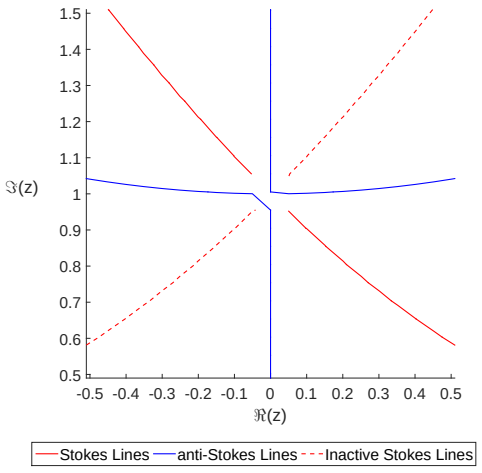
in which $Q(z)$ will be addressed shortly. Let us first assume ν is in the form of $\nu=\varepsilon N$ which is influenced by the truncation point (3.13). The straightforward substitution of (3.23) into (3.12), under the consideration of ν, leads to a singular



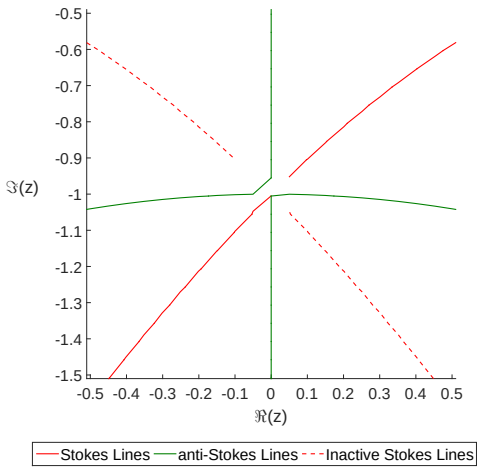
(a) $z = i$



(b) $z = -i$



(c) $z = i$



(d) $z = -i$

Figure 3.4 Red lines show Stokes lines of the equation (3.1), blue and green lines show the anti-Stokes lines originating at $z = i$ and $z = -i$ in Example 3.3.4 for chosen $A(z) = 1 - z^2$, respectively. Figure 3.4c and Figure 3.4d demonstrate the behaviour of the Stokes lines near the turning points. They behave similar to the lines in Example 3.3.1.

differential equation as

$$\varepsilon Q'(z) + \left(u'(z) - \nu \frac{u'(z)}{u(z)} + \varepsilon \frac{u''(z)}{u'(z)} \right) Q(z) \sim 1. \tag{3.24}$$

For ε small, the leading parts of pre-factor of $Q(z)$ in (3.24) is

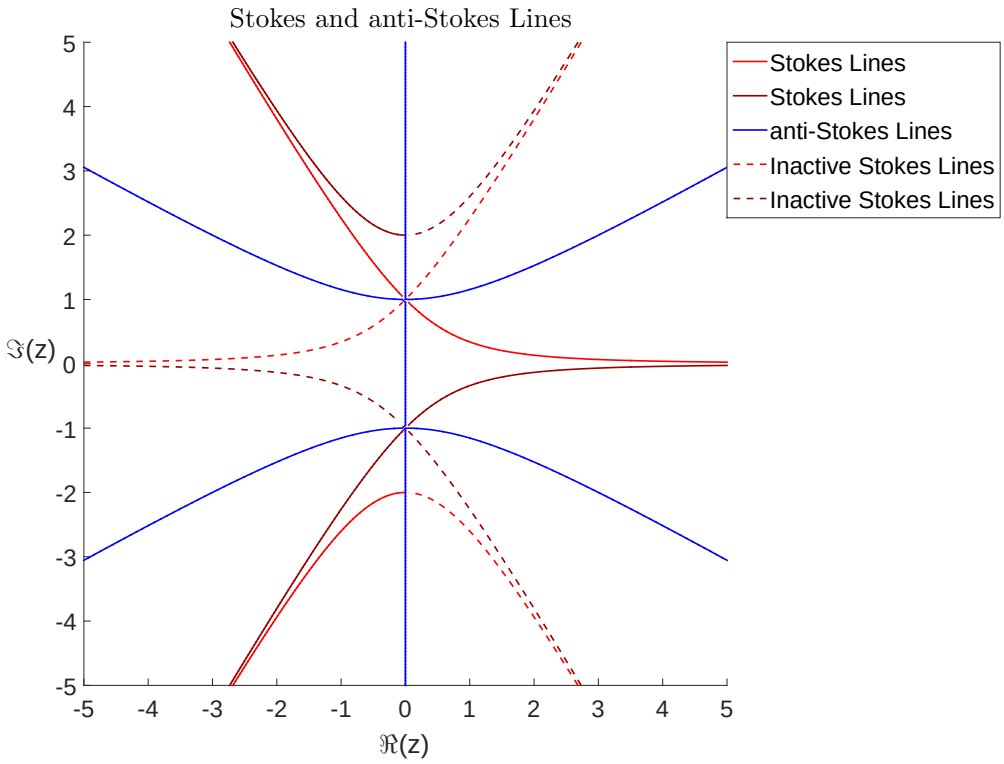


Figure 3.5 For the case turning points $z = i$ and $z = -i$, the figure shows the Stokes and anti-Stokes lines of Example 3.3.4 which are symmetric about x axis.

$$\varepsilon Q'(z) + u'(z)\left(1 - \frac{\nu}{u(z)}\right) Q(z) \sim 1. \tag{3.25}$$

Hence, the first level differential equation which is in the form of (3.1) is established. Therefore, for given $A(z)$ and so its relation with the singulant, we can execute the systematic analysis of hyperasymptotics in the first level upon expansion of $Q(z)$, or directly begin the examination from the first level for either the optimal or arbitrary selection of the truncation point in the zeroth level for the first level differential equations. Although we do not conduct first level analysis in this chapter, we could determine the generic form of the first level singulant for the first order singular differential equations with the formula derived in (3.6). Let us assume the first level singulant of $Q(z)$ is $u_1(z)$. Applying the formula (3.6) in the pre-factor of (3.25) gives the first level singulant as a function of level zero singulant as

$$u_1(z) = u(z) - \nu \ln(u(z)) + c_1, \tag{3.26}$$

where c_1 is an integration constant and can be derived by the singularity of the expansion. It is crucial to note we observe a logarithmic branch cut at the singular points of level zero for the first level of hyperasymptotics. Hence, the preceding level singularity disappears in the succeeding level. For instance, in the case of $u(z) = z$, (3.25) and the singulant (3.26) are equivalent to (4.16) and (4.23) of §4.5, respectively. Therefore, this (3.25) and the associated singulant will indeed be observed and investigated for the every level of the exponential integral in §§4.5, 4.9, 4.10 and for the error function in §5.2.

3.5 Summary

To summarise, through scrutinising the equation in (3.1), we have found the general representation of the optimal truncation point and expressed the relationship obtained in (3.6) between the singulant of the expansion and $A(z)$ function for the first order singular perturbation problem. Throughout the thesis, this relationship will be employed in the higher levels of the hyperasymptotics and clarify the understanding of the Stokes phenomenon. We have determined the Stokes and anti-Stokes lines of the equation emerging from the singular points of the expansion, by examining of the turning points of the expansion in light of various values of pre-factor $A(z)$. In §3.4, the general representation of the inhomogeneous singular differential equation of the resultant reminder (3.25) was determined so that the first level investigation of any differential equation in the form of (3.1) can be done straightaway. Although this will be clearer in the further sections of the thesis, it is important to highlight that a singular differential equation generated by the remainder function in higher levels is a generic feature of the hyperasymptotics studied in this thesis.

Chapter 4

Exponential integral

4.1 Introduction

In this chapter, by applying the methods in exponential asymptotics, we will study another singularly perturbed differential equation depending on a small parameter, ε, in which Stokes and anti-Stokes lines emerge. While inspecting the equation, we will introduce multi-level asymptotics (or hyperasymptotics in the sense of this thesis). Application of this method will enable us to derive an exponentially more accurate approximated solution than that of the superasymptotics [25]. For more details on how to obtain such accuracy or usual hyperasymptotics, see [25, 43] and [47]. The equation to be addressed in the present chapter is

$$\varepsilon \frac{dy(z)}{dz} + y(z) = \frac{1}{z}\,, \qquad y(z) \to 0 \ \text{ as } \ z \to -\infty, \tag{4.1}$$

in which $0 < \varepsilon \ll 1$. In addition to illustrating how a multi-level asymptotics can be performed in a differential equation, we aim to derive the main features which arise in this example.

First, we will describe in detail the technique of hyperasymptotics: as argued in §2, exponential asymptotics deals with the divergent asymptotic expansion which

must be truncated in order to obtain a meaningful approximation. After optimally truncating such divergent series, the truncated remainder of the expansion appears to be exponentially small, and is governed by an inhomogeneous differential equation. In addition to the superasymptotic expansion addressed in §2, the hyperasymptotic approach analyses the differential equation by explicitly considering the remainder of the each level expansion explicitly. This method is based on the re-expansion of the truncated remainder [25]. This process of re-expansion of the remainder can be repeated, and each time it will give a better approximation than the previous level. The objective of the hyperasymptotics, therefore, is to obtain the most accurate result using the optimum number of terms at each level.

Exponential integral can be studied via the differential equation and the integral representation (given in §4.2). Byatt-Smith in [75] studied the exponential integral through the formulation of the hyperasymptotics through the integral representations. Although both methods aim to have an exponentially accurate approximation for the asymptotic expansions, Byatt-Smith uses the integrals by implementing the Laplace's method in each stage. This method is applicable to functions expressible as Stieltjes transforms. It is this point where the method used in this thesis differ from those used by Byatt-Smith. Byatt-Smith uses the change of variables by which the singularity of the integrand transforms moves away from its corresponding point for the integrands. No integral representation is involved in our method. On the other hand, we use the asymptotic expansion technique for approximating the exponential integral, and receive inhomogeneous remainder differential equations for each level. In our case, when we go to the higher levels, singularity of the previous levels approaches to infinity and leading to logarithmic branch cut. Although both the methods inspect the hyperasymptotics by arbitrary truncation points, in our approach we go beyond the first level and study the higher levels and their remainders in terms of truncation points in the preceding stages. We use the 'Factorial/Power' method after the first level to interpret the late order terms. As used widely in the

literature, both methods study the divergence of the asymptotic series, and both express the error estimate exponentially decreases like in Olde Daalhuis [45] when the optimal number of the terms needed for each series increases. Thus, hyperasymptotic expansion is not finite. Moreover, the methods obtain the exponentially smaller error than that given by the successive optimal truncations, however, they do not guarantee that the approximate value converges to the exact values of the exponential integral. Nevertheless, the size of the argument (the width) near the Stokes line doing the smoothing of the error function is same in both techniques.

Stokes and anti-Stokes lines as well as the switching on (and off) behaviour of the subdominant exponentials by the dominant ones can be determined by optimally truncating the divergent series solution of a differential equation near the singularities. These lines play a critical role in exponential asymptotics due to their capacity to impact the switching on (and off) behaviour of the exponentials across the Stokes lines, and their growing by the anti-Stokes lines and ability to become dominant. By locating them, we can uncover the locations where the subdominant contributions are present in the z-plane. These features of the exponentials have already discussed in previous sections of this thesis.

The present chapter is organised as follows: §4.2 is devoted to discussing the equation in (4.1) by direct integration and representing it via an exponential integral function. The essence of the Stokes phenomenon will be addressed through this example by focusing on the method of exponential asymptotics in the remainder of the chapter. The procedure of investigation is similar to previous chapters; for the calculations of this chapter, the same steps of §2 will be repeated from the beginning step by step, which is superasymptotics or equivalently the zeroth level of expansion in hyperasymptotics in §4.3. In §4.4 the Stokes and anti-Stokes lines will be located which will allow us to determine which exponentials are present in different sectors of the complex plane. In §4.5, in addition to the analysis of §2, the minimal remain-

der of the zeroth level will be re-scaled and re-expanded in powers of ε. Therein, the asymptotic series solution of the remainder equation will be truncated optimally and arbitrarily, and its asymptotic behaviour will be analysed near the singularities. We will keep the zeroth level truncation as a free parameter and increase it arbitrarily, and we will investigate how this influences the next level. In §4.6, we will explore the first level error estimate based on zeroth and first level truncation points. We will continue this repeating process of expansion, which for our own purposes we term as hyperasymptotics (multi-level asymptotics), in four levels. Finally in §4.11, we will present relevant conclusions along with discussion.

4.2 Asymptotic behaviour of a differential equation and Stokes phenomenon

Our purpose is to find the approximate solution of this model problem by obtaining the best possible minimum error, and to analyse its asymptotic behaviour by examining the late-order terms, and to locate the Stokes and anti-Stokes lines. Prior to initiating this procedure, let us first solve the equation directly. Using the integration factor method [67] enables us to obtain the exact integral representation of (4.1) which can be represented in terms of the well known special function exponential integral [28, 76] as,

$$\begin{aligned} y(z) &= \frac{\exp\left(-\frac{z}{\varepsilon}\right)}{\varepsilon}\int_{-\infty}^{\frac{z}{\varepsilon}}\frac{\exp(t)}{t}dt + C\exp\left(-\frac{z}{\varepsilon}\right) \\ &= \frac{\exp\left(-\frac{z}{\varepsilon}\right)}{\varepsilon}\mathrm{Ei}\left(\frac{z}{\varepsilon}\right), \end{aligned} \tag{4.2}$$

where C equals zero by the boundary condition at $-\infty$. Because there is a logarithmic singularity at 0 in the above integrand of (4.2), exponential integral has a branch point at the origin [74, 76]. Given the integral representation, repeatedly performing integration by parts method produces the corresponding series solution of the problem such that

$$y(z) = \sum_{n=0}^{N_0-1} \varepsilon^n \frac{n!}{z^{n+1}} + R_{N_0}(z), \tag{4.3}$$

where a singularity exists at $z = 0$ which should be considered in exponential asymptotics. In order to observe subdominant exponential(s) of such an expansion and determine its switching behaviour in the vicinity of the Stokes lines, we need to consider the truncated remainder equation after the series solution is optimally truncated. Hence, in the following section we will attain this investigation procedure for the exponential integral in the zeroth level. In fact, we will repeat expansion and truncation of the remainders process at four levels naively, and therefore our use of hyperasymptotics differs from that found in literature. By successively repeating this process we aim to reduce the error and obtain an exponentially more accurate approximation compared to that attained in the previous stages. At each level of hyperasymptotics, we focus on the singular points of the expansions, as they are going to play central roles for determining the structure of Stokes and anti-Stokes lines and their relevant switching behaviour. However, in the literature, the hyperasymptotic expansion method is mostly employed by using repeated Borel' resummation technique, the integral representation of the factorial terms, to obtain the new expansions in [43]. Another way this method is adopted is demonstrated by Berry and Howls in [71] where they approximate the integrals with saddles based on the steepest descent method in order to study the exponentially small terms or Olde Daalhuis' method in [44] with the similar results obtained in [71] was based on the properties of the Borel-Laplace transform.

4.3 Zeroth level of hyperasymptotics

In this example (4.1), although the late-order terms of the equation were obtained by conducting repeated differentiation, we use the regular perturbation expansion method and then truncate the series solution. We begin solving (4.1) in the usual asymptotical way by expanding it in powers of ε. Let us assume the asymptotic

series solution of (4.1) is

$$y(z) \sim \sum_{n=0}^{\infty} \varepsilon^n y_n(z). \tag{4.4}$$

Since the series solution has to satisfy the differential equation (4.1), we take the first derivative of (4.4) and substitute it back into (4.1). Equating like powers of ε yields the leading-order equation at $\mathrm{O}(1)$

$$y_0(z) = \frac{1}{z}, \tag{4.5}$$

which typically contains a singularity at $z = 0$, and the two term differential recursion equation at $\mathrm{O}(\varepsilon^{n+1})$

$$y_{n+1}(z) + y_n'(z) = 0 \quad \forall \ n \geqslant 0. \tag{4.6}$$

It is worth remarking that the leading order term in (4.5) corresponds to the RHS of the differential equation. In order to solve this recursive relationship, the previous term requires to be differentiated once to derive its successor term. This means that the strength of the singularity increases in each successive term. After recursively performing (4.6), the general term of the expansion is obtained as

$$y_n(z) = \frac{n!}{z^{n+1}} := \frac{\Gamma(n+1)}{u_0(z)^{n+1}} \quad \forall \ n \geqslant 0, \tag{4.7}$$

where the singulant $u_0(z) = z$, and it has a singularity at $z = 0$. This result with the singularity, in fact, is consistent with the general term of (4.3) as determined by successive integration. Deriving this general term, given in (4.7), shows further that the expansion is in the expected factorial divided by function form without the need for performing the factorial-over-a-power method. Before carrying out the procedure of truncation on (4.4), it is important to notice that the series diverges. Upon carrying out the ratio test, we observe that

$$\begin{aligned} \lim_{n\to\infty} \left| \frac{\varepsilon^{n+1} y_{n+1}(z)}{\varepsilon^n y_n(z)} \right| &= \lim_{n\to\infty} \left| \varepsilon^{n+1} \frac{(n+1)!}{z^{n+2}} \frac{z^{n+1}}{\varepsilon^n n!} \right| \\ &= \lim_{n\to\infty} \left| \frac{\varepsilon(n+1)}{z} \right| \ \longrightarrow \infty \quad \text{as } n \longrightarrow \infty. \end{aligned} \tag{4.8}$$

The series (4.4) is unbounded; hence, it diverges for all fixed values of z and ε as anticipated. Interpretation of this series with the usual perturbation method is not useful, because it is divergent. Indeed, in exponential asymptotics, asymptotic series are frequently divergent, since the factorial term in the series increases faster than the whole series in the expansion. Therefore rather than at a fixed point, these series must be truncated where it takes its minimum value to obtain a good approximation. In order to achieve this, let us first introduce a truncated sum of the zeroth level expansion which occurs after $N_0 \gg 1$ terms as

$$y(z) = \sum_{n=0}^{N_0-1} \varepsilon^n \frac{n!}{z^{n+1}} + R_{N_0}(z). \tag{4.9}$$

The remainder $R_{N_0}(z)$ must be exponentially small when the optimal truncation point is determined; hence, analysing the remainder term allows us to work on exponentially small terms. Firstly, taking the first derivative of (4.9) and plugging it back into (4.1), we confirm that the remainder is a solution of the inhomogeneous differential equation

$$\varepsilon R'_{N_0}(z) + R_{N_0}(z) = \varepsilon^{N_0} \frac{N_0!}{z^{N_0+1}}. \tag{4.10}$$

This shows the truncated reminder is in $\mathrm{O}(\varepsilon^{N_0})$ and will be algebraically small in ε if it is not truncated after optimum numbers of terms when N_0 is large and $\varepsilon \to 0$. In order to derive the required optimum number, the RHS of (4.10) must be minimised. In particular, taking the derivative of the RHS of (4.10) with respect to N_0 and equating it to zero for sufficiently large N_0 for small ε, we deduce the value of zeroth level optimal truncation as

$$N_0^{(0)} \sim \frac{|z|}{\varepsilon}, \tag{4.11}$$

which is in the form of "function divided by ε", and the remainder term of the expansion is supposed to be in order $\exp(-|z|/\varepsilon)$. Upon minimising the remainder, we have identified the optimal truncation point $N_0^{(0)}$, the minimum value of the re-

mainder can be obtained by using the known values of z and ε. We alternatively can derive $N_0^{(0)}$ by comparing the successive terms of the series, see (2.9) of §2.3 for details. As it is clear, the optimal truncation point depends on ε, which means as ε approaches to zero the truncation point increases, which is illustrated in Figure 4.1 for three different values of ε. For this level, the error occurring due to truncation is called the "superasymptotic error" [1] which is the magnitude of the first term neglected in the expansion. Hence, the truncation error of the zeroth level is

$$E_{N_0}(z) := \varepsilon^{N_0} \frac{N_0!}{z^{N_0+1}}. \tag{4.12}$$

In Figure 4.1, the error estimate of the expansion decreases at first, and once it reaches its minimum value, it diverges to infinity for both fixed z and ε. Because the truncation point is an integer, it should be added that $N_0 = |z|/\varepsilon + \alpha$ where α is bounded when ε approaches to zero as discussed in (3.14) of §3.2. Utilising the truncation point derived in (4.11) yields

$$E_{N_0}(z) \sim \frac{\sqrt{\dfrac{2\pi|z|}{\varepsilon}}}{z} \exp\left[-\left(\frac{|z|}{\varepsilon}+\alpha\right)\left(1+\ln\left(\frac{z}{|z|}\right)-\frac{\varepsilon}{|z|}\alpha\right)\right], \tag{4.13}$$

in which we use the log function properties for small values of ε and α. Since optimal truncation point $N_0^{(0)}$ varies with $|z|$, this minimum error of the zeroth level is obtained with an exponential accuracy, which follows Stirling's approximation of factorial. Since the optimal truncation point is defined by a magnitude, it is convenient to use polar coordinates and set $z = |z|e^{i\theta}$, where θ denotes the phase of z. Setting $|z| = r$ and varying θ for r fixed change the derivative as described in (2.27) of §2.5. Substitution of this transformation by applying (2.27) into (4.10) allows us to write the remainder differential equation in terms of polar coordinates

$$-\frac{\varepsilon \exp(i(\pi/2-\theta))}{r}\frac{dR_{N_0}(re^{i\theta})}{d\theta} + R_{N_0}(re^{i\theta}) \sim \frac{\varepsilon^{N_0} N_0!}{(r\exp(i\theta))^{N_0+1}}. \tag{4.14}$$

We anticipate that the RHS of (4.14) is exponentially small if (4.9) is truncated optimally; hence, employing the optimal truncation point $N_0^{(0)}$ with Stirling's formula for the factorial term makes the RHS small in exponential

$$\begin{aligned}
&\sim \frac{\varepsilon^{N_0}\sqrt{2\pi N_0}}{(r\exp(i\theta))^{N_0+1}}\left(\frac{N_0}{e}\right)^{N_0} \\
&\sim \sqrt{\frac{2\pi}{r\varepsilon}}\exp\left(-\frac{r}{\varepsilon}-\alpha\right)\exp\left(-i\theta\left(\frac{r}{\varepsilon}+\alpha+1\right)\right),
\end{aligned}$$

as seen from the factor $\exp(-r/\varepsilon)$.

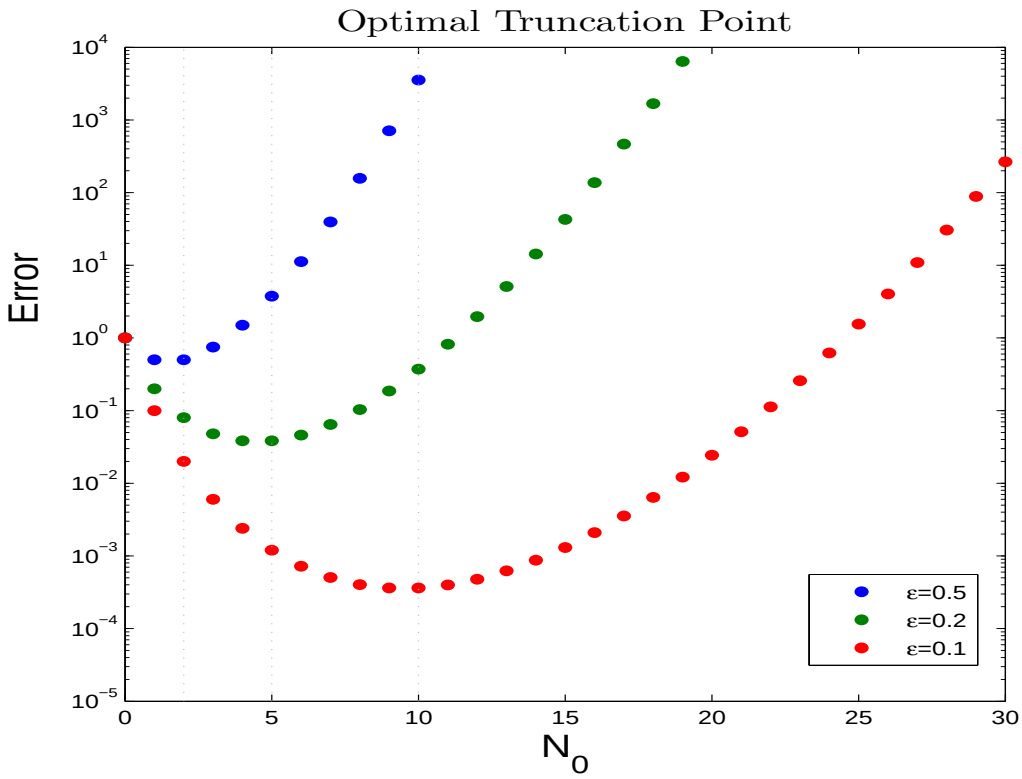


Figure 4.1 Magnitude of the error in (4.12) plotted for $|z| = 1$ while $ph(z) = 60$. The figure denotes the ε dependency of the error and how the optimal truncation point varies as ε varies for a fixed $|z|$. For a selected z and $\varepsilon = 0.1$, the optimal truncation point is $N_0 = 10$, which is consistent with the result in (4.11).

4.4 Stokes and anti-Stokes lines

From (v) of §3, we easily observe that the Stokes line of the level zero expansion lies along $\theta = 0$, where exponentials behave without oscillating. Furthermore, it is also known from §3 that if the late-order terms of the expansion is determined fully, we are able to identify the Stokes and anti-Stokes lines via its singulant $u_0(z)$ [67, 77]. Thus, Stokes lines of the zeroth level can be found when the singulant satisfies

$$\Im(u_0(z)) = 0 \quad \text{and} \quad \Re(u_0(z)) > 0,$$

where $z = x + iy$. This implies that the zeroth level Stokes line lies along

$$y = 0 \quad \text{and} \quad x > 0.$$

This means that Stokes switching occurs along this line. Similarly, an anti-Stokes line can be obtained when the singulant fulfils the condition in (vi) of §3. This implies that the anti-Stokes lines occurs at

$$x = 0.$$

To expand on this, it is important to note the anti-Stokes line is pivotal, as sub-dominant exponentials increase by this line, become dominant as the limit $\varepsilon \to 0$. However, it has no impact on the switching on and off. These effects are presented in Figure 4.2 where the positive real axis is the Stokes lines and the imaginary axis is the anti-Stokes lines. Similar to the steps introduced in §2, we can initiate circuting around the complex plane as the Stokes and anti-Stokes lines are located. This is necessary to pinpoint the appearance and disappearance of the exponentials across the Stokes line. In this figure, the contribution $\exp(-z/\varepsilon)$ and the term $\exp(0)$ on the RHS of the equation are labelled by ① and ⓪, respectively. Let us begin to move from Sector III through Sector IV in a counterclockwise direction with an assumption that ⓪ is present in Sector III. The blue line represents an anti-Stokes line, and

hence no change is observed when we reach Sector IV. Moving upward to Sector I, ① is switched on by ⓪ across the Stokes line; hence, ① and ⓪ are both present in Sector I. From Sector I to Sector II, no switching on or off is observed across the anti-Stokes lines, therefore ① and ⓪ are present in Sector II. Since the exponential integral is discontinuous across the branch cut, there is no inconsistency with having different representations on each side of the cut. Hence, we can say it leads to the removal of the exponential ① while moving downward to Sector III from Sector II. This means that ⓪ is the only exponential present in Sector III which was the assumption made prior to the travel. We reach the initiation sector with the same solution as the travel is complete. Through this travel, we have presented which exponentials are present in which sectors of the z-plane. See Figure 4.2 for details.

The sudden appearance and disappearance (switching on/off) of the subdominant exponentials often happens smoothly via error function. In order to observe this effect, we need to conduct local analysis around the Stokes lines. This calculation is similar to that illustrated in §2.5. Therefore, it is not shown here. Having minimised the error estimate and determined the Stokes lines of the exponential integral in zeroth level, we will now examine the first level of the hyperasymptotics to obtain a better approximation.

4.5 First level of hyperasymptotics

In this section, we present the first level hyperasymptotic expansion for the approximation of the truncated remainder of the zeroth level presented in (4.10). As discussed earlier, the procedure for level one is very similar to that of the zeroth level. The construction of level one starts with re-expansion of the remainder $R_{N_0}(z)$ into a new asymptotic power series. We then truncate the new series, and then analyse it, and finally determine the exponentially small remainder. Although we investigate the equation in a similar fashion, we will keep the zeroth level truncation point as a

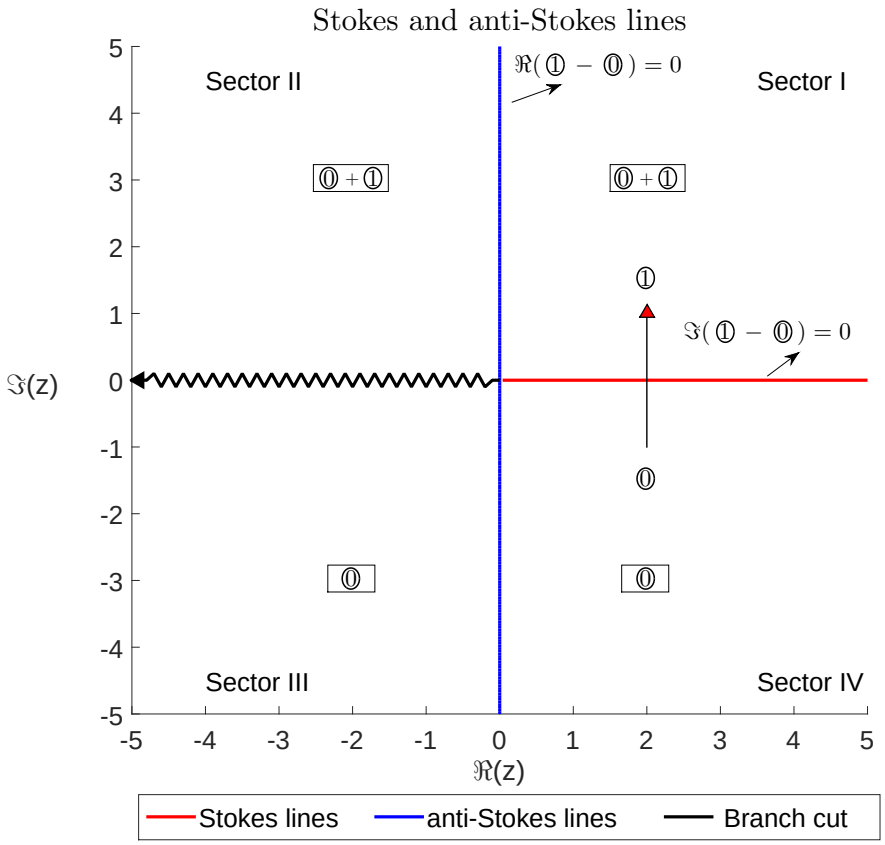


Figure 4.2 The Stokes and the anti-Stokes lines of the zeroth level expansion (4.9) are shown in red and blue, respectively. The Stokes lines across which the subdominant exponential switches on and off are demonstrated. Since exponential integral is discontinuous across the branch cut, ① is not present in Sector III for this travel. The present exponentials of sectors are illustrated in boxes.

free parameter in our hyperasymptotic approach. In the rest of the thesis, we use this approach in our work and discuss how this influences the error estimate. In order to analyse the remainder, the first step in the investigation is to re-scale the original remainder expression according to the RHS of the remainder differential equation (4.10) such that

$$R_{N_0}(z) = \varepsilon^{N_0} \frac{N_0!}{z^{N_0+1}} Q(z), \tag{4.15}$$

where $Q(z)$ is an unknown function of z. Once this equation (4.15) is substituted into the inhomogeneous remainder equation (4.10), we are left with a new singular differential equation for $Q(z)$:

$$\varepsilon \frac{dQ(z)}{dz} + \left(1 - \frac{\nu_0}{z}\right) Q(z) = 1, \tag{4.16}$$

where $\nu_0 \sim N_0\varepsilon$. It is apparent from the pre-factor of $Q(z)$ that singularity of (4.16) appears at $z = \nu_0$. This will be imposed during the derivation of the asymptotic solution for the differential equation. The singular point of the differential equation is illustrated using the contour plot in Figure 4.3. On the other hand, we observe here that (4.16) is in the same fashion with equation (3.1) addressed in §3; thus, it should have similar outcomes. After employing the truncation point N_0, we continue to analyse the equation (4.16) in an asymptotic sense with the same steps carried out for the zeroth level. We begin with the standard form of the perturbation theory where the corresponding asymptotic series solution of (4.16) in powers of ε is

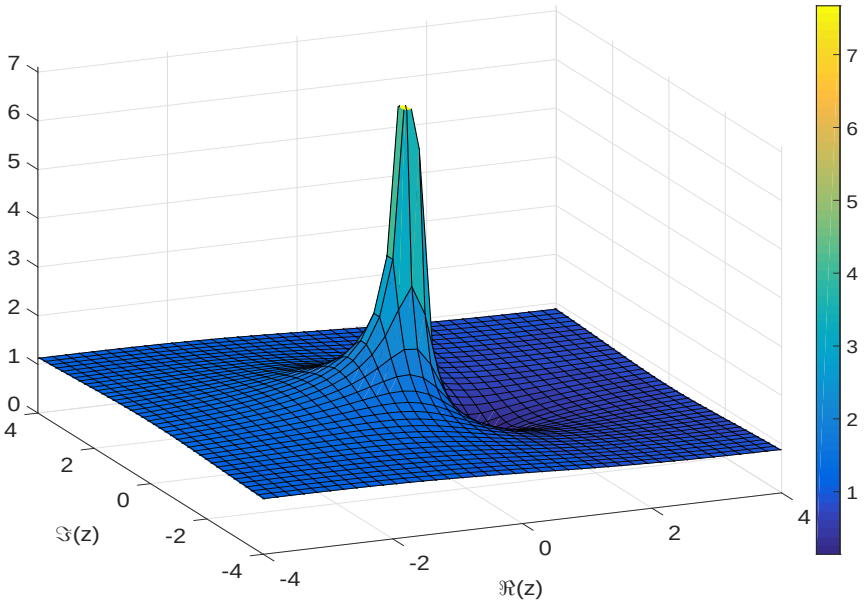
$$Q(z) \sim \sum_{n=0}^{\infty} \varepsilon^n Q_n(z). \tag{4.17}$$

In a similar manner to the previous level, we need to derive $Q_n(z)$ to inspect the asymptotic behaviour of $Q(z)$ in the limit $n \to \infty$. Substituting the series expansion of $Q(z)$ back into the differential equation (4.16) and then equating like powers of ε, we obtain at the leading order $\mathrm{O}(1)$ and at $\mathrm{O}(\varepsilon^n)$, respectively,

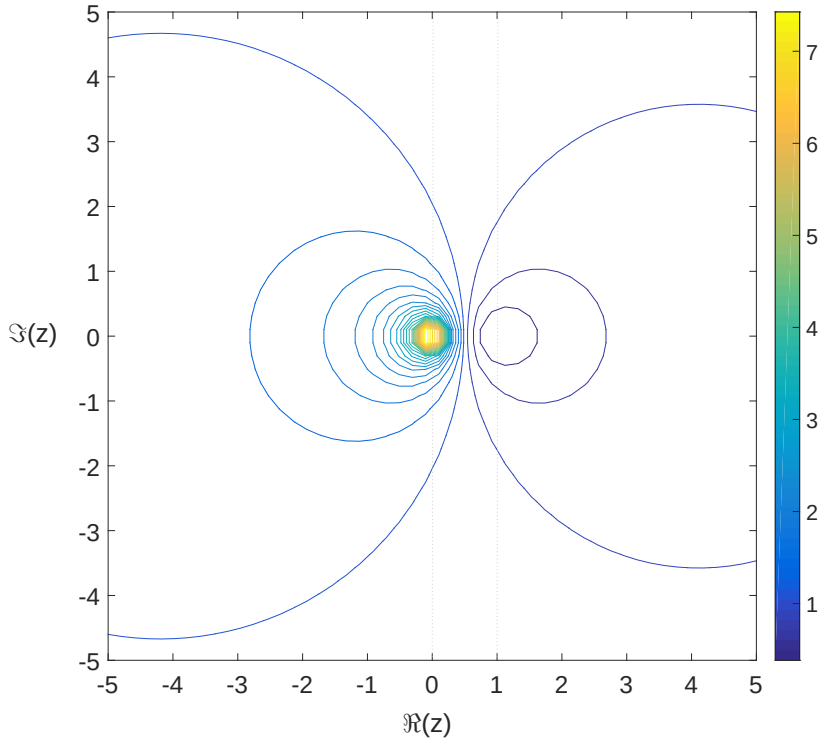
$$Q_0(z) = \frac{z}{z - \nu_0}, \tag{4.18}$$

$$\frac{dQ_{n-1}(z)}{dz} + \left(1 - \frac{\nu_0}{z}\right) Q_n(z) = 0, \qquad \text{for } n \geq 1. \tag{4.19}$$

In zeroth level, the leading order term (4.5) corresponds to the RHS of the original differential equation. However, in this level the leading order is obtained by the prefactor of $Q(z)$ and its zeros. Upon using the above recurrence relationship, $Q_n(z)$ may be determined by using the first derivative of the previous term $Q_{n-1}(z)$ at each further order of the expansion in (4.17). Therefore, all the $Q_n(z)$'s must have a singularity at $z = \nu_0$, since they are generated by $Q_0(z)$ which has a singularity at this point. This indeed means, at each order, the strength of the singularity is going



(a)



(b)

Figure 4.3 Magnitude of the pre-factor of $Q(z)$ in (4.16) in the complex plane and its contour plot for arbitraily chosen $z = 1/2 + i\sqrt{3}/2$ giving $\nu_0 = 1$. The figures clearly show $Q(z)$ is not ubiquitously small in the complex plane. The singular point plays a key role and cannot be ignored, and in this case the singular point is 1. The spike at $z = 0$ represents the singularity of the pre-factor at this point.

to increase by adding 1 to the power of the singularity of the previous term, which ensures the protection of singularity at each level. To establish the optimal truncation point and the Stokes lines, we first need to determine the general representation of the n^{th} term of the expansion for large n. As there is no simple representation for the late order term $Q_n(z)$ by performing the recursive relation successively, the late term can be expressed in the factorial-over-a-power form unlike that shown in §4.3. Hence, it is reasonable to seek a solution of (4.19) in this nature

$$Q_n(z) \sim \frac{\Gamma(n+\gamma_1)}{u_1(z)^{n+\gamma_1}} \left(A_0(z) + \frac{1}{n} A_1(z) + \frac{1}{n^2} A_2(z) + \dots \right) \quad \text{as } n \to \infty, \tag{4.20}$$

where $\gamma_1 = \mathrm{O}(1)$ is an arbitrary constant; and $u_1(z), \gamma_1$, and $A_i(z)$'s are independent of n. Functions $u_1(z)$ and $A_i(z)$ are to be determined. To attain an easy cancellation in (4.20) upon its substitution into (4.19), γ_1 is added as a power of $u_1(z)$ in the denominator to ensure consistency with $\Gamma(n+\gamma_1)$. After taking the first derivative of this ansatz and substituting back into the equation (4.19), we arrive at

$$\frac{\Gamma(n+\gamma_1)}{u_1(z)^{n+\gamma_1}} \left[\left(-u_1'(z) + 1 - \frac{\nu_0}{z} \right) A_0 + \sum_{i=1}^{\infty} \left(\frac{1}{n} \right)^i \left(\left(-u_1'(z) + 1 - \frac{\nu_0}{z} \right) A_i + A_{i-1}' u_1(z) \right) \right] = 0. \tag{4.21}$$

If, here, we use the method of dominant balance for large n, we have

$$-u_1'(z) + 1 - \frac{\nu_0}{z} = 0. \tag{4.22}$$

It is worth remarking that $A_0(z)$ cannot be zero; indeed, if $A_0(z)$ was zero, the rest of $A_i(z)$ would be zero for every i unless (4.22) is satisfied. Solving the derivative (4.22) gives

$$u_1(z) = z - \nu_0 \ln(z) + c_1, \tag{4.23}$$

where c_1 is an integration constant. Since the singularity of $Q_n(z)$ must be the same as the singularity of $Q_0(z)$, $u_1(z)$ has to zero at $z = \nu_0$, that is

$$u_1(v_0) = 0 \implies c_1 = v_0 \ln(v_0) - v_0,$$

which implies the singulant $u_1(z)$ is established as

$$u_1(z) = z - v_0 \ln(z) - v_0 + v_0 \ln(v_0), \tag{4.24}$$

which could equivalently be written in terms of $u_0(z)$ in (4.7) as

$$u_1(z) = u_0(z) - v_0 - v_0 \ln(u_0(z)) + v_0 \ln(v_0). \tag{4.25}$$

The log function must have a branch cut when its argument lies along the negative real axis due to its multivaluedness. Thus, $u_1(z)$ has a branch cut when

$$\Im(z) = 0 \qquad \text{and} \qquad \Re(z) < 0. \tag{4.26}$$

In fact, logarithmic branch cut appears for preserving the zeroth level singularity in the first level equation (4.19); particularly, integration of the pre-factor of $Q(z)$ in (4.19) turns out to be the singulant of the first level expansion. Since the terms in summation in (4.21) is supposed to be zero applying the method of dominant balance, we deduce that

$$A_i'(z) = 0 \implies A_i(z) = C_i \quad \forall \ i,$$

where C_is are constants of direct integration. Hence, the determination of the form of the late-order terms in (4.20) is completed by using the factorial-over-a-power nature. Using this information, the ansatz (4.20) can be written as follows at the leading order

$$Q_n(z) \sim \frac{\Gamma(n+\gamma_1)}{u_1(z)^{n+\gamma_1}} C_0 \quad \text{as } n \to \infty, \tag{4.27}$$

in which γ_1, C_0 are arbitrary constants and they are independent of n. An asymptotic representation of $Q(z)$ is obtained in powers of ε. As the asymptotic expansion given

by (4.17) is divergent, we need to truncate and calculate the required optimum numbers of the terms in order to attain a meaningful approximation prior to investigating the remainder. Thus, our strategy is to substitute (4.27) back into the summation (4.17) and truncate the algebraic expansion after $N_1 \gg 1$ terms,

$$Q(z) \sim \sum_{n=0}^{N_1-1} \varepsilon^n Q_n(z) + \mathscr{R}_{N_1}(z), \tag{4.28}$$

where $\mathscr{R}_{N_1}$ is a remainder and $\mathscr{R}_{N_1} = \mathrm{O}(\varepsilon^{N_1})$. Here, N_1 will be derived at the point where it minimises the remainder of the asymptotic expansion. Taking the first derivative of (4.28) and substituting it into the equation (4.19), we obtain that the remainder is a solution of the inhomogeneous differential equation of

$$\varepsilon \frac{d\mathscr{R}_{N_1}(z)}{dz} + \left(1 - \frac{\nu_0}{z}\right) \mathscr{R}_{N_1}(z) \approx \varepsilon^{N_1} Q_{N_1}(z) \left(1 - \frac{\nu_0}{z}\right). \tag{4.29}$$

Suppose N_1 is the optimal truncation point of (4.28) in the first level such that the remainder $\mathscr{R}_{N_1}(z)$ takes its minimum value. In order to determine such N_1, we minimise the general term of (4.28) for large n, yielding

$$0 = \frac{d}{dn}\left(\varepsilon^n \frac{\Gamma(n+\gamma_1)}{u_1(z)^{n+\gamma_1}} C\right) \implies \ln\left(\frac{\varepsilon(n+\gamma_1)}{u_1(z)}\right) - \frac{1}{n+\gamma_1} \approx 0. \tag{4.30}$$

Then the optimal truncation point, for a large $n \approx N_1$, occurs when

$$\begin{aligned} N_1 &\sim \frac{|u_1(z)|}{\varepsilon}, \\ &= \frac{|z - \nu_0 - \nu_0 \ln(z) + \nu_0 \ln(\nu_0)|}{\varepsilon}, \end{aligned} \tag{4.31}$$

whereby the optimal truncation point of level zero is

$$N_0 \sim \frac{|z|}{\varepsilon}. \tag{4.32}$$

We use the optimal truncation point only when finding the first level optimal error, which corresponds to the blue lines in Figure 4.4. We will keep the truncation point

arbitrary throughout this chapter. Here, for $z = \nu_0$, N_1 is not large; this means, if z is real and if the zeroth level optimal truncation is taken into consideration as $N_0 \sim \nu_0/\varepsilon$, the optimal value of N_1 will not approach to infinity when ε tends to zero. Furthermore, as evident through the rightmost term of the equation (4.29); if $z = \nu_0$, we cannot proceed any further as $z = \nu_0$ stops the analysis. Until now, we have treated z as a real parameter. From now on, z will be treated as a complex parameter. By back-substitution of (4.28) and (4.15) into (4.9), we determine the optimally truncated series of the first level after $N_0 + N_1$ terms is

$$y(z) = \sum_{n=0}^{N_0-1} \varepsilon^n \frac{n!}{z^{n+1}} + \varepsilon^{N_0} \frac{N_0!}{z^{N_0+1}} \sum_{n=0}^{N_1-1} \varepsilon^n Q_n(z) + \varepsilon^{N_0} \frac{N_0!}{z^{N_0+1}} \mathscr{R}_{N_1}(z). \tag{4.33}$$

In comparison to the superasymptotics expansion (4.9), N_1 more terms are added into the expansion; allowing us obtain a higher precision with hyperasymptotics than with superasymptotics. Herein, we define the first level truncation error using (4.33) by

$$\begin{aligned} E_{N_1}(z) :&= \varepsilon^{N_0} \frac{N_0!}{z^{N_0+1}} \mathscr{R}_{N_1}(z) \\ &\sim \varepsilon^{N_0} \frac{N_0!}{z^{N_0+1}} \varepsilon^{N_1} Q_{N_1}(z). \end{aligned} \tag{4.34}$$

Whilst calculating the order of error, the factorial terms are replaced by Stirling's approximation formula, which leads to

$$E_{N_1}(z) \sim \varepsilon^{N_0+N_1} \frac{N_0^{N_0+\frac{1}{2}} N_1^{N_1+\gamma_1-\frac{1}{2}}}{z^{N_0+1} u_1(z)^{N_1+\gamma_1} e^{N_0+N_1+\gamma_1-1}} C_1, \tag{4.35}$$

where $C_1 = 2\pi C$. Rewriting the expression above in terms of ν_1 and ν_0, the next step is then to minimise the magnitude of the error estimate by the conventional method as it is currently in a complex form; specifically, we take its first derivative with respect to ν_1 and ν_0. Since the series is divergent, there is no need to check the sign

of the second derivatives. Hence, after some computations, the derivations yield

$$\begin{aligned}
\frac{d\,|E_{N_1}(z)|}{d\nu_1} &\sim \left| \frac{\nu_0^{\frac{\nu_0}{\varepsilon}+\frac{1}{2}} \nu_1^{\frac{\nu_1}{\varepsilon}+\gamma_1-\frac{1}{2}}\, C_1}{z^{\frac{\nu_0}{\varepsilon}+1} e^{\frac{\nu_0}{\varepsilon}+\frac{\nu_1}{\varepsilon}+\gamma_1-1} \varepsilon^{\gamma_1+1} (z-\nu_0+\nu_0 \ln\left(\frac{\nu_0}{z}\right))^{\frac{\nu_1}{\varepsilon}+\gamma_1}} \left[\ln\left(\frac{\nu_1}{z-\nu_0+\nu_0\ln\left(\frac{\nu_0}{z}\right)} \right) \right] \right|, \\
\frac{d\,|E_{N_1}(z)|}{d\nu_0} &\sim \left| \frac{\nu_0^{\frac{\nu_0}{\varepsilon}+\frac{1}{2}} \nu_1^{\frac{\nu_1}{\varepsilon}+\gamma_1-\frac{1}{2}}\, C_1 \ln\left(\frac{\nu_0}{z}\right)}{z^{\frac{\nu_0}{\varepsilon}+1} e^{\frac{\nu_0}{\varepsilon}+\frac{\nu_1}{\varepsilon}+\gamma_1-1} \varepsilon^{\gamma_1+1} (z-\nu_0+\nu_0 \ln\left(\frac{\nu_0}{z}\right))^{\frac{\nu_1}{\varepsilon}+\gamma_1}} \left(1 - \frac{\nu_1}{z-\nu_0+\nu_0\ln\left(\frac{\nu_0}{z}\right)} \right) \right|,
\end{aligned} \tag{4.36}$$

where $\nu_1 = N_1\varepsilon$. The minimum value of $|E_{N_1}(z)|$ over ν_1 and ν_0 can be obtained by equating each derivative to zero. These imply that the minimum value occurs when

$$\nu_1 \sim \left| z - \nu_0 + \nu_0 \ln\left(\frac{\nu_0}{z}\right) \right|, \tag{4.37}$$

which corresponds to the optimal truncation point of the first level without ε in the denominator computed in (4.31). Minimising the error estimate (4.35) with respect to ν_1, ν_1 is derived as a function of ν_0, whence the error can be written in terms of ν_0 and z. This means, if we set z real and N_0 free parameter, $E_{N_1}(z)$ does not depend on N_0 as seen in Figure 4.4f. Plots in Figure 4.4 and Figure 4.5 show that the first level error decreases as the truncation point of the zeroth level is increased; particularly, this is to say that the error estimate with arbitrary truncation point is less than the first level of hyperasymptotics obtained by the optimal truncation. These figures also illustrate that if the truncation points of the zeroth level are increased arbitrarily, and the phase of z is decreased, the error increases, which is also shown in Table 4.1. In Figure 4.4, the green lines are plotted by substituting the value of ν_1 given in (4.37) into the error estimate. Green lines illustrate the agreement between the plots. Note that as the value of ν_0 increases, it touches the minimum points of the first level figures in black for both optimally and arbitrarily selected truncation points.

Additionally, the figures demonstrate the behaviour of the error depends on the argument of z. Particularly, while it stops at $\theta = 0$ corresponding the Stokes lines,

it increases as we move away from the Stokes lines by the argument of z. See, for example, Figure 4.4f and Figure 4.4a. Equivalently, Figure 4.5 enables us to identify which direction the error declines and to understand the difference of the behaviour of the error in relation to the Stokes lines.

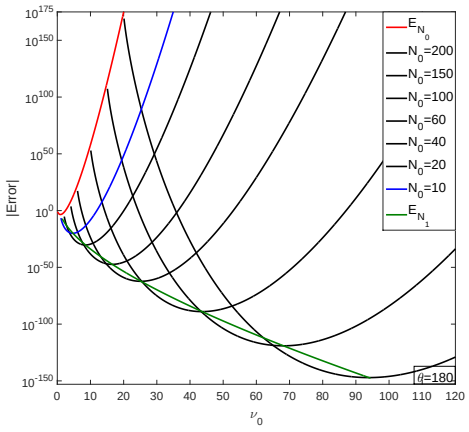
In summary, by considering the first level error (4.35) as a function of truncation points and allowing them to vary, we discovered that the error declines as we increase the zeroth level truncation point. Moreover, expressing the first level truncation point in terms of the zeroth level truncation point upon minimisation as well as increasing it causes the error estimate to converge in theory; see Figure 4.4. However, in practice ν_0 cannot be arbitrarily large. Hence, in the next section, we will inspect the behaviour of the error estimate and discuss this convergence in greater detail. We note that the detailed discussion of the relationship between this method and that of Byatt-Smith [75] on the exponential integral made in the introduction §4.1.

4.6 Error analysis

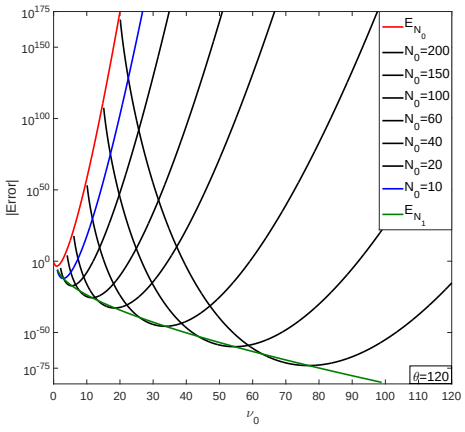
In this section, the error estimate of the first level, given in (4.34), will be examined for different cases in order to test whether there is a complete agreement between the analytical analysis and the Figure 4.4. To recap, the estimate is

$$E_{N_1}(z) \sim \varepsilon^{N_0+N_1} \frac{N_0^{N_0+1/2} N_1^{N_1+1/2}}{z^{N_0+1} u_1(z)^{N_1+1} e^{N_0+N_1}}, \tag{4.38}$$

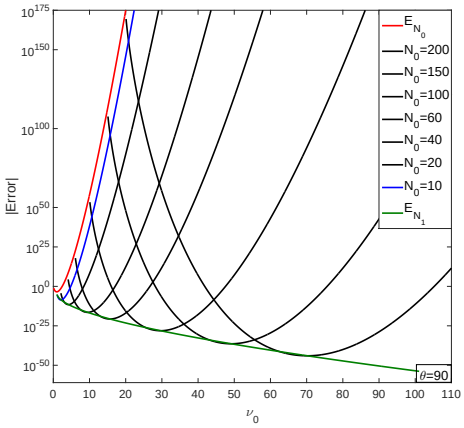
in which $u_1(z) = z - \nu_0 + \nu_0 \ln(\nu_0/z)$. Without loss of generality, the constants of (4.34), i.e. γ_1 and C_1, are taken to be 1 in (4.38). Moreover, to investigate the error,



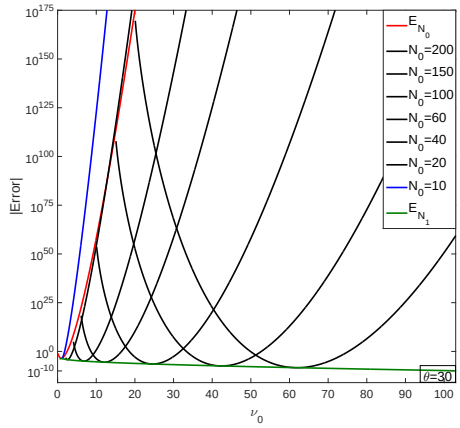
(a) $\arg(z) = \pi$



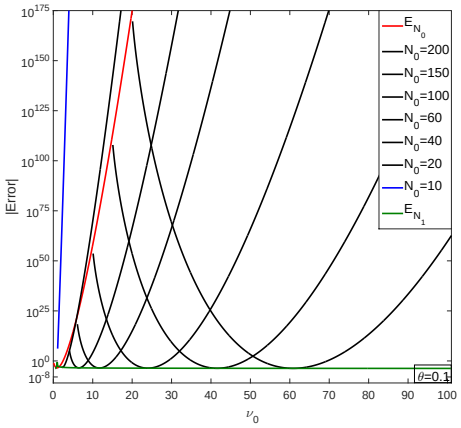
(b) $\arg(z) = \frac{2\pi}{3}$



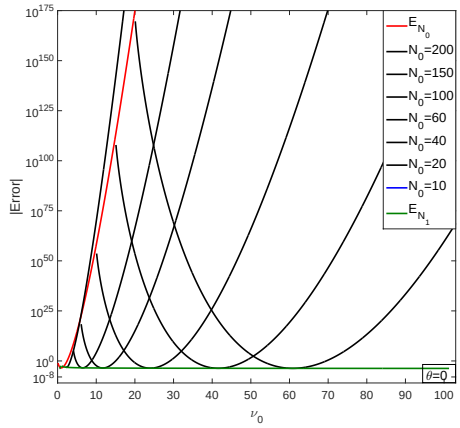
(c) $\arg(z) = \frac{\pi}{2}$



(d) $\arg(z) = \frac{\pi}{6}$

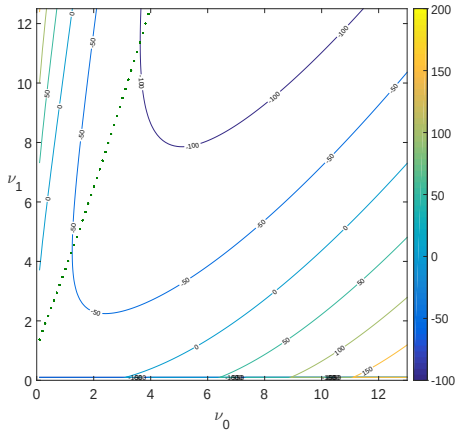


(e) $\arg(z) = \frac{\pi}{1800}$

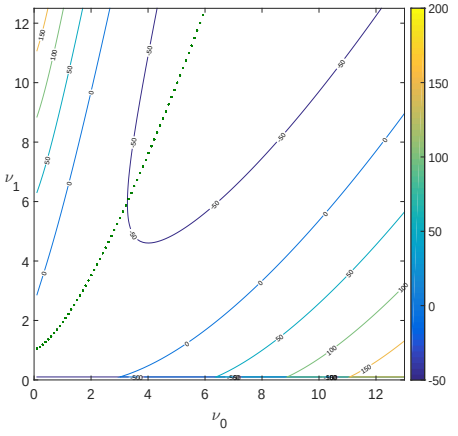


(f) $\arg(z) = 0$

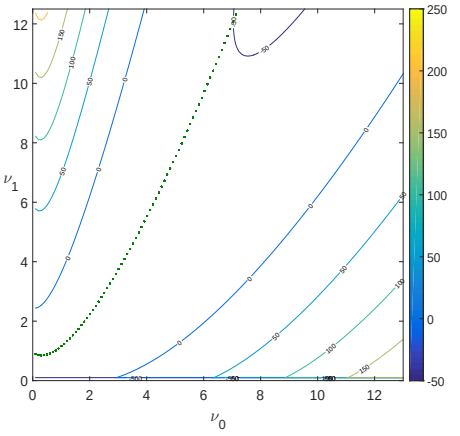
Figure 4.4 Magnitude of the errors (4.12) and (4.34) in 2 levels where the series are truncated optimally, which are represented by red and blue lines, respectiely, the series is truncated arbitrarily at $N_0^i = 20, 40, 60, 100, 150$ and 200, respectiely, which are represented by black lines, at the first level for $\varepsilon = 0.1$ with fixed value of $|z| = 1$ and various values of $\arg(z) = 180, 120, 90, 30, 0.1$ and 0, respectively. The figure further shows the improvement obtained by hyperasymptotics. Green lines demonstrate the behaviour of the first level error (4.34) when it is expressed as a function of ν_0.



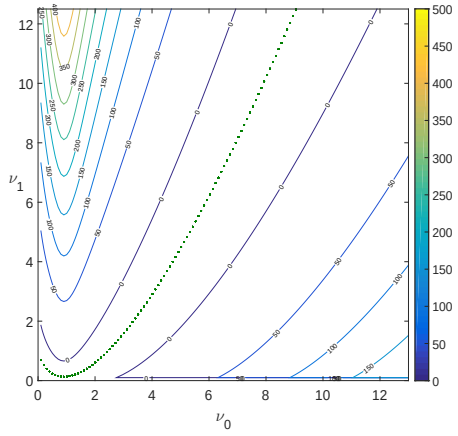
(a) $\arg(z) = \pi$



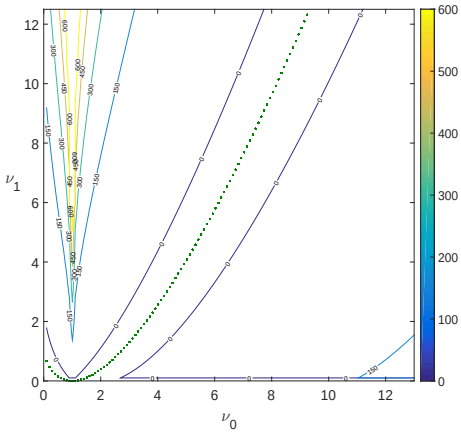
(b) $\arg(z) = \frac{2\pi}{3}$



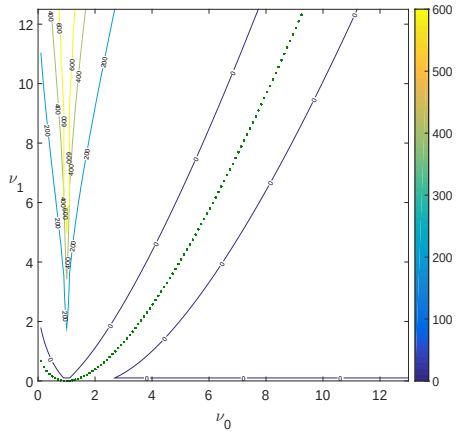
(c) $\arg(z) = \frac{\pi}{2}$



(d) $\arg(z) = \frac{\pi}{6}$



(e) $\arg(z) = \frac{\pi}{1800}$



(f) $\arg(z) = 0$

Figure 4.5 The contour plots of (4.34) for fixed value of $|z| = 1$ with values of $\arg(z) = 180, 120, 90, 30, 0.1$ and 0, respectively. Green dots illustrate the relation between ν_0 and ν_1 found in (4.37) in the contour plot and it is equivalent to lines in green in Figure 4.4. They show the behaviour and the direction of the estimate near and away from the Stokes lines.

	Truncation points and magnitude of the error estimate									
θ	(N_0^0, N_1^0)	$\ln(\lvert E_{N_1}\rvert)$	(N_0^1, N_1^1)	$\ln(\lvert E_{N_1}\rvert)$	(N_0^2, N_1^2)	$\ln(\lvert E_{N_1}\rvert)$	(N_0^3, N_1^3)	$\ln(\lvert E_{N_1}\rvert)$	(N_0^4, N_1^4)	$\ln(\lvert E_{N_1}\rvert)$
0	$(0,10)$	3.63×10^{-4}	$(5,1)$	5.098×10^{-4}	$(10,-)$	$-$	$(20,3)$	6.55×10^{-4}	$(60,57)$	2.916×10^{-4}
0.01	$(0,10)$	3.63×10^{-4}	$(5,1)$	5.098×10^{-4}	$(10,0)$	2383	$(20,3)$	6.55×10^{-4}	$(60,57)$	2.916×10^{-4}
0.1	$(0,10)$	3.63×10^{-4}	$(5,1)$	5.098×10^{-4}	$(10,0)$	23.83	$(20,3)$	6.55×10^{-4}	$(60,57)$	2.916×10^{-4}
15	$(0,10)$	3.63×10^{-4}	$(5,1)$	3.921×10^{-4}	$(10,0)$	1.061×10^{-3}	$(20,4)$	3.51×10^{-4}	$(60,58)$	9.185×10^{-5}
30	$(0,10)$	3.63×10^{-4}	$(5,2)$	1.758×10^{-4}	$(10,1)$	1.961×10^{-4}	$(20,6)$	6.07×10^{-5}	$(60,62)$	2.934×10^{-6}
45	$(0,10)$	3.63×10^{-4}	$(5,3)$	5.144×10^{-5}	$(10,3)$	2.577×10^{-5}	$(20,8)$	3.48×10^{-6}	$(60,67)$	1.008×10^{-8}
60	$(0,10)$	3.63×10^{-4}	$(5,4)$	1.049×10^{-5}	$(10,5)$	1.925×10^{-6}	$(20,12)$	7.60×10^{-8}	$(60,75)$	4.14×10^{-12}
75	$(0,10)$	3.63×10^{-4}	$(5,6)$	1.5×10^{-6}	$(10,8)$	9.049×10^{-8}	$(20,16)$	6.82×10^{-10}	$(60,85)$	2.32×10^{-16}
90	$(0,10)$	3.63×10^{-4}	$(5,8)$	1.637×10^{-7}	$(10,11)$	2.667×10^{-9}	$(20,22)$	2.73×10^{-12}	$(60,96)$	2.1×10^{-21}

Table 4.1 The table shows that for a fixed truncation point in the zeroth level, as $\arg(z) = \theta$ where $z = \exp(i\theta)$ is increased, the required number of the terms increases for the first level optimal truncation where $\ln(|E_{N_1}(z)|)$ in (4.34) takes its minimum value. The table further illustrates that for fixed θ, as the truncation point in the zeroth level is arbitrarily increased, the error estimate decreases except near the Stokes line $\theta = 0$.

we substitute $z = e^{i\theta}$ into the error (4.38). Analysing the estimate for large ν_1, we find that

$$E_{N_1}(z) \sim \frac{\nu_0^{\frac{\nu_0}{\varepsilon}+\frac{1}{2}} \exp\left(-\frac{\nu_0}{\varepsilon}\right)}{\varepsilon \exp\left(i\theta\left(\frac{\nu_0}{\varepsilon}+1\right)\right)} \frac{\exp\left(-\frac{\nu_1}{\varepsilon}\right) \nu_1^{\frac{\nu_1}{\varepsilon}+\frac{1}{2}}}{\left(e^{i\theta}-\nu_0+\nu_0 \ln\left(\frac{\nu_0}{e^{i\theta}}\right)\right)^{\frac{\nu_1}{\varepsilon}+1}}, \tag{4.39}$$

which, as expected, is divergent for sufficiently large ν_1 with fixed θ and ν_0. Indeed, this happens as the first level error is in the nature of a factorial-over-a-power, and, therefore, its numerator overpowers the whole expression when ν_1 is large.

The next step is to examine the error estimate (4.39) analytically for large ν_0 and large ν_1. In order to find the best relation between ν_0 and ν_1, we first minimise the estimate (4.39) with respect to ν_1, whereupon we found that this occurs when

$$\nu_1 = |\exp(i\theta) - \nu_0 + \nu_0 \ln(\nu_0) - i\nu_0\theta|. \tag{4.40}$$

Substitution of this relationship into the error estimate yields an estimate in terms of the variables ν_0 and θ, such that

$$E_{N_1}(z) \sim \frac{\nu_0^{\frac{\nu_0}{\varepsilon}+\frac{1}{2}} e^{\frac{-\nu_0}{\varepsilon}}}{\varepsilon e^{i\theta\left(\frac{\nu_0}{\varepsilon}+1\right)}} \frac{\exp\left(-\frac{\left|e^{i\theta}-\nu_0+\nu_0\ln\left(\frac{\nu_0}{e^{i\theta}}\right)\right|}{\varepsilon}\right)}{\sqrt{\left|e^{i\theta}-\nu_0+\nu_0\ln\left(\frac{\nu_0}{e^{i\theta}}\right)\right|}} \left[\frac{\left|e^{i\theta}-\nu_0+\nu_0\ln\left(\frac{\nu_0}{e^{i\theta}}\right)\right|}{e^{i\theta}-\nu_0+\nu_0\ln\left(\frac{\nu_0}{e^{i\theta}}\right)}\right]^{\frac{\left|e^{i\theta}-\nu_0+\nu_0\ln\left(\frac{\nu_0}{e^{i\theta}}\right)\right|}{\varepsilon}+1}. \tag{4.41}$$

Now this estimate (4.41) can be investigated for a large enough ν_0 when $\theta = 0$ and when $\theta \neq 0$. For when $\theta = 0$, we have to be careful whether or not ν_0 is obtained by the optimal truncation. In particular, we derive from (4.37) that if the series is truncated optimally and continued to the next level for z real,; N_1 is not large, so that the corresponding ν_1 is zero. We, therefore, consider that θ equals zero and ν_0 is different from 1 in this case; whereby, applying these to the error estimate (4.41)

implies

$$\begin{aligned} E_{N_1}(z) &\sim \frac{\nu_0^{\nu_0/\varepsilon+1/2}\exp\left(-\frac{\nu_0}{\varepsilon}\right)}{\varepsilon}\frac{\exp\left(-\frac{1-\nu_0+\nu_0\ln(\nu_0)}{\varepsilon}\right)}{\sqrt{1-\nu_0+\nu_0\ln(\nu_0)}} \\ &\sim \frac{1}{\varepsilon\exp(1/\varepsilon)}\sqrt{\frac{\nu_0}{1-\nu_0+\nu_0\ln(\nu_0)}} \\ &\sim \frac{\exp(-1/\varepsilon)}{\varepsilon}\sqrt{\frac{1}{\ln(\nu_0)-1}} \sim \frac{\exp(-1/\varepsilon)}{\varepsilon}\frac{1}{\sqrt{\ln(\nu_0)}}, \end{aligned}$$

which depends on ν_0 slightly and decreases very slowly as demonstrated in Figure 4.4f.

Next, the error estimate will be examined for fixed θ and large ν_0. Calculation of the magnitude in (4.40) gives,

$$\nu_1 = \sqrt{(f(\nu_0)+\cos(\theta))^2+(\sin(\theta)-\nu_0\theta)^2}, \tag{4.42}$$

where $f(\nu_0) = \nu_0\ln(\nu_0)-\nu_0$. Since we are interested in the behaviour of the error in magnitude, the numerator and the denominator of the rightmost term in (4.41) cancel each other out. Upon back substitution of (4.42) into the estimate (4.41) and taking its magnitude, the expression becomes

$$|E_{N_1}(z)| \sim \left|\frac{\sqrt{\nu_0}\ \exp\left(\dfrac{\nu_0\ln(\nu_0)-\nu_0-\sqrt{(f(\nu_0)+\cos(\theta))^2+(\sin(\theta)-\nu_0\theta)^2}}{\varepsilon}\right)}{\varepsilon\exp(i\theta(1+\nu_0/\varepsilon))\left(\sqrt{(f(\nu_0)+\cos(\theta))^2+(\sin(\theta)-\nu_0\theta)^2}\right)^{1/2}}\right|. \tag{4.43}$$

After taking out the term $(f(\nu_0)+\cos(\theta))^2$ from the square-root in exponential and performing the square-root function expansion for the large ν_0, we arrive at

$$|E_{N_1}(z)| \sim \left| \frac{1}{\varepsilon\sqrt{\ln(\nu_0)}} \frac{\exp\left(-\frac{1}{2\varepsilon}\frac{\nu_0^2\theta^2}{f(\nu_0)+\cos(\theta)}\right)\exp\left(-\frac{\cos(\theta)}{\varepsilon}\right)}{\left(1+\frac{1}{2}\left(\frac{\sin(\theta)-\nu_0\theta}{f(\nu_0)+\cos(\theta)}\right)^2\right)^{1/2}} \right|. \tag{4.44}$$

Pulling out the forcing term of (4.44) yields

$$\exp\left(-\frac{1}{2\varepsilon}\frac{\nu_0^2\theta^2}{f(\nu_0)+\cos(\theta)}\right), \tag{4.45}$$

which, for large enough ν_0, approximates to

$$\sim \exp\left(-\frac{1}{2\varepsilon}\frac{\nu_0\theta^2}{\ln(\nu_0)}\right). \tag{4.46}$$

We observe that this term reduces exponentially as ν_0 is increased; furthermore, it decreases more rapidly if θ is large. We may, hence, conclude that (4.44) reduces for the large ν_0, but the conclusion is not valid for small θ; in particular, when it is in $\theta = \mathrm{O}\left(\sqrt{2\varepsilon\ln(\nu_0)}/\sqrt{\nu_0}\right)$. This situation will be considered in the following case.

Motivated by the above discussion, our next step is to analyse the error estimate (4.41) when θ is small and ν_0 is sufficiently large. Therefore, first having the expansion of $\exp(i\theta)$ for small θ, and then substituting it into the estimate leads to

$$\begin{aligned} E_{N_1}(z) \sim & \frac{\sqrt{\nu_0}\exp\left[\left(\nu_0\ln(\nu_0)-\nu_0-\left|1+i\theta-\nu_0+\nu_0\ln\left(\nu_0/\exp(i\theta)\right)\right|\right)/\varepsilon\right]}{\varepsilon\exp\left[i\theta\left(\nu_0/\varepsilon+1\right)\right]\sqrt{\left|1+i\theta-\nu_0+\nu_0\ln\left(\nu_0/\exp(i\theta)\right)\right|}} \\ & \times\left(\frac{\left|1+i\theta-\nu_0+\nu_0\ln\left(\nu_0/\exp(i\theta)\right)\right|}{1+i\theta-\nu_0+\nu_0\ln\left(\nu_0/\exp(i\theta)\right)}\right)^{\left|1+i\theta-\nu_0+\nu_0\ln\left(\nu_0/\exp(i\theta)\right)\right|/\varepsilon+1}. \end{aligned} \tag{4.47}$$

Since we are interested in studying the magnitude of the error estimate, using the magnitude of (4.47) and employing the properties of log function gives

$$|E_{N_1}(z)| \sim \left| \frac{\exp\left[\left(\nu_0 \ln(\nu_0) - \nu_0 - f(\nu_0)\right)/\varepsilon\right] \exp\left(-\theta^2(1-\nu_0)^2/2\varepsilon f(\nu_0)\right)}{\varepsilon\sqrt{f(\nu_0)}\sqrt{1+\theta^2(1-\nu_0)^2/2f(\nu_0)^2}} \right|$$
$$\sim \left| \frac{\exp(-1/\varepsilon)}{\varepsilon} \frac{\exp\left(-\theta^2\left(1-\nu_0\right)^2/2\varepsilon f(\nu_0)\right)}{\sqrt{\ln(\nu_0)-1}\sqrt{1+\theta^2(1-\nu_0)^2/2f(\nu_0)^2}} \right|, \tag{4.48}$$

in which $f(\nu_0) = \nu_0 \ln(\nu_0) - \nu_0 + 1$. This decreases slowly as seen Figure 4.4f. This can be seen if the leading term is pulled out like in the previous case when ν_0 is sufficiently large, whereupon the term approximates to

$$\exp\left(-\frac{1}{2\varepsilon}\frac{\theta^2\left(1-\nu_0\right)^2}{f(\nu_0)}\right) \sim \exp\left(-\frac{1}{2\varepsilon}\frac{\theta^2\nu_0}{\ln(\nu_0)}\right). \tag{4.49}$$

Note that this approximation is the same as (4.46). Carrying out the procedure, (4.49) is exponentially small for large ν_0 except when θ depends on ν_0, such that

$$\theta = \mathrm{O}\left(\frac{\sqrt{2\varepsilon\ln(\nu_0)}}{\sqrt{\nu_0}}\right). \tag{4.50}$$

If this is the case, for large ν_0, the remainder will slightly depend on ν_0 as in the case $\theta = 0$, and it will not be exponentially convergent. This agreement can also be observed in the last two plots of Figure 4.4. Since the error (4.41) decreases for all cases, we minimise it with respect to ν_0 to attain a consistency with the above cases

$$\frac{dE_{N_1}(\theta)}{d\nu_0} = \frac{\sqrt{\nu_0}\exp\left[\left(\nu_0\ln(\nu_0) - \nu_0 - \left|e^{i\theta} - \nu_0 + \nu_0\ln\left(\nu_0/e^{i\theta}\right)\right|\right)/\varepsilon\right]}{\varepsilon\sqrt{\left|e^{i\theta} - \nu_0 + \nu_0\ln\left(\nu_0/e^{i\theta}\right)\right|}}$$
$$\times \begin{pmatrix} \dfrac{\ln(\nu_0)}{\varepsilon} + \dfrac{1}{2\nu_0} - \\ \dfrac{(\nu_0\ln(\nu_0) - \nu_0 + cos(\theta))\ln(\nu_0) - (sin(\theta) - \nu_0\theta)\theta)}{\varepsilon\sqrt{(\nu_0\ln(\nu_0) - \nu_0 + cos(\theta))^2 + (sin(\theta) - \nu_0\theta)^2}} + \\ \dfrac{(\nu_0\ln(\nu_0) - \nu_0 + cos(\theta))\ln(\nu_0) - (sin(\theta) - \nu_0\theta)\theta)}{2((\nu_0\ln(\nu_0) - \nu_0 + cos(\theta))^2 + (sin(\theta) - \nu_0\theta)^2)} \end{pmatrix}. \tag{4.51}$$

For the large enough value of ν_0, the derivative approximates to

$$\sim \frac{\sqrt{\nu_0}\exp\left[\dfrac{\nu_0\ln(\nu_0)-\nu_0-|\exp(i\theta)-\nu_0+\nu_0\ln(\nu_0/\exp(i\theta))|}{\varepsilon}\right]}{\varepsilon\sqrt{|\exp(i\theta)-\nu_0+\nu_0\ln(\nu_0/\exp(i\theta))|}}\left[\frac{\ln(\nu_0)}{\varepsilon}-\frac{\ln(\nu_0)}{\varepsilon}\right]$$

$$=0. \tag{4.52}$$

Hence, the derivative is equal to zero for large ν_0, which implies that the error estimate reduces when ν_0 is sufficiently large.

We will repeat the same process over ν_0 by fixing ν_1 in order to test the agreement with all the plots and expressions. Minimising the first level of the error estimate given in (4.38) with respect to ν_0 for fixed ν_1 yields

$$\frac{dE_{N_1}(\theta)}{d\nu_0}\sim\frac{\exp(-i\theta)\nu_0^{\nu_0/\varepsilon+1/2}}{\varepsilon^2\exp\left((1+i\theta)\nu_0/\varepsilon\right)}\frac{\nu_1^{\nu_1/\varepsilon+1/2}}{\exp(\nu_1/\varepsilon)}\frac{(\ln(\nu_0)-i\theta)}{\left(e^{i\theta}-\nu_0+\nu_0\ln(\nu_0/e^{i\theta})\right)^{\nu_1/\varepsilon+1}}$$
$$\times\left(1-\frac{\nu_1}{e^{i\theta}-\nu_0+\nu_0\ln(\nu_0/e^{i\theta})}\right). \tag{4.53}$$

We then have two cases;

(i) If $\ln(\nu_0)=i\theta$ which implies $e^{i\theta}-\nu_0+\nu_0\ln(\nu_0)-i\nu_0\theta=0$,

(ii) If $\ln(\nu_0)\neq i\theta$ which implies $\nu_1=|e^{i\theta}-\nu_0+\nu_0\ln(\nu_0)-i\nu_0\theta|$.

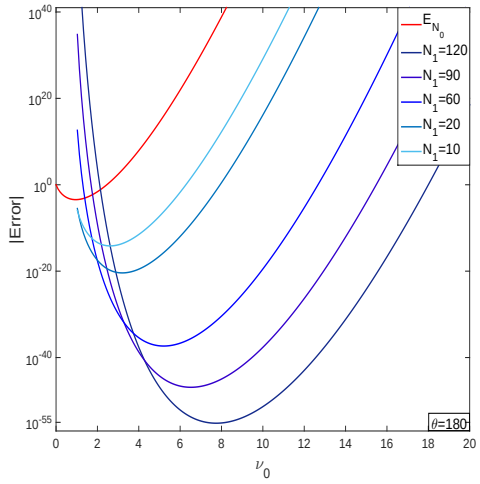
The first case takes us to the zeroth level of hyperasymptotics. Had we assumed that $\ln(\nu_0)=i\theta$, then we would have gone back to the zeroth level and stopped after the superasymptotics, as it corresponds with the optimal truncation point of zeroth level. However, in the latter case, by fixing ν_1, and varying θ and ν_0, we observe that the error first decreases and then increases except around the Stokes line $\theta=0$. To visualise this, as seen in Figure 4.6, if the fixed value of ν_1 is increased, the error estimate reduces depending on its location in relation near or away from the Stokes lines. The above results are obtained for various combination of truncation points N_0, N_1 and θ as well as considerations of the exponentially small terms, which are

hidden behind divergent series. Thus, as can be observed from Figures 4.4- 4.7, a satisfactory agreement between all the figures have been established; particularly, Figure 4.6 and Figure 4.7 clearly show the consistency with Figure 4.4. From these figures we observe that the error estimate decreases as the fixed values of ν_1 increase. It is further true that as θ increases the error reduces. It is worth remarking that the error estimate in this level also diverges as it is in the factorial-over-a-power nature and the 'factorial-over-a-power' series are necessarily divergent as discussed in (4.8) and as the late order terms in the expansions are governed by the nearest singularity or singularities (see Darboux's theorem [24]).

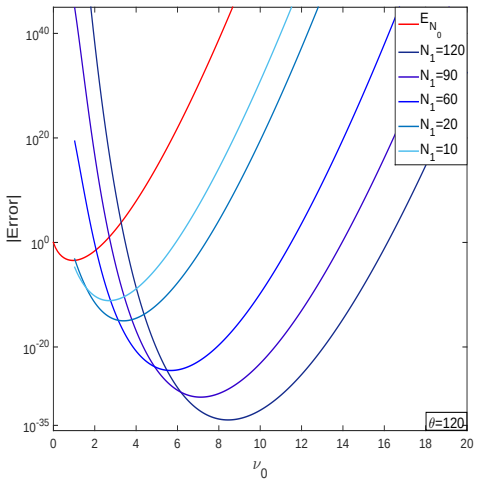
In summary, having derived the error estimate as a function of the level zero truncation point and increased it arbitrarily, we deduced that the error gets exponentially smaller away from its phase at $\theta = 0$, which corresponds to the Stokes line. We will discuss Stokes and anti-Stokes lines in the forthcoming section.

4.7 Stokes and anti-Stokes lines in first level

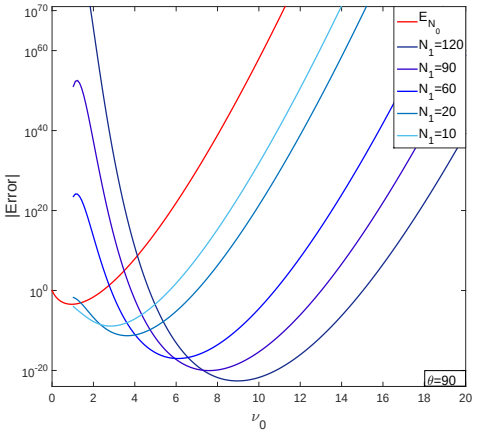
Having completely determined the late-order terms of $Q(z)$ and analysed the error estimates in sections §4.5 and §4.6, we can proceed to the investigation of Stokes lines at the first level of hyperasymptotics. Henceforth, we use the shorthand for the Stokes lines calculations at this and higher levels and write, for instance, "first level Stoke lines". These Stokes lines indeed carry the same smoothing at every level and always has to turn on the same quantity. In §3, the nature of the Stokes (and anti-Stokes) lines were discussed by considering the differential equation appearing in the form of (3.1). Additionally, determining the singulant was argued to be the central step for finding these lines. These lines are associated with the pre-factor of $y(z)$ in the equation (3.1), and the relation between the pre-factor and the singulant was determined as in (3.6). Since the first level differential equation (4.16) is similar to that in (3.1), the same technique of §3 will be used in this section. The distinguishing



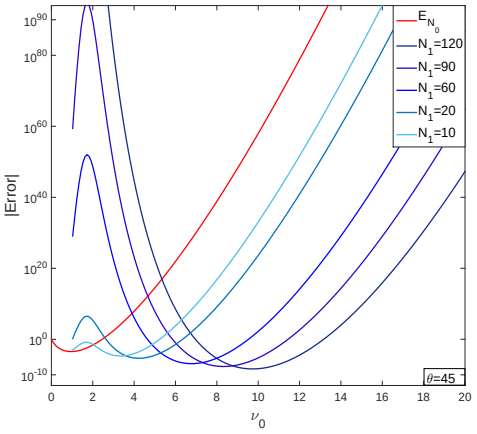
(a) $\theta = \pi$



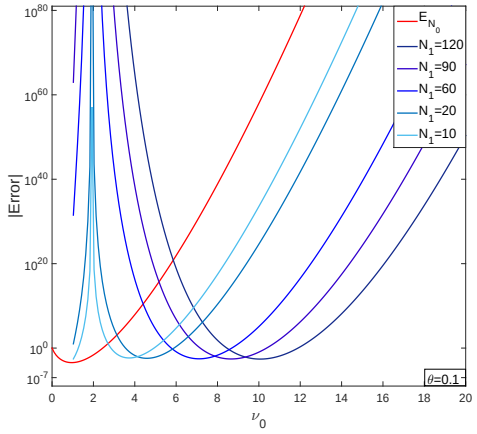
(b) $\theta = \frac{2\pi}{3}$



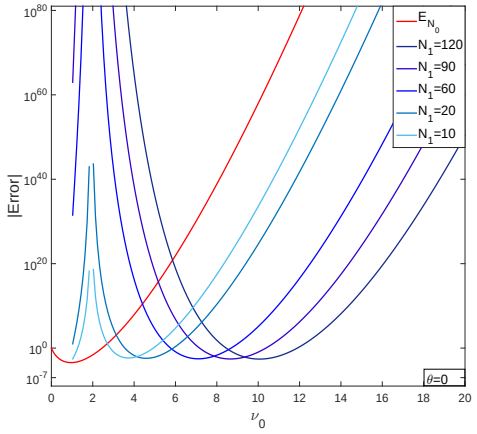
(c) $\theta = \frac{\pi}{2}$



(d) $\theta = \frac{\pi}{4}$



(e) $\theta = \frac{\pi}{1800}$



(f) $\theta = 0$

Figure 4.6 Behaviours of the zeroth level of error estimate in (4.12) shown by red lines and the first level estimate in (4.34) shown by blue coloured lines. They are plotted for $N_1 = 120, 90, 60, 20, 10$ and $\theta = 180, 120, 90, 45, 0.1, 0$ in which $z = \exp(i\theta)$. They demonstrate that the error decreases as they are increased, except near the Stokes line, Figure 4.6f.

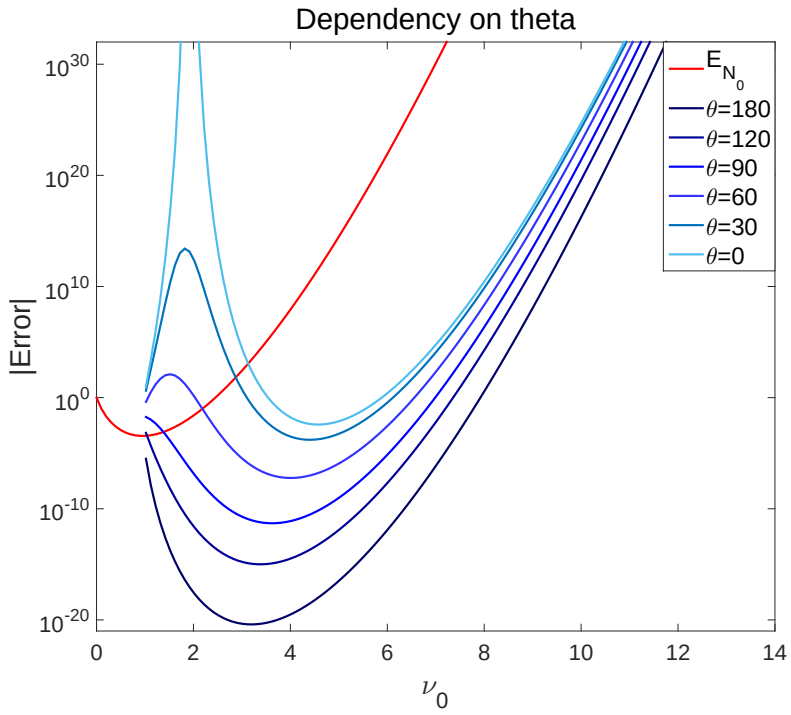


Figure 4.7 Red and blue lines represent the estimates given in (4.12) and (4.34). Plotted for fixed $N_1 = 20$, and $\theta = 180, 120, 90, 60, 30$ and 0 where $z = \exp(i\theta)$. As θ is increased the error estimate decreases, and the expansion breaks down at $\theta = 0$ as it corresponds to the singular point.

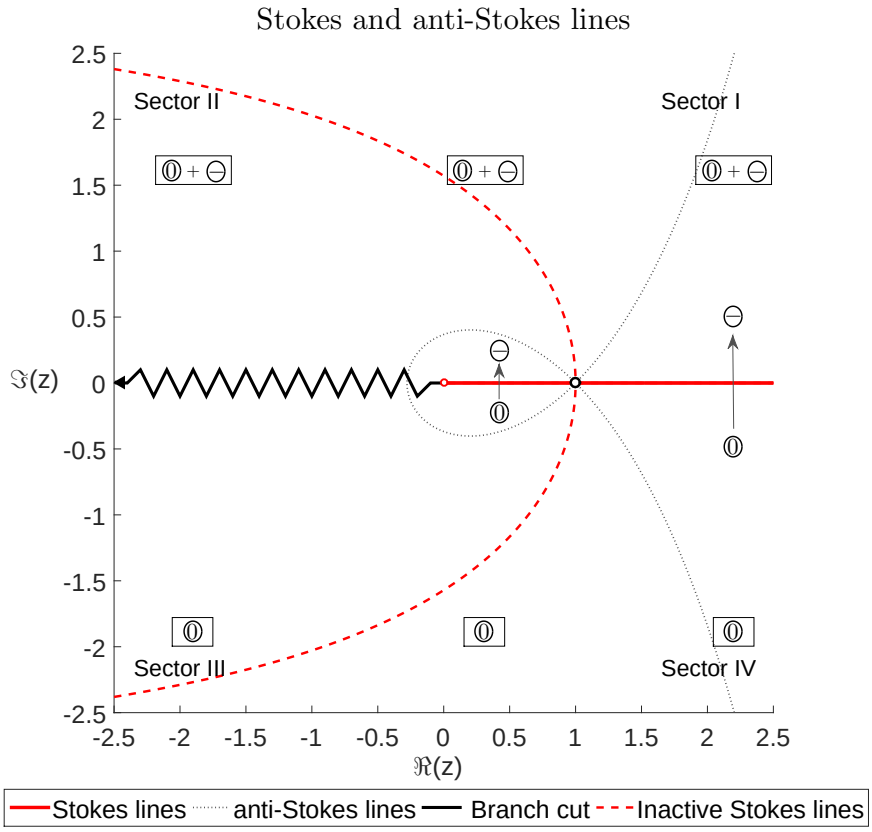
feature of these types of differential equations, if they are in the form of (3.1), lies at the turning points that possess Stokes lines where new exponential terms arise. Hence, the first step is to derive the turning point of (4.16). Before doing so, however, it is useful to refer to the equation (4.16)

$$\varepsilon \frac{dQ(z)}{dz} + \left(1 - \frac{\nu_0}{z}\right) Q(z) = 1. \tag{4.54}$$

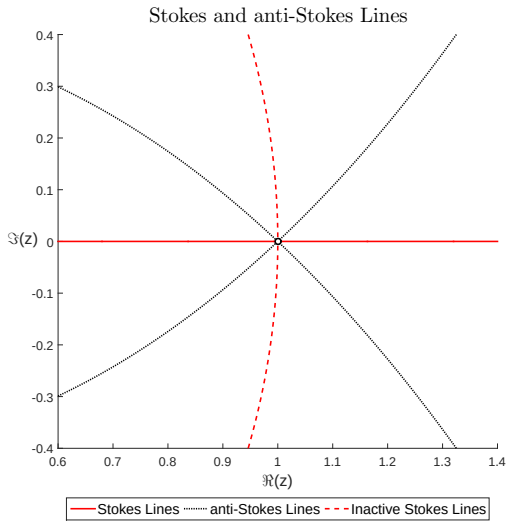
The turning point, which occurs when the pre-factor of (4.54) is equal to zero, lies at $z = \nu_0$ in which the singulant is required to vanish. In light of the relationship given in (3.6) between the singulant of (4.54) and the pre-factor $(1 - \nu_0/z)$, integrating the pre-factor once determines the singulant directly. Imposing the turning point completes the process which yields

$$u_1(z) = z - \nu_0 \ln(z) - \nu_0 + \nu_0 \ln(\nu_0). \tag{4.55}$$

See §3.1 for further details. Notice that the singulant is the same with the one obtained by the factorial-over-a-power method in (4.24), and has the branch point at $z = 0$ as discussed in §4.5. The birth of the Stokes and anti-Stokes lines occur at singularities of expansions, and Stokes lines occur when $u_1(z)$ is purely real and positive, anti-Stokes lines occur when $u_1(z)$ is purely imaginary [17] as addressed in §4.4. Having determined the form of $u_1(z)$, the Stokes and anti-Stokes lines of (4.16) may now be represented in Figure 4.8 for randomly chosen $z = 1/2 + i\sqrt{3}/2$. To demonstrate what happens while crossing the Stokes lines as well as which exponentials are present in which regions of the complex plane, we travel along the complex plane starting from any sector. Assume we are in Sector IV and $\exp(0)$ denoted by ⓪ is present there and let us see whether or not we return to our assumption ⓪ when the travel is complete. Moving in a counterclockwise direction upward to Sector I, the subdominant exponential term $\exp(-u_1(z))$ represented by ⊖ gets switched on by ⓪ across the Stokes line. Hence, ⓪ and ⊖ are both present in Sector I. They are also present in Sector II, since there is no active Stokes lines crossed while proceeding from Sector I to Sector II. Moving downward to Sector III, the branch cut leads to the removal of ⊖ by discontinuity. Hence, ⓪ is the only exponential present in Sector III. Likewise, nothing gets turned on or off since the relevant Stokes line is not active whilst travelling from Sector III to Sector IV; hence, ⓪ is present in Sector IV. The travel is complete with ⓪ which was the assumption before beginning the travel. This is to say that we arrive where we started. In doing so, we have pinpointed which exponentials are contributed in the different sectors of the plane. See Figure 4.8a. Furthermore, since the first level expansion is the multiplication of the zeroth level, whenever ⊖ is switched on, the subdominant exponential of level zero switches on; hence, ⊖ also represents both subdominant exponentials of two levels.



(a)



(b)

Figure 4.8 Red lines represent the first level active Stokes lines of the expansion (4.54) for $\nu_0 = 1$ given by $\Im(u_1(z)) = \Im(0)$ while $\Re(u_1(z)) > \Re(0)$. Inactive Stokes lines are represented with dashed red lines given by $\Im(u_1(z)) = \Im(0)$ while $\Re(u_1(z)) < \Re(0)$. Dotted black lines represent the second level anti-Stokes lines of (4.54), given by $\Re(u_1(z)) = \Re(0)$. Second Figure 4.8b is a closer view of the first Figure 4.8a near the singularity. It shows that the first level Stokes and anti-Stokes lines behave similar to those in Example 3.3.1. While crossing the Stokes line, $\ominus$ gets turned on, and across the brach cut, the logarithmic discontinuity leads to the removal of $\ominus$.

In order to see the closer picture of the Stokes lines given in Figure 4.8b, we need to study the behaviour of the Stokes lines close to the root of $u_1(z)$, i.e. near ν_0. We set $z = \nu_0 + \delta$, and this implies the singulant for small $|\delta| \ll 1$ becomes

$$\begin{aligned} u_1(\nu_0+\delta) &= \delta - \nu_0\left(\frac{\delta}{\nu_0} - \frac{\delta^2}{2\nu_0^2}\right) \\ &\approx \frac{\delta^2}{2\nu_0}. \end{aligned}$$

The Stokes and anti Stokes lines close to ν_0 should be the same as those in Figure 3.1, since the singulant in terms of δ is in the same form as that in Example 3.3.1 of §3. To demonstrate this without loss of generality, we transform δ into the polar coordinates such that we set $\delta = \exp(i\tilde{\theta})$ and analyse the singulant in terms of $\tilde{\theta}$. Relevant computations reveal that the active and inactive Stokes lines lie along $\tilde{\theta} = 0, \pi$ and $\pi/2, 3\pi/2$, respectively, and anti-Stokes lines lie along $\tilde{\theta} = \pi/4, 3\pi/4$, $5\pi/4$ and $7\pi/4$, respectively. These yield Figure 4.8b, which is indeed identical to Figure 3.1.

Additionally, the analysis of Stokes lines in the first level expansion (4.17) can also be performed by investigating the RHS of (4.29), i.e.,

$$\varepsilon\frac{d\mathscr{R}_{N_1}(z)}{dz} + \left(1 - \frac{\nu_0}{z}\right)\mathscr{R}_{N_1}(z) \approx \varepsilon^{N_1} Q_{N_1}(z)\left(1 - \frac{\nu_0}{z}\right).$$

In §3.3 (ii), we infer that Stokes lines emanate when the dominant factor of RHS of (4.29) is maximal at θ. In order to demonstrate this, we first need to write the RHS in terms of θ. After convenient substitutions, i.e., polar coordinates $z = r\exp(i\theta)$ and Stirling's formula, we obtain that

$$\begin{aligned} \text{RHS} \sim \frac{\sqrt{2\pi}}{\sqrt{\varepsilon}} \frac{\exp\left(-\frac{|re^{i\theta} - \nu_0 + \nu_0 \ln(\frac{\nu_0}{re^{i\theta}})|}{\varepsilon}\right)}{\sqrt{|re^{i\theta} - \nu_0 + \nu_0\ln(\frac{\nu_0}{re^{i\theta}})|}} \left(\frac{|re^{i\theta} - \nu_0 + \nu_0\ln(\frac{\nu_0}{re^{i\theta}})|}{re^{i\theta} - \nu_0 + \nu_0\ln(\frac{\nu_0}{re^{i\theta}})}\right)^{\frac{|re^{i\theta} - \nu_0 + \nu_0\ln(\frac{\nu_0}{re^{i\theta}})|}{\varepsilon}+1} \\ \times \left(1 - \frac{\nu_0}{re^{i\theta}}\right). \end{aligned} \tag{4.56}$$

Taking the controlling factor of (4.56) out and analysing it for θ leads to

$$\frac{\exp\left(-\dfrac{(r\sin(\theta)-\nu_0\theta)^2}{2\varepsilon f(\nu_0,\theta)}\right)}{\exp\left(\dfrac{f(\nu_0,\theta)}{\varepsilon}\right)} \sim \frac{\exp\left(-\dfrac{\theta^2\nu_0}{2\varepsilon\ln(\nu_0)}\right)}{\exp\left(\dfrac{f(\nu_0,\theta)}{\varepsilon}\right)}, \tag{4.57}$$

where $f(\nu_0,\theta) = r\cos(\theta) + \nu_0\ln(\nu_0) - \nu_0\ln(r) - \nu_0$. If $\theta = 0$, then the RHS takes its maximum value, although it is still exponentially small for the large ν_0. Thus, $\theta = 0$ is the Stokes lines of the first level differential equation whereby at $\theta = 0$ the behaviour of the remainder switches. Furthermore, if the size of θ is in the order of

$$\sqrt{2\varepsilon\ln(\nu_0)/\nu_0}, \tag{4.58}$$

we then have the distinguished limit which is consistent with the previous one calculated in (4.50). Note that this limit takes us back to the zeroth level expansion.

4.8 Stokes line smoothing

In this section, we will turn our attention to the thickness of the first level Stokes lines by investigating the first level remainder equation (4.29) in detail. Thickness, in this thesis, refers to the scaling of the error function smoothing. We keep ν_0 arbitrary and ν_1 optimally truncated as given in (4.37) as a function of ν_0. Let us begin the analysis by looking at the homogeneous solution of (4.29) which takes form as

$$\mathscr{R}_{N_1} := \exp\left(\frac{-z+\nu_0\ln(z)}{\varepsilon}\right) M(z), \tag{4.59}$$

where $M(z)$ will be discussed shortly. Straightforward substitution of this into the remainder equation (4.29) leads to

$$\begin{aligned}\frac{dM(z)}{dz} &= \varepsilon^{\nu_1-1}\exp\left(\frac{z-\nu_0\ln(z)}{\varepsilon}\right)Q_{\nu_1}\left(1-\frac{\nu_0}{z}\right)\\ &\sim \frac{\sqrt{2\pi}}{\varepsilon\sqrt{\varepsilon}}\frac{\nu_1^{\nu_1/\varepsilon+1/2}\exp\left(\dfrac{z-\nu_0\ln(z)}{\varepsilon}\right)}{\exp\left(\dfrac{\nu_1}{\varepsilon}\right)u_1(z)^{\nu_1/\varepsilon+1}}\left(1-\frac{\nu_0}{z}\right),\end{aligned} \tag{4.60}$$

in which (4.27) is performed using Stirling's formula. As before, the polar coordinates are introduced under the consideration that there is a singularity at ν_0. Particularly, for the case where $\nu_0 > 1$,

$$z = \nu_0 + re^{i\theta},$$

in which $r = \nu_0 - 1$ is the radial distance to the singularity . By using polar coordinates, we allow Stokes lines to vary as θ varies; in fact, the width of the Stokes line in the exponential asymptotics is defined near the singularity. In order to determine the width, we transform θ in the vicinity of Stokes line and perturbate about it, i.e.,

$$\theta = \pi + \delta\widehat{\theta}, \tag{4.61}$$

where $\delta \ll 1$ and $\widehat{\theta} = \mathrm{O}(1)$. Here, δ of the above transformation (4.61) will be determined using the same method employed in the previous level. Employing the polar coordinates by considering the transformation of θ changes (4.60) into

$$\begin{aligned}\frac{dM}{d\widehat{\theta}} \sim \frac{\delta\sqrt{2\pi}}{\varepsilon\sqrt{\varepsilon}}&\frac{\exp\left(\dfrac{f(\nu_0)-1+i\delta\widehat{\theta}(\nu_0-1)^2}{\varepsilon}-\dfrac{(\delta\widehat{\theta})^2(\nu_0-1)^4}{2\varepsilon f(\nu_0)}+\mathrm{O}(\varepsilon)\right)}{\sqrt{f(\nu_0)}}\\ &\times\left(\frac{1+\dfrac{\left(\delta\widehat{\theta}(\nu_0-1)^2\right)^2}{2f(\nu_0)^2}}{1+i\dfrac{\delta\widehat{\theta}(\nu_0-1)^2}{f(\nu_0)}}\right)^{f(\nu_0)/\varepsilon+O(\varepsilon)}\cdot\frac{(\nu_0-1)^2}{1+i(1-\nu_0)\delta\widehat{\theta}},\end{aligned} \tag{4.62}$$

where $f(\nu_0) = 1+\nu_0\ln(\nu_0)-\nu_0$. Here, the terms of lower order for small ε were omitted. Using the properties of logarithmic function and expanding the relevant

parts for small δ, we obtain

$$\frac{dM}{d\widehat{\theta}} \sim \frac{\delta\sqrt{2\pi}}{\varepsilon\sqrt{\varepsilon}} \frac{\exp\left(\dfrac{f(\nu_0)-1}{\varepsilon} - \dfrac{(\delta\widehat{\theta})^2(\nu_0-1)^4}{2\varepsilon f(\nu_0)}\right)}{\sqrt{f(\nu_0)}} (\nu_0-1)^2 . \tag{4.63}$$

This suggests that the critical scaling in the vicinity of the Stokes line should be

$$\delta = \frac{\sqrt{2\varepsilon}\sqrt{f(\nu_0)}}{(\nu_0-1)^2}. \tag{4.64}$$

We easily verify that (4.64) is small when ν_0 is large for fixed ε. Accordingly, after substitution of this scaling into (4.62), the RHS of the expression becomes

$$\frac{dM}{d\widehat{\theta}} \sim \frac{2\sqrt{\pi}}{\varepsilon} \exp\left(\frac{f(\nu_0)-1}{\varepsilon}\right) \exp\left(-\widehat{\theta}^2\right), \tag{4.65}$$

where the rightmost exponential term with $\widehat{\theta}$ recovers the classic error function. In particular, integrating (4.65) directly with respect to $\widehat{\theta}$ allows us to establish the error function

$$M(\widehat{\theta}) \sim \frac{\pi}{\varepsilon} \exp\left(\frac{f(\nu_0)-1}{\varepsilon}\right) \operatorname{erf}\left(\widehat{\theta}\right). \tag{4.66}$$

By this transformed δ in (4.64), we determine the width of the Stokes line about $\theta = \pi$, which is

$$(\nu_0-1)\left(\frac{\sqrt{2\varepsilon f(\nu_0)}}{(\nu_0-1)^2}\right) = \frac{\sqrt{2\varepsilon f(\nu_0)}}{\nu_0-1}. \tag{4.67}$$

For the large values of ν_0 in above $f(\nu_0)$, the width becomes

$$\frac{\sqrt{2\varepsilon \ln(\nu_0)}}{\sqrt{\nu_0}}. \tag{4.68}$$

In comparison, the thickness of the Stokes line calculated above is identical to the distinguishing limit derived in (4.58), which defines the width of the Stokes line using different angles. Substituting the scaling into z enables us to define z in terms

of the thickness of the Stokes lines such that

$$\begin{aligned} z &= \nu_0 + (\nu_0 - 1)\exp\left(i\pi + i\delta\widehat{\theta}\right) \\ &\sim 1 - i\frac{\sqrt{2\varepsilon f(\nu_0)}}{\nu_0 - 1}\widehat{\theta} \\ &\sim 1 - i\frac{\sqrt{2\varepsilon \ln(\nu_0)}}{\sqrt{\nu_0}}\widehat{\theta}, \quad \text{for large } \nu_0. \end{aligned}$$

To sum up, it is possible that seemingly simple differential equations may sometimes lack an exact solution or have a relatively complicated solution. In order to attain more information about these types of differential equations, studying the turning points and singular points of the equations essentially play key roles using exponential asymptotics. In fact, these points are the distinguishing features of the equations. Particularly, by analysing the first level remainder equation using its distinguishing features, we obtain more information about the Stokes lines and the first level remainder equation, even though we cannot obtain the exact solution of the remainder equation yet. In the zeroth level, we calculate the width of the Stokes line as $\sqrt{2\varepsilon/r}$. However, in the first level it appears that the width of the Stokes line depends on ν_0 and ε; hence, the width reduces as ν_0 gets bigger.

Next, we will perform the second level analysis of the hyperasymptotic approach. The technique consists of expanding the remainder differential equation, truncating the expansion and inspecting the second level error estimate based on arbitrary truncation points.

4.9 Second level of hyperasymptotics and Stokes lines

As in the first level, we continue to analyse the remainder from (4.29) for the second level of the hyperasymptotic expansion. We follow similar steps of the first level investigation. However, since we approximate the RHS of the equation by its factorial-over-a-power representation (which is not exact) from the previous level, some of the

results which follow maybe questionable, thus the analysis requires greater care. Let us first re-scale the remainder $\mathscr{R}_{N_1}(z)$ according to the RHS of (4.29)

$$\mathscr{R}_{N_1}(z) = \varepsilon^{N_1} Q_{N_1}(z) \left(1 - \frac{\nu_0}{z}\right) S(z), \tag{4.69}$$

where $S(z)$ is an unknown function of z, and will be determined shortly. After finding the first derivative of (4.69) and applying it to the differential equation (4.29), we compute that the function $S(z)$ satisfies the differential equation

$$\varepsilon \left(\frac{dS(z)}{dz} + \frac{S(z)\nu_0}{z(z-\nu_0)} - \frac{S(z)(N_1+\gamma_1)}{z-\nu_0+\nu_0 \ln(\frac{\nu_0}{z})} \left(\frac{z-\nu_0}{z}\right) \right) + \left(\frac{z-\nu_0}{z}\right) S(z) \sim 1. \tag{4.70}$$

For sufficiently large N_1 when ε is small, it becomes

$$\varepsilon \frac{dS(z)}{dz} + \left(1 - \frac{\nu_1}{z-\nu_0+\nu_0 \ln(\frac{\nu_0}{z})}\right) \left(\frac{z-\nu_0}{z}\right) S(z) \sim 1, \tag{4.71}$$

which preserves the pre-factor of previous levels. It is worth remarking that (4.71) is the same in nature as (3.25) established in §3.4 for the general first level equations, since it corresponds to the first level equation according to the preceding level. In light of the discussions in previous steps, singularities of $S(z)$ occur where the pre-factors of $S(z)$ equal to zero, that is

$$\left(\frac{z-\nu_0+\nu_0 \ln\left(\frac{\nu_0}{z}\right) - \nu_1}{z-\nu_0+\nu_0 \ln\left(\frac{\nu_0}{z}\right)} \right) \left(\frac{z-\nu_0}{z}\right) = 0.$$

In particular, they occur when $z = \nu_0$ and when z is a solution of

$$z - \nu_0 + \nu_0 \ln\left(\frac{\nu_0}{z}\right) = \nu_1.$$

Since $z = \nu_0$ is the solution of the previous level singulant u_1, it is not a turning point of the expansion; in fact, it turns out to be a branch point of the present level.

Figure 4.9 shows the singular points of the leftmost pre-factor of $S(z)$ in (4.71). Expanding $S(z)$ into powers of ε in the usual way of asymptotics

$$S(z) \sim \sum_{n=0}^{\infty} \varepsilon^n S_n(z), \tag{4.72}$$

and substituting the ansatz back into (4.71) derives the leading order term at $\mathrm{O}(1)$ as well as the two terms differential recursive relation for the general term at $\mathrm{O}(\varepsilon^n)$ for the expansion of $S(z)$

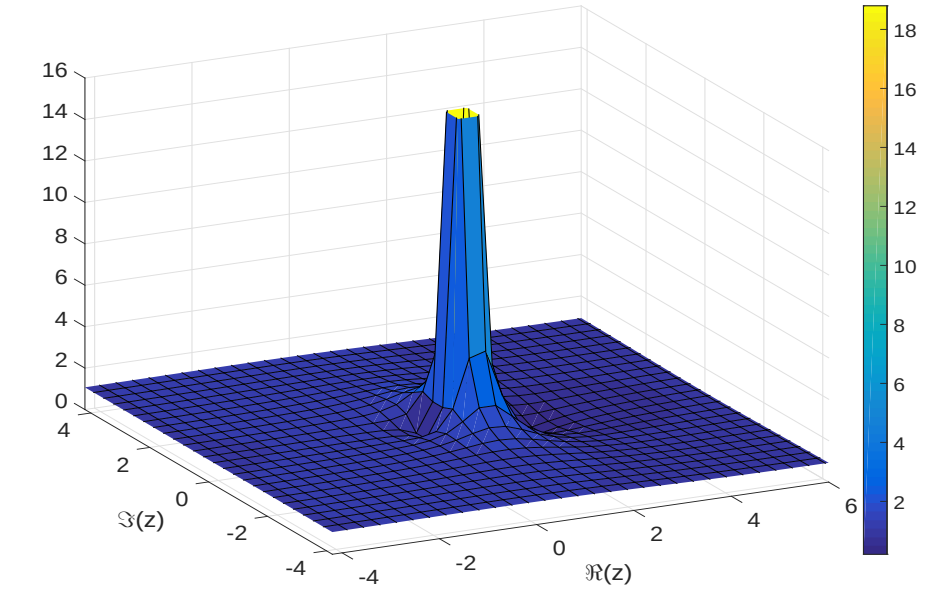
$$\begin{aligned} S_0(z) &= \left(\frac{z}{z-\nu_0}\right)\left(\frac{z-\nu_0+\nu_0\ln(\frac{\nu_0}{z})}{z-\nu_0+\nu_0\ln(\frac{\nu_0}{z})-\nu_1}\right), \\ \frac{dS_{n-1}(z)}{dz} &+ \left(1-\frac{\nu_1}{z-\nu_0+\nu_0\ln(\frac{\nu_0}{z})}\right)\left(\frac{z-\nu_0}{z}\right)S_n(z) = 0, \end{aligned} \tag{4.73}$$

where $n \geq 1$. The key point to note is that as $S_n(z)$ is produced by $S_0(z)$, all the singular points of $S_n(z)$ will be the same for $S_0(z)$. Since it is impossible to obtain the general representation by repeated integration using the recurrence relation, we seek a solution of $S_n(z)$ in the familiar 'factorial/power' form, that is,

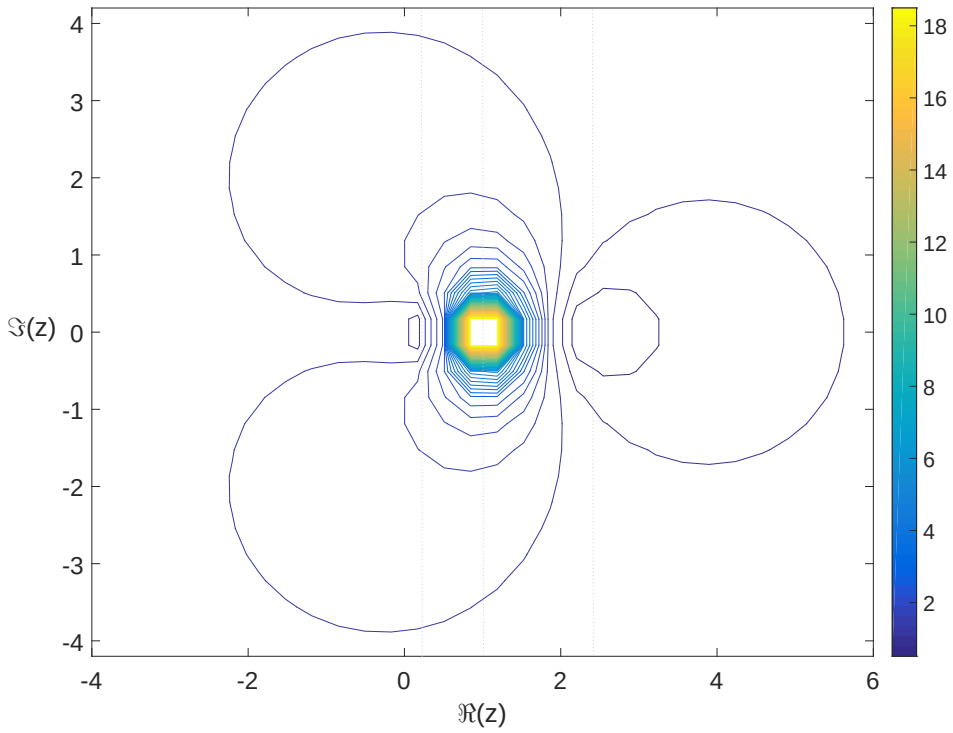
$$S_n(z) \sim \frac{\Gamma(n+\gamma_2)}{u_2(z)^{n+\gamma_2}}\left(B_0(z)+\frac{1}{n}B_1(z)+\frac{1}{n^2}B_2(z)+\ldots\right) \quad \text{as } n\to\infty, \tag{4.74}$$

where $\gamma_2 = \mathrm{O}(1)$ is an arbitrary constant and $u_2(z), \gamma_2$, and $B_i(z)$'s are independent of n. After substitution of the first derivative of (4.74) and (4.74) itself into (4.73), it is not difficult to show that

$$\frac{\Gamma(n+\gamma_2)}{u_2(z)^{(n+\gamma_2)}}\left(\begin{array}{c} \left(u_2'(z)+\left(\frac{z-\nu_0+\nu_0\ln(\frac{\nu_0}{z})-\nu_1}{z-\nu_0+\nu_0\ln(\frac{\nu_0}{z})}\right)\left(\frac{z-\nu_0}{z}\right)\right)B_0+ \\ \sum_{i=1}^{\infty}\left(\frac{1}{n}\right)^i\left[\left(u_2'(z)+\left(\frac{z-\nu_0+\nu_0\ln(\frac{\nu_0}{z})-\nu_1}{z-\nu_0+\nu_0\ln(\frac{\nu_0}{z})}\right)\left(\frac{z-\nu_0}{z}\right)\right)B_i+B_{i-1}'\right] \end{array}\right) = 0. \tag{4.75}$$



(a)



(b)

Figure 4.9 Magnitude of the pre-factor of $(1-\nu_0/z)S(z)$ in (4.71) in the complex plane and its contour plot for randomly picked $z = 1/2 + i\sqrt{3}/2$ which yields $\nu_0 = 1$ and $\nu_1 = 0.53$. The spike shows that $S(z)$ is not universally small across the plane.

For large n, the dominant balanced term should be zero:

$$\left(u_2'(z)+\left(\frac{z-\nu_0+\nu_0\ln(\frac{\nu_0}{z})-\nu_1}{z-\nu_0+\nu_0\ln(\frac{\nu_0}{z})}\right)\left(\frac{z-\nu_0}{z}\right)\right)B_0=0. \tag{4.76}$$

As thoroughly explained in previous sections such as (4.21) of §4.5, B_0 must not be zero. Moreover, substitution of (4.76) into the summation of (4.75) deduces that all B_i terms are indeed constants upon integration. Having solved the derivation of $u_2(z)$ in (4.76), the singulant of the second level is obtained as

$$u_2(z)=z-\nu_0\ln(z)-\nu_1\ln\left(z-\nu_0+\nu_0\ln\left(\frac{\nu_0}{z}\right)\right)+C_1 \;\text{ and }\; B_i=C_i, \tag{4.77}$$

where $0\leq i\leq n$ and C_is are arbitrary constants and C_1 is a constant to be determined soon based on the singulant subject to the singularity. Because $u_2(z)$ is located in the denominator of $S_n(z)$, it needs to be zero at the singularities of $S_n(z)$ which yields

$$\begin{aligned}u_2(z)&=\nu_1\ln\left(z-\nu_0+\nu_0\ln\left(\frac{\nu_0}{z}\right)\right)-z+\nu_0\ln(z)-\nu_1\ln(\nu_1)-\nu_0\ln(\nu_0)+\nu_1+\nu_0\\&=\nu_1\ln(u_1(z))-\nu_1\ln(\nu_1(z))+\nu_1-u_1(z).\end{aligned} \tag{4.78}$$

Hence, the determination of the unknown function $S(z)$ for late order terms is completed with recovering the singulant $u_2(z)$ by the factorial-over-a-power method. Moreover, the singulant has branch points at $z=0$ and $z=\nu_0$. Now we need to find Stokes and anti-Stokes lines of the equation (4.71), which are to be the second level Stokes and anti-Stokes lines of (4.1). As already discussed, Stokes lines appear whenever $u_2(z)$ satisfies the following conditions

$$\Im(u_2(z))=0 \qquad \text{while} \qquad \Re(u_2(z))>0.$$

Anti-Stokes lines appear whenever $\Re(u_2(z))=0$. However, since the singular points of the second level expansion cannot approach separately unlike in the other levels and chapters, Stokes lines may overlap with each other; hence, further analysis is

necessary. Therefore, we only plot the putative active Stokes lines in Figure 4.10 according to the above description.

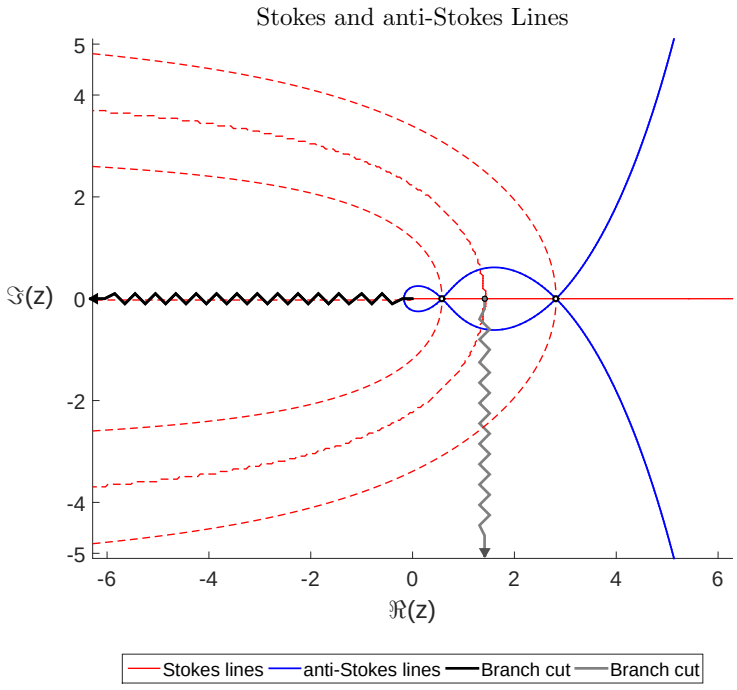


Figure 4.10 Red lines and blue lines are the Stokes and anti-Stokes lines of the equation (4.71) plotted via the singulant in (4.78), respectively, while branch cuts are represented by the zigzag lines in black and grey for arbitrarily chosen $\nu_0 = |1+i|$ whereby $\nu_1 = 0.428$ in accordance with (4.31).

Having established the general term of the series $S(z)$ in the factorial-over-a-power nature in the limit $n \to \infty$, the series can now be truncated directly after $N_2 \gg 1$ terms which is the second level truncation point

$$S(z) \sim \sum_{n=0}^{N_2-1} \varepsilon^n \frac{\Gamma(n+\gamma_2)}{u_2(z)^{n+\gamma_2}} + \mathfrak{R}_{N_2}(z), \tag{4.79}$$

where $\mathfrak{R}_{N_2}(z) = \mathrm{O}(\varepsilon^{N_2})$. Substituting the truncated series (4.79) into the equation (4.71), we find that the second level remainder term $\mathfrak{R}_{N_2}(z)$ is a solution of

$$\varepsilon\mathfrak{R}'_{N_2}(z)+\left(1-\frac{\nu_0}{z}\right)\left(1-\frac{\nu_1}{z-\nu_0+\nu_0\ln\left(\frac{\nu_0}{z}\right)}\right)\mathfrak{R}_{N_2}(z)\approx \varepsilon^{N_2}\left(1-\frac{\nu_0}{z}\right)\left(1-\frac{\nu_1}{z-\nu_0+\nu_0\ln\left(\frac{\nu_0}{z}\right)}\right)S_{N_2}(z). \tag{4.80}$$

In order to derive the point of optimal truncation, the RHS of (4.80) needs to be minimised with respect to N_2 in the same way whereby N_1 is determined in (4.30). Such truncation point can be obtained as usual, in the form of "function divided by ε",

$$N_2 \sim \frac{|u_2(z)|}{\varepsilon}. \tag{4.81}$$

As in the previous stages, we will also consider the truncation point of zeroth, first and second levels arbitrarily. Once (4.79) and (4.69) are back-substituted into (4.33), we find that such a truncated series of the second level expansion consists of $N_0+N_1+N_2$ terms plus the remainder such that

$$y=\sum_{n=0}^{N_0-1}\frac{\varepsilon^n n!}{z^{n+1}}+\frac{\varepsilon^{N_0}N_0!}{z^{N_0+1}}\sum_{n=0}^{N_1-1}\varepsilon^n Q_n(z)+\frac{\varepsilon^{N_0+N_1}N_0!}{z^{N_0+1}}\left(\frac{z-\nu_0}{z}\right)Q_{N_1}(z)\sum_{n=0}^{N_2-1}\varepsilon^n S_n(z) +\frac{\varepsilon^{N_0+N_1}N_0!}{z^{N_0+1}}\left(\frac{z-\nu_0}{z}\right)Q_{N_1}(z)\mathfrak{R}_{N_2}(z). \tag{4.82}$$

We obtained a more accurate approximation than the zeroth and the first level expansions, since N_2 more terms have been added into the solution of the preceding level. Herein, we define the second level truncation error by the first neglected term, which is the rightmost term in (4.82),

$$\begin{aligned} E_{N_2}(z) :&= \frac{\varepsilon^{N_0+N_1}N_0!}{z^{N_0+1}}Q_{N_1}\left(\frac{z-\nu_0}{z}\right)\mathfrak{R}_{N_2}(z)\\ &= \frac{\varepsilon^{N_0+N_1+N_2}N_0!}{z^{N_0+1}}\left(\frac{z-\nu_0}{z}\right)Q_{N_1}(z)S_{N_2}(z). \end{aligned} \tag{4.83}$$

The order of the second level error, after employing Stirling's approximation for factorial terms, becomes

$$E_{N_2}(z) \sim \frac{\varepsilon^{N_0+N_1+N_2} N_0^{N_0+\frac{1}{2}} N_1^{N_1+\gamma_1-\frac{1}{2}} N_2^{N_2+\gamma_2-\frac{1}{2}}}{z^{N_0+1} \exp\left(N_0+N_1+N_2+\gamma_1+\gamma_2-2\right) u_1(z)^{N_1+\gamma_1} u_2(z)^{N_2+\gamma_2}} \left(1-\frac{\nu_0}{z}\right) C_1, \tag{4.84}$$

in which $C_1 = 2\pi\sqrt{2\pi}C$. After rearranging the error (4.84) in terms of $\nu_2 \sim \varepsilon N_2$, $\nu_1 \sim \varepsilon N_1$ and $\nu_0 \sim \varepsilon N_0$, the magnitude of (4.84) may be minimised with respect to ν_2, ν_1 and ν_0. To do this directly, the first derivative of $E_{N_2}(z)$ are taken over ν_2, ν_1 and ν_0, respectively, such that

$$\begin{aligned}
\frac{dE_{N_2}(z)}{d\nu_2} &\sim \frac{\nu_0^{\frac{\nu_0}{\varepsilon}+\frac{1}{2}} \nu_1^{\frac{\nu_1}{\varepsilon}+\gamma_1-\frac{1}{2}} \nu_2^{\frac{\nu_2}{\varepsilon}+\gamma_2-\frac{1}{2}} \left(1-\frac{\nu_0}{z}\right) C_2}{z^{\frac{\nu_0}{\varepsilon}+1} \varepsilon^{\gamma_1+\gamma_2+\frac{1}{2}} e^{\frac{\nu_0}{\varepsilon}+\frac{\nu_1}{\varepsilon}+\frac{\nu_2}{\varepsilon}+\gamma_1+\gamma_2-2} \left(u_1(z)\right)^{\frac{\nu_1}{\varepsilon}+\gamma_1} \left(u_2(z)\right)^{\frac{\nu_2}{\varepsilon}+\gamma_2}} \ln\left(\frac{\nu_2}{u_2(z)}\right), \\
\frac{dE_{N_2}(z)}{d\nu_1} &\sim \frac{\nu_0^{\frac{\nu_0}{\varepsilon}+\frac{1}{2}} \nu_1^{\frac{\nu_1}{\varepsilon}+\gamma_1-\frac{1}{2}} \nu_2^{\frac{\nu_2}{\varepsilon}+\gamma_2-\frac{1}{2}} \left(1-\frac{\nu_0}{z}\right) C_2}{z^{\frac{\nu_0}{\varepsilon}+1} \varepsilon^{\gamma_1+\gamma_2+\frac{1}{2}} e^{\frac{\nu_0}{\varepsilon}+\frac{\nu_1}{\varepsilon}+\frac{\nu_2}{\varepsilon}+\gamma_1+\gamma_2-2} \left(u_1(z)\right)^{\frac{\nu_1}{\varepsilon}+\gamma_1} \left(u_2(z)\right)^{\frac{\nu_2}{\varepsilon}+\gamma_2}} \ln\left[\frac{\nu_1}{u_1(z)}\right] \left[1+\frac{\nu_2}{u_2(z)}\right], \\
\frac{dE_{N_2}(z)}{d\nu_0} &\sim \frac{\nu_0^{\frac{\nu_0}{\varepsilon}+\frac{1}{2}} \nu_1^{\frac{\nu_1}{\varepsilon}+\gamma_1-\frac{1}{2}} \nu_2^{\frac{\nu_2}{\varepsilon}+\gamma_2-\frac{1}{2}} \left(1-\frac{\nu_0}{z}\right) C_2 \ln\left(\frac{\nu_0}{z}\right)}{z^{\frac{\nu_0}{\varepsilon}+1} \varepsilon^{\gamma_1+\gamma_2+\frac{1}{2}} e^{\frac{\nu_0}{\varepsilon}+\frac{\nu_1}{\varepsilon}+\frac{\nu_2}{\varepsilon}+\gamma_1+\gamma_2-2} u_1(z)^{\frac{\nu_1}{\varepsilon}+\gamma_1} u_2(z)^{\frac{\nu_2}{\varepsilon}+\gamma_2}} \left[1-\frac{\nu_1}{u_1(z)}\right] \left[1+\frac{\nu_2}{u_2(z)}\right].
\end{aligned} \tag{4.85}$$

The minimum value of $|E_{N_2}(z)|$ over ν_0, ν_1 and ν_2 occurs when each derivative is equal to zero. Thus it happens when

$$N_2 \sim \frac{|u_2(z)|}{\varepsilon}, \tag{4.86}$$

or

$$N_1 \sim \frac{|u_1(z)|}{\varepsilon}, \tag{4.87}$$

or

$$N_0 \sim \frac{|z|}{\varepsilon}, \tag{4.88}$$

respectively, and z should be complex as explicated earlier. Herein, (4.86), (4.87) and (4.88) correspond to the optimal truncation points of each stage. Upon performing these minimisations and using the above results, the error estimate may be expressed in terms of only ν_0 and ν_1. Hence, increasing either the values of ν_0 or ν_1 arbitrarily, irrespective of the relevant optimal truncation points, will minimise

the error. Figure 4.11 shows the improvement obtained by hyperasymptotics in three levels. Increasing the first level truncation point N_1 arbitrarily decreases the error, which is illustrated by the green dots in this figure. Furthermore, as demonstrated by the black dots in the figure, if the truncation point of the zeroth level is increased freely, we obtain even a greater accuracy than that in the accuracy obtained in three levels by repeated optimal truncation. Grey and light blue lines illustrate the reducing behaviour of the error estimates for the zeroth and first levels, respectively. Level one decreases faster than level zero as can be seen from the same figure. Figure 4.11 also shows that the truncated series grow like factorial-over-a-power form.

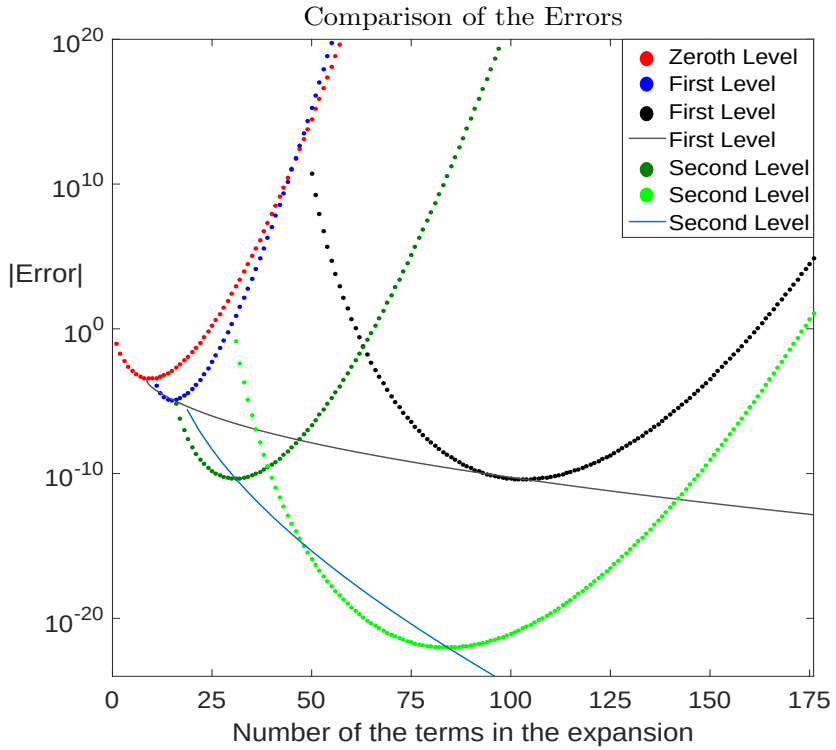


Figure 4.11 Magnitude of the errors, respectively given by (4.12), (4.34) and (4.84) in 3 levels of the expansion where the series are truncated optimally at each level and arbitrarily at the zeroth and the first levels for chosen $\varepsilon = 0.1$ with $z = 1/2 + i\sqrt{3}/2$. The figure clearly shows the improvement obtained by hyperasymptotics; the error decreases at each level. Black and light green dots respectively correspond to the various truncation points of the zeroth and the first levels rather than optimal truncation. Blue and grey lines show the behaviour of level one and two errors when they are written as a function of ν_0 and ν_1, respectively. They touch the minimum points of the green and black dots, respectively, whilst decreasing; indeed, the speed observed in the second level is faster than that in the first level.

Having selected the zeroth level and the first level truncation points arbitrarily and increased them, the second level error is diminished as it did in the preceding level.

4.10 Third level of hyperasymptotics and Stokes lines

Finally, the corresponding calculation of this level will be done briefly without going into much detail. In order to continue to the third level of expansion, we first re-scale the remainder equation of (4.80) such that

$$\mathfrak{R}_{N_2}(z) := \varepsilon^{N_2}\left(1-\frac{\nu_0}{z}\right)\left(1-\frac{\nu_1}{z-\nu_0+\nu_0\ln\left(\frac{\nu_0}{z}\right)}\right)S_{N_2}(z)T(z), \tag{4.89}$$

where $T(z)$ is an unknown function of z and will be discussed shortly. Similar to that in the previous level, it is worth pointing out that since we approximate the RHS of the equation by its factorial-over-a-power representation, which we applied twice so far, first and second levels are not exact. Thus, the third level expansion does not have an exact representation. Therefore, some of the results may be questionable. Since (4.89) has to satisfy (4.80), back substitution of this last equation into the second level remainder differential equation given in (4.80) yields a new differential equation involving only derivatives for $T(z)$ when N_2 is large for small ε,

$$\varepsilon\frac{dT(z)}{dz}+\left(1-\frac{\nu_0}{z}\right)\left(1-\frac{\nu_1}{z-\nu_0+\nu_0\ln\left(\frac{\nu_0}{z}\right)}\right)\left(1-\frac{\nu_2}{u_2(z)}\right)T(z)\sim 1. \tag{4.90}$$

Note that the third level equation preserves all the pre-factors of the previous levels which will cause branch cuts. As in the second level, (4.90) satisfies the equation (3.25) given in §3.4. To proceed, let us expand $T(z)$ as a usual perturbation series into powers of ε

$$T(z)\sim\sum_{n=0}^{\infty}\varepsilon^n T_n(z). \tag{4.91}$$

Back substitution of this expansion into (4.90) generates the leading order term at

O(1) and the differential recurrence relation of $T_n(z)$ at $\mathrm{O}(\varepsilon^n)$

$$\begin{aligned} T_0(z) &= \left(\frac{z}{z-\nu_0}\right)\left(\frac{z-\nu_0+\nu_0\ln\left(\frac{\nu_0}{z}\right)}{z-\nu_0+\nu_0\ln\left(\frac{\nu_0}{z}\right)-\nu_1}\right)\left(\frac{u_2(z)}{u_2(z)-\nu_2}\right), \\ \frac{dT_{n-1}(z)}{dz} &+ \left(1-\frac{\nu_0}{z}\right)\left(1-\frac{\nu_1}{z-\nu_0+\nu_0\ln\left(\frac{\nu_0}{z}\right)}\right)\left(1-\frac{\nu_2}{u_2(z)}\right)T_n(z)=0, \end{aligned} \tag{4.92}$$

where $n \geq 1$. It is crucial to emphasise that the leading order term $T_0(z)$ has singularities at $z=\nu_0$ and where z is the solution of

$$z-\nu_0+\nu_0\ln\left(\frac{\nu_0}{z}\right)=\nu_1 \quad \text{and} \quad u_2(z)=\nu_2, \tag{4.93}$$

but, as explicated earlier, $z=\nu_0$ and the solution of the leftmost equation of (4.93) are actually not singular points, since each preceding level solves its succeeding level singulant; in fact, they will appear as the branch points of the current level soon. All $T_n(z)$ terms must have singularities at the same points with $T_0(z)$; hence, $T_n(z)$ is more singular than $T_0(z)$. As in the previous steps, because it is impossible to generalise the late-order terms by successively integrating the recursion relation in (4.92), a general solution of the terms $T_n(z)$ is sought to be in the factorial-over-a-power form, that is,

$$T_n(z) \sim \frac{\Gamma(n+\gamma_3)}{u_3(z)^{n+\gamma_3}}\left(D_0(z)+\frac{1}{n}D_1(z)+\frac{1}{n^2}D_2(z)+\ldots\right) \quad \text{as } n\to\infty, \tag{4.94}$$

where $\gamma_3=\mathrm{O}(1)$ is an arbitrary constant; and $u_3(z), \gamma_3$, and $D_i(z)$'s are independent of n. Note that $u_3(z)$ is required to vanish at the singularities of the leading order term. Hence, performing the first derivative of (4.94) as well as (4.94) itself into the recursive relation of (4.92), we deduce the singulant after some computations as

$$\begin{aligned} u_3(z) =& \nu_2\ln\left[\nu_1\ln\left(\frac{z-\nu_0+\nu_0\ln(\nu_0/z)}{\nu_1}\right)+\nu_0\ln\left(\frac{z}{\nu_0}\right)-z+\nu_0+\nu_1\right] \\ &+z-\nu_0\ln(z)-\nu_1\ln\left[z-\nu_0+\nu_0\ln\left(\frac{\nu_0}{z}\right)\right]+C_4, \end{aligned} \tag{4.95}$$

where C_4 is a constant of direct integration which may be calculated similarly to (4.76). Because singularities of $T_0(z)$ given in (4.93) are the zeros of $u_3(z)$, and since we know the following equation from the zeros of previous singulant $u_2(z)$ of the second level, we can substitute the equation

$$\nu_1 \ln\left[z-\nu_0+\nu_0\ln\left(\frac{\nu_0}{z}\right)\right]+\nu_0\ln(z)-z=\nu_2+\nu_1\ln(\nu_1)+\nu_0\ln(\nu_0)-\nu_0-\nu_1, \tag{4.96}$$

into (4.95), whereupon the constant C_4 can be derived accordingly as below

$$C_4=-\nu_2\ln(\nu_2)+\nu_1\ln(\nu_1)+\nu_0\ln(\nu_0)+\nu_2-\nu_1-\nu_0. \tag{4.97}$$

Hence, the third level singulant, $u_3(z)$, of the exponential integral (4.1) is completely determined by means of

$$\begin{aligned} u_3(z)=\nu_2\ln&\left[\frac{\nu_1\ln\left(\dfrac{z-\nu_0+\nu_0\ln(\nu_0/z)}{\nu_1}\right)+\nu_0\ln(z/\nu_0)-z+\nu_0+\nu_1}{\nu_2}\right]\\ &+z+\nu_2-\nu_1-\nu_0+\nu_0\ln\left(\frac{\nu_0}{z}\right)+\nu_1\ln\left[\frac{\nu_1}{z-\nu_0+\nu_0\ln(\nu_0/z)}\right], \end{aligned} \tag{4.98}$$

which equivalently can be rewritten in terms of $u_1(z)$ and $u_2(z)$ as

$$\begin{aligned} u_3(z)&=\nu_2\ln\left[\frac{\nu_1\ln\left(\dfrac{u_1(z)}{\nu_1}\right)-u_1(z)+\nu_1}{\nu_2}\right]+\nu_2-\nu_1+u_1(z)+\nu_1\ln(\nu_1)-\nu_1\ln(u_1(z))\\ &=\nu_2\ln(u_2(z))-\ln(\nu_2)+\nu_2-u_2(z). \end{aligned} \tag{4.99}$$

It is worth expressing here that, besides the main branch cut of level zero at $z=0$, the above singulant has branch cuts at $z=\nu_0$, and when z is a solution of $z-\nu_0+\nu_0\ln(\nu_0/z)=\nu_1$ due to the logarithmic singularities at these points. This will be shown in Figure 4.12 by grey and green zigzag lines. Although we will not investi-

gate the third level remainder in detail, having determined the third level singulant allows us to truncate the series in addition to examining the truncated remainder; in particular, that is

$$T(z) \sim \sum_{n=0}^{N_3-1} \varepsilon^n T_n(z) + \mathscr{R}_{N_3}(z). \tag{4.100}$$

For the sake of brevity, we only note that $D_i(z)$ in (4.94) are constants which could be calculated as in (4.21). Since the general term of the expansion has been determined, the third level error arising due to truncation can be defined by back substitution of (4.89) into (4.82) as

$$E_{N_3}(z) := \frac{\varepsilon^{N_0+N_1+N_2+N_3} N_0!}{z^{N_0+1}} \left(\frac{z-\nu_0}{z}\right)^2 \left(1 - \frac{\nu_1}{z-\nu_0+\nu_0 \ln\left(\frac{\nu_0}{z}\right)}\right) Q_{N_1} S_{N_2}(z) T_{N_3}(z), \tag{4.101}$$

which will be used while comparing the errors of each level with each other in Figure 4.13. However, at each level, since we obtain more accurate approximations than in the previous levels and more importantly due to the diminishing behaviour of the first level error estimate, this particular problem is analysed only in four levels without remainder analysis for the third level. Furthermore, as the singulant is derived precisely, the third level putative Stokes and anti-Stokes lines of the expansion can be plotted as in §4.4. Third level Stokes lines emerge when $u_3(z)$ satisfies $\Im(u_3(z)) = 0$ while $\Re(u_3(z)) > 0$, and third level anti-Stokes lines emerge when $\Re(u_3(z)) = 0$. As similar calculations have been conducted in the previous sections and chapters in detail, in this section the illustration of the Stokes and anti-Stokes lines and the associated branch cuts are only provided in Figure 4.12. As discussed earlier, because the singularities of the expansion cannot be approached by the singulant individually, we plot the putative Stokes lines. The figure demonstrates that across the anti-Stokes lines active Stokes lines become inactive; particularly, beyond these lines real part of the singulant changes its sign which happens by the turning points.

On the other hand, the successive optimal truncation points for selected $\varepsilon = 0.1$ and $z = 1/2 + i\sqrt{3}/2$ to the nearest integer values are

$$N_0 = 10, \;\; N_1 = 5, \;\; N_2 = 16, \;\; \text{and} \;\; N_3 = 35, \tag{4.102}$$

respectively, which may also be seen in Figure 4.13. It is interesting that the relative lengths of the optimally truncated series first decrease in the first level and then increase in the further levels. Hence, for this particular problem the hyperasymptotics do not terminate. Moreover, how this behaviour of the length of truncated series relates to the size of the singulants is unclear in this conjecture.

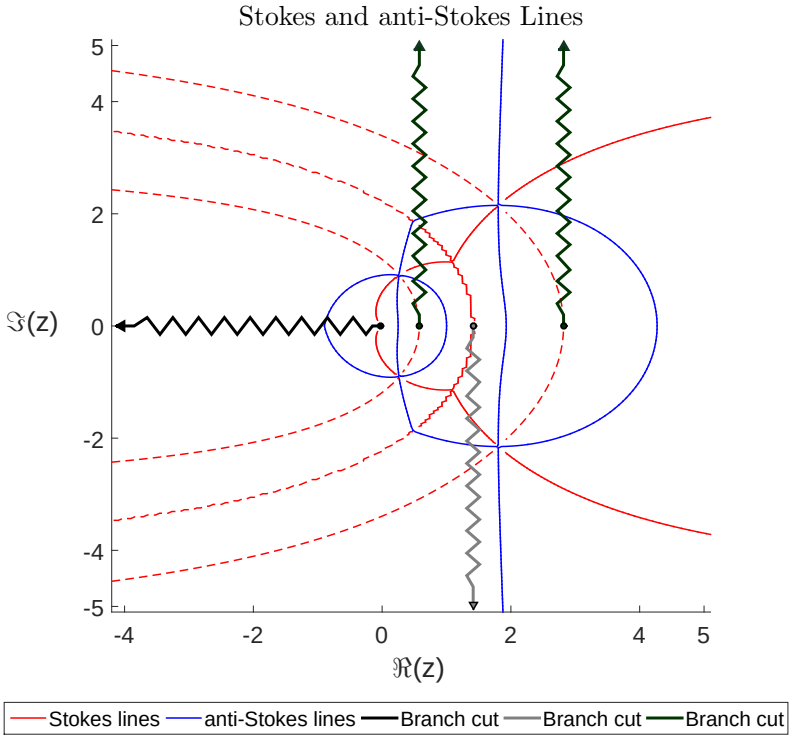


Figure 4.12 Red and blue lines demonstrate the Stokes and anti-Stokes lines of the equation (4.90) plotted by its singulant (4.98), respectively, with the branch cuts of the equation shown in black, grey and green. In this figure, $\nu_0 = |1+i|$ derives $\nu_1 = 0.4288$ and $\nu_2 = 1.405$ in accordance with their definitions in (4.31) and (4.81), respectively.

We conclude the present section with expository figures. Because all four level sin-

gulants and the remainders of the expansions are determined, they can be plotted together. Figure 4.13 demonstrates the exponential accuracy we obtain via hyperasymptotics at four levels when the relevant series are truncated optimally. Moreover, the figure also shows that if we increase the truncation point of the first level arbitrarily, we decrease the associated error estimate better than the estimate obtained by successive optimal truncations by the third level; specifically, see and compare the dots representing the second level error in green with the dots representing the third level error in black. In fact, increasing the zeroth level truncation point arbitrarily in level one even decreases the level one error $E_{N_1}(z)$ faster than the third level error of successive optimal truncation. To visualise this, compare the dotted line in light blue with the black dots of the third level in Figure 4.14. Nonetheless, as discussed in the previous section, increasing N_0 in $E_{N_2}(z)$ decreases the error, but not as fast as increasing N_1; particularly, compare the green dashed lines with the green dots in Figure 4.14, in which N_0 and N_1 are increased respectively. Note that to avoid confusion with colours in the figure, some of the error plots are represented with dashes rather than dots.

4.11 Comparison and conclusions

In conclusion, we have derived the asymptotic series solution of the exponential integral and investigated its approximate solution by successfully applying the methods of hyperasymptotics. We conducted the investigations by expressing the truncated remainders as an asymptotic power series containing its own remainder and went beyond the superasymptotic expansion. Compared to the previous chapters, three more levels of analysis in hyperasymptotics were performed subsequently to ensure agreement with the results of each level. In fact, the resultant remainder differential equations, as well as their relevant singulants, were much more complicated with increasing levels. Investigations of the remainders showed that information extracted by hyperasymptotics cannot be attained by the Poincaré's asymptotic techniques.

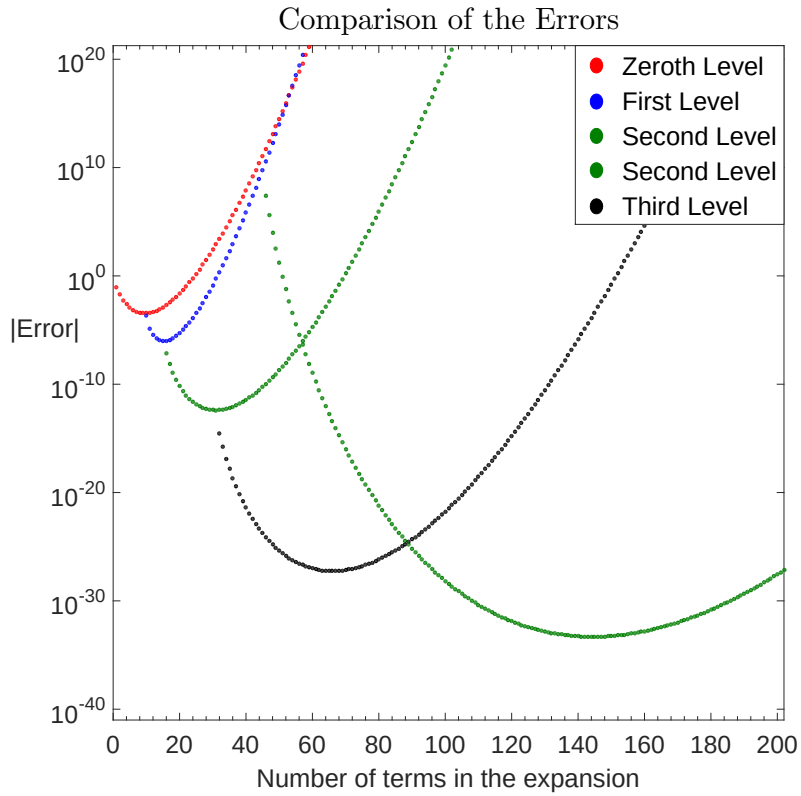


Figure 4.13 Magnitudes of the errors, given in (4.12), (4.34), (4.84) and (4.101), in 4 levels of the expansion where the series are truncated optimally at each level for randomly chosen $\varepsilon = 0.1$ with $z = 1/2 + i\sqrt{3}/2$. The figure shows the improvement obtained by the hyperasymptotics at four levels. The error decreases at every further level, and the corresponding optimal truncation points are $10, 5, 16$, and 35, respectively. Comparing the green dots shows that increasing the truncation point of the first level arbitrarily in the second level error increases the accuracy exponentially.

In addressing the hyperasymptotics, some common features arising by exponential asymptotics have been demonstrated.

To perform the methods in exponential asymptotics after the zeroth level, the examination process consists of to re-scaling the remainders according to the RHS of the remainder differential equations. The system, hence, produced new singular perturbation equations, which were expanded as a power series of small parameter, ε. Their associated divergent series have been obtained by performing 'factorial/power' method. Because the general terms were found by this method, we have not obtained

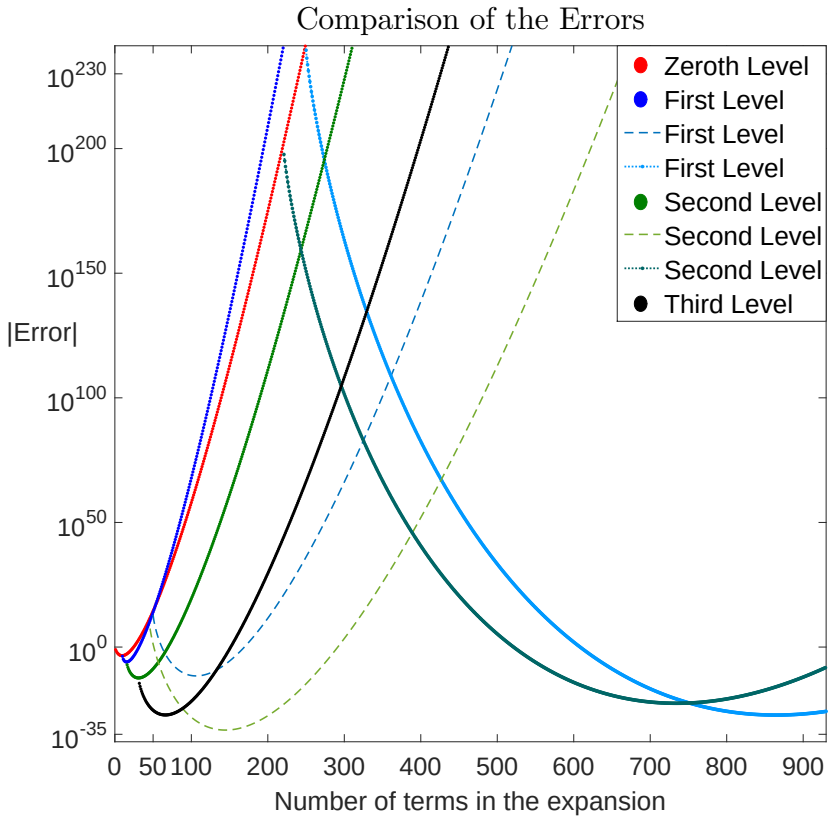


Figure 4.14 Red, blue, green and black lines indicate magnitudes of the errors in (4.12), (4.34), (4.84) and (4.101), respectively for arbitrarily chosen $\varepsilon = 0.1$ and $z = 1/2 + i\sqrt{3}/2$. Figure represents the comparisons of the errors with each other in four levels truncated optimally and arbitrarily. It shows that the first and the second level errors decrease as the number of the terms is increased.

the close expressions for them contrary to the general term in the zeroth level. Therefore, these levels of calculations and their relevant figures needed to be treated with caution. Analysing the leading order behaviour, we derived the singularities of the expansions, from which the relevant singulants were completely determined. Having located the Stokes lines, we were able to demonstrate the switching on and off behaviour of the subdominant exponential terms across the Stokes lines. However, second and third level singulants need further analysis since they are not separately factored out by their singular points.

Analysis of the truncation errors was conducted in sections §4.5 and §4.9 more gen-

erally, instead of analysing only one truncation point. Specifically, in the first level it was represented as a function of ν_0 and θ, and the reducing behaviour of error as the number of the terms in the first level is increased was established. In fact, having written out the level one truncation point ν_1 as a function of the level zero truncation point ν_0 by minimising the error, we have further confirmed that the error decreases as we increase ν_0. In the latter cases, the error has been expressed in terms of ν_1, ν_0 and θ. Likewise, increasing the zeroth or the first level truncation points decreased the error; however, the first level truncation point reduced the error faster than the zeroth level. Examining the errors in terms of θ showed that the accuracy of the error further depends on θ; importantly, at the Stokes lines, the improvement of the hyperasymptotics is stopped. However, as we moved away from the Stokes lines, the improvement is increased dramatically. The analytical analysis and figures for both the first and second levels of errors showed an agreement. Furthermore, as seen in figures such as Figure 4.13, optimal truncation points increased after the first level; hence, hyperasymptotics by optimal truncation is not finite.

Throughout the current chapter, it is interesting to point out that, although the singularities of previous levels are not turning points in each subsequent level, the singular points of all preceding levels appeared in the logarithmic function of the singulants at the next levels. Therefore, they generated logarithmic branch cuts. To conclude, each level of investigation produced an exponential improvement through each level. Through a simple differential equation we described how the method of hyperasymptotics can be studied and focused on presenting the details of the hyperasymptotics. The concept of multi-level asymptotics was introduced by investigating the inhomogeneous remainder differential equation of the resultant remainders. Figure 4.13 and Figure 4.14 briefly illustrate the present outcomes. We aim to apply this method to more complex problems throughout the rest of the thesis. Particularly, in §§5, 6 and 7, the main idea of this chapter will be performed while investigating the behaviour of the error, Airy and confluent hypergeometric functions using the multi-

level asymptotics.

In comparison with the hyperasymptotic expansion method of Berry and Howls [33], their implementation of method is discussed for integrals with saddles and they applied the steepest descent method to expand the integrands, and no Borel's summation was employed. Berry and Howls discovered that the number of the terms in each hyperseries is half the number of the terms at the preceding stage, and concluded that the hyperasymptotics is finite. In that paper, the error of the final remainder roughly approximated to $\exp(-2.39A|k|)$. However, our approach differs from that of [33], as we develop a scheme of reexpansion of the remainders by obtaining and interpreting the inhomogeneous remainder differential equation. Each truncated remainder is expressed as a new asymptotic series and we do not use integral representations. In our method optimal number of the terms needed in the each series increases; whence, hyperasymptomatic expansion does not halt and the process can be repeated any number of times. We also interpreted the errors as a function of the preceding stages truncation points and allowed all the values of truncation points to vary (to reduce the error), not only the last truncation point. The singularity of the expansion moves to infinity and causes a logarithmic discontinuity at the succeeding and higher levels. Moreover, our expansion is valid at locations both near and far from the Stokes lines. The error almost stops at the Stokes lines, and decreases dramatically faster as we move away from the Stokes lines.

Chapter 5

Error function

5.1 Introduction

In §4, the methodology of hyperasymptotics was illustrated considering the exponential integral. In this chapter, we will discuss this technique applied to differential equations and express the asymptotic behaviours of the equations. The illustrative examples of the present chapter are differential equations of the error function which are a simple form of the hyperasymptotics. We will consider the following first and second order differential equations for $g(z)$

$$\frac{dg(z)}{dz} = -\frac{1}{\varepsilon^2}\exp\left(-\frac{z^2}{\varepsilon^2}\right), \tag{5.1}$$

and for $y(z)$

$$\varepsilon^2\frac{d^2y(z)}{dz^2} + 2z\frac{dy(z)}{dz} = 0, \tag{5.2}$$

in which $0 < \varepsilon \ll 1$, and from both the error function occurs [78]. These equations can be analysed with the method of exponential asymptotics since the highest derivatives are multiples of the small parameter ε. In fact, because we often address the exponential asymptotics in the limit of some small parameter, (5.2) is obtained after rescaling the large parameter $z_1 = z/\varepsilon$ where $z = \mathrm{O}(1)$ to ensure a similar form to

the first one. Note that similar rescaling will be done in §§6-8. In a similar manner to chapters §§2-4, the analysis of these equations will enable us to demonstrate the hyperasymptotics. Particularly, this chapter presents the hyperasymptotic solutions of the error function in two levels with two different equations. In addition to hyperasymptotic investigation, while discussing their asymptotic behaviours and presenting the Stokes switching near their singularities along with other features, we will demonstrate how the new method developed throughout §4 may be applied to the examination of these differential equations.

The present chapter is organised as follows: In §5.2 the differential equation (5.1) will be solved exactly by direct integration so that the error function can be observed. In this section we will analyse the differential equation asymptotically by expanding it in powers of ε. The crucial point of the expansion is to derive its leading order term which contains a singularity that must be preserved in the general term. It will, then, be truncated optimally to examine the truncated remainder which is to be exponentially small at this stage. Hence, the next step is to analyse the remainder and to present the exponential terms of the expansion. In §5.2.2, Stokes and anti-Stokes lines will be located, and the switching behaviour of the subdominant exponentials will be illustrated; in particular, we will discover which exponentials are present in which sectors of the z plane, which will be the last step of the zeroth level. In §5.2.3, we will begin the analysis of the first level; specifically, we will re-expand the zeroth level remainder and then repeat the process of truncation optimally and arbitrarily, then examine the new remainder and consider its behaviour near the singularities to obtain the location of the first level Stokes (and anti-Stokes) lines. Furthermore, to observe the accuracy of the hyperasymptotic expansion, the error of the zeroth and the first levels expansions will be compared. By the end of this subsection, we minimise the first level error with respect to the arbitrary truncation points with the same manner as explained in §4. Finally in §5.2.5, first level Stokes (and anti-Stokes) lines, as well as the presence and absence of the exponential contributions will be

illustrated. In §5.3, the same investigation described above will be performed for the second order differential equation (5.2) in two levels. §5.4 contains the comparison and conclusion of both equations with a discussion of the present chapter.

5.2 First order differential equation for the error function

We begin this section by constructing an asymptotic expansion of the error function using power series. Before illustrating the hyperasymptotic technique, however, we first solve the differential equation in (5.1) with direct integration, which yields the error function erf

$$g(z) = -\frac{\sqrt{\pi}}{2\varepsilon}\text{erf}\left(\frac{z}{\varepsilon}\right) + C, \tag{5.3}$$

where C is an unknown constant of integration. More information on the behaviour of the solutions of the differential equation, given in (5.1), can be obtained by transformation of the equation. Particularly, motivated by the form of the RHS of (5.1), let us re-scale $g(z)$ such that

$$g(z) = \exp\left(-\frac{z^2}{\varepsilon^2}\right) f(z). \tag{5.4}$$

Straightforward substitution of (5.4) into the original differential equation enables us to obtain a differential equation for $f(z)$

$$\varepsilon^2 \frac{df(z)}{dz} - 2zf(z) = -1, \tag{5.5}$$

where we seek to determine the asymptotic behaviour of the solution of (5.5) for sufficiently small ε. We observe that the pre-factor of $f(z)$ is equal to zero at $z = 0$, which is the turning point. In fact, this point must be present in a denominator of the late order terms, when it is expanded, like the examples investigated earlier in §§3

and 4. Additionally, notice particularly that it is similar to the example 3.3.1 considered in §3 so that they should have similar outcomes, such as optimal truncation points, singulants and Stokes (and anti-Stokes) lines which will be addressed shortly. Before embarking on the asymptotic analysis of (5.5), solving this differential equation directly by integration factor method generates

$$f(z) = \left(-\frac{\sqrt{\pi}}{2\varepsilon} \mathrm{erf}\left(\frac{z}{\varepsilon}\right) + C \right) \exp\left(\frac{z^2}{\varepsilon^2}\right), \tag{5.6}$$

which is exactly the same as (5.3) when multiplied with $\exp(-z^2/\varepsilon^2)$. The differential equation of $f(z)$ is in the form of the highest derivative multiplied by the small term ε^2; therefore, we can employ exponential asymptotics in this differential equation.

5.2.1 Zeroth level of hyperasymptotics: superasymptotics

We next focus on solving the transformed differential equation using hyperasymptotic techniques; in particular, we will discuss the superasymptotics in this subsection. In order to do so, let us begin to expand $f(z)$ in (5.5) in powers of ε^2 with the conventional method such that

$$f(z) \sim \sum_{n=0}^{\infty} \varepsilon^{2n} f_n(z), \tag{5.7}$$

in which we are interested in determining the asymptotic behaviour of the solution and investigating the remainder in the truncation point. To achieve this, we must first identify the general terms of the series as $n \to \infty$. Substituting the perturbation expansion (5.7) into the differential equation (5.5) yields

$$\sum_{n=0}^{\infty} \varepsilon^{2n+2} \left(\frac{df_n(z)}{dz} - 2z f_{n+1}(z) \right) - 2z f_0(z) = -1. \tag{5.8}$$

Balancing like powers of ε at the leading order $\mathrm{O}(\varepsilon^0)$ gives the first term explicitly

$$f_0(z) = \frac{1}{2z}. \tag{5.9}$$

We note that this uniquely determined leading order term of (5.9) contains a singularity lying at $z = 0$, which agrees with the statement made earlier regarding the prefactor of the equation (5.5). The two-term recursion relation of the perturbation expansion at $\mathrm{O}(\varepsilon^{2n+2})$ can be obtained from (5.8) as

$$\frac{df_n(z)}{dz} - 2zf_{n+1}(z) = 0. \tag{5.10}$$

This shows that the $(n+1)^{th}$ term of the expansion can be derived from the first derivative of the n^{th} term. Moreover, since each term of the expansion is derived by differentiation of its predecessor, the strength of the singularity will grow in each level. To proceed, making use of the recursion relation repeatedly between the $(n+1)^{th}$ term and the previous n^{th} term gives the general term of the expansion in the complete form, that is,

$$f_n(z) = \frac{(-1)^n(2n)!}{n!\,(2z)^{2n+1}}, \tag{5.11}$$

which is consistent with the well known approximation of the usual error function [73, 74]. In this case, we have been able to establish the complete derivation of the asymptotic expansion $f_n(z)$ easily. Although it could be explicitly determined by repeated differentiation via recursion relation, in general it is not straightforward to directly derive the exact representation of the n^{th} term $f_n(z)$ in the expansion. For such cases, we employ the factorial-over-a-power method to obtain the late-order term and make sure that the singularity of the leading order term is consistent with $f_n(z)$ [62] at every order; we use this method in §5.2.3. It is worth remarking here that substitution of $f_n(z)$ into (5.4) via (5.7) produces an asymptotic expansion of erf(z), which could also be shown by repeated differentiation of (5.1). As the

asymptotic behaviour of such a solution is already obtained for small ε, it is now natural to ask in which point we can obtain the greatest accuracy if this divergent asymptotic series is truncated. The next step is hence to truncate this expansion (5.7) after N_0 terms

$$f(z) = \sum_{n=0}^{N_0-1} \varepsilon^{2n} \frac{(-1)^n (2n)!}{n! \, (2z)^{2n+1}} + R_{N_0}(z), \tag{5.12}$$

where $R_{N_0}(z)$ is the remainder of the truncated expansion, whereby the zeroth level truncation error may be defined as

$$E_{N_0}(z) := \varepsilon^{2N_0} \frac{(-1)^{N_0} (2N_0)!}{N_0! \, (2z)^{2N_0+1}}. \tag{5.13}$$

The remainder must be exponentially small rather than algebraically small in ε as $\varepsilon \to 0$ when the expansion truncated optimally, since the optimal truncation cancels out the ε^{N_0} terms in the expansion. Therefore, we need to pay attention to investigating the remainder terms after truncation. Substitution of the truncated expansion (5.12) into the original differential equation gives an inhomogeneous remainder differential equation for $R_{N_0}(z)$

$$\begin{aligned} \varepsilon^2 \frac{dR_{N_0}(z)}{dz} - 2zR_{N_0}(z) &= -\varepsilon^{2N_0} \frac{df_{N_0-1}(z)}{dz} \\ &= \varepsilon^{2N_0} \frac{(-1)^{N_0+1} (2N_0)!}{N_0! \, (2z)^{2N_0}}. \end{aligned} \tag{5.14}$$

The RHS of (5.14) can be obtained easily by the recursive relation (5.10) or can be deduced by differentiating (5.11) once. To derive the optimal number of terms needed in (5.7), the optimisation methods provided in (2.9) of §2 deduce that the optimal truncation point occurs approximately for sufficiently large n as $\varepsilon \to 0$ at

$$N_0 \sim \frac{|z^2|}{\varepsilon^2}. \tag{5.15}$$

To make sure that the point of optimal truncation takes an integer value, α is added into (5.15), giving

$$N_0 = \frac{|z^2|}{\varepsilon^2} + \alpha, \tag{5.16}$$

where α is bounded as in (3.14) of §3.2 while $\varepsilon \to 0$. The magnitude of the divergent expansion takes its minimum value at this point; which in turn means that the error of the zeroth level of the expansion has been minimised. Note that the optimal truncation point is the same as the magnitude of the power of the exponential term obtained in the homogeneous solution (5.3).

Once the singularities and the general term of the expansion are obtained, we expect to find the Stokes and anti-Stokes lines which stem from the singularities as well as what happens on and across these lines. Therefore, in the next subsection, the Stokes lines and their switching behaviour in the neighbourhood of the singularities will be discussed in detail.

5.2.2 Stokes and anti-Stokes lines

Having established the asymptotic series solution and the optimal truncation point, we are now ready to present more information regarding the Stokes (and anti-Stokes) lines of the differential equation in (5.5) from its singulant and observe the switching on and off behaviour of the exponentials across them. Specifically, we anticipate to have a Stokes line when the singulant satisfies the condition (i) in §3.3, i.e.,

$$\Im(-z^2) = 0 \quad \text{while} \quad \Re(-z^2) > 0, \tag{5.17}$$

where $z = x + iy$. This implies they occur when

$$x = 0 \quad \text{while} \quad y^2 > 0, \tag{5.18}$$

in which Stokes switching occurs and forcing of the remainder becomes maximal. We remark that the real part of the singulant being negative in above (5.17) corresponds to inactive Stokes lines. Likewise, the position of the anti-Stokes lines can

be obtained via

$$\Re(-z^2) = 0, \tag{5.19}$$

which transpires when

$$x = \pm y. \tag{5.20}$$

Across the anti-Stokes lines exponentials change their behaviour from being dominant to subdominant or vice-versa which means anti-Stokes lines indicate the region of the complex plane where the exponential is dominant. Stokes and anti-Stokes lines can be determined through the exponential terms of (5.3): one can be obtained from the homogeneous solution as $\exp(z^2/\varepsilon^2)$ while the other is derived from the RHS of the differential equation as $\exp(0)$, which will yield the same result as above. These are all shown in Figure 5.1, in which $\exp(z^2/\varepsilon^2)$ and $\exp(0)$ are labelled by ① and ⓪, respectively. This figure further illustrates the sectors in the z-plane where these exponential terms are present. In order to see it, we need to make a full circuit around the complex plane. Suppose we are in Sector II of Figure 5.1 and ⓪ is present there. We travel through Sector I, IV and III in the clockwise direction. As we cross the Stokes line from Sector II to Sector I, ① gets turned on by ⓪ and it must be added to the solution. Thus, ⓪ and ① are both present in Sector I. As the Stokes line from Sector I to Sector IV is inactive, no change is observed as we move downward, i.e., ⓪ and ① are also present in Sector IV. However, crossing through Sector III, ① is switched off by ⓪ across the Stokes line. Therefore, ① is not present in Sector III. Since the Stokes line is inactive while travelling upward from Sector III toward to Sector II, again nothing gets turned on and off; hence, ⓪ stays present in Sector II. As we arrive at the point of initiation, we conclude that we return to where we started in which we began with an assumption that ⓪ was present. In other words, through this circuit around the plane, we have observed that the resultant asymptotic contribution is identical to the initial contribution. Note that Figure 5.1 is in the same form as Figure 3.1 since their corresponding differential equations come from the same family.

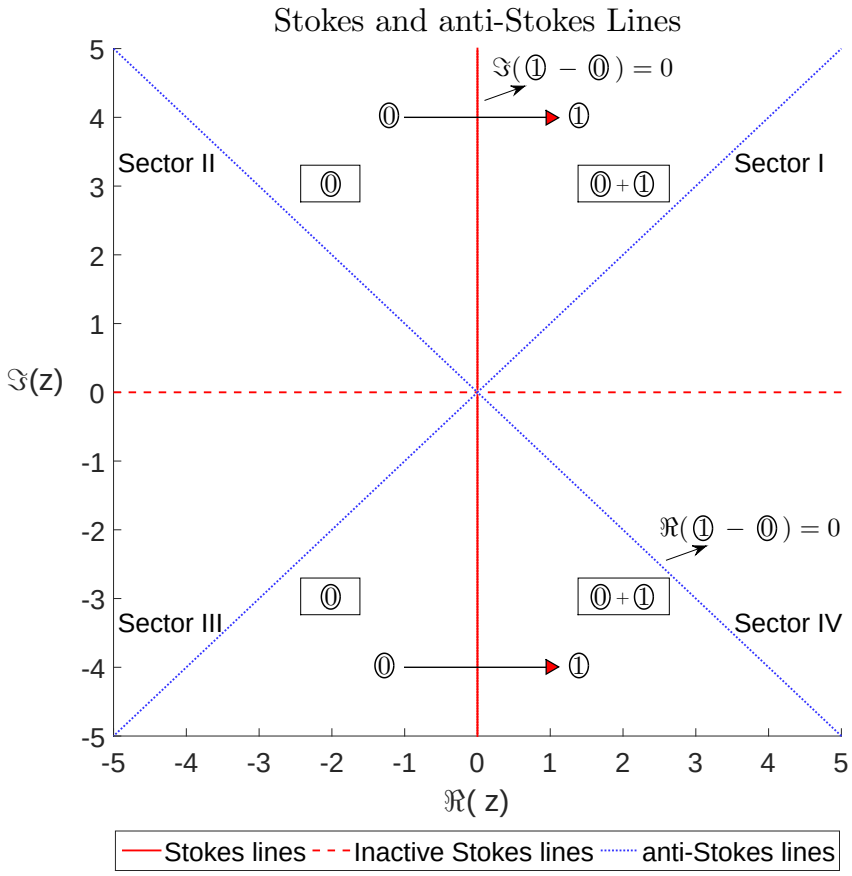


Figure 5.1 Red lines indicate the Stokes lines while dotted blue lines represent the anti-Stokes lines. Across the Stokes lines, ① is switching on and off by ⓪. Present exponentials of the relevant sectors are shown in boxes.

The main observation is that the Stokes switching on and off of the subdominant exponentials across the Stokes lines mostly happens smoothly by the error function. We can investigate this smoothing through the local analysis near the singularity. In order to avoid repetition, we will not present the error function smoothing of the error function. Refer to §2.5 for details. This process is also detailed by Berry in [51].

The idea of hyperasymptotics lies under a simple question: "can we do better?". As the level zero in hyperasymptotics is fully completed, we ask ourselves whether we can do better and improve the precision of the expansion. Therefore, in the subsequent subsections we will answer this question. We begin in §5.2.3 by re-expanding

the level zero remainder. This method involves deriving the form of the later order terms, truncating the series in the sense of §4 and keeping the truncation points arbitrary to minimise the first level error. While considering the behaviour of the remainder, we will observe the Stokes (and anti-Stokes) lines.

5.2.3 First level of hyperasymptotics

This section goes beyond superasymptotics since it seeks further improvement of the exponentially small remainder. As the procedure of investigation in the first level of hyperasymptotics is similar with the one we performed in §4, we will therefore begin straightaway to re-scale and re-expand the remainder function $R_{N_0}(z)$ asymptotically in order to analyse (5.14), yielding

$$R_{N_0}(z) = \varepsilon^{2N_0} \frac{(-1)^{N_0+1}(2N_0)!}{N_0!\,(2z)^{2N_0}} Q(z), \tag{5.21}$$

where $Q(z)$ is to be determined. Substituting (5.21) in (5.14) yields a differential equation involving only $Q(z)$

$$\varepsilon^2 \frac{dQ(z)}{dz} - 2z\left(1 + \frac{\nu_0}{z^2}\right) Q(z) = 1, \tag{5.22}$$

where ν_0 is set to be $\nu_0 \sim \varepsilon^2 N_0$ which is motivated by the form of N_0 given in (5.15), but corresponds to the arbitrary selection of N_0. As elucidated in §3, the first level differential equation of hyperasymptotics is in the form of equation (3.1) which was analysed for various pre-factors of $Q(z)$. The differential equation has turning points at $z = \pm i\sqrt{\nu_0}$ each of which will be a term of the singulants [79]. For a detailed discussion of this type of differential equation that is faced on the first level, refer to §3. As in §5.2.1, the second step in the procedure is expansion; thus, expanding $Q(z)$ with respect to the small parameter ε as in (5.7) yields:

$$Q(z) \sim \sum_{n=0}^{\infty} \varepsilon^{2n} Q_n(z), \tag{5.23}$$

and substituting the expansion (5.23) back into equation (5.22), we find

$$\sum_{n=0}^{\infty} \varepsilon^{2n+2} \left(\frac{dQ_n(z)}{dz} - \left(2z + \frac{2\nu_0}{z} \right) Q_{n+1}(z) \right) - \left(2z + \frac{2\nu_0}{z} \right) Q_0(z) = 1. \quad (5.24)$$

Equating like powers of ε produces the leading-order term of the perturbation expansion explicitly

$$Q_0(z) = -\frac{z}{2z^2 + 2\nu_0}, \quad (5.25)$$

from which it is easily observed that the leading order term contains two symmetrical singularities at $z = \pm i\sqrt{\nu_0}$, and they are in fact to be the singularities of each term of the expansion. Therefore, we expect to have two series solutions, each of which must involve the relevant singularity in its singulants. Later we will establish that these are the singularities from which the switching on and off behaviour of the exponentially small terms sprout. After matching the asymptotic expansion at $\mathrm{O}(\varepsilon^{2(n+1)})$, $Q_n(z)$ and its successor satisfy the differential recurrence relation such that

$$\frac{dQ_n(z)}{dz} - \left(2z + \frac{2\nu_0}{z} \right) Q_{n+1}(z) = 0, \quad (5.26)$$

for $n \geq 0$. Having $Q_0(z)$ term and applying it directly in this recurrence formula to derive the next term, we obtain

$$Q_1(z) = -\frac{z\left(-z^2 + \nu_0\right)}{4\left(z^2 + \nu_0\right)^3}. \quad (5.27)$$

Although, in practice it is possible to derive next $Q_n(z)$ term via employing the recurrence relation repeatedly, since the numerators of the terms in each further level become more complicated than the previous one, these cannot be formulated in a certain form for large values of n. Meanwhile, note that the power of the singularities increases as odd numbers; in particular, their degree for any $Q_n(z)$ term becomes $2n+1$. This will be used later while establishing the general term of the expansion. Additionally, it is important to note that the expansion will be dominated by the

singularity based on the region when n gets larger. Thus, each singularity must be discussed separately in the neighbourhood of the Stokes lines. To locate Stokes lines of level one hyperasymptotics, it suffices to know the form of the late-order terms with its exact singulant. Hence, since it is not possible to write down the general term of the expansion via repeated differentiation and impose the recursion relation as in level zero. Therefore, let us assume it is in the form of a factorial-over-a-power, that is,

$$Q_n(z) = \frac{\Gamma(n+\gamma)}{u_1(z)^{n+\gamma}} \sum_{k=0}^{\infty} \frac{A_k(z)}{n^k}, \tag{5.28}$$

as $n \to \infty$, where γ is a constant, the singulant $u_1(z)$ and $A_k(z)$'s are independent from n; but they could be a function of z and are to be determined shortly. The next step is to apply this ansatz into the recursive relationship (5.26), which yields

$$\frac{\Gamma(n+\gamma)}{u_1^{n+\gamma}} \left[n \left(\frac{du_1}{dz} + 2z + \frac{2\nu_0}{z} \right) \frac{A_0(z)}{u_1} + \sum_{i=0}^{\infty} \frac{1}{n^i} \left[\left(\frac{du_1}{dz} + 2z + \frac{2\nu_0}{z} \right) \frac{A_{i+1}(z)}{u_1} - \frac{dA_i(z)}{dz} \right] \right] = 0. \tag{5.29}$$

Balancing the coefficients of the same powers of n, we find that the singulant $u_1(z)$ satisfies

$$\frac{du_1}{dz} + 2z + \frac{2\nu_0}{z} = 0, \tag{5.30}$$

in which $A_0(z) \neq 0$. It is worth remarking that assuming $A_0(z) = 0$ makes the general term of the expansion to be zero, therefore, it should not be zero. Nevertheless, notice that the derivative of $u_1(z)$ in (5.30) is exactly the same as the pre-factor of $Q(z)$ in (5.22). After applying (5.30) in (5.29), it is easy to evaluate that the part in summation gives

$$\frac{dA_i(z)}{dz} = 0, \tag{5.31}$$

from which, upon direct integration, it is apparent that

$$A_i(z) = c_i \quad \text{for } \forall \ i, \tag{5.32}$$

where c_is are arbitrary constants, and we take the leading order solution c_0 for large n in (5.28). Next we need to determine the singulant; therefore, integrating the equation (5.30) straightaway yields

$$u_1(z) = -z^2 - 2\nu_0 \ln(z) + C, \tag{5.33}$$

in which C is a constant of integration which can be determined from the singularities of the leading order term. Imposing the singular points into the singulant $u_1(z)$ derives the unknown constant in (5.33) exactly as

$$\begin{aligned} C_1 &= 2\nu_0 \ln(i\sqrt{\nu_0}) - \nu_0 \qquad \text{for} \quad z_1 = i\sqrt{\nu_0}, \\ C_2 &= 2\nu_0 \ln(-i\sqrt{\nu_0}) - \nu_0 \qquad \text{for} \quad z_2 = -i\sqrt{\nu_0}. \end{aligned} \tag{5.34}$$

Combining these constants of the singularities with (5.33) fully determines the singulants of the n^{th} term in the expansion such that

$$u_1^{\pm}(z) = -z^2 - 2\nu_0 \ln(z) + 2\nu_0 \ln(\pm i\sqrt{\nu_0}) - \nu_0, \tag{5.35}$$

in which the subscripts of the singulant $u_1(z)$ refer to the level of the hyperasymptotic expansion and the superscripts $\pm$ denote the the singulants of the level. Particularly, in the above equation, $u_1^+(z)$ corresponds to the singulant with the constant C_1, $u_1^-(z)$ is the singulant obtained with the constant C_2. The singulants $u_1^+(z)$ and $u_1^-(z)$ have logarithmic branch cuts when $z = 0$ due to the underlying factors discussed in §4.5. Substitution of both singulants including with the above constant A_i into the factorial-over-a-power method introduced in (5.28), we formally obtain two distinct expressions of the asymptotic expansion with respect to the turning points obtained in (5.25)

$$Q_n(z) \sim \frac{\Gamma(n+\gamma)}{\left(-z^2 - 2\nu_0 \ln(z) + 2\nu_0 \ln(\pm i\sqrt{\nu_0}) - \nu_0\right)^{n+\gamma}} c_0. \tag{5.36}$$

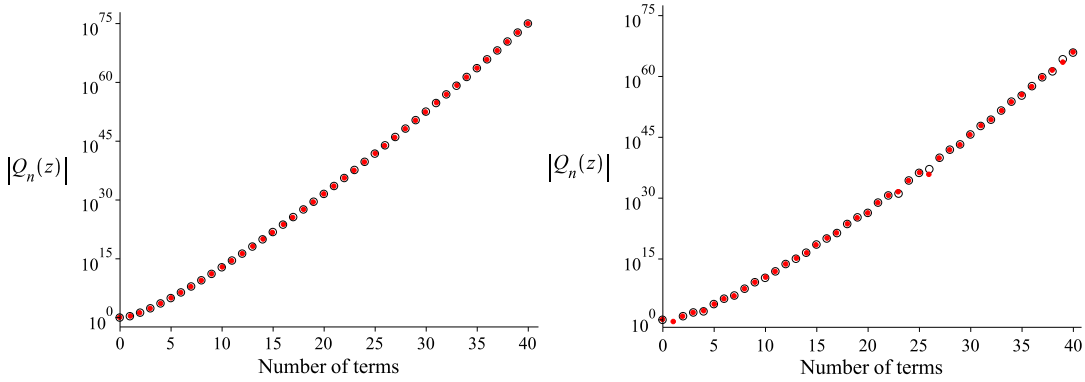
The asymptotic series solution of differential equation (5.22) is a linear combination of these two. Both contributions have the same strength for large n; particularly, based on the region we are in, the general term involving the relevant singularity becomes the dominant solution in the limit $n \to \infty$. This can be observed from Figure 5.3. As the sector is changed, such as from $\Im(z) > 0$ to $\Im(z) < 0$, the colours of the plots representing the relevant errors shift from green to blue or vice-versa. Another observation that can be made from Figure 5.3d is that if the values of z are to be chosen purely real, the errors occurring by $u_1^+(z)$ and $u_1^-(z)$ overlap each other since both have the same strength and cannot overpower each other as shown in Figure 5.3a, Figure 5.3b and Figure 5.3c. In light of the discussion made earlier in this subsection, we have sufficient information to derive the constant γ introduced in (5.26). The degree of the poles for the general term Q_n should have odd numbers; therefore, it is in fact $\gamma = 1/2$ due to

$$2(n+\gamma) = 2n+1 \implies \gamma = \frac{1}{2},$$

which ensures that the late-order terms of the expansion are consistent with each other. The only undetermined parameter of (5.36) is the constant c as yet. Unlike the subsection §5.2.1, because the factorial-over-a-power method is performed in order to determine the late order terms of the expansion in a certain form, there is a constant in (5.36). Indeed, this constant may be found via

$$c \approx \lim_{n\to\infty} \left(Q_n(z) \frac{\left(-z^2 - 2\nu_0 \ln(z) + 2\nu_0 \ln(\pm i\sqrt{\nu_0}) - \nu_0\right)^{n+\gamma}}{\Gamma(n+\gamma)} \right), \tag{5.37}$$

where $Q_n(z)$ represents the general term to be determined by employing the recursive relation given in (5.36) successively; in detail, starting from the leading order term $Q_0(z)$ in (5.25) through the n^{th} term, its predecessor must be differentiated $n-1$ times. As discussed earlier in the present subsection, in practice, deriving the late order terms of the expansion becomes harder as the number of the terms is increased. We have compared the two ways of obtaining the late order terms via only iterating



(a) $z = 0.3 + 0.4i$ (b) $z = 0.3$

Figure 5.2 The solid circles in red represent the magnitude of the general term found by using the factorial-over-a-power method in (5.36) for $u_1^+(z)$ for $\gamma = 0.5$, while the black-dots represent the first 40 exact terms of the expansion derived through repeated use of the recurrence relation in (5.26) in Figure 5.2a and Figure 5.2b, respectively. They show a very good agreement between the two ways if the constant c of (5.36) is $0.2i$.

the terms of the expansion up to the first 40 terms using the recurrence relation with the one deduced in (5.36) in Figure 5.2. In fact, the constant c converges to $0.2i$, and if we pick $0.2i$ in (5.36), the figures show how good the agreement is between the two ways for selected values of z.

5.2.4 Truncation

Next we will truncate the expansion and examine the asymptotic behaviour of its truncated remainder in the same manner as in the zeroth level. Therefore, truncation of (5.23) after $N_1 \gg 1$ terms yields

$$Q(z) = \sum_{n=0}^{N_1-1} \varepsilon^{2n} Q_n(z) + \mathscr{R}_{N_1}(z), \tag{5.38}$$

where $\mathscr{R}_{N_1}(z)$ is the new remainder term of the expansion which will be investigated via the method of exponential asymptotics and will be exponentially small in ε if the truncation point N_1 is selected optimally. Substitution of this truncated expansion into the differential equation produces the first level remainder differential equation,

$$\begin{aligned}\varepsilon^2\frac{d\mathscr{R}_{N_1}(z)}{dz}-\left(2z+\frac{2\nu_0}{z}\right)\mathscr{R}_{N_1}(z) &= -\varepsilon^{2N_1}\frac{dQ_{N_1-1}(z)}{dz}\\ &= -\varepsilon^{2N_1}\left(2z+\frac{2\nu_0}{z}\right)Q_{N_1}(z),\end{aligned} \tag{5.39}$$

in which the successive relationship between terms Q_{N_1-1} and Q_{N_1} derived from (5.26) is performed on the RHS. Minimising the general term of the expansion as a function of n in the limit when n is sufficiently large in order to derive the optimal number of the terms, we obtain that the magnitude of the RHS of (5.39) takes its minimum value at

$$\frac{d}{dn}\left(\varepsilon^{2n}\frac{\Gamma(n+\gamma)}{|u_1^{\pm}(z)|^{n+\gamma}}c\right)=0, \tag{5.40}$$

from which its evaluation at N_1 deduces

$$N_1(z)\sim\frac{|u_1^{\pm}(z)|}{\varepsilon^2}. \tag{5.41}$$

Notice that if $-z^2=\nu_0$, the first level optimal truncation point N_1 becomes zero due to the boundary condition of the singulants given in (5.35); in fact if this is the case, it stops the calculation of the first level. In particular, this can be further observed from the RHS of (5.39) or from Figure 5.3c, for randomly selected values of $z=0.4i$ if the truncation value is chosen as 16, the corresponding blue curve of the error estimate for $u_1^{+}(z)$ does not occur. However, it starts to occur if $-z^2$ is not equal to ν_0, for instance in the nearest neighbourhood of the optimal truncation point when $\nu_0=17$, which corresponds to the first blue dotted figure in Figure 5.3c. In order to carry out the procedure, $-z^2$ must not be equal to ν_0.

Using exponential asymptotics, we have obtained first N_0+N_1 terms of $f(z)$ with the resultant remainder,

$$f(z)=\sum_{n=0}^{N_0-1}\frac{(-1)^n(2n)!}{n!\,(2z)^{2n+1}}+\varepsilon^{2N_0}\frac{(-1)^{N_0+1}(2N_0)!}{N_0!\,(2z)^{2N_0}}\sum_{n=0}^{N_1-1}\varepsilon^{2n}Q_n(z)+\varepsilon^{2N_0}\frac{(-1)^{N_0+1}(2N_0)!}{N_0!\,(2z)^{2N_0}}\mathscr{R}_{N_1}(z), \tag{5.42}$$

with an exponential accuracy. We compare this result with the zeroth level outcome of the expansion: as N_1 more terms are added, the accuracy of the first level becomes greater than the zeroth level. Next, let us introduce the first level truncation error of the hyperasymptotics

$$\begin{aligned}E_{N_1}(z):&=\varepsilon^{2N_0}\frac{(-1)^{N_0+1}(2N_0)!}{N_0!\,(2z)^{2N_0}}\mathscr{R}_{N_1}(z)\\&=\varepsilon^{2N_0+2N_1}\frac{(-1)^{N_0+1}(2N_0)!}{N_0!\,(2z)^{2N_0}}Q_{N_1}(z).\end{aligned} \tag{5.43}$$

Exponentiation of (5.43) via employing the Stirling's formula gives

$$\begin{aligned}E_{N_1}(z)&\sim C_1\varepsilon^{2N_0+2N_1}\frac{(-1)^{N_0+1}N_0^{N_0}N_1^{N_1+\gamma-\frac{1}{2}}}{z^{2N_0}u_1^{\pm}(z)^{N_1+\gamma}\exp\left(N_0+N_1+\gamma-1\right)}\\&\sim C_1\left(-\frac{\nu_0}{ez^2}\right)^{\frac{\nu_0}{\varepsilon^2}}\left(\frac{\nu_1}{eu_1^{\pm}(z)}\right)^{\frac{\nu_1}{\varepsilon^2}+\gamma-\frac{1}{2}}\frac{1}{\sqrt{u_1^{\pm}(z)}},\end{aligned} \tag{5.44}$$

in which $C_1=-2\sqrt{\pi e}C$, and ν_0 and ν_1 are defined as $\nu_0\sim N_0\varepsilon^2$ and $\nu_1\sim N_1\varepsilon^2$. Before minimisation of the relative error estimate, let us compare the level one error given in (5.43) with its level zero error estimate obtained in (5.13).

	Magnitude of the error estimate	
Level	$\Im(z)>0$	$\Im(z)<0$
0th	1.964×10^{-11}	1.964×10^{-11}
1st for $u_1^+(z)$	9.489×10^{-20}	8.062×10^{-84}
1st for $u_1^-(z)$	9.62×10^{-77}	9.489×10^{-20}

Table 5.1 Comparison of the hyperasmptotic errors given in (5.13) and (5.43) according to relevant optimal truncation points for $C=0.2i$, $\gamma=0.5$ and arbitrarily chosen $\varepsilon=0.1$ while $z=0.3+0.4i$ for $\Im(z)>0$ and while $z=-0.3-0.4i$ for $\Im(z)<0$.

The table clearly shows that the magnitude of the relative error reduces exponentially which can further be deduced from Figure 5.3a. Due to the error diminution,

we can comment that the accuracy of the hyperasymptotic expansion has increased exponentially, which is the exponential improvement of the first level.

Figure 5.3 shows that if the hyperasymptotic expansion is truncated optimally at level one, the error gets exponentially smaller. Furthermore, the figures also show that when the level zero truncation point is increased arbitrarily in the first level, the error of the expansion decreases faster than the optimally truncated values. In order to see this, the next step is to minimise this error with respect to ν_1 and ν_0, that are,

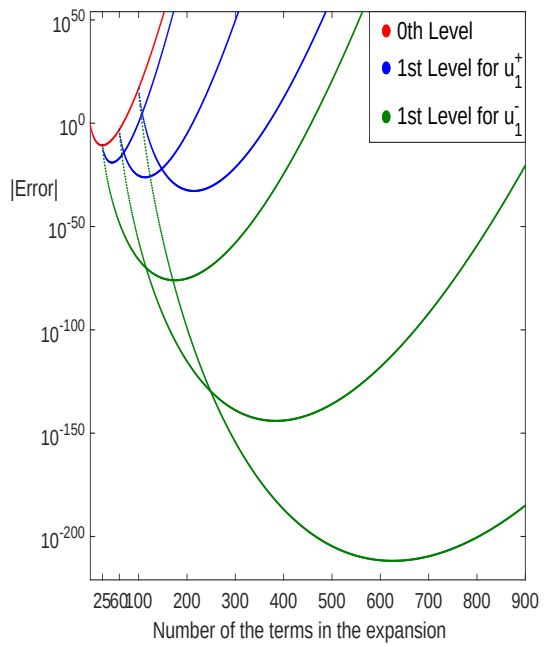
$$\begin{aligned}
\frac{dE_{N_1}(z)}{d\nu_1} &\sim \frac{C_1}{\varepsilon^2}\left(-\frac{\nu_0}{ez^2}\right)^{\frac{\nu_0}{\varepsilon^2}}\left(\frac{\nu_1}{eu_1^{\pm}(z)}\right)^{\frac{\nu_1}{\varepsilon^2}+\gamma-\frac{1}{2}}\frac{1}{\sqrt{u_1^{\pm}(z)}}\ln\left(\frac{\nu_1}{u_1^{\pm}(z)}\right),\\
\frac{dE_{N_1}(z)}{d\nu_0} &\sim \frac{C_1}{\varepsilon^2}\left(-\frac{\nu_0}{ez^2}\right)^{\frac{\nu_0}{\varepsilon^2}}\left(\frac{\nu_1}{eu_1^{\pm}(z)}\right)^{\frac{\nu_1}{\varepsilon^2}+\gamma-\frac{1}{2}}\frac{1}{\sqrt{u_1^{\pm}(z)}}\ln\left(-\frac{\nu_0}{z^2}\right)\left(1-\frac{\nu_1}{u_1^{\pm}(z)}\right).
\end{aligned} \tag{5.45}$$

Equating each derivative to zero, we find that the error takes its minimum value at

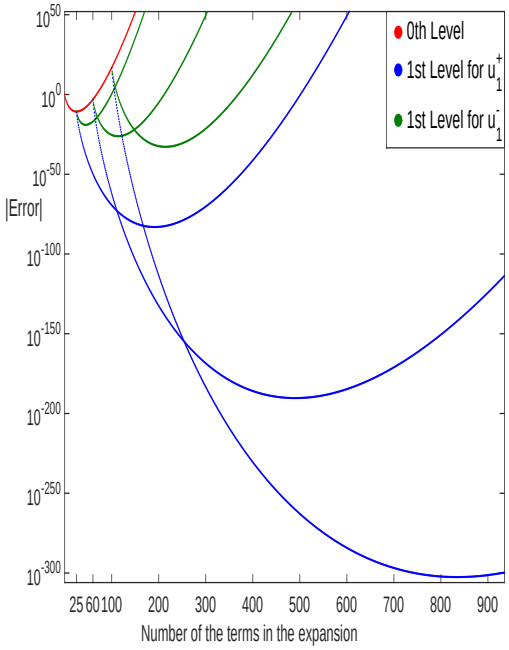
$$\nu_1 \sim \left|u_1^{\pm}(z)\right|, \tag{5.46}$$

when $\nu_0 \neq -z^2$. Notice from (5.46) that this is the same as the first level optimal truncation point without ε^2 in the denominator. Upon minimising the first level error over ν_0 and ν_1, ν_1 is expressed in both as a function of ν_0. By establishing this result, the first level of error is derived in terms of ν_0 and z, and it is reduced by increasing ν_0 and ν_1 in the correct way. The absolute values of the terms of the expansion together in the first level are plotted in the following figures with various values of z and various values of truncation points.

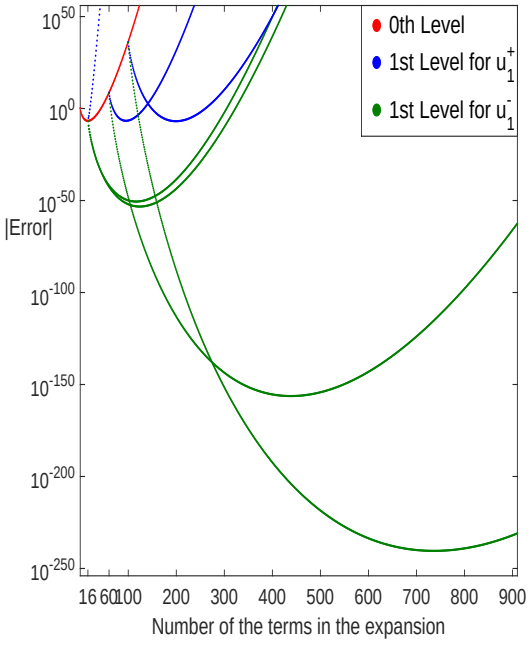
Figure 5.3, Figure 5.4, Figure 5.5 and Figure 5.6 all illustrate the behaviour of the first level error estimate with respect to various values of z and $phz = \theta$. The green lines in Figure 5.4 and Figure 5.5 show the diminishing of the error. In fact, while



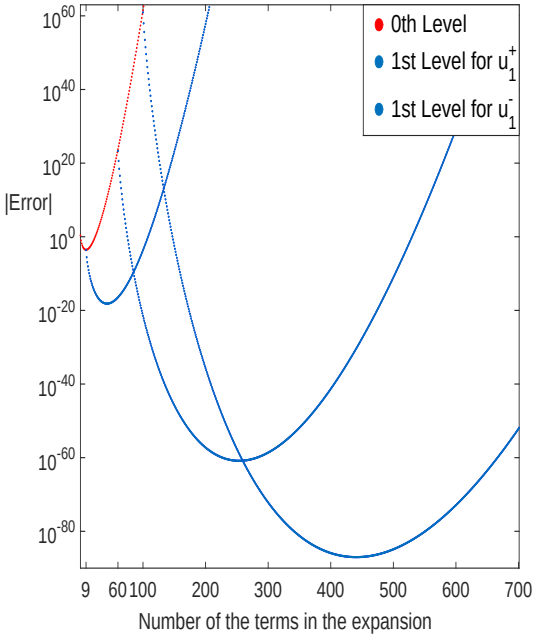
(a) $z = 0.3 + 0.4i$



(b) $z = -0.3 - 0.4i$



(c) $z = 0.4i$



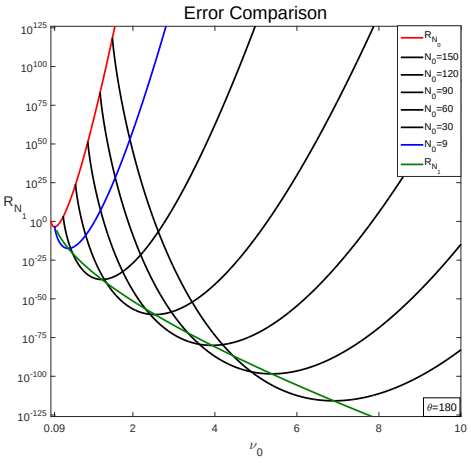
(d) $z = 0.3$

Figure 5.3 Comparisons of the error of the expansion at two levels given in (5.44). Red dotted line illustrates the level zero error in (5.13). The figures are plotted according to $u_1^+(z)$ and $u_1^-(z)$ for $C = 0.2i$ and $\gamma = 1/2$ while $\varepsilon = 0.1$ for randomly selected values of z in $\Im(z) > 0$ and $\Im(z) < 0$. Blue dots correspond to the error estimate in (5.44) occurring via $u_1^+(z)$ while green dots correspond to the error estimate in (5.44) occurring via $u_1^-(z)$ for an optimal truncation point and various truncation points. In Figure 5.3d, corresponding error estimates occurring via $u_1^+(z)$ and $u_1^-(z)$ overlap on each other for purely real values of z.

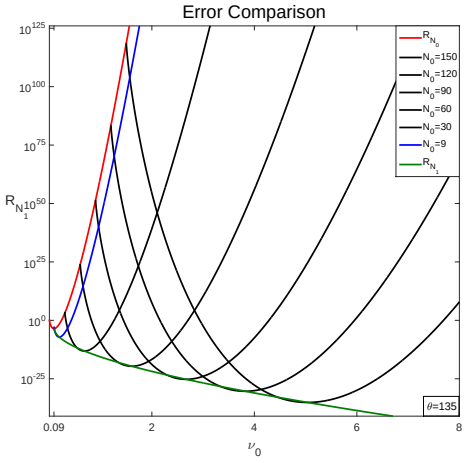
it decreases, it crosses the optimally minimum values of the first level error in each case. Depending on the values of θ, another observation which could be made from the figures is that as we move away from singularities of the relevant late order terms by θ, the error reduces faster. Notice that Figure 5.4d and Figure 5.5b; and Figure 5.4f and Figure 5.5d are identical to each other; the former happens because they are in the singularities, and the latter happens due to them moving away from the singularities with the same distance, i.e., $\pi/2$. It is worth mentioning here again that these show that both singularities have the same strength as argued earlier. Thence, the error of the expansion is dependent on also the values of θ. Figure 5.6a and Figure 5.6b of Figure 5.6 are plotted in light of this idea. Increasing the number of the terms in the expansion for fixed values of θ exponentially reduces the error. Moreover, using the same truncation values of the error in both figures, we observe that increasing solely the values of θ reduces the error exponentially.

To conclude the present subsection, it is shown that the error of the expansion in the first level decreases as the number of the terms, ν_0, is increased in theory. Furthermore, the speed of the decreasing behaviour of the error depends upon the phase of z, whether it is close to the Stokes lines; at the Stokes lines it stops (see Figure 5.4d and Figure 5.5b), and away from the Stokes lines the speed increases.

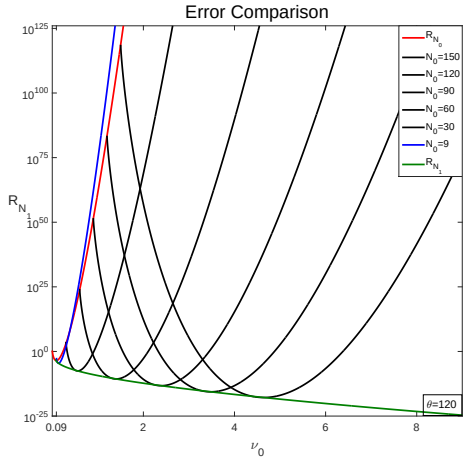
In general, obtaining which exponential contributions of the expansion are present or absent in different sectors of the z-plane is possible through determining the singulants without having the full series solution. As we have completely derived the form of the late order terms and located its singularities explicitly, we can next discuss the Stokes phenomenon in the first level of hyperasymptotics in the following subsection.



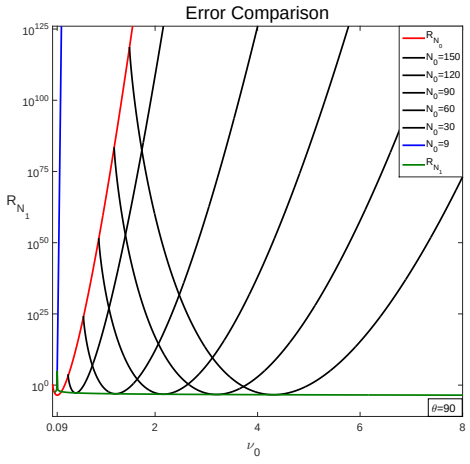
(a) $\theta = \pi$



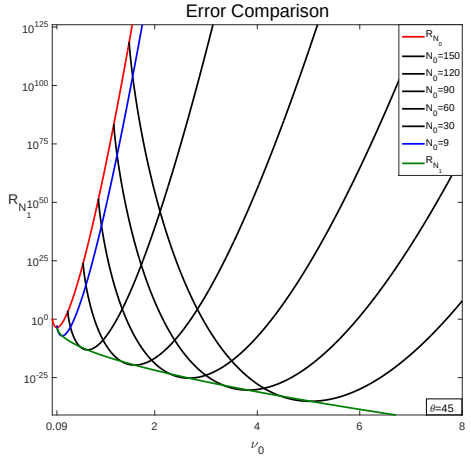
(b) $\theta = \frac{3\pi}{4}$



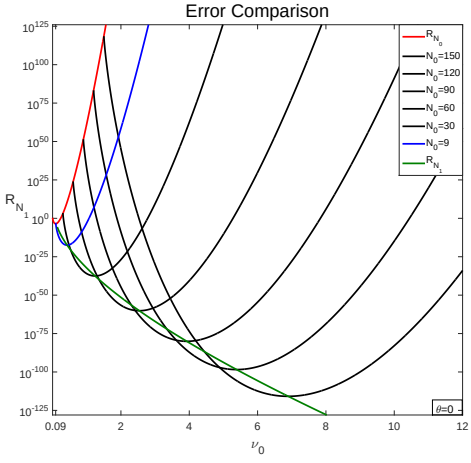
(c) $\theta = \frac{2\pi}{3}$



(d) $\theta = \frac{\pi}{2}$

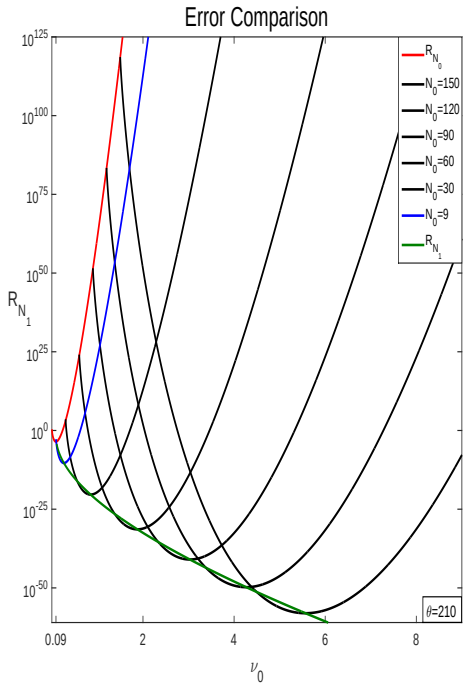


(e) $\theta = \frac{\pi}{4}$

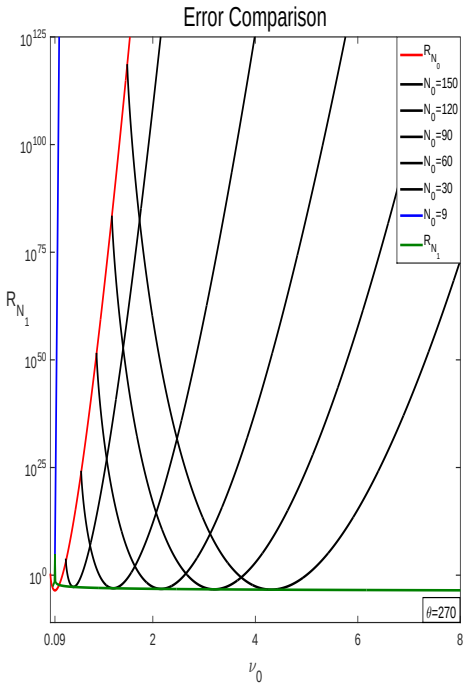


(f) $\theta = 0$

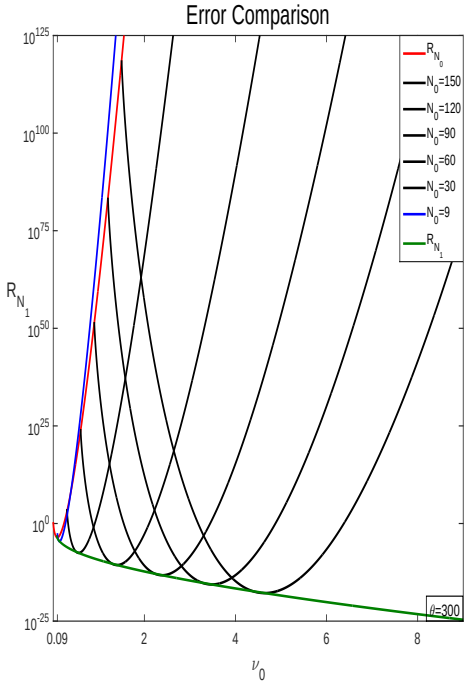
Figure 5.4 Error comparison at two levels given in (5.13) and (5.44) plotted according to $u_1^+(z)$, for $|z| = 0.3$ when $\theta = \arg(z) = \pi$, $3\pi/4$, $2\pi/3$, $\pi/2$, $\pi/4$ and $\theta = 0$, respectively, for $\gamma = 1/2, C = 0.2i$ while $\varepsilon = 0.1$. They demonstrate that the decreasing behaviour of the error depends on both the truncation points and θ.



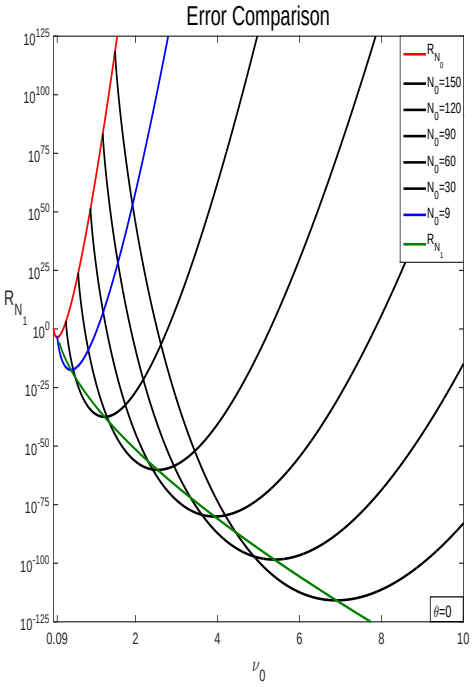
(a) $\theta = \frac{7\pi}{6}$



(b) $\theta = \frac{3\pi}{2}$

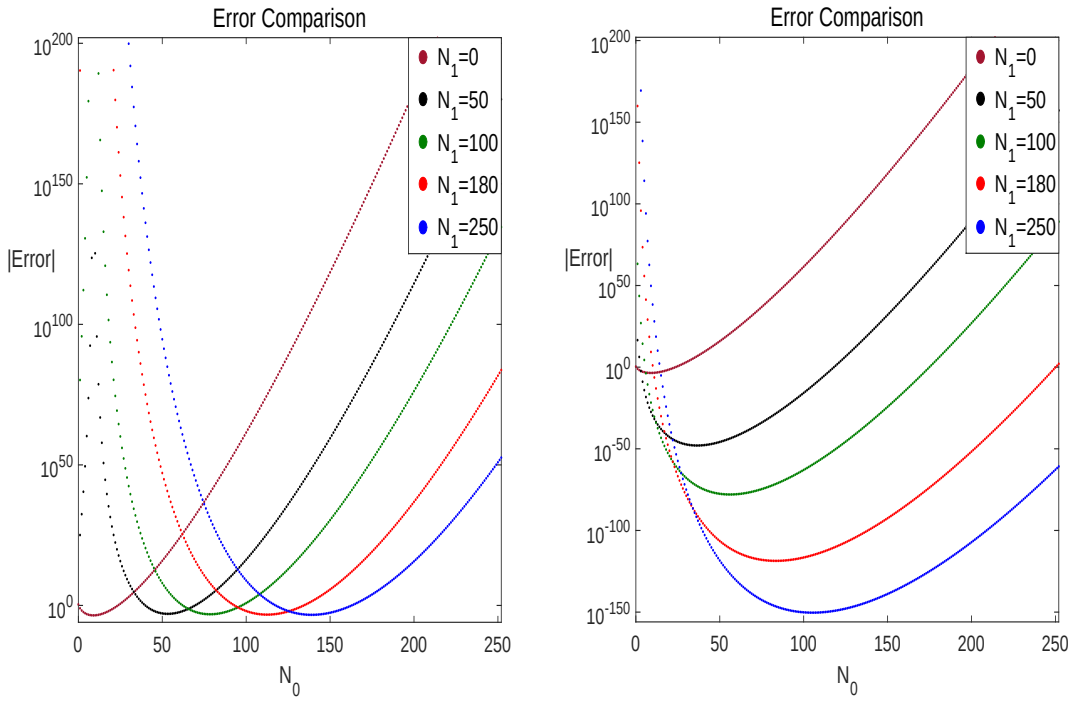


(c) $\theta = \frac{5\pi}{3}$



(d) $\theta = 0$

Figure 5.5 Comparison of the errors (5.13) and (5.44) plotted according to $u_1^-(z)$, for $|z| = 0.3$ when $\theta = \arg(z) = 7\pi/6, 3\pi/2, 5\pi/3$ and $\theta = 0$, respectively, for $\gamma = 1/2$, $C = 0.2i$ while $\varepsilon = 0.1$. They show that the behaviour of the error depends on both truncation points and θ.



(a) $\theta = \frac{\pi}{2}$ (b) $\theta = \frac{3\pi}{2}$

Figure 5.6 Behaviour of the error (5.44) according to $u_1^+(z)$, for $|z| = 0.3$ when $\theta = \arg(z) = \pi/2$ and $\theta = \arg(z) = 3\pi/2$, respectively, for $\gamma = 1/2$, $C = 0.2i$ while $\varepsilon = 0.1$. Black, green, red and blue dots correspond to the error estimate while N_0 and N_1 both increase at the same time. Here N_1 is selected as $0, 50, 100, 180, 250$, respectively, in order to see the agreement. While both N_0 and N_1 are increased, the error decreases faster, especially at 180^o away from the singularity.

5.2.5 Stokes and anti-Stokes lines

Similar to §5.2.2 where we determined the zeroth level Stokes phenomenon, in this subsection we are interested in finding the first level Stokes and anti-Stokes lines; in fact, the details of Stokes lines analysis are similar. Stokes (and anti-Stokes) lines of the first level are associated with the prefactor of $Q(z)$ in (5.22) which emanate from its zeros or singularities as they complete the derivation of the singulants. From §5.2.2, it is already known that Stokes lines occur along the line in which they fulfil the following conditions,

$$\Im(u_1^{\pm}(z)) = 0 \quad \text{and} \quad \Re(u_1^{\pm}(z)) > 0, \tag{5.47}$$

where $u_1^+(z)$ and $u_1^-(z)$ are the singulants of the level one obtained upon the inspection of the late order terms associated with the two different singularities in (5.25). Because $u_1^+(z)$ and $u_1^-(z)$ are defined by the complex conjugate singularities, Stokes and anti-Stokes analysis will be addressed only according to $u_1^+(z)$ rather than considering both contributions of the late order terms separately; the analyses are also symmetrical and give the complex conjugate contribution with each other. Hence, analysis of the Stokes and anti-Stokes lines occurring via $u_1^-(z)$ defined by the singularity at $z=-i\sqrt{\nu_0}$ from which relevant exponentially small behaviour being switched on will be just illustrated in Figure 5.7 in which the logarithmic branch cut is represented by hatched lines. Without loss of generality, we introduce the polar coordinate, $z=r\exp(i\theta)$. Evaluating the singulant $u_1^+(z)$ based on (5.47) in terms of the polar coordinates yields the expression

$$-r^2\sin(2\theta)-2\nu_0(\theta)+\nu_0\pi=0 \quad \text{and} \quad -r^2\cos(2\theta)-2\nu_0\ln(r)+\nu_0\ln(\nu_0)-\nu_0>0. \tag{5.48}$$

This implies that the Stokes line lies along $\pi/2$. Similarly, anti-Stokes lines take place when θ satisfies

$$-r^2\cos(2\theta)-2\nu_0\ln(r)+\nu_0\ln(\nu_0)-\nu_0=0. \tag{5.49}$$

Across these Stokes lines, subdominant exponentially small terms switch on and off, as discussed in detail in the §2.5. Hence, with this information, we aim to identify which of these subdominant contributions are present in different sectors of the z-plane. Stokes and anti-Stokes lines, as well as the sudden appearance and disappearance of the exponentials, across the Stokes lines in the relevant sectors, are to be illustrated in Figure 5.7 with an offset at 0. In this figure, ① and ② represent the contributions induced by singulants $u_1^+(z)$ and $u_1^-(z)$, respectively, while ⓪ represents the exponential $\exp(0)$ in the RHS of the first level equation (5.22). To proceed, we start travelling from Sector II through Sector I in a clockwise direction. Crossing the active Stokes line in red switches the contribution ① on by ⓪ as it is present in Sec-

tor I; hence, ⓪ and ① are present in Sector I. Since the Stokes line is inactive while travelling from Sector I to Sector IV, nothing turns off, so that ⓪ and ① are present in Sector IV. Carrying on the travel through Sector III as the relevant Stokes line is irrelevant for ①, ⓪ and ① stay present in Sector III. Moving upward through Sector II, crossing the branch cut leads to the removal of the exponential ① due to the discontinuity. Hence, we return to where we started. For the sake of brevity, the same travel along the complex plane for the contribution ② is demonstrated in Figure 5.7. We conclude this subsection by commenting that the asymptotic series has different asymptotics in different sectors of the $z-$plane. In fact, this can be observed through Figure 5.7.

To sum up this section, the first order differential equation has been inspected by the techniques in hyperasymptotics. As the truncation point of the zeroth level is increased arbitrarily, we observed that the optimal truncation point of the first level increases and the truncation error of the expansion in this stage reduces exponentially. Moreover, the decreasing behaviour of the error estimate further depends on the phase of the expansion whether it is near or away from the Stokes lines. In order to have a consistency and an agreement in our results, the second order differential equation of the error function will be investigated using the same steps in the next section. Therefore, the detailed conclusion of the present section are left to the last section, §5.4.

5.3 Second order differential equation for the error function

In this section, we will investigate the second level differential equation of the error function given in (5.2), which is

$$\varepsilon^2 \frac{d^2y(z)}{dz^2} + 2z\frac{dy(z)}{dz} = 0, \tag{5.50}$$

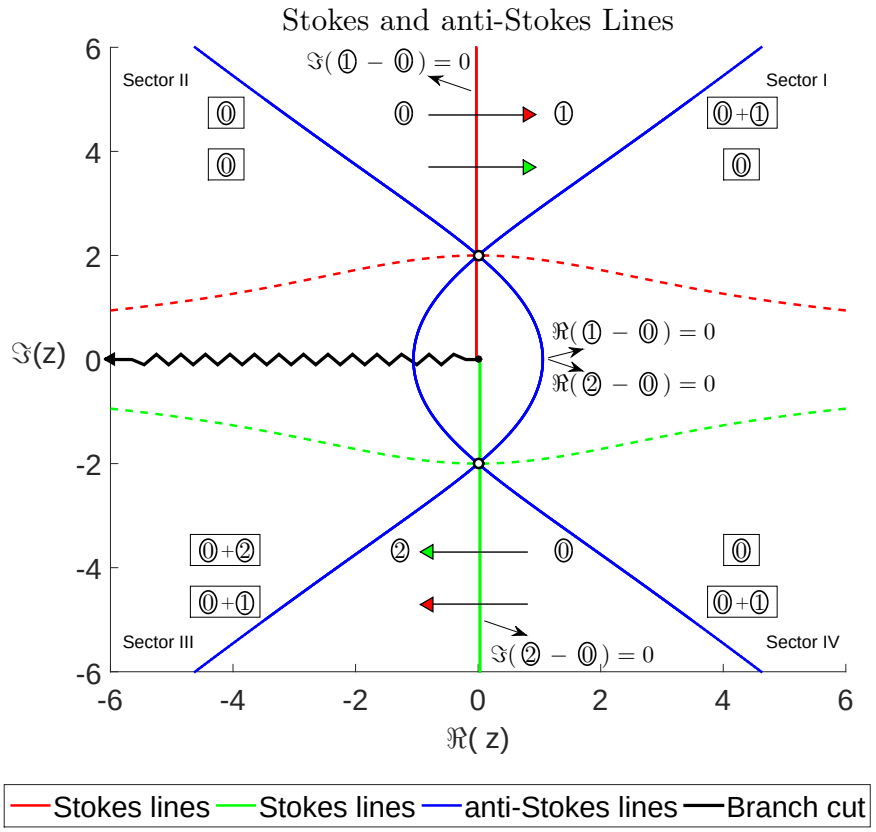


Figure 5.7 Red and green lines represent the active Stokes lines for $u_1^+(z)$ and $u_1^-(z)$, while dashed lines represent the inactive Stokes lines for randomly chosen $\nu_0 = 4$ and $\varepsilon = 0.1$. Blue lines show the anti-Stokes lines for both $u_1^+(z)$ and $u_1^-(z)$. Turning points are demonstrated with the black circle. Zigzag in black along the negative real axis below zero indicates the branch cut in which the discontinuity appears. Arrows indicate the direction of the travel.

in which the turning point appears when z equals to 0. We may easily verify that the constant function is a solution of this differential equation in addition to the error function. Before inspecting the equation via exponential asymptotics, let us first derive the second solution, i.e., erf function. Equation (5.50) is equal to

$$\frac{dy'(z)}{y'(z)} = -\frac{2z}{\varepsilon^2}dz. \tag{5.51}$$

Integrating this (5.51) once gives

$$y'(z) = \exp\left(-\frac{z^2}{\varepsilon^2}\right), \tag{5.52}$$

which is the same as the 'first order' equation in (5.1). Hence, we can compare the results of both equations coming from the same family if they are consistent or have any meaningful differences. Next, integration of (5.52) gives the desired solution

$$\begin{aligned} y(z) &= C\int \exp\left(-\frac{z^2}{\varepsilon^2}\right) dz \\ &= C\frac{\sqrt{\pi}\varepsilon}{2}\mathrm{erf}\left(\frac{z}{\varepsilon}\right), \end{aligned} \tag{5.53}$$

where C is a constant. Since the error function is represented by an application of the direct integration, it is verified that erf function is the solution of (5.50).

On the other hand, employing the WKB approximation, we find two solutions of the differential equation; one is a constant, whereas the other is $y(z) \sim \exp(-z^2/\varepsilon^2)$. Note that the detailed explanation of the WKB approach with its application will be given in the confluent hypergeometric function chapter in §7 in order to avoid redundancy. We rescale $y(z)$ based on its WKB solution as in the following form

$$y(z) = \exp\left(-\frac{z^2}{\varepsilon^2}\right) f(z), \tag{5.54}$$

which also agrees with the rescaling of the function (5.4) in the previous section. Substitution of (5.54) leads to a differential equation for the newly introduced $f(z)$

$$\varepsilon^2 \frac{d^2 f(z)}{dz^2} - 2z\frac{df(z)}{dz} - 2f(z) = 0. \tag{5.55}$$

Indeed, it is in the same nature with $y(z)$, as its highest derivative is multiplied by ε. By the same token, in order to analyse this differential equation with the techniques of hyperasymptotics, we next need to expand the solution by the conventional perturbation. As we already discussed the related issues of the hyperasymptotics in the previous section §5.2 in greater detail, this section will be kept brief.

5.3.1 Zeroth level of hyperasymptotics: superasymptotics

We begin this subsection by seeking the asymptotic expansion of $f(z)$ expanding in powers of ε^2 such that

$$f(z) \sim \sum_{n=0}^{\infty} \varepsilon^{2n} f_n(z). \tag{5.56}$$

Substitution of this series solution into the differential equation (5.54) yields

$$\sum_{n=0}^{\infty} \varepsilon^{2n+2} \left(\frac{d^2 f_n(z)}{dz^2} - 2z \frac{df_{n+1}(z)}{dz} - 2f_{n+1}(z) \right) - 2z \frac{df_0(z)}{dz} - 2f_0(z) = 0. \tag{5.57}$$

As already apparent in (5.57), like powers of ε gives at the leading order $\mathrm{O}(\varepsilon^0)$

$$2z \frac{df_0(z)}{dz} + 2f_0(z) = 0. \tag{5.58}$$

Upon solving this, we establish the leading order term of the expansion as

$$f_0(z) = \frac{c_0}{z}, \tag{5.59}$$

where c_0 is a constant of integration. It is worth remarking herein that the leading term has a singularity at $z = 0$ which must be present in the late order terms. Furthermore, from expression (5.57), matched asymptotic expansion produces the differential recursion relationship at $\mathrm{O}\left(\varepsilon^{2n+2}\right)$

$$\frac{d^2 f_n(z)}{dz^2} - 2z \frac{df_{n+1}(z)}{dz} - 2f_{n+1}(z) = 0. \tag{5.60}$$

Applying the leading term (5.59) into the recurrence relation, and similarly performing this relation for $n = 1, 2$ recursively determines the next three successive terms of the expansion by means of

$$f_1(z) = -\frac{c_0}{2z^3}, \quad f_2(z) = \frac{3c_0}{4z^5}, \quad f_3(z) = -\frac{15c_0}{8z^7}. \tag{5.61}$$

Thence, using the recursive equation repeatedly, we compute the late order term of the expansion as

$$f_n(z) = (-1)^n \frac{(2n)!c_0}{n!2^{2n}z^{2n+1}}, \tag{5.62}$$

which completes the determination of the asymptotic series solution. To point out, the general term of (5.56) agrees with the general term of the first order differential equation derived in (5.11). Establishing the general term of the expansion has further enabled us to have the form of the asymptotic expansion of the error function; particularly, this could be seen with back substitution of the expansion (5.56) in (5.54).

5.3.2 Truncation

We may truncate the asymptotic series solution as the general term of the expansion is already derived. Thus, writing down the expansion after N_0 terms yields

$$f(z) = \sum_{n=0}^{N_0-1} \varepsilon^{2n} f_n(z) + R_{N_0}(z), \tag{5.63}$$

where $R_{N_0}(z)$ is asymptotic to the first neglected term of the expansion. While investigating the truncated error of the expansion in the first order error function in §5.2, we examined the corresponding $f(z)$ rather than $g(z)$ in (5.4). To have a different perspective, in this second order error function, we will inspect $y(z)$ given in (5.54) with its exponential pre-factor. Thence, the error estimate of the error function in (5.54) occurring due to the truncation becomes

$$E_{N_0}(z) := \exp\left(-\frac{z^2}{\varepsilon^2}\right) \frac{(-1)^{N_0}\varepsilon^{2N_0}(2N_0)!}{(N_0)!2^{2N_0}z^{2N_0+1}}. \tag{5.64}$$

Once the truncated expansion is substituted into (5.55), it yields a differential equation of the remainder, that is

$$\varepsilon^2 \frac{d^2R_{N_0}(z)}{dz^2} - 2z\frac{dR_{N_0}(z)}{dz} - 2R_{N_0}(z) = (-1)^{N_0} \frac{\varepsilon^{2N_0}(2N_0)!}{(N_0-1)!2^{2N_0-2}z^{2N_0+1}}. \tag{5.65}$$

It is worth commenting that (5.65) is in the same form as (5.55), but it is not homogeneous. Using one of the methods given in (2.9) of §2, we obtain that the optimal truncation point occurs at

$$N_0 \sim \frac{|z^2|}{\varepsilon^2}. \tag{5.66}$$

As the singulant of the expansion is the same as the singulant of the previous section and since we already analysed it in §5.2.2, the same Stokes lines analysis will not be repeated in this level. Therefore, the zeroth level Stokes lines and its structure may be seen in the Figure 5.1 and §5.2.2 in detail. We next begin the level one analysis of the hyperasymptotics in which we discuss the first level error in terms of arbitrary truncation points.

5.3.3 First level of hyperasymptotics

In order to obtain a more accurate approximation than the superasymptotics, we need to analyse the truncated remainder of the previous level in hyperasymptotics. Hence, the next natural step is to rescale the remainder according to the RHS of (5.65) such that

$$R_{N_0}(z) = (-1)^{N_0} \frac{\varepsilon^{2N_0+2}(2N_0)!}{(N_0-1)!2^{2N_0-2}z^{2N_0+1}} Q(z), \tag{5.67}$$

in which $Q(z)$ will be discussed shortly. Substituting this expression in the equation (5.65), we establish that $Q(z)$ satisfies for large N_0

$$\varepsilon^4 \frac{d^2Q(z)}{dz^2} - \varepsilon^2 \left(2z + \frac{4\nu_0}{z}\right) \frac{dQ(z)}{dz} + \left(4\nu_0 + \frac{4\nu_0^2}{z^2}\right) Q(z) \sim 1. \tag{5.68}$$

where $\nu_0 = N_0\varepsilon^2$ which is influenced by the truncation point in (5.66). It is worth remarking that had we assumed the remainder differential equation of the zeroth level as stated by Olde Daalhuis et al. in [27] and carried out the first level of hyperasymptotics directly based on their analysis, we would have arrived at the same differential equation for above $Q(z)$, which reinforces the consistency between the two pieces of

analysis. We next come to the usual step: expansion. To have the asymptotic series solution of (5.68), we need to expand $Q(z)$ as a power series in ε^2; hence, we attempt the asymptotic series solution of the form

$$Q(z) \sim \sum_{n=0}^{\infty} \varepsilon^{2n} Q_n(z). \tag{5.69}$$

Substituting and matching like powers of ε straightaway help to determine the first two terms and the differential recurrence equation, from which we may derive each term of the asymptotic expansion

$$Q_0(z) = \frac{z^2}{4\nu_0\left(z^2+\nu_0\right)}, \qquad Q_1(z) = \frac{z^2\left(z^2+2\nu_0\right)}{4\nu_0\left(z^2+\nu_0\right)^3}, \tag{5.70}$$

$$\frac{d^2Q_n(z)}{dz^2} - \left(2z + \frac{4\nu_0}{z}\right)\frac{dQ_{n+1}(z)}{dz} + \left(4\nu_0 + \frac{4\nu_0^2}{z^2}\right)Q_{n+2}(z) = 0, \tag{5.71}$$

in which the leading order term has singularities while $z^2 = -\nu_0$ from which the expansion breaks down. Since the general term does not occur at a certain form by repeatedly using the recursive relation in (5.71), we may use the factorial-over-a-power method as usual. Thence, let us suppose the late order term is in this nature

$$Q_n(z) = \frac{\Gamma(n+\gamma)}{u_1(z)^{n+\gamma}} \sum_{n=0}^{\infty} \frac{B_k(z)}{n^k}, \tag{5.72}$$

where $u_1(z)$ and $B_k(z)$ will be derived shortly. To proceed, employing this ansatz in the differential recursive relation in (5.71) and matching the same powers of n, we find at order $1/n^2$

$$\frac{B_0(z)}{\left(u_1(z)\right)^2}\left(u_1'(z) + \frac{2\nu_0}{z}\right)\left(u_1'(z) + \frac{2\nu_0}{z} + 2z\right) = 0, \tag{5.73}$$

and at order $1/n$

$$u_1''(z)B_0 + \left(2u_1'(z) + 2z + \frac{4\nu_0}{z}\right)B_0'(z) = 0, \tag{5.74}$$

which is obtained after performing (5.73) at this order. As explicated in previous chapters, B_0 in (5.73) cannot be zero. Therefore, we are left with two options:

$$u_1'(z)+\frac{2\nu_0}{z}=0 \quad \text{and} \quad u_1'(z)+\frac{2\nu_0}{z}+2z=0. \tag{5.75}$$

Upon direct integration, singulants are found as

$$u_1^1(z)=-2\nu_0\ln(z)+C_1 \quad \text{and} \quad u_1^2(z)=-2\nu_0\ln(z)-z^2+C_2. \tag{5.76}$$

By the definition of the late order terms, the constants C_1 and C_2 are to be determined subject to the singularities of the leading order term derived in (5.70). We have then two cases: first, based on the singular point in $\Im(z)>0$, the constants are

$$\begin{aligned} C_1&=2\nu_0\ln(i\sqrt{\nu_0}) && \text{for} \quad z_1=i\sqrt{\nu_0},\\ C_2&=2\nu_0\ln(i\sqrt{\nu_0})-\nu_0 && \text{for} \quad z_2=i\sqrt{\nu_0}, \end{aligned} \tag{5.77}$$

and second, based on the singularity in $\Im(z)<0$, the constants become

$$\begin{aligned} C_1&=2\nu_0\ln(-i\sqrt{\nu_0}) && \text{for} \quad z_1=-i\sqrt{\nu_0},\\ C_2&=2\nu_0\ln(-i\sqrt{\nu_0})-\nu_0 && \text{for} \quad z_2=-i\sqrt{\nu_0}. \end{aligned} \tag{5.78}$$

As discussed in §4.5, both singulants have the logarithmic branch cuts which we place along the negative real axis. Combining these constants of the singulants with (5.76) fully determines the singulants of the n^{th} term in the expansion as

$$u_1^1(z)=-2\nu_0\ln(z)+2\nu_0\ln(\pm i\sqrt{\nu_0}), \tag{5.79}$$

$$u_1^2(z)=-z^2-2\nu_0\ln(z)+2\nu_0\ln(\pm i\sqrt{\nu_0})-\nu_0, \tag{5.80}$$

where the signs $\pm$ correspond to the choice of having the singularities $z_{1,2}$. In addition, we observe that the singulant (5.80) is exactly the same as the corresponding singulant in (5.35) of the preceding section. Having used these singulants in (5.74) enables us to produce the leading order terms in the summation of the factorial-over-

a-power ansatz in (5.71), giving

$$B_{0_{u_1^1}}(z) = \exp\left(\frac{\nu_0}{2z^2}\right) \qquad \text{and} \qquad B_{0_{u_1^2}}(z) = \frac{1}{z}\exp\left(-\frac{\nu_0}{2z^2}\right). \tag{5.81}$$

Notice that in the same level of the previous section, these functions are determined as constants. However, in this level, they are attained as a function of ν_0 which may effect the speed of the diminishing in the error once it is increased. Determining these functions concludes the derivation of the leading order solution of the expansion for large n. Thence, the asymptotic solution of the first level differential equation of the hyperasymptotic expansion is the linear combination of the late order terms depending on the singulants

$$Q_n(z) \sim C_3 \frac{\Gamma(n+\gamma)}{\left(u_1^1(z)\right)^{n+\gamma}}\exp\left(\frac{\nu_0}{2z^2}\right) + C_4 \frac{\Gamma(n+\gamma)}{\left(u_1^2(z)\right)^{n+\gamma}}\frac{1}{z}\exp\left(-\frac{\nu_0}{2z^2}\right), \tag{5.82}$$

in which $C_{3,4}$ represent the combinations of the constants which are obtained after the integration of the singulants and $B_{0_{u_1^{1,2}}}(z)$. Before discussing truncation, it is important to highlight that since singulants have the same strength in the expansion, and they are defined according to the singularities; as we approach either singularity in $\Im(z) > 0$ and $\Im(z) < 0$, the denominator of the expansion becomes smaller so that the relevant late order term overpowers the another one. If, however, z is purely real, because the singularities are a complex conjugate of each other, the above situation does not happen and so the late order terms overlap each other. A more detailed explanation supported by the figures of Figure 5.3 were addressed in §5.2.3.

5.3.4 Truncation

Having established the general representation of the expansion, we now have sufficient information to truncate the expansion after N_1 terms, which is

$$Q(z) \sim \sum_{n=0}^{N_1-1} \varepsilon^{2n} Q_n(z) + \mathscr{R}_{N_1}(z), \tag{5.83}$$

where $\mathscr{R}_{N_1}$ is a remainder of the series and $\mathscr{R}_{N_1} = \mathrm{O}(\varepsilon^{2N_1})$. By performing the back substitution of this truncated series into (5.54) via (5.63), we obtain the power series solution of the error function in the first level; in other words, first N_0 plus N_1 terms of the expansion with the remainder can be written out as

$$y(z) \sim \exp\left(-\frac{z^2}{\varepsilon^2}\right)\sum_{n=0}^{N_0-1}\varepsilon^{2n}f_n(z) + \exp\left(-\frac{z^2}{\varepsilon^2}\right)\frac{(-1)^{N_0}\varepsilon^{2N_0+2}(2N_0)!}{(N_0-1)!2^{2N_0-2}z^{2N_0+1}}\sum_{n=0}^{N_1-1}\varepsilon^{2n}Q_n(z) + \exp\left(-\frac{z^2}{\varepsilon^2}\right)\frac{(-1)^{N_0}\varepsilon^{2N_0+2}(2N_0)!}{(N_0-1)!2^{2N_0-2}z^{2N_0+1}}\mathscr{R}_{N_1}(z), \quad (5.84)$$

which is established with an application of (5.67). In comparison with the zeroth level, since N_1 more terms are added into the asymptotic solution, the accuracy of the expansion has increased. Furthermore, the first level truncation error of the error function in (5.54) emerges as the first neglected term of the above summation

$$E_{N_1}(z) := \exp\left(-\frac{z^2}{\varepsilon^2}\right)\frac{(-1)^{N_0}\varepsilon^{2N_0+2N_1+2}(2N_0)!}{(N_0-1)!2^{2N_0-2}z^{2N_0+1}}Q_{N_1}(z). \quad (5.85)$$

Following the methods in (2.9) by making use of the ansatz forms for $Q_{N_1}(z)$, we confirm that the first level optimal truncation occurs at

$$N_1 \sim \frac{|u_1^{1,2}(z)|}{\varepsilon^2}, \quad (5.86)$$

for both singulants $u_1^1(z)$ and $u_1^2(z)$. However, we keep the truncation points arbitrary and investigate the behaviour of the error in the sense of §4. Next, we plot it. Thence, Figure 5.8 and Figure 5.9 demonstrate the behaviour of the errors depending on both the argument of z and the number of the terms. Particularly, increasing the zeroth level truncation point arbitrarily reduces the errors exponentially as shown by the green lines. Since the first level truncation point is a function of the zeroth level truncation point, we write the error in terms of the zeroth level truncation point. While decreasing, the green lines in both figures cross the minimum points of the first level errors shown in blue and black. Furthermore, we observe that its speed

depends upon the argument. In particular, moving away from the singularity by the argument, increases the speed of diminishing exponentially, whereas at the Stokes lines the speed takes its slowest value.

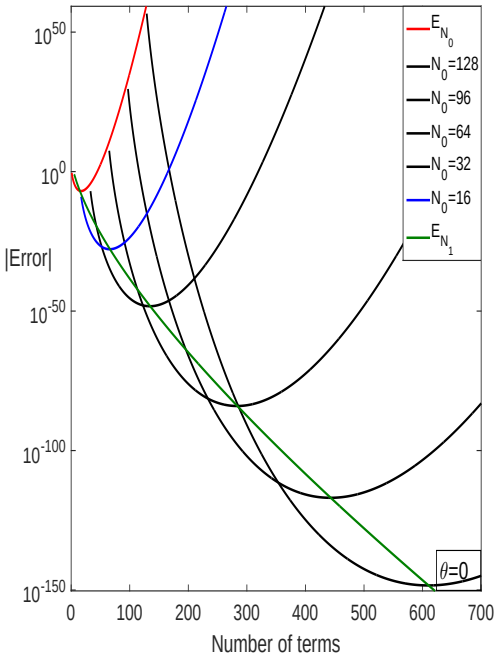
5.3.5 Stokes phenomenon

Having established the singulants, we can next locate the Stokes and anti-Stokes lines using both singulants. However, as the singulant found in (5.80) is identical to the singulant in (5.35) of the previous section, the Stokes calculation of this level will be presented for the singulant (5.79) to avoid redundancy. For more information regarding the Stokes phenomenon of the singulant $u_1^2(z)$ in (5.80), refer to §5.2.5. The first level differential equation of the 'first order' error function contains two exponentials: one particular integral and one complementary function as found in the previous section. However, in this section, (5.68) contains two complementary functions, each of which could be turned on, with a particular integral in practice. In addition to addressing this, we will also discuss the higher order Stokes lines (HOSL) briefly, since we have the three exponentials. In order to proceed, we set the polar coordinates $z = r\exp(i\theta)$ and express both singulant in terms of it, giving

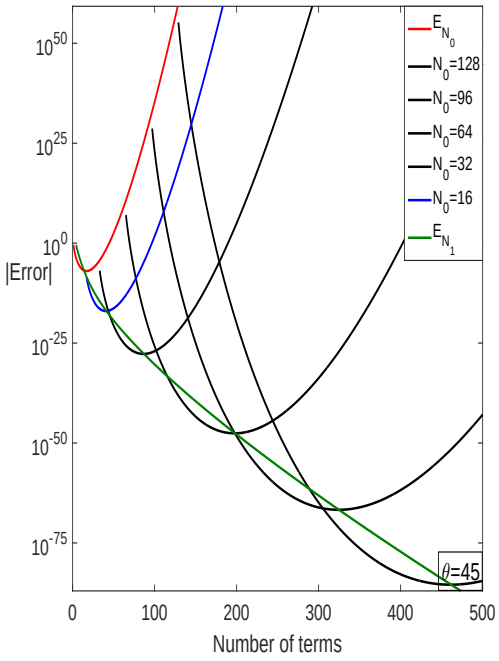
$$\begin{aligned} u_1^1\left(re^{i\theta}\right) &= -2\nu_0 \ln\left(r\exp(i\theta)\right) + 2\nu_0 \ln\left(\pm i\sqrt{\nu_0}\right) \\ &= 2\nu_0 \ln\left(\frac{\sqrt{\nu_0}}{r}\right) + 2\nu_0\left(\pm\frac{\pi}{2} - \theta\right) i. \end{aligned} \tag{5.87}$$

We know that the active Stokes lines occur whenever the imaginary part of the singulant (5.87) equals zero, while its real part is positive. Therefore, they lie along $\theta = \pm\pi/2$ by the condition of $\sqrt{\nu_0}$ greater than r. Hence, the symmetrical lines emerge when $\theta = \pi/2$ and $\theta = -\pi/2$ for the singularities $z = i\sqrt{\nu_0}$ and $z = -i\sqrt{\nu_0}$, respectively. In a similar manner, anti-Stokes lines occur whenever the real part of (5.87) equals to zero, that is

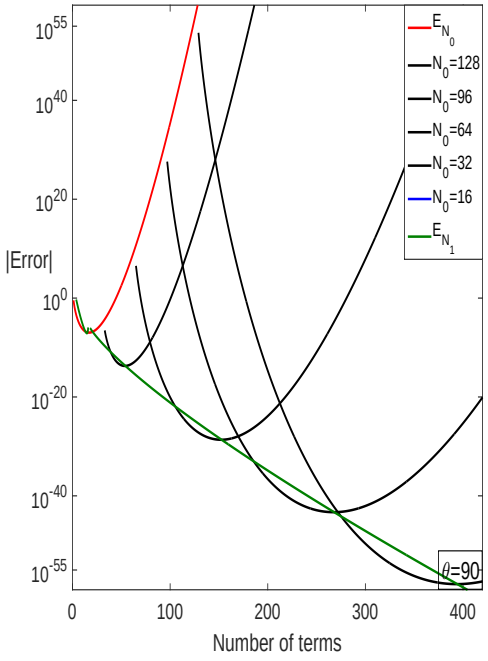
$$2\nu_0 \ln\left(\frac{\sqrt{\nu_0}}{r}\right) \implies r = \sqrt{\nu_0}. \tag{5.88}$$



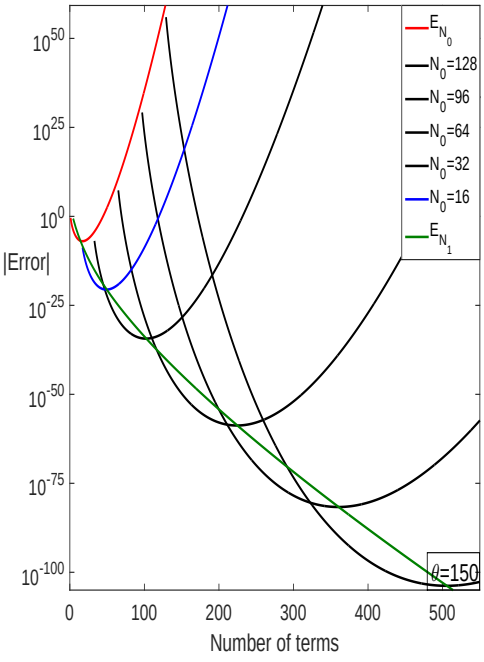
(a) $\theta = 0$



(b) $\theta = \frac{\pi}{4}$

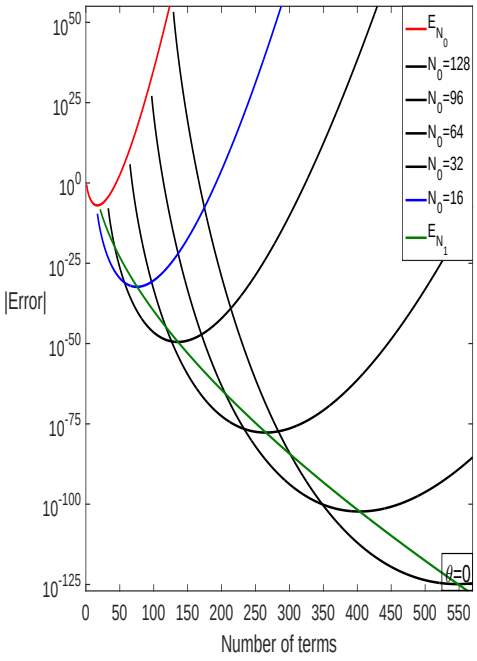


(c) $\theta = \frac{\pi}{2}$

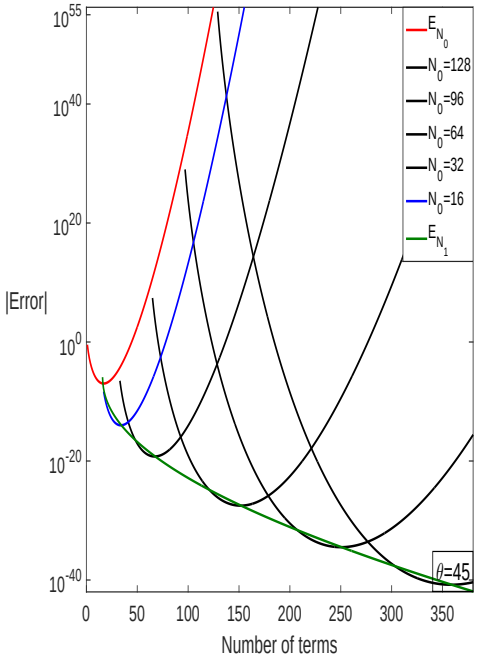


(d) $\theta = \frac{5\pi}{6}$

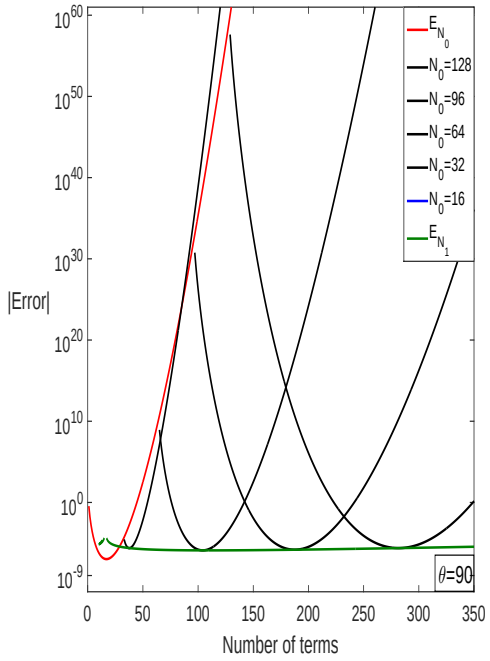
Figure 5.8 The behaviour of the zeroth and first level error estimates in (5.64) and (5.85) plotted according to $u_1^1(z)$ in (5.79) for the singularity in $\Im(z) > 0$ while $|z| = 1$ for $\theta = \arg(z) = 0, \pi/4, \pi/2$ and $\theta = 5\pi/6$, respectively, for randomly chosen $\gamma = 1$, $C_3 = 1$ while $\varepsilon = 0.25$. They show that the behaviour depends on both truncation points and θ.



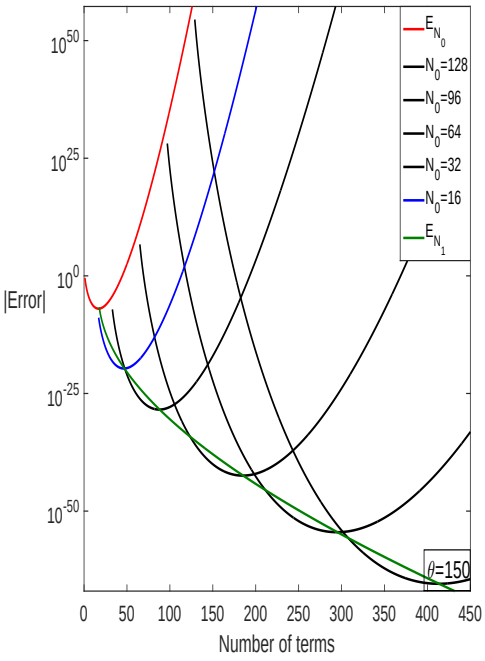
(a) $\theta = 0$



(b) $\theta = \frac{\pi}{4}$



(c) $\theta = \frac{\pi}{2}$



(d) $\theta = \frac{5\pi}{6}$

Figure 5.9 Demonstrating the error estimate found in (5.85) plotted according to $u_1^2(z)$ in (5.80) corresponding the singularity (5.77) in $\Im(z) > 0$ while $|z| = 1$ for $\theta = \arg(z) = 0$, $\pi/4$, $\pi/2$ and $\theta = 5\pi/6$, respectively, for randomly picked $\gamma = 1, C_4 = 1$ while $\varepsilon = 0.25$. Red lines show the level zero estimate in (5.64). The plots reveal that the error decreases exponentially when both truncation points are increased. The error further depends on θ.

This means that anti-Stokes lines lie along the circle whose radius is $\sqrt{\nu_0}$, and as ν_0 is increased, the circle gets larger. Since we have provided both the Stokes and anti-Stokes lines, we can now illustrate them. Particularly, these lines with the branch cut are illustrated in Figure 5.10 with an offset at zero. Stokes plot of $u_1^2(z)$ in (5.80) is also given in Figure 5.11.

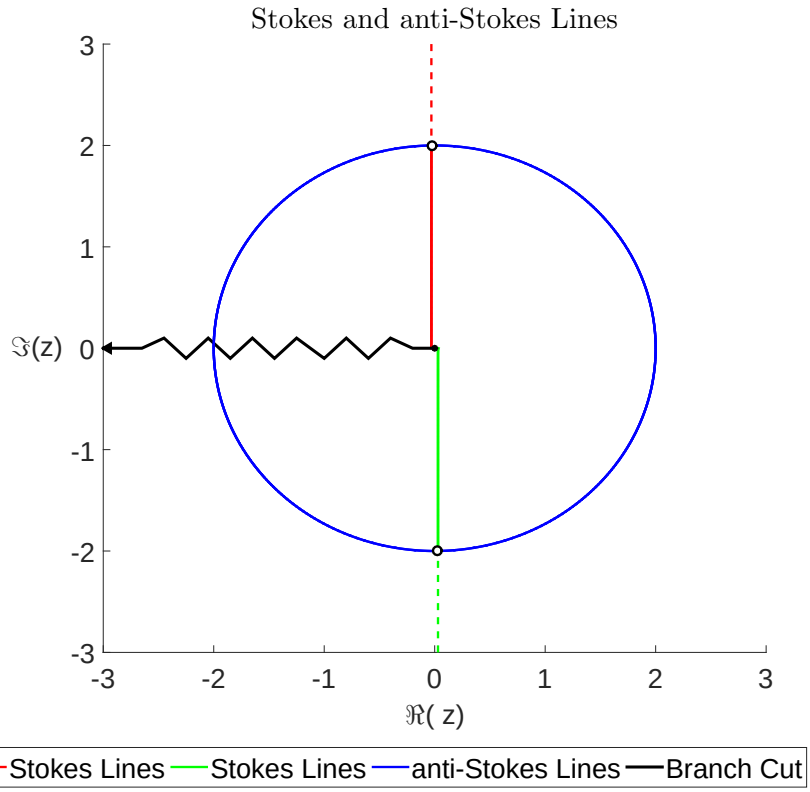


Figure 5.10 Red and green lines show the active Stokes lines for $u_1^1(z)$ given in (5.79) based on the turning points when $\Im(z) > 0$ and $\Im(z) < 0$, respectively, for $\nu_0 = 4$ and $\varepsilon = 0.1$. Blue circle is the anti-Stokes lines for $u_1^1(z)$. Turning points in which the both Stokes and anti-Stokes lines cross are represented by the black circles. Black zigzag on the negative real axis below 0 illustrates the branch cut.

However, we notice that circulating around the turning points in Figure 5.10 does not bring us back to where we started. Hence, we will conduct the local analysis near one of the turning points in order to see the behaviour of the first level differential equation. Let us assume

$$z = i\sqrt{\nu_0} + \delta\zeta, \tag{5.89}$$

in which $0 < \delta \ll 1$. Substitution of this under the consideration of the chain rule into (5.68) gives

$$\frac{\varepsilon^4}{\delta^2}\frac{d^2Q(\zeta)}{d\zeta^2} + \frac{2i\varepsilon^2\sqrt{v_0}}{\delta}\frac{dQ(\zeta)}{d\zeta} - 8i\sqrt{v_0}\delta\zeta Q(\zeta) \sim 1, \tag{5.90}$$

for small δ. Balancing δ scaling in terms of ε will provide the behaviour. Suppose $\varepsilon = \delta$, and then (5.90) turns out to be

$$2\varepsilon i\sqrt{v_0}\frac{dQ(\zeta)}{d\zeta} - 8\varepsilon i\sqrt{v_0}\zeta Q(\zeta) \sim 1, \tag{5.91}$$

in which only the leading order terms are considered. It is in the form of error function, and therefore it should behave like an error function near the turning point as plotted in Figure 5.11 for $u_1^2(z)$. Next, assume $\varepsilon^2 = \delta$. In this case, (5.90) becomes

$$\frac{d^2Q(\zeta)}{d\zeta^2} + 2i\sqrt{v_0}Q(\zeta) \sim 1. \tag{5.92}$$

Since it does not involve any multiplication of ζ in it unlike to (5.91), it does not generate a divergent series. In this situation, the associated Stokes lines are inactive. Therefore, in Figure 5.10, red and green lines illustrate the inactive Stokes lines and switching does not occur.

Although the detailed explanation will be given later on in §8, since the second order inhomogeneous differential equation for the remainder in (5.65), which is simplified as (5.68), has two exponentials with the RHS, there is a possibility for emerging of HOSL. Hence, we will briefly discuss this here. The condition for the HOSL to occur is to have at least three or more exponential terms. Particularly, HOSL stems from the crossing point (regular point) of Stokes lines in which the Stokes lines may terminate. However, usual Stokes lines begins from the turning points in which the expansion(s) diverges. HOSL can be located when the exponentials fulfil the condition [56, 60],

$$\frac{u_0 - u_1^2(z)}{u_0 - u_1^1(z)} \in \mathbb{R}, \tag{5.93}$$

where u_0 represents the power in exponential, $\exp(-u_0) = 1$, from the RHS of (5.68). Hence, it equivalently is the locus of the points when the following is purely real and positive

$$\frac{-z^2 - 2\nu_0 \ln(z) + 2\nu_0 \ln(i\sqrt{\nu_0}) - \nu_0}{-2\nu_0 \ln(z) + 2\nu_0 \ln(i\sqrt{\nu_0})}. \tag{5.94}$$

The only crossing point is the singular point of the singulants from which Stokes lines emerge so that the associated HOSL is inactive. Hence, it is only plotted in Figure 5.11. Furthermore, this could also be seen by the Stokes lines; in particular, since both the Stokes lines lie along $\pm\pi/2$, they do not cross each other, and therefore Stokes crossing point does not exist.

5.4 Conclusion and discussion

Using the techniques in multi-level asymptotics, we have presented the asymptotic series solution of the error function in addition to the general features of the exponential asymptotics. To achieve the most accurate approximate solution of $\mathrm{erf}(z/\varepsilon)$ with minimum error for sufficiently small ε, we first expressed the behaviour of the function as an asymptotic power series. Once the late order term of the expansion was identified, we used this information to examine the exponentially small variations of the asymptotic series solution. Secondly, and more importantly, in the investigations, we have truncated the series solutions at the point where they take their absolute least value in order to obtain a meaningful approximation. In fact, determining the late order term for large values of n, was the critical point of the exponential asymptotics to be able to investigate asymptotic behaviours of the remainders. We established that if the divergent series of such expansions are truncated after the optimal number, the remainders turned out to be exponentially small and their behaviour was demonstrated in the error figures of this chapter.

In §§5.2.2, 5.2.5 and 5.3.5, we have addressed the complete Stokes analysis by

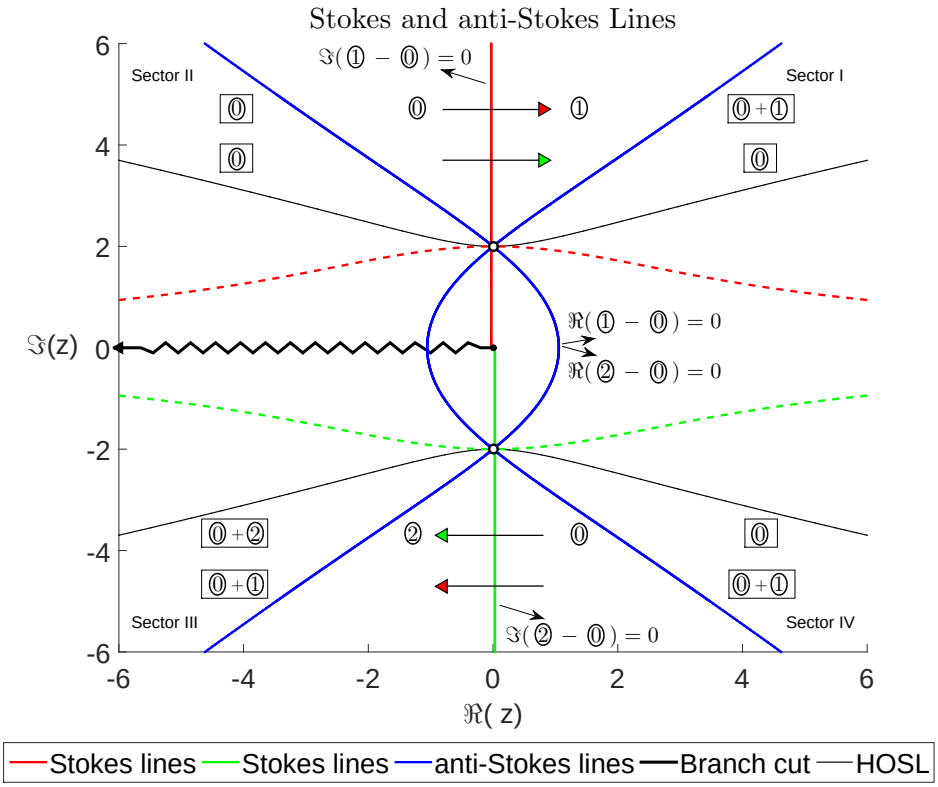


Figure 5.11 Red and green lines represent the Stokes lines for $u_1^2(z)$ in (5.80), whilst blue lines represent the anti-Stokes lines for arbitrarily chosen $\nu_0 = 4$ and $\varepsilon = 0.1$. Thin black lines show inactive HOSL whilst the zigzag shows the branch cut which leads to removal of the relevant exponential across. Turning points where the Stokes, HOSL and anti-Stokes lines cross each other are represented by the black dots. ① and ② indicate the exponential occurred by the singulants in $\Im(z) > 0$ and $\Im(z) < 0$ respectively, and ⓪ shows the exponential in the RHS. Present exponentials of the sectors are shown in boxes.

considering the late-order terms of the asymptotic expansions, and hence observed that the singularities of the leading order terms are associated with the Stokes phenomenon. Having determined the complete form of the general term or the power of the exponentials investigated after optimal truncation, we were able to determine the Stokes and anti-Stokes lines. We demonstrated that upon crossing the Stokes lines, the subdominant exponentials switched on and off, whereas upon crossing the anti-Stokes lines they changed their characteristics; in particular, the subdominant exponentials grew exponentially as $\varepsilon \to 0$ by the anti-Stokes lines. As a result of the investigation, the way the switching behaviour occurs across the Stokes lines was

illustrated in Figure 5.1 and Figure 5.7. Travelling along the complex-z plane, we established that subdominant exponentially small terms cannot be neglected as they become dominant near the anti-Stokes lines.

With the re-expansion of level zero remainders and having repeated the same steps of level zero, we established the hyperasymptotic solutions of the error function in two levels. However, in the level one analysis of §§5.2.3 and 5.3.3, the late order terms have been constructed by the application of the factorial-over-a-power method, and so that the close form of these terms was not found. Hence, the analysis required more care. On the other hand, the turning points of both equations in level zero were not a turning point in the first level. Further analysis showed that there were logarithmic singularities which caused a branch cut in this conjecture for the first level expansions generated by these turning points.

In this chapter we have employed a new approach of hyperasymptotic expansion by focusing on the truncated remainder functions of the $\mathrm{erf}(z)$ function. By repeated optimal truncations we illustrated that the error of the expansions gets exponentially smaller compared to the previous level for sufficiently small ε, a similar observation as those addressed in the Table 5.1. Moreover, in our technique, by minimising the first level of the error estimates in terms of the truncation points and increasing the zeroth level truncation points arbitrarily in the first level, we have reduced the first level error. We obtained this behaviour of the error estimate by considering the level one error as a function of the level zero truncation point. These exponential improvements of the hyperasymptotic expansion and comparisons of the error plots are illustrated in figures, such as Figure 5.3, Figure 5.4, Figure 5.5, Figure 5.6, Figure 5.8, Figure 5.9. Nevertheless, the accuracy also depends on the parameter θ; indeed, as we moved away from the Stokes lines with the argument, we observed that the error decreases faster, see for example Figure 5.6. In light of the results gathered in this chapter, the present findings agree with the findings of the previous chapter.

Chapter 6

Airy function

6.1 Introduction

This chapter addresses the well-known Airy function [78] within the context of hyperasymptotics. While analysing the Airy function, we aim to illustrate the new approach of hyperasymptotics explained in previous chapters throughout. Using exponential asymptotic techniques, exponentially small terms will be identified and the subdominant changing behaviour of these terms across the Stokes lines will be investigated in two levels. Airy function occurs in solutions of the Schrödinger equation in some particular cases and has applications in areas such as in physics, quantum mechanics, radiative transfer [80, pp. 137]. A more detailed explanation of the Airy function may be found in [77], [81, pp. 195-212], and its Stokes picture can be seen such as in [51] by Berry. Additionally, Airy function was the function Stokes himself studied in [38], and where he first observed the discontinuous changing behaviours of the exponential terms.

The outline of the chapter is as follows: first, we will find the WKB solution of the Airy differential equation in §6.2. Upon doing this, we will rescale the function according to its WKB solution and obtain a new differential equation. The rest of the steps are similar to the steps of previous chapters. In particular, we expand and derive

the approximate series solution in terms of a small parameter. To truncate the series after an optimal number of terms, we need to derive the general representation of the expansion. Hence, after deriving it, we will truncate the asymptotic series solution where it takes its minimum value in §6.3. Once this is done, Stokes phenomenon of the Airy function will be presented in §6.4, which completes the zeroth level of the hyperasymptotics. In §6.5 and afterwards, we will repeat the similar analyses of the zeroth level in the sense of hyperasymptomatics. In particular, we will truncate the first level expansion and discuss its behaviour in terms of arbitrary truncation points. Moreover, in §6.7, the error occurring after the first level truncation will be investigated near and away from the singularities based on the singulants of the first level expansion in detail. Finally, we will conclude the present chapter by addressing the conclusion in §6.9.

6.2 Airy function expansion

Let us first introduce the differential equation also known as the Airy equation [82] that will be examined in this chapter,

$$\frac{d^2}{dz_1^2}y(z_1) - z_1 y(z_1) = 0, \tag{6.1}$$

which has a turning point at $z_1 = 0$. One of two solutions of this differential equation is called the Airy function [27]. Performing the WKB approximation method for large z_1 enables us to determine two solutions as

$$y(z_1)_\pm \sim C_\pm \frac{\exp\left(\pm\frac{2}{3}z_1^{3/2}\right)}{z_1^{1/4}}, \tag{6.2}$$

where $C_\pm$ is an unknown constant and $\pm$ is associated with the sign of the powers in exponential term. The two linearly independent solutions $y(z_1)_+$ and $y(z_1)_-$ are also denoted by $\mathrm{Ai}(z)$ and $\mathrm{Bi}(z)$, respectively, [68, 78]. These two WKB solutions of the

Airy functions have a branch point at $z = 0$ as they are multivalued for the complex z. It is worth remarking that the detailed discussion of the WKB approach will be presented when studying the confluent hypergeometric function in §7, since the WKB analysis of the Airy function is already done in [81, pp. 195-212] and in [67, pp. 484-496] in more detail. In what follows, since there are two solutions, without loss of generality we are going to proceed with one; however, a similar calculation may also be done with the other solution. To obtain the asymptotic expansion, we rescale $y(z_1)$ according to (6.2) as they solve Airy equation (6.1), yielding

$$y(z_1)_- = C_- \frac{\exp\left(-\frac{2}{3}z_1^{3/2}\right)}{z_1^{1/4}} W(z_1)\,. \tag{6.3}$$

Substitution of this rescaled equation into the original equation (6.1) leaves a differential equation solely involving $W(z_1)$ as

$$W''(z_1) - \frac{W'(z_1)}{2z_1} - 2\sqrt{z_1}W'(z_1) + \frac{5}{16z_1^2}W(z_1) = 0. \tag{6.4}$$

The exponential asymptotics is often discussed with a small parameter, ε; hence, we rescale large z_1

$$z_1 = \frac{z}{\varepsilon^{2/3}}, \tag{6.5}$$

when $\varepsilon \to 0$, without loss of generality. Making the substitution of newly introduced (6.5) under the consideration of the chain rule produces the differential equation for $W(z)$, giving

$$\varepsilon W''(z) - \frac{\varepsilon}{2z}W'(z) - 2\sqrt{z}W'(z) + \frac{5\varepsilon}{16z^2}W(z) = 0, \tag{6.6}$$

whose highest derivative is a multiple of ε. As usual, we expand $W(z)$ into small powers of ε

$$W(z) \sim \sum_{n=0}^{\infty} \varepsilon^n w_n(z). \tag{6.7}$$

First we perform back substitution and then equating like powers of ε yield

$$\sum_{n=0}^{\infty} \varepsilon^{n+1} \left(w_n''(z) - \frac{1}{2z} w_n'(z) - 2\sqrt{z} w_{n+1}'(z) + \frac{5}{16z^2} w_n(z) \right) - 2\sqrt{z} w_0'(z) = 0. \tag{6.8}$$

As it is already clear from the above expression, using the matched asymptotic expansion, we find the leading order term at $\mathrm{O}(1)$ as

$$w_0'(z) = 0, \tag{6.9}$$

and the differential recursive equation for the coefficients of the expansion at $\mathrm{O}(\varepsilon^{n+1})$ satisfying

$$w_n''(z) - \frac{1}{2z} w_n'(z) - 2\sqrt{z} w_{n+1}'(z) + \frac{5}{16z^2} w_n(z) = 0, \tag{6.10}$$

in which $n \geq 0$. From (6.9), it is apparent that w_0 is a constant, so rather than introducing a new constant term, we use w_0 as an integration constant. Performing the recurrence relation (6.10) for $n = 0$ and 1 and recursively, we compute the first two successive terms of the expansion in terms of w_0 as follows

$$w_1(z) = -\frac{5}{3.4^2} \frac{w_0}{z^{3/2}} + c_1, \qquad w_2(z) = \frac{5.7.11}{3^2.4^4.2} \frac{w_0}{z^3} - \frac{5}{3.4^2} \frac{c_1 w_0}{z^{3/2}} + c_2. \tag{6.11}$$

We must ensure the singularity of (6.11) at $z = 0$ is stored in all the later order terms. We notice that the second and third terms of $w_2(z)$ have the same form as $w_1(z)$. Moreover, we can always absorb these terms into the previous term, which is why the constants c_1, c_2 can be setted to 0. By repeatedly using the recursive relationship, we find out that the general term of the asymptotic series can be expressed as

$$w_n(z) \sim \left(-\frac{3}{4} \right)^n \frac{\Gamma(n+5/6)\Gamma(n+1/6)}{2\pi z^{3n/2}\Gamma(n+1)} w_0, \tag{6.12}$$

and the late order term secures the singularity. Since in the recurrence relation each further term of the expansion are defined by differentiation of the preceding term twice, the power of the singularity increases in each subsequent term calculated. Therefore, the general term diverges in the nature of a factorial-over-a-power. To be more precise, using Stirling's formula for the factorial terms in (6.12), we see that it approximates indeed in this nature as

$$w_n(z) \sim \left(-\frac{3}{4}\right)^n \frac{\Gamma(n)}{2\pi z^{3n/2}} w_0, \tag{6.13}$$

Since a general term of an expansion in exponential asymptotics must diverge in this form; in order to ensure consistency, let us assume its late order term takes the following expression in the limit $n \to \infty$

$$w_n(z) = \frac{\Gamma(n+\gamma)}{u_0(z)^{n+\gamma}} \sum_{k=0}^{\infty} \left(\frac{1}{n^k} A_k(z)\right), \tag{6.14}$$

where γ, $u_0(z)$ and $A_k(z)$'s are independent of n, and $\gamma = \mathrm{O}(1)$ is an arbitrary constant like in the earlier chapters. Here, the key point to be noted for the ansatz is that the singulant is subject to

$$u_0(z) = 0 \quad \text{when} \quad z_1 = 0. \tag{6.15}$$

After straightforward substitution of (6.14) into the differential recursive relation (6.10), and solving the singulant subject to the singularity, we establish that

$$u_0(z) = -\frac{4}{3} z^{3/2} \qquad \text{and} \qquad A_k = c_k \quad \forall\, k, \tag{6.16}$$

where c_ks are constants of integrations. Ideally, by inserting these values into the ansatz (6.14), we arrive at

$$w_n(z) \sim \left(-\frac{3}{4z^{3/2}}\right)^{n+\gamma} \Gamma(n+\gamma)\, c_0, \tag{6.17}$$

in which c_0 is the leading order term of the summation in (6.14) for large n. Matching both late order terms found by repeated use of the recursion equation in (6.13) and by the factorial-over-a-power method in (6.17) leads to

$$\frac{3n}{2} = \frac{3}{2}(n+\gamma) \implies \gamma = 0,$$

and the constant c_0 is $w_0/2\pi$. Hence, we show both late order terms agree with each other. As the determination of the general term of the expansion is complete, the expansion can be truncated next.

6.3 Optimal truncation

We now truncate the asymptotic series solution in (6.7) after N_0 terms, yielding

$$W(z) = \sum_{n=0}^{N_0-1} \varepsilon^n w_n(z) + R_{N_0}(z), \tag{6.18}$$

in which R_{N_0} is the remainder, and this resultant term shares some general features of the exponential asymptotics which will be considered soon. Here we introduce the zeroth level truncation error by the first neglected term of the expression, that is,

$$E_{N_0}(z) := \varepsilon^{N_0} \left(-\frac{3}{4z^{3/2}}\right)^{N_0} \frac{\Gamma(N_0)}{2\pi} w_0. \tag{6.19}$$

After substituting the truncated sum with the remainder into the original differential equation, we find the inhomogeneous remainder differential equation

$$\begin{aligned} \varepsilon R''_{N_0}(z) - \frac{\varepsilon}{2z} R'_{N_0}(z) - 2\sqrt{z} R'_{N_0}(z) + \frac{5\varepsilon}{16z^2} R_{N_0}(z) &= -2\varepsilon^{N_0} \sqrt{z} w'_{N_0}(z) \\ &= -2\varepsilon^{N_0} \left(-\frac{3}{4}\right)^{N_0+1} \frac{\Gamma(N_0+1)}{\pi} \frac{w_0}{z^{\frac{3N_0}{2}+\frac{1}{2}}}. \end{aligned} \tag{6.20}$$

Herein, the RHS of (6.20) is written by using the general term of the expansion in (6.12). Using one of the methods of optimal truncation introduced in (2.9) of §2, we

obtain that the truncation point of the expansion in which the series takes its least value in magnitude occurs at

$$N_0 \sim \frac{4}{3\varepsilon}\left|z^{3/2}\right|, \tag{6.21}$$

which approaches to infinity in the limit $\varepsilon \to 0$. We observe that the optimal truncation is the magnitude of the singulant divided by ε. Moreover, once this point is applied to the remainder term, they appear in the exponential power; in fact, this makes the remainder exponentially small. We now have enough information to obtain the existence of the Stokes phenomenon employing the singulants from the previous sections.

6.4 Stokes and anti-Stokes lines

In this section, we will discuss the Stokes and anti-Stokes lines of the Airy function. Based on the analysis in §6.2, we have the exponential terms as in the form of $\exp(-u_0/\varepsilon)$ from the WKB solution obtained in (6.2), given by

$$u_0^1(z) = -\frac{2}{3}z^{3/2} \qquad \text{and} \qquad u_0^2(z) = \frac{2}{3}z^{3/2}, \tag{6.22}$$

where the subscript of $u_0(z)$ refers to the level of the hyperasymptotic expansion and the superscripts denote the singulants of the associated levels. Hence, Stokes lines emerge whenever they fulfil the conditions

$$\Im\left(u_0^i(z) - u_0^j(z)\right) = 0 \qquad \text{and} \qquad \Re\left(u_0^i(z) - u_0^j(z)\right) > 0, \tag{6.23}$$

where $i, j = 1, 2$ such that $i \neq j$. According to (6.23), we have

$$u_0^{\mathbf{1}}(z) \text{ turns } \mathbf{on} \; u_0^{\mathbf{2}}(z) \text{ when :} \qquad \Im\left(z^{3/2}\right) = 0 \quad \text{and} \quad \Re\left(-z^{3/2}\right) > 0, \tag{6.24}$$

$$u_0^{\mathbf{2}}(z) \text{ turns } \mathbf{on} \; u_0^{\mathbf{1}}(z) \text{ when :} \qquad \Im\left(z^{3/2}\right) = 0 \quad \text{and} \quad \Re\left(z^{3/2}\right) > 0. \tag{6.25}$$

For convenience, let us suppose $z = r\exp(i\theta)$ as usual. In light of the polar coordinates, active Stokes lines for (6.24) occur along $ph(z) = \pm 2\pi/3$. Likewise, the active Stokes line for (6.25) lies at $ph(z) = 0$. For $\mathrm{Ai}(z)$, only the subdominant exponential is present on this line as shown in Figure 6.1a; whence, Stokes phenomenon does not occur. However, as both exponentials are present for $\mathrm{Bi}(z)$, as illustrated in Figure 6.1b, Stokes switching on and off occurs. Hence, $ph(z) = 0$ is an active Stokes line for Bi(z), but it is irrelevant for Ai(z). Likewise, anti-Stokes lines appears when

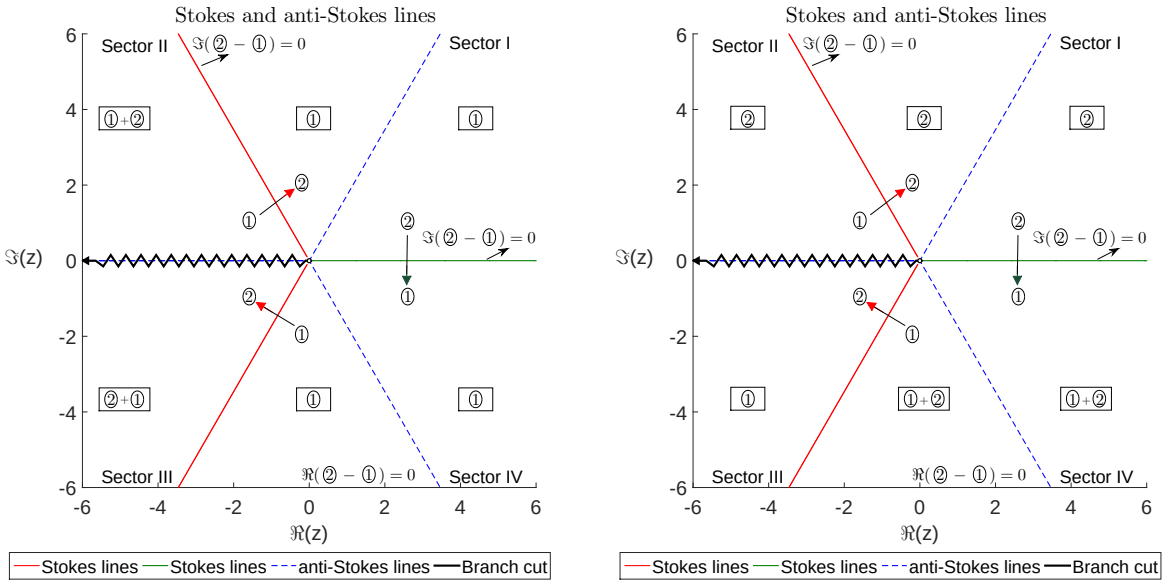
$$\Re\left(u_0^1(z) - u_0^2(z)\right) = 0, \tag{6.26}$$

whence they occur along $ph(z) = \pm\pi/3, \pi$. Thus, the Stokes structure of the Airy function in level zero can now be pictured. Although the Airy equation does not have a branch cut, its WKB solutions in (6.2) have a square root branch cut where we chose it to lie along the negative real axis. Therefore, in the WKB approximation the exponentials swap identities, so that the Airy function itself does not see the branch cut. In Figure 6.1, we have illustrated these lines. Associated exponentials $\exp\left(-u_0^1(z)/\varepsilon\right)$ and $\exp\left(-u_0^2(z)/\varepsilon\right)$ are labelled by ① and ②, respectively. Through circuiting along the complex plane, we return to where we started in both figures. Present exponentials of the relevant sectors are shown in boxes in Figure 6.1.

As level zero is completed, we can begin the first level hyperasymptotic analysis of the Airy function in the following section to obtain a better approximation than the zeroth level expansion. Upon deriving the late order term, we truncate the series and discuss the error by the arbitrary truncation points of both zeroth and first levels.

6.5 First level of hyperasymptotics

In this section, to attain the asymptotic expansion of the remainder, we first rescale the zeroth level remainder according to the RHS of (6.20) such that



(a) (b)

Figure 6.1 Stokes structure of the zeroth level expansion, relevant exponentials are represented by ① and ②. While red lines correspond to (6.24), where $\Re\left(u_0^2(z)-u_0^1(z)\right)>0$, green lines correspond to (6.25), where $\Re\left(u_0^1(z)-u_0^2(z)\right)>0$. Zigzag in black shows the branch cut across which the exponentials switch identities. In Figure 6.1a, only ① is present in the relevant sectors, hence no switching occurs across the green line and the Stokes line is irrelevant. In Figure 6.1b, green line is active and the switching on and off occurs.

$$R_{N_0}(z) := -2\varepsilon^{N_0+1}\left(-\frac{3}{4}\right)^{N_0+1}\frac{\Gamma(N_0+1)}{\pi}\frac{w_0}{z^{\frac{3N_0}{2}+\frac{1}{2}}}Q(z), \tag{6.27}$$

where $Q(z)$ is to be discussed, and without loss off generality the constant w_0 can be taken as 1. As in the zeroth level, substitution of this re-scaled remainder into (6.20) provides a differential equation for $Q(z)$

$$\begin{aligned}\varepsilon^2 Q''(z)-\varepsilon\left(\frac{3\nu_0}{z}+2\sqrt{z}\right)Q'(z)-\frac{3\varepsilon^2}{2z}Q'(z)+\left(\frac{9\nu_0^2}{4z^2}+\frac{3\nu_0}{\sqrt{z}}\right)Q(z)\\ +\varepsilon\left(\frac{15\nu_0}{4z^2}+\frac{1}{\sqrt{z}}\right)Q(z)+\frac{31\varepsilon^2}{16z^2}Q(z)=1,\end{aligned} \tag{6.28}$$

in which we set $\nu_0=\varepsilon N_0$ for convenience. Next, in order to derive the asymptotic series solution, we expand $Q(z)$ into powers of ε

$$Q(z) \sim \sum_{n=0}^{\infty} \varepsilon^n Q_n. \tag{6.29}$$

Substituting (6.29) into (6.28), we derive the leading order term at $\mathrm{O}(1)$, and the recursive relationship at $\mathrm{O}\left(\varepsilon^{n+2}\right)$ respectively

$$\begin{aligned} Q_0(z) &= \frac{4z^2}{3\nu_0\left(3\nu_0+4z\sqrt{z}\right)}, \\ Q_n''(z) - \left(\frac{3\nu_0}{z}+2\sqrt{z}\right)Q_{n+1}'(z) - \frac{3}{2z}Q_n'(z) + \left(\frac{9\nu_0^2}{4z^2}+\frac{3\nu_0}{\sqrt{z}}\right)Q_{n+2}(z) \\ + \left(\frac{15\nu_0}{4z^2}+\frac{1}{\sqrt{z}}\right)Q_{n+1}(z) + \frac{31}{16z^2}Q_n(z) = 0, \end{aligned} \tag{6.30}$$

in which the leading order term $Q_0(z)$ has singularities at $z = (-3\nu_0/4)^{2/3}$. As the singularities cause the asymptotic series solution to diverge in the form of a factorial-over-a-power, let us define the general term of the expansion as

$$Q_n(z) = \frac{\Gamma(n+\gamma)}{u_1(z)^{n+\gamma}} \sum_{k=0}^{\infty} \left(\frac{1}{n^k} B_k(z)\right), \tag{6.31}$$

where γ is a constant, and $u_1(z)$ and $B_i(z)$s are to be determined; in particular, the singulant satisfies $u((-3\nu_0/4)^{2/3}) = 0$. Direct substitution of this ansatz, after following the method of matched asymptotic expansions, at order n^2 reveals

$$\frac{B_0}{(u_1(z))^2}\left(u_1'(z)+\frac{3\nu_0}{2z}\right)\left(u_1'(z)+\frac{3\nu_0}{2z}+2\sqrt{z}\right) = 0. \tag{6.32}$$

As explained in the previous chapters, B_0 cannot be zero for the same reason; whence, we have two options as

$$u_1'(z)+\frac{3\nu_0}{2z} = 0 \qquad \text{and} \qquad u_1'(z)+\frac{3\nu_0}{2z}+2\sqrt{z} = 0. \tag{6.33}$$

After integration, solving them subject to singular points of the leading order term completes the determination of the singulants of the first level expansion

$$u_1^1(z) = \nu_0 \ln\left(-\frac{3\nu_0}{4z^{\frac{3}{2}}}\right) \qquad \text{and} \qquad u_1^2(z) = \nu_0 \ln\left(-\frac{3\nu_0}{4z^{\frac{3}{2}}}\right) - \frac{4}{3}z^{\frac{3}{2}} - \nu_0, \quad (6.34)$$

in which the subscript refers to the level of the hyperasymptotic expansion, and the superscripts denote the singulants of the first level. It is important to note that both singulants have the logarithmic branch cut, lying along the negative axis when inspecting the Stokes structure of the first level Airy function. To proceed, in a similar manner to (6.32), application of (6.31) enables us to obtain the expression at order n

$$\begin{aligned}\frac{B_1}{(u_1(z))^2}\left(u_1'(z)+\frac{3\nu_0}{2z}\right)\left(u_1'(z)+\frac{3\nu_0}{2z}+2\sqrt{z}\right)\\ +\left(-u_1''(z)+\frac{3u_1'(z)}{2z}+\frac{15\nu_0}{4z^2}+\frac{1}{\sqrt{z}}\right)\frac{B_0(z)}{u_1(z)}-\left(2u_1'(z)+\frac{3\nu_0}{z}+2\sqrt{z}\right)\frac{B_0'(z)}{u_1(z)}=0.\end{aligned} \quad (6.35)$$

Solving this expression according to relevant singulants $u_1^{1,2}(z)$ derived in (6.34) establishes the leading order term $B_0(z)$ of the ansatz by means of

$$B_{0_{u_1^{1,2}}}(z) = \sqrt{z}. \quad (6.36)$$

Thence, the series solution of the first level equation turns out to be a linear combination of these two,

$$Q_n(z) \sim C_2 \frac{\Gamma(n+\gamma)}{\left(u_1^1(z)\right)^{n+\gamma}} B_{0_{u_1^1}}(z) + C_3 \frac{\Gamma(n+\gamma)}{\left(u_1^2(z)\right)^{n+\gamma}} B_{0_{u_1^2}}(z), \quad (6.37)$$

in which both C_2 and C_3 are constants. Since the late order terms are derived, the next step is to truncate the divergent series. The error estimate of the Airy function will be also investigated in the following section by keeping the truncation points arbitrary and writing the first level truncation point as a function of level zero truncation point and how it influences behaviour of the error estimate.

6.6 Truncation

Motivated by the discussion in §6.3, truncating the series after $N_1 \gg 1$ terms yields

$$Q(z) \sim \sum_{n=0}^{N_1-1} \varepsilon^n Q_n(z) + \mathscr{R}_{N_1}(z), \tag{6.38}$$

where $\mathscr{R}_{N_1}$ is a remainder of the series and $\mathscr{R}_{N_1} = \mathrm{O}(\varepsilon^{N_1})$. Applying this truncated expression in (6.18), we find the first $N_0 + N_1$ terms of the hyperasymptotic expansion with the first level resultant

$$\begin{aligned} W(z) \sim \sum_{n=0}^{N_0-1} \varepsilon^n w_n(z) - 2\varepsilon^{N_0+1} \left(-\frac{3}{4}\right)^{N_0+1} \frac{\Gamma(N_0+1)}{\pi} \frac{w_0}{z^{\frac{3N_0}{2}+\frac{1}{2}}} \sum_{n=0}^{N_1-1} \varepsilon^n Q_n(z) \\ - 2\varepsilon^{N_0+1} \left(-\frac{3}{4}\right)^{N_0+1} \frac{\Gamma(N_0+1)}{\pi} \frac{w_0}{z^{\frac{3N_0}{2}+\frac{1}{2}}} \mathscr{R}_{N_1}(z). \end{aligned} \tag{6.39}$$

The first level error which occurs due to both N_0 and N_1 truncations can be defined as

$$E_{N_1}(z) := 2(-1)^{N_0} \varepsilon^{N_0+N_1+1} \left(\frac{3}{4}\right)^{N_0+1} \frac{\Gamma(N_0+1)}{\pi} \frac{w_0}{z^{\frac{3N_0}{2}+\frac{1}{2}}} Q_{N_1}(z). \tag{6.40}$$

Substitution of the truncated expansion plus the remainder term in (6.38) into (6.28) generates the first level inhomogeneous differential equation of the remainder,

$$\begin{aligned} \mathscr{L}(\mathscr{R}_{N_1}(z);\varepsilon) &\sim -\varepsilon^{N_1} \left(\frac{9\nu_0^2}{4z^2} + \frac{3\nu_0}{\sqrt{z}}\right) Q_{N_1} + \varepsilon^{N_1+1} \left(Q''_{N_1-1} - \frac{3}{2z} Q'_{N_1-1} + \frac{31\varepsilon}{16z^2} Q_{N_1-1}\right) \\ &\sim -\varepsilon^{N_1} \frac{3\nu_0(3\nu_0 + 4z\sqrt{z})}{4z^2} Q_{N_1}(z), \end{aligned} \tag{6.41}$$

for ε small and N_1 large, whereby the parameter $\mathscr{L}$ is defined as

$$\begin{aligned} \mathscr{L}(\mathscr{R}_{N_1}(z);\varepsilon) :=& \varepsilon^2 \mathscr{R}''_{N_1}(z) - \frac{3\varepsilon^2}{2z} \mathscr{R}'_{N_1}(z) - \varepsilon \left(\frac{3\nu_0}{z} + 2\sqrt{z}\right) \mathscr{R}'_{N_1}(z) + \frac{31\varepsilon^2}{16z^2} \mathscr{R}_{N_1}(z) \\ &+ \varepsilon \left(\frac{15\nu_0}{4z^2} + \frac{1}{\sqrt{z}}\right) \mathscr{R}_{N_1}(z) + \left(\frac{9\nu_0^2}{4z^2} + \frac{3\nu_0}{\sqrt{z}}\right) \mathscr{R}_{N_1}(z), \end{aligned} \tag{6.42}$$

which is the same operator as in the (6.28). In light of the technique of optimal truncation given in (2.9), the minimum required number of terms based on both singulants $u_1^{1,2}(z)$ arises at

$$N_1(z) \sim \frac{\left|u_1^{1,2}(z)\right|}{\varepsilon}, \tag{6.43}$$

in which the asymptotic series solution is minimal in magnitude. It is worth to emphasise herein that, if $4z\sqrt{z} = -3\nu_0$, these above truncation points vanish by the definition of $u_1^{1,2}(z)$, and hence the first level expansion stops. Moreover, this could also be seen from the RHS of (6.41). Thus, we must subsequently ensure that $4z\sqrt{z} \neq -3\nu_0$.

The next stage of the analysis is to minimise the first level error estimate (6.40) according to the free truncation points. Firstly, upon rewriting the estimate in terms of ν_0 and ν_1 for brevity, and performing Stirling's approximation; the error is transformed into

$$E_{N_1}(z) \sim A\sqrt{\frac{\nu_0}{\nu_1}}\left(-\frac{3\nu_0}{4ez^{3/2}}\right)^{\nu_0/\varepsilon}\left(\frac{\nu_1}{eu_1^{1,2}(z)}\right)^{\nu_1/\varepsilon+\gamma}, \tag{6.44}$$

in which we set $\nu_1 = \varepsilon N_1$ and $A = 3e^2 w_0/\varepsilon^{\gamma-1}$. Since the estimate is in the factorial-over-a-power form, taking the derivative with respect to ν_1 yields that the derivative equals to zero at the optimal truncation point; in other words, it occurs when $\nu_1 = |u_1^{1,2}(z)|$. Let us now differentiate the estimate over ν_0, which gives

$$\begin{aligned}\frac{dE_{N_1}(z)}{d\nu_0} \sim A\sqrt{\frac{\nu_0}{\nu_1}}\left(-\frac{3\nu_0}{4ez^{3/2}}\right)^{\nu_0/\varepsilon}&\left(\frac{\nu_1}{eu_1^{1,2}(z)}\right)^{\nu_1/\varepsilon+\gamma}\\ &\times\left(\frac{\ln\left(-\dfrac{3\nu_0}{4z^{3/2}}\right)}{\varepsilon} - \frac{\nu_1}{\varepsilon}\frac{\left(u_1^{1,2}(z)\right)'}{u_1^{1,2}(z)}\right).\end{aligned} \tag{6.45}$$

For sufficiently small ε and sufficiently large ν_0, the derivative becomes equal to zero either when

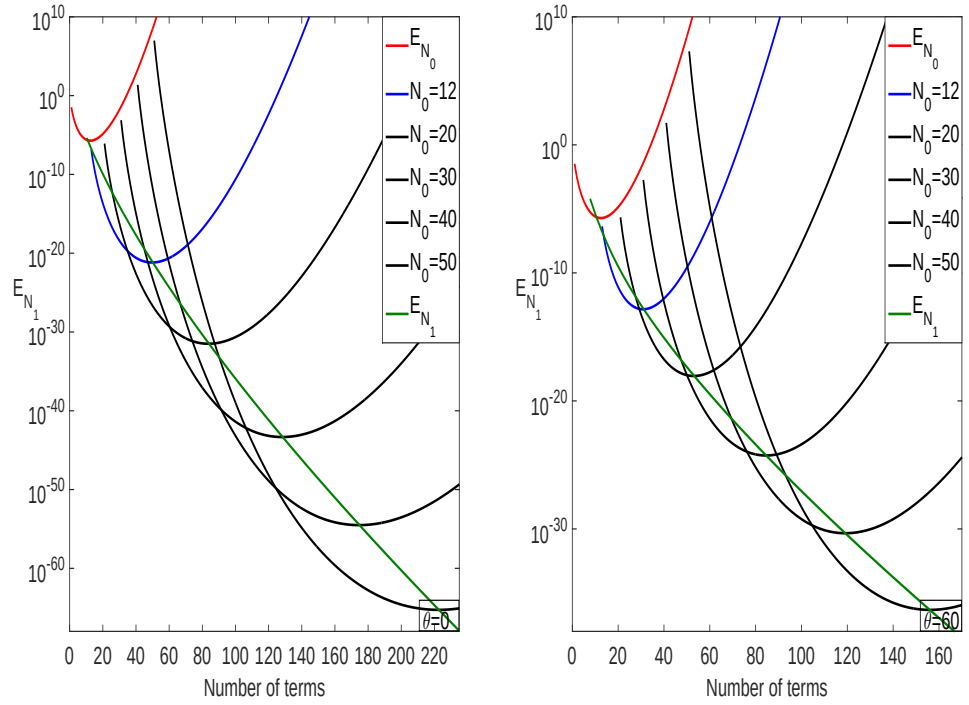
$$\nu_1(z) \sim \left| u_1^{1,2}(z) \right|, \tag{6.46}$$

or

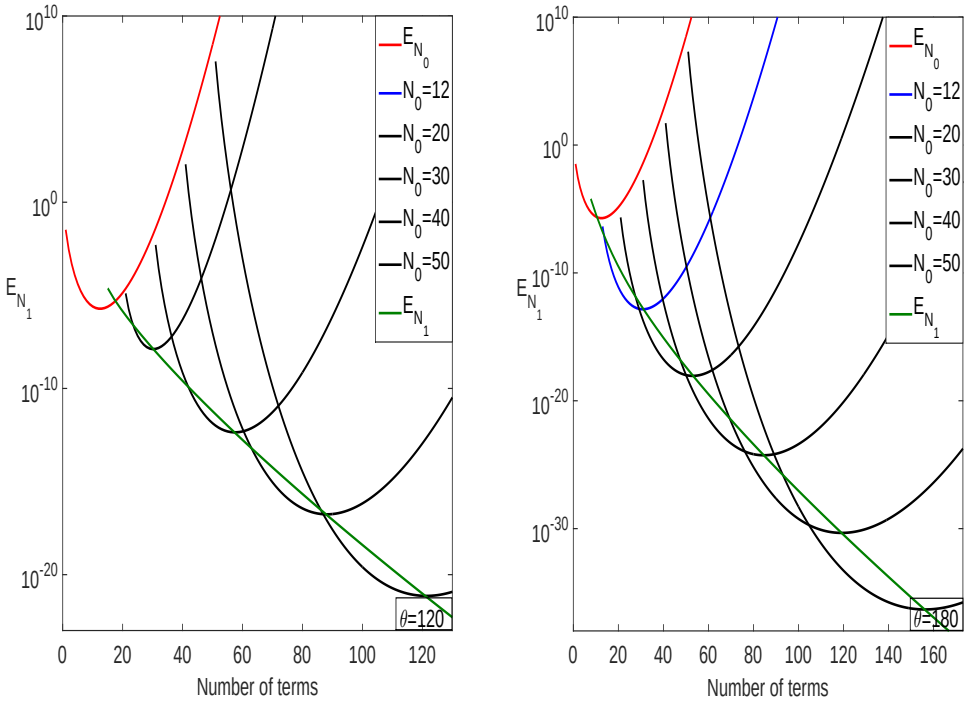
$$\nu_0(z) = \frac{4}{3} \left| z^{3/2} \right|, \tag{6.47}$$

which are respectively the first and the zeroth levels optimal truncation points without ε in their denominators. Thence, the estimates take their absolute least value at these points. Particularly, minimising the errors with respect to ν_1 allows us to derive ν_1 in terms of ν_0 as done previously. Achieving this enables us to have the error estimate (6.40) as a function of ν_0, and see its behaviour for a large ν_0 as explained in the earlier chapters.

Next, we plot the first level error estimate in (6.40). Particularly, Figure 6.2 and Figure 6.3 illustrate the behaviour of the estimate both near and away from the singular point. In all figures, increasing both truncation points together decreases the estimate. Additionally, the figures show that speed of the diminishing error reduces as we approach to the singularity by the phase of z, whereas moving away from the singularity increases the speed. Furthermore, green lines in figures demonstrate the behaviour of the error written by ν_0; in addition to this, while decreasing, they touch the minimum points of the each plots due to the first level optimal truncation point. Moreover, note that Figure 6.2b and Figure 6.2d of Figure 6.2 are similar to each other when they are the same distance away from the Stokes lines by the argument. The same is true for Figure 6.3b and Figure 6.3d. As we carry out the linear problem, it has a rotational symmetry away from the Stokes lines. Figure 6.3d and Figure 6.3c show that the hyperasymptotic method improves again, once the Stokes line at $2\pi/3$ is crossed corresponding to Figure 6.3c. Hence, Figure 6.3d and Figure 6.3c have the same behaviour.

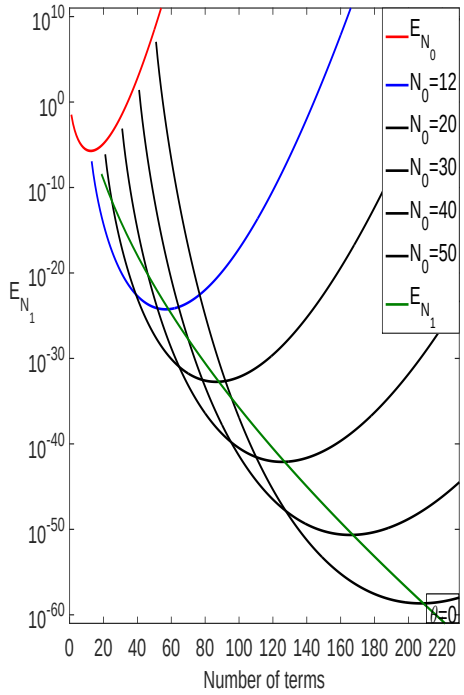


(a) $\theta = 0$ (b) $\theta = \frac{\pi}{3}$

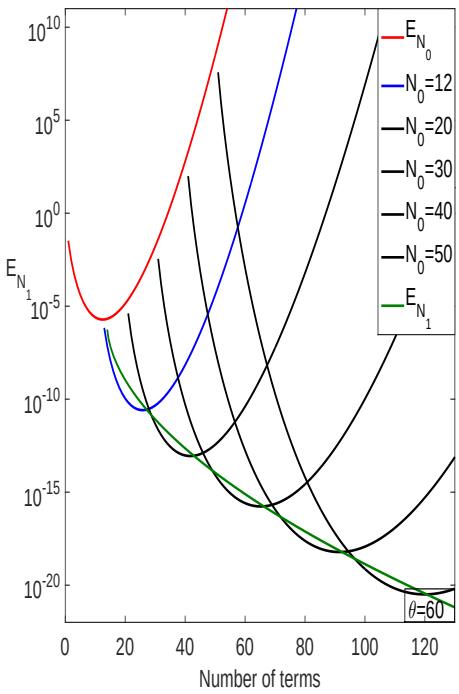


(c) $\theta = \frac{2\pi}{3}$ (d) $\theta = \pi$

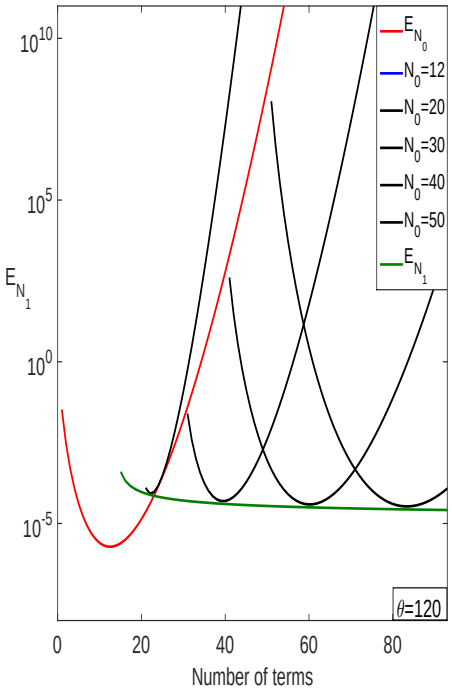
Figure 6.2 Magnitude of the error at two levels (6.40) plotted according to $u_1^1(z)$ in (6.34), for $|z| = 1$ when $\theta = \arg(z) = 0$, $\pi/3$, $2\pi/3$ and $\theta = \pi$, respectively, for $\gamma = 1/2$, $w_0 = 1$ while $\varepsilon = 1/9$. As the level zero truncation point is increased, the error reduces. Moreover, if the second level error (6.40) is written in terms of ν_0 via (6.43) and as the number of the terms are increased, the error decreases as illustrated by the green lines. Optimaly truncated error in blue line disappears in Figure 6.2c since it is on the Stokes line.



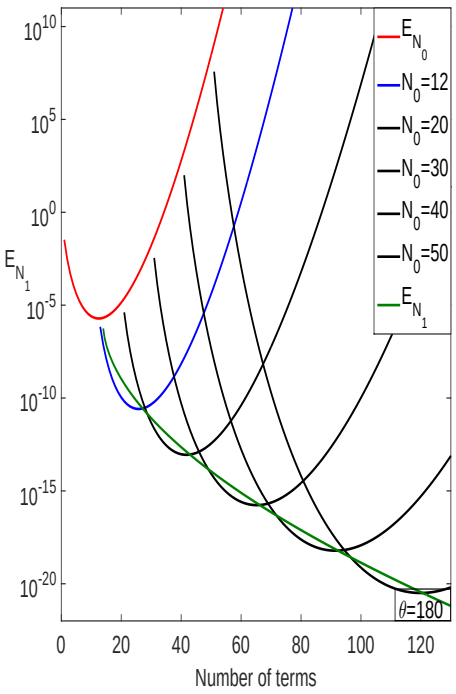
(a) $\theta = 0$



(b) $\theta = \frac{\pi}{3}$



(c) $\theta = \frac{2\pi}{3}$



(d) $\theta = \pi$

Figure 6.3 Magnitude of the second level error estimate (6.40) plotted according to $u_1^2(z)$ in (6.34), for $|z| = 1$ when $\theta = \arg(z) = 0$, $\pi/3$, $2\pi/3$ and $\theta = \pi$, respectively, for $\gamma = 1/2$, $w_0 = 1$ while $\varepsilon = 1/9$. As the number of the terms are increased, the error reduces, and the improvement of the hyperasymptotics increases away from the Stokes line. Blue line disappears in Figure 6.3c as it corresponds to the Stokes line at the optimal truncation for given z.

The forthcoming section is devoted to analytical analysis of the error estimate; in order to ensure the figures of the present section are consistent with analytical results.

6.7 Error analysis

This section demonstrates the behaviour of the error estimate mentioned in the preceding section based on its argument. Since we are interested in the behaviour of the estimate in magnitude, it is easy to verify that ν_1 and $u_1^{1,2}(z)$ cancel each other out by their relation given in (6.46). Thence, we find that the controlling factor of the estimate for sufficiently large ν_0 and ν_1 is

$$E_{N_1}(z) \sim \left(-\frac{3\nu_0}{4ez^{3/2}}\right)^{\nu_0/\varepsilon} \exp\left(-\frac{\nu_1}{\varepsilon}\right), \tag{6.48}$$

with no loss of generality. Before beginning the analysis based on the two singulants, we first suppose that $z = re^{i\theta}$, and then a direct substitution yields

$$E_{N_1}(z) \sim \left(-\frac{3\nu_0}{4r^{3/2}\exp\left(1+\dfrac{3i\theta}{2}\right)}\right)^{\nu_0/\varepsilon} \exp\left(-\frac{\nu_1}{\varepsilon}\right). \tag{6.49}$$

6.7.1 Analysis for $u_1^1(z)$

Let us first examine the error estimate at $2\pi/3$ in which the estimate is in its slowest speed. Substitution of $\theta = 2\pi/3$ into the estimate leads to

$$\begin{aligned} E_{N_1}(z) &\sim \left(\frac{3\nu_0}{4r^{3/2}}\right)^{\nu_0/\varepsilon} \exp\left(-\frac{\nu_0}{\varepsilon}\left(1+\ln\left(\frac{3\nu_0}{4r^{3/2}}\right)\right)\right) \\ &\sim \exp\left(-\frac{\nu_0}{\varepsilon}\right), \end{aligned} \tag{6.50}$$

which is exponentially small as in Figure 6.2c when ν_0 is large. Similarly, moving

away from the singularity while $\theta = 0$, for instance, yields

$$E_{N_1}(z) \sim \exp\left(-\frac{\nu_0}{\varepsilon} - \frac{\nu_0 \pi^2}{2\varepsilon \ln\left(3\nu_0/(4r^{3/2})\right)}\right), \tag{6.51}$$

which gets exponentially smaller for sufficiently small ε as ν_0 gets bigger like in the Figure 6.2a.

6.7.2 Analysis for $u_1^2(z)$

In a similar manner, we first inspect the error estimate at $2\pi/3$ where it is in the slowest speed and almost comes to a halt. In order to observe this, performing $2\pi/3$ in the estimate of $u_1^2(z)$ for large ν_0 gives

$$\begin{aligned} E_{N_1}(z) &\sim \left(\frac{3\nu_0}{4er^{3/2}}\right)^{\nu_0/\varepsilon} \exp\left[\frac{\nu_0}{\varepsilon}\left(1 - \ln\left(\frac{3\nu_0}{4r^{3/2}}\right)\right) - \frac{4r^{3/2}}{3\varepsilon}\right] \\ &\sim \exp\left(-\frac{4r^{3/2}}{3\varepsilon}\right), \end{aligned} \tag{6.52}$$

which is independent from ν_0 and in $\mathrm{O}(1)$ for ν_0 as in Figure 6.3c. Likewise, when $\theta = 0$, the estimate becomes

$$E_{N_1}(z) \sim \exp\left(-\frac{\pi^2 \nu_0^2}{2\varepsilon\left(\ln\left(3\nu_0/(4r^{3/2})\right) - 4r^{3/2}/3 - \nu_0\right)} + \frac{4r^{3/2}}{3\varepsilon}\right), \tag{6.53}$$

which gets exponentially smaller while ν_0 gets larger.

To compare both singulants $u_1^1(z)$ and $u_1^2(z)$, the exponential term $\exp(-\nu_0/\varepsilon)$ of (6.48) which comes from the zeroth level error is not cancelled out in $u_1^1(z)$, whereas it took place in $u_1^2(z)$ by the definition of both singulants in (6.34). Particularly, the rightmost term ν_0 of $u_1^2(z)$ cancels the exponential term coming from the zeroth level which makes the first level error estimate in order one at the argument $2\pi/3$ according to ν_0. Therefore, the error almost stops at this phase. However, since the zeroth

level exponential term is not cancelled out at the same phase, we obtain the estimate based on $u_1^1(z)$ at the slowest speed.

6.8 Stokes and anti-Stokes lines

Having calculated the singulants $u_1^1(z)$ and $u_1^2(z)$ which will appear in the exponentials as in the form of $\exp(-u_1(z)/\varepsilon)$, we now discuss the Stokes structure of the first level expansion. Therefore, in light of the conditions given in (6.23) for $u_1^{1,2}(z)$ with the RHS of (6.28), i.e. $\exp(0)$, we determine the Stokes and anti-Stokes lines of the first level. On the other hand, the singulant $u_1^1(z)$ is calculated in a similar fashion to the singulant (5.79) in the previous chapter. We can easily observe that after the local analysis near the turning point a divergent series from this singulant does not occur, and therefore the associated Stokes lines are inactive. See (5.90) of §5.3.5 for a detailed analysis. Let us locate the Stokes lines emerging via $u_1^2(z)$, which suggests the condition that

$$\Im\left(\nu_0 \ln\left(-\frac{3\nu_0}{4z^{\frac{3}{2}}}\right)-\frac{4}{3}z^{\frac{3}{2}}-\nu_0\right)=0 \quad \text{while} \quad \Re\left(\nu_0 \ln\left(-\frac{3\nu_0}{4z^{\frac{3}{2}}}\right)-\frac{4}{3}z^{\frac{3}{2}}-\nu_0\right)>0. \tag{6.54}$$

We next set the polar coordinates $z = re^{i\theta}$, then the singulant in (6.54) may be written down as

$$\nu_0 \ln\left(\frac{3\nu_0}{4r^{3/2}}\right)-\frac{4}{3}r^{3/2}\cos\left(\frac{3\theta}{2}\right)+i\nu_0\left(\pm\pi-\frac{3}{2}\theta\right)-i\frac{4}{3}r^{3/2}\sin\left(\frac{3\theta}{2}\right). \tag{6.55}$$

Thence, Stokes lines lie along when $\theta = \pm 2\pi/3$. Anti-Stokes lines of the singulant $u_1^2(z)$ occurs whenever the real part of (6.55) is equal to zero, that is

$$\nu_0 \ln\left(\frac{3\nu_0}{4r^{3/2}}\right)-\frac{4}{3}r^{3/2}\cos\left(\frac{3\theta}{2}\right)=0. \tag{6.56}$$

Stokes structure of this stage is demonstrated in Figure 6.4 along with the branch cut. As it is seen from the figure, since the only crossing point of the Stokes lines are

the actual turning points, HOSL is inactive.

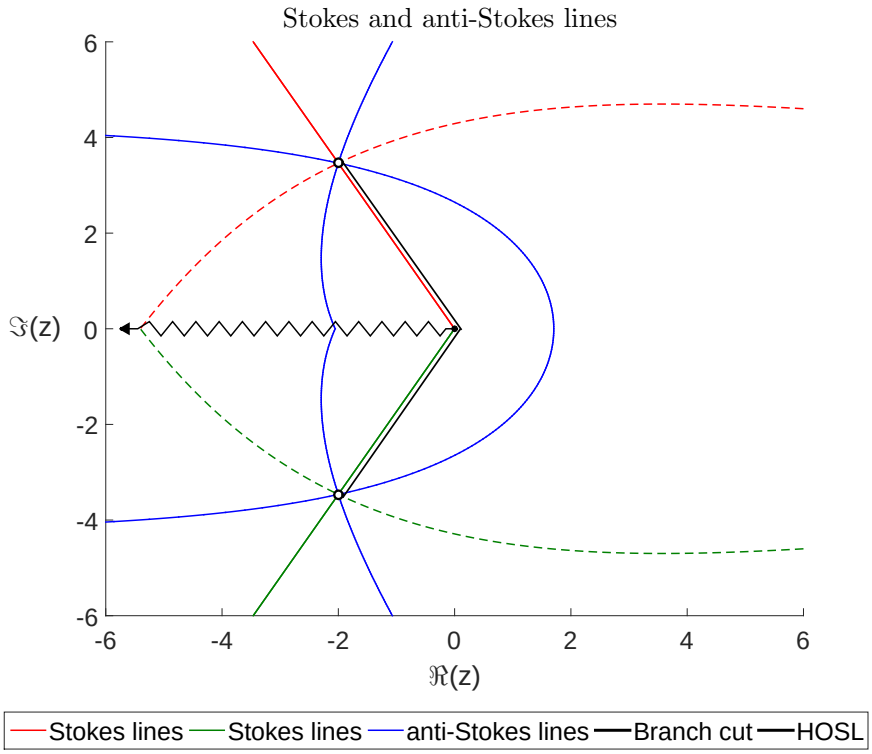


Figure 6.4 The figure is plotted according to $u_1^2(z)$ in (6.34) and 0 for randomly chosen $\nu_0 = 32/3$. Corresponding turning points for ν_0 occur at $z = 2 \pm 2\sqrt{3}i$ from each emerging Stokes lines demonstrated in red and green. Dashed lines represent the inactive-Stokes lines while the lines in black represent the inactive HOSL, and zigzags are the branch cuts.

6.9 Conclusion

In this chapter, we inspected the Airy function within the framework of hyperasymptotics at two levels. In both levels, we represented the asymptotic series solutions of Airy function and its first level differential equation and truncated the expansions and located the Stokes and anti-Stokes lines of each level. Focusing on the truncated remainder of the expansion in the first level, we observed and demonstrated that increasing the zeroth level truncation point arbitrarily increases the first level optimal truncation point whence the first level error estimate is reduced exponentially. Af-

ter having found out the first level truncation point as a function of the zeroth level truncation point and increasing the level zero truncation point, we observed that the first level estimate is decreasing. Nevertheless, we observed that this decreasing behaviour of the error depends on the argument; in particular, moving away from the Stokes line exponentially increases the speed and on the Stokes lines the speed takes its slowest value. Moreover, the singular points of the level zero expansion turned out to be the branch points of the first level expansion, and so such turning points were not involved in the first level. To sum up, present outcomes of this chapter agree with the results of the previous chapters §§4 and 5.

Chapter 7

The confluent hypergeometric function

7.1 Introduction

Confluent hypergeometric functions play an important role in quantum mechanics, optics, statistics and engineering, where they are widely used [83]. Many special functions of mathematical physics can be expressed by the confluent hypergeometric functions (abbreviated as CHF), such as, the exponential integral, the error function, the Airy function, the two-body Coulomb scattering wave function of quantum mechanics, incomplete gamma function, Hermite polynomials, modified Bessel function and parabolic cylinder functions [78, 84–87]. For instance in quantum mechanics, the two-body Coulomb of Schrödinger equation is reduced to the CHF and can be written in terms of it [87, 88]. The second order differential equation

$$z_1(1-z_1)\frac{d^2W(z_1)}{dz_1^2}+\{c-(a+b+1)z_1\}\frac{dW(z_1)}{dz_1}-abW(z_1)=0, \tag{7.1}$$

in which a, b and c are real or complex parameters, is called the hypergeometric equation [74, 84]. Although it is considered as a function of z_1, in some physical problems a and b are considered as a variable. Series solution of this equation is

valid in the neighbourhoods of its singularities $z_1 = 0$, 1 or ∞ and can be constructed using the techniques in exponential asymptotics. The series solution

$$F(a,b;c;z_1) = \frac{\Gamma(c)}{\Gamma(a)\Gamma(b)} \sum_{n=0}^{\infty} \frac{\Gamma(a+n)\Gamma(b+n)}{\Gamma(c+n)} \frac{z_1^n}{n!}, \tag{7.2}$$

is called the hypergeometric function [89–91]. The CHF emerges if two singular points of (7.1) merge into one singular point [92]. Particularly, in the equation (7.1), if z_1 is replaced by z_1/b, and then if we take the limit for b large and set $c = b$, the confluent hypergeometric differential equation [24, 45] is obtained as

$$z_1 \frac{d^2W(z_1)}{dz_1^2} + (b - z_1) \frac{dW(z_1)}{dz_1} - aW(z_1) = 0, \tag{7.3}$$

which has regular and irregular singularities at $z_1 = 0$ and $z_1 = \infty$, respectively. It is also known as Kummer's equation [24]. Hence, the relation between the hypergeometric function and the confluent hypergeometric function can be briefly expressed as

$$M(a,b;z_1) = \lim_{b\to\infty} F\left(a,b;b;\frac{z_1}{b}\right). \tag{7.4}$$

There are two well known series solutions of the confluent equation [63, 93]. One of them is

$$M(a,b;z_1) = \sum_{n=0}^{\infty} \frac{(a)_n}{(b)_n} \frac{z_1^n}{n!}, \tag{7.5}$$

where $(a)_n$, which is known as the Pochhammer's symbol, is defined by

$$(a)_0 = 1, \;\; (a)_n = a(a+1)(a+2)\ldots(a+n-1) = \frac{\Gamma(a+n)}{\Gamma(a)}, \;\; n = 1,2,3..., \tag{7.6}$$

which will be used, for brevity, in the rest of the chapter. The series (7.5) converges for all complex z_1. An explicit integral representation of $M(a,b;z_1)$ is

$$M(a,b,z_1) = \frac{\Gamma(b)}{\Gamma(a)\Gamma(b-a)} \int_0^1 \exp(z_1 t) t^{a-1} g_1(t) dt, \tag{7.7}$$

in which $g_1(t) = (1-t)^{b-a-1}$, and $\Re(b) > \Re(a) > 0$. The other solution of the confluent differential equation (7.3) is

$$U(a,b,z_1) = \sum_{n=0}^{\infty} (-1)^n \frac{(a)_n (a-b+1)_n}{n! z_1^{a+n}}, \tag{7.8}$$

and its integral representation is

$$U(a,b,z_1) = \frac{1}{\Gamma(a)} \int_0^{\infty} \exp(-z_1 t) t^{a-1} g_2(t) dt, \tag{7.9}$$

in which $g_2(t) = (1+t)^{-a+b-1}$, and $\Re(a) > 0$. CHFs are more complicated than the other special functions as they have additional parameters a and b. By taking appropriate values of a and b in (7.3), many special functions may be expressed in terms of CHFs, including the exponential integral, the error function and the Airy function, which we discussed in our earlier chapters, and many more in [68, 78]. Particularly, they can be obtained by means of

$$U(1,1,-z_1) = -\exp(-z_1)\mathrm{Ei}(z_1), \tag{7.10}$$

$$M\left(\frac{1}{2},\frac{3}{2},-z_1^2\right) = \frac{\sqrt{\pi}}{2z_1}\mathrm{erf}(z_1) \quad \text{and} \quad U\left(\frac{1}{2},\frac{1}{2},z_1^2\right) = \sqrt{\pi}\exp\left(z_1^2\right)\mathrm{erfc}(z_1), \tag{7.11}$$

$$U\left(\frac{5}{6},\frac{5}{3},\frac{4z_1^{3/2}}{3}\right) = \frac{3^{5/6}\sqrt{\pi}}{2^{2/3}z_1}\exp\left(\frac{2z_1^{3/2}}{3}\right)\mathrm{Ai}(z_1). \tag{7.12}$$

The purpose of this chapter is to investigate and compute the CHF in the asymptotic sense of this thesis so that the subdominant exponentials and their behaviour on the complex plane can be addressed; to do so, the theory of exponential asymptotics will be needed. In this chapter, the hyperasymptotic method which we employed throughout the previous chapters, such as in §4, will be applied to the CHF.

The procedure of the present chapter is as follows: we will first transform (7.3) by rescaling the large z_1 with a small parameter since we often study expansions with small ε in the limit. In comparison with Olde Daalhuis [45], rather than ex-

panding $g_2(t)$ of (7.9) around $t = 0$ and truncating the relevant expansion optimally for large z_1, we will obtain the hypergeometric function in terms of a small variable by re-scaling. In a similar manner, Olver [63] investigated the CHF for large z_1 using the integral representation of the remainder function and expanded it by Taylor expansion, which is not convenient to apply for the higher levels [45]; hence, our approach to the CHF is different from both Olde Daalhuis's and Olver's works. Upon re-scaling, we will have the singularly perturbed differential equation, then we will follow the usual perturbation technique. After determining the late-order terms of the asymptotic expansion, in §7.3 we will optimally truncate it. Therein, we will perform the WKB method to find the quadratic solution of CHF whereupon the Stokes and anti-Stokes lines will be located in §7.4. In order to inspect the truncated remainder, we will substitute the truncated series into the CHF equation which produces an inhomogeneous resultant differential equation. Next, in §7.5 we will observe the error function smoothing by investigating the remainder near the Stokes line where the remainder is maximal. This process of expansion, truncation and investigation of the behaviour of the remainder, will be performed at two levels. We will discuss the behaviour of the first level error in terms of arbitrary truncation points in the subsequent sections. Finally in §7.7, the conclusion and relevant comparisons will be addressed.

7.2 Rescaled confluent hypergeometric function

Motivated by the discussion above, before we begin the process of examination of the CHF by expansion, let us first transform the CHF (7.3) by letting

$$z_1 = \frac{z}{\varepsilon}, \tag{7.13}$$

where $0 < \varepsilon \ll 1$ and $z = \mathrm{O}(1)$. Considering this transformation, employing the chain rule [69] into the derivatives of the CHF (7.3) enables us to compute the first and second derivatives of $W(z_1)$ in terms of a new variable z, using

$$\frac{dW(z_1)}{dz_1} = \varepsilon \frac{dW(z)}{dz} \quad \text{and} \quad \frac{d^2W(z_1)}{dz_1^2} = \varepsilon^2 \frac{d^2W(z)}{dz^2}. \tag{7.14}$$

Hence, it follows that the CHF with the fast scale z/ε takes the form of a singular perturbation with ε in

$$\varepsilon z \frac{d^2W(z)}{dz^2} + (\varepsilon b - z) \frac{dW(z)}{dz} - aW(z) = 0, \tag{7.15}$$

The approximate solution of the new re-scaled CHF (7.15) can be obtained using the exponential asymptotics; thus, we can carry out the hyperasymptotic technique by expanding $W(z)$ of the new CHF in powers of ε in the usual way. To obtain the zeroth level hyperasymptotic expansion, the calculation begins with the assumption that the series solution of $W(z)$ is

$$W(z) \sim \sum_{n=0}^{\infty} \varepsilon^n w_n(z). \tag{7.16}$$

Because this solution (7.16) has to satisfy the CHF given by (7.15), substituting it into the differential equation yields

$$\sum_{n=0}^{\infty} \varepsilon^{n+1} \left(z \frac{d^2w_n(z)}{dz^2} + b \frac{dw_n(z)}{dz} - z \frac{dw_{n+1}(z)}{dz} - aw_{n+1}(z) \right) - \left(z \frac{dw_0(z)}{dz} + aw_0(z) \right) = 0. \tag{7.17}$$

Comparing like powers of ε in the above summation (7.17) provides us a leading order relation at $\mathrm{O}(1)$ and a differential recursion relation between terms of the expansion at higher order $\mathrm{O}(\varepsilon^n)$ such that

$$\begin{aligned} z \frac{dw_0(z)}{dz} + aw_0(z) &= 0, \\ z \frac{d^2w_n(z)}{dz^2} + b \frac{dw_n(z)}{dz} - z \frac{dw_{n+1}(z)}{dz} - aw_{n+1}(z) &= 0 \quad \text{for } n \geq 0. \end{aligned} \tag{7.18}$$

By exact integration, the solution at the leading order is

$$z \frac{dw_0(z)}{dz} + aw_0(z) = 0 \implies w_0(z) = c_0 z^{-a}, \tag{7.19}$$

where c_0 is a constant of integration, and the leading order term is associated with the singularity at $z = 0$. As earlier, we need the general term of the expansion for further analysis; hence, our analysis relies on the recurrence relation, which corresponds to the CHF. For instance at $\mathrm{O}(\varepsilon)$, we have

$$z\frac{d^2w_0(z)}{dz^2} + b\frac{dw_0(z)}{dz} - z\frac{dw_1(z)}{dz} - aw_1(z) = 0. \tag{7.20}$$

Imposing the first and second derivatives of $w_0(z)$ into (7.20) enables us to establish $w_1(z)$ upon integration

$$z\frac{dw_1(z)}{dz} + aw_1(z) = a(a-b+1)c_0z^{-a-1} \implies w_1(z) = -a(a-b+1)c_0z^{-a-1} + c_1z^{-a}, \tag{7.21}$$

for constants c_0 and c_1. We can set $c_1 = 0$, since we can always absorb c_1z^{-a} into the leading order solution (7.19). Similarly, by successively repeating this process between the n^{th} term and the $(n+1)^{th}$ term of the recurrence relation, we find that the general term of the expansion (7.15) corresponds to

$$w_n(z) \sim (-1)^n\frac{\Gamma(a+n)}{\Gamma(a)}\frac{\Gamma(a-b+n+1)}{\Gamma(a-b+1)}\frac{c_0}{z^{a+n}n!}, \tag{7.22}$$

where c_0 can be taken as 1 with no loss of generality. We know that the general terms of such expansions have to be in the factorial-over-a-power nature in exponential asymptotics, whence we can easily see performing Stirling's formula to approximate the factorial terms in the above equation (7.22) for large n yields

$$w_n(z) \sim (-1)^n\frac{\exp(a)n^{a-b-\frac{1}{2}}}{2\pi(a-1)^{a-\frac{1}{2}}(a-b)^{a-b-\frac{1}{2}}}\frac{(a+n)!}{z^{a+n}} := (-1)^n\frac{\Gamma(a+n+1)}{u_0(z)^{a+n}}n^{a-b-\frac{1}{2}}C, \tag{7.23}$$

in which C is a constant depending on a and b, and general term is indeed in this nature, which confirms that the late order ansatz must diverge as n goes to infinity.

$-u_0(z)$ is the singulant. The crucial step of analysing the remainder in exponential asymptotics is to determine the late terms of an expansion. Although we have exactly obtained it in this particular differential equation by successively employing the recurrence relation, establishing the general term is not always straigtforward, and be impossible at times. Hence, in order to have a complete agreement, the nature of late-order terms will be proven assuming that it is in the 'factorial/power' form. In this way, the singulant must be represented as in the same fashion that we obtained in (7.22). Therefore, let us assume the general term of the expansion when $n \to \infty$ is

$$w_n(z) = (-1)^n \frac{\Gamma(n+\gamma)}{u_0(z)^{n+\gamma}} \left(B_0(z) + \frac{1}{n} B_1(z) + \frac{1}{n^2} B_2(z) + \dots \right), \tag{7.24}$$

where γ, $u_0(z)$ and $B_i(z)$s are defined as before and do not depend on the large parameter n. Firstly, we take the first and second derivative of the ansatz (7.24) with respect to z and substitute them into the recurrence equation (7.18). Equating like powers of n, we obtain at the leading-order in which we aim to determine the singulant $-u_0(z)$ as

$$\frac{z}{(u_0(z))^2} B_0(z) \frac{du_0(z)}{dz} \left(\frac{du_0(z)}{dz} - 1 \right) = 0. \tag{7.25}$$

Here, we have three possibilities which may satisfy the equation (7.25): first, if $B_0(z)$ is assumed to equal zero, it makes all $B_i(z)$s zero, which is indeed the trivial solution. Hence, $B_0(z)$ is not zero. The singularities of the expansion has to be consistent with singularities of the leading order term since each successive term is determined by the derivative of the previous term, which can be verified by the recurrence relation (7.18). We know from (7.19) that the expansion has a singular point at $z_1 = 0$. Hence, assuming $du_0(z)/dz = 0$ makes the singulant function equal to a constant which has to be zero due to the singularity at zero; indeed, this cannot happen. We, therefore, assume that

$$\frac{du_0(z)}{dz} - 1 = 0, \tag{7.26}$$

which can be evaluated by direct integration, yielding

$$u_0(z) = z + c, \tag{7.27}$$

where c is a constant of integration. Solving (7.27) subject to the singular point, 0, completes the determination of $u_0(z)$

$$u_0(z) = z. \tag{7.28}$$

After taking the first and second derivative of the ansatz (7.24) and substituting them into the recurrence relation of (7.18) with $u_0(z)$, we establish that

$$B_0(z) = z^{a-b}. \tag{7.29}$$

Obtaining $B_0(z)$ completes the derivation of the form of the factorial-over-a-power ansatz at the leading-order. Therefore, the substitution of $u_0(z)$ and $B_0(z)$ in (7.24) leads to

$$w_n(z) \sim (-1)^n \frac{\Gamma(n+\gamma)}{z^{n+\gamma}} z^{a-b} \left(1 + \mathrm{O}\left(n^{-1}\right)\right), \qquad \text{as} \quad n \to \infty. \tag{7.30}$$

Finally, the constant γ is defined such that $\gamma = 2a - b$; particularly, we can see that the ansatz (7.30) is the same as the ansatz (7.23) which was determined using repeated differentiation of the differential difference equation (7.18) for large n. Hence, the agreement between the two ways has been deduced. The corresponding series solution of the CHF (7.3) is fully determined by direct application of the hyperasymptotic method by means of

$$W(z) \sim \sum_{n=0}^{\infty} (-1)^n \varepsilon^n \frac{(a)_n \, (a-b+1)_n}{z^{a+n} n!}, \tag{7.31}$$

which diverges for any fixed ε and z. As explicated in [23, 94], $U(a,b,z_1)$ corresponding to $W(z)$ has a branch point at $z = 0$ with a branch cut in the complex z-plane since z^a is a multivalued function at $z = 0$. As we explicitly expressed the

asymptotic series solution of the CHF in light of the differential difference equation, our next step is to truncate the divergent expansion (7.31) to investigate the behaviour of its remainder which will be introduced in the upcoming section.

7.3 Optimal truncation and the WKB approach

Derivation of the truncation point in which the divergent series takes its minimum value in magnitude, is one of the key features of exponential asymptotics. In this section, we first truncate the series and obtain its optimal value, whereupon we use the WKB method [67] in order to establish the late order approximate solution of the quadratic CHF and locate the Stokes and anti-Stokes lines. Let us truncate the expansion after $N_0 \gg 1$ terms and introduce the remainder term. This yields

$$W(z) \sim \sum_{n=0}^{N_0-1} (-1)^n \varepsilon^n \frac{(a)_n (a-b+1)_n}{z^{a+n} n!} + R_{N_0}(z), \tag{7.32}$$

where the remainder, $R_{N_0}(z)$, is of the order

$$R_{N_0}(z) = \mathrm{O}\left(\varepsilon^{N_0} \frac{(a)_{N_0} (a-b+1)_{N_0}}{z^{a+N_0} N_0!} \right).$$

As before, the zeroth level truncation error can be defined based on the first neglected term or equivalently the general term at N_0 such that

$$E_{N_0}(z) := \varepsilon^{N_0} \frac{(a)_{N_0} (a-b+1)_{N_0}}{z^{a+N_0} N_0!}. \tag{7.33}$$

The optimal truncation point can be found by comparing the magnitude of successive terms of the expansion and equating their ratio to one, i.e.,

$$\left| \frac{\varepsilon^{N_0+1} (-1)^{N_0+1} \dfrac{(a)_{N_0+1} (a-b+1)_{N_0+1}}{z^{a+N_0+1} (N_0+1)!}}{\varepsilon^{N_0} (-1)^{N_0} \dfrac{(a)_{N_0} (a-b+1)_{N_0}}{z^{a+N_0} N_0!}} \right| \sim 1. \tag{7.34}$$

After carrying out the simplifications, we deduce that such a point appears where

$$N_0 \sim \frac{|z|}{\varepsilon}. \tag{7.35}$$

If in case a and b are real, the truncation point then approximates to $N_0 \sim |z|/\varepsilon - 2a + b$; however, a and b are negligible for small $\varepsilon \to 0$. Because N_0 is an integer, we add α

$$N_0 = \frac{|z|}{\varepsilon} + \alpha, \tag{7.36}$$

where α is bounded in the limit $\varepsilon \to 0$ as discussed previously in (3.14) of §3.2. Figure 7.1 illustrates the behaviour of the zeroth level error estimate (7.33); it first decreases, then starts to grow infinity after the least value for fixed z and ε, which is the typical behaviour of the divergent series in exponential asymptotics. It shows the point of optimal truncation appears at 15, which is consistent with the result of (7.35) if we have the same values of $z,\ \varepsilon$, a and b that we use for plotting Figure 7.1.

7.3.1 WKB analysis

In §7.2 one general solution of the quadratic CHF (7.15) is derived; however, in order to find the second approximate solution of (7.15), we perform the WKB approximation method from which the exponential terms appear explicitly. To do so, let us assume the series solution of the CHF, that we seek a solution of the form, is

$$W(z) \sim \exp\left[\frac{1}{\delta}\sum_{n=0}^{\infty}\delta^n S_n(z)\right], \qquad \delta \to 0, \tag{7.37}$$

where δ is a function of ε to be determined soon. Differentiating (7.37) twice by employing the chain rule, we have

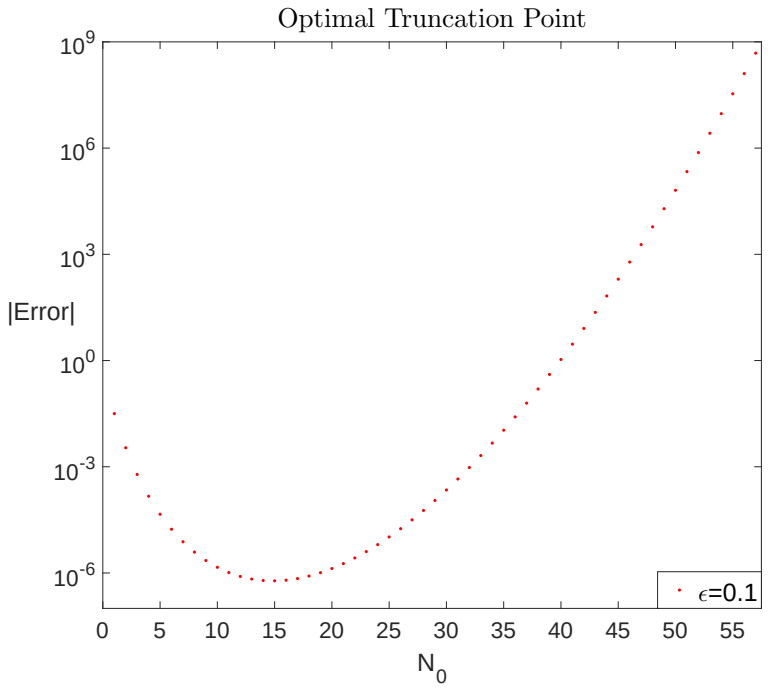


Figure 7.1 The magnitude of the error given in (7.33) for chosen $z = 1.5i$ while $a = 1/2$, $b = 1/3$. The error is at minimum when the optimal term is $N_0 = 15$.

$$\frac{dW(z)}{dz} \sim \left(\frac{1}{\delta}\sum_{n=0}^{\infty}\delta^n S_n'(z)\right)\exp\left[\frac{1}{\delta}\sum_{n=0}^{\infty}\delta^n S_n(z)\right], \qquad \delta \to 0,$$
$$\frac{d^2W(z)}{dz^2} \sim \left[\frac{1}{\delta^2}\left(\sum_{n=0}^{\infty}\delta^n S_n'(z)\right)^2 + \frac{1}{\delta}\sum_{n=0}^{\infty}\delta^n S_n''(z)\right]\exp\left[\frac{1}{\delta}\sum_{n=0}^{\infty}\delta^n S_n(z)\right], \qquad \delta \to 0. \tag{7.38}$$

Upon employing the WKB series (7.37) in (7.15), we derive the exponential terms in ε; whence, we can derive the Stokes lines. In particular, carrying out the substitution of these derivatives given in (7.38) into the CHF (7.15) and dividing off the common exponential factors, we are left with derivatives of $S_n(z)$

$$\varepsilon z\left[\frac{1}{\delta^2}\left(\sum_{n=0}^{\infty}\delta^n S_n'(z)\right)^2 + \frac{1}{\delta}\sum_{n=0}^{\infty}\delta^n S_n''(z)\right] + (\varepsilon b - z)\left(\frac{1}{\delta}\sum_{n=0}^{\infty}\delta^n S_n'(z)\right) = a. \tag{7.39}$$

Expanding the series in the equation (7.39) and considering the leading terms of the left hand side (LHS) of the equation, we obtain

$$\varepsilon z\left[\frac{\left(S_0'\right)^2}{\delta^2}+\frac{2S_0'S_1'}{\delta}+2S_0'S_2'+\left(S_1'\right)^2+2\delta S_1'S_2'+\delta^2\left(S_2'\right)^2+\cdots+\frac{S_0''}{\delta}+S_1''+\delta S_2''+\mathrm{O}(\delta^3)\right]$$
$$+(\varepsilon b-z)\left(\frac{S_0'}{\delta}+S_1'+\delta S_2'+\delta^2 S_3'+\mathrm{O}(\delta^3)\right)=a. \quad (7.40)$$

By using the method of dominant balance, the largest term of the equation (7.40) on the LHS is

$$\frac{\varepsilon z}{\delta^2}\left(S_0'\right)^2-\frac{z}{\delta}\left(S_0'\right), \quad (7.41)$$

for small δ. The terms on the LHS of (7.40) must equal to the terms on the RHS; particularly, they must have the same order. This suggests that δ must be determined in terms of ε, that is, $\delta=\varepsilon$. Substituting this distinguishing value of δ in (7.40) will enable us to derive S_0, S_1 and S_n for $n\geq 2$ from the following sequence of differential equations

$$\begin{aligned}
&\text{at} \quad \mathrm{O}(\varepsilon^{-1}) && z\left(S_0'\right)^2-zS_0'=0,\\
&\text{at} \quad \mathrm{O}(\varepsilon^{0}) && 2zS_0'S_1'+zS_0''+bS_0'-zS_1'=a,\\
&\text{at} \quad \mathrm{O}(\varepsilon^{n-1}) && 2zS_0'S_n'+zS_{n-1}''+z\textstyle\sum_{k=1}^{n-1}S_k'S_{n-k}'+bS_{n-1}'-zS_n'=0, \quad n\geq 2.
\end{aligned} \quad (7.42)$$

We will only calculate the first three terms of the WKB series as they are sufficient at this point. The first equation in the system of (7.42), $\mathrm{O}(\varepsilon^{-1})$, can be integrated directly; hence, it yields two solutions for $S_0'(z)$ such that

$$S_0'(z)=0 \quad \text{and} \quad S_0'(z)=1, \quad (7.43)$$

in which the solution occurring by $S_0'(z)=0$ leads to the algebraic order solution that was derived without using the WKB approach. However, in order to be consistent with the results, we carry on the calculation. Determining $S_0(z)$, therefore, requires

an integration with respect to the above equations, yielding

$$S_0(z) = c_0 \quad \text{and} \quad S_0(z) = z + c_1, \tag{7.44}$$

where c_0 and c_1 are constants. In fact, these c_0 and c_1 must be zero since the leading order exponents have to satisfy the singularities of the leading order term introduced in (7.19). Let us next consider the second equation of the system (7.42) at O(1) according to $S_0(z)$s. Imposing the first solution of (7.43) where $S_0'(z) = 0$, we have

$$2zS_0'S_1' + zS_0'' + bS_0' - zS_1' = a \implies S_1' = -\frac{a}{z},$$

which upon a single direct integration gives

$$S_1(z) = -a\ln(z) + c_2. \tag{7.45}$$

Accordingly, imposing the second solution of (7.43) where $S_0'(z) = 1$, we have

$$2zS_0'S_1' + zS_0'' + bS_0' - zS_1' = a \implies S_1' = \frac{a-b}{z},$$

which by a single direct integration becomes

$$S_1(z) = (a-b)\ln(z) + c_3. \tag{7.46}$$

By the same token, we are able to determine $S_2(z)$ from the third of (7.42) at O(ε) as

$$S_2(z) = -\frac{a(a-b+1)}{z} + c_4 \qquad \text{when } S_1(z) = -a\ln(z) + c_2, \tag{7.47}$$

$$S_2(z) = -\frac{(b-a)(a-1)}{z} + c_5 \qquad \text{when } S_1(z) = (b-a)\ln(z) + c_3, \tag{7.48}$$

where c_2, c_3, c_4 and c_5 are constants all of which can be determined by the boundary values or initial values. We also need to know the values of a and b to derive them.

As it is sufficient, according to these values of $S_0(z)$, $S_1(z)$, and $S_2(z)$, corresponding exponential solutions of the CHF (7.15), which are well approximated via WKB approach, are derived as follows in the limit $\varepsilon \to 0$

$$W(z) \sim C_0 \exp\left(-a\ln(z) - \varepsilon\frac{a(a-b+1)}{z} + \mathrm{O}\left(\varepsilon^2\right)\right), \qquad \text{at } \mathrm{O}(z^{-a}), \tag{7.49}$$

$$W(z) \sim C_1 \exp\left(\frac{z}{\varepsilon} + (a-b)\ln(z) - \varepsilon\frac{(b-a)(a-1)}{z} + \mathrm{O}\left(\varepsilon^2\right)\right), \tag{7.50}$$

where C_0 and C_1 are constants, and the constants of the WKB solutions are absorbed into them if they are in $\mathrm{O}(1)$ and $\mathrm{O}(\varepsilon)$, and the higher orders are included in $\mathrm{O}(\varepsilon^2)$. Meanwhile, because the accuracy of the approximation depends on the number of terms in the WKB ansatz, for a more accurate approximation to $W(z)$ higher order terms can be determined from the recurrence relation of (7.42) by performing repeated differentiations. We have the leading-order WKB approximate solution of the CHF as a linear combination of (7.49) and (7.50) for small ε such that

$$\begin{aligned} W(z) \sim & C_0 \exp\left(-a\ln(z) - \varepsilon\frac{a(a-b+1)}{z}\right) \\ & + C_1 \exp\left(\frac{z}{\varepsilon} + (a-b)\ln(z) - \varepsilon\frac{(b-a)(a-1)}{z}\right) + \mathrm{O}\left(\varepsilon^2\right). \end{aligned} \tag{7.51}$$

To point out here, (7.49) is the solution we already found by factorial-over-a-power method. Employing the WKB approach enabled us to derive the second exponential solution of a quadratic CHF (7.15) in the limit $\varepsilon \to 0$.

Having established the late-order terms of the expansion and the general solutions through WKB analysis, we can now embark on the Stokes lines analysis of the CHF.

7.4 Stokes and anti-Stokes lines

Our purpose in this section is to furnish the Stokes and anti-Stokes lines of the CHF; in order to find these lines, we introduce the polar coordinates using $z = r\exp(i\theta)$,

where $-\pi \leq \theta \leq \pi$. To be more precise, let us begin this section by formally substituting these coordinates into the WKB approximate solutions, which holds

$$W(z) \sim C_0 \exp\left(-a\ln(r) - i\theta a - \varepsilon \frac{a(a-b+1)}{r\exp(i\theta)}\right), \tag{7.52}$$

$$W(z) \sim C_1 \exp\left(\frac{r\exp(i\theta)}{\varepsilon} + i\theta(a-b)\ln(r) - \varepsilon \frac{(b-a)(a-1)}{r\exp(i\theta)}\right). \tag{7.53}$$

The controlling factors of the above WKB solutions are respectively

$$\exp\left(-a\ln(r) - i\theta a\right) \quad \text{and} \quad \exp\left(\frac{r\exp(i\theta)}{\varepsilon}\right). \tag{7.54}$$

We find the Stokes lines via (7.54)) using (6.23) of Airy §6.4

$$\Im\left(-r\exp(i\theta)\right) = \Im\left(0\right) \quad \text{and} \quad \Re\left(-r\exp(i\theta)\right) > \Re\left(0\right). \tag{7.55}$$

This confirms that the Stokes lines of the CHF lie along $\pm\pi$. Similarly, the anti-Stokes lines of the CHF occur when the real parts of the exponential powers of the WKB solutions are purely imaginary, i.e.,

$$\Re\left(0\right) = \Re\left(-r\exp(i\theta)\right) \quad \Longrightarrow \quad 0 = \cos(\theta). \tag{7.56}$$

The anti-Stokes lines, therefore, lie along $\theta = \pm\pi/2$. In Figure 7.2, the Stokes and anti-Stokes lines of the zeroth level expansion are illustrated as discussed above. As before, the next step is to travel around the complex plane. However, since we have done it in previous chapters in detail, such as in Figure 4.2 of §4, the Figure 7.2 will be explained briefly. Let us start the travel from Sector II through Sector III in a counter clockwise direction. In doing this, $\exp\left(-z/\varepsilon\right)$ represented by ① is switched on by $\exp\left(0\right)$ represented by ⓪ across the Stokes line. As we continue the process and reach to Sector II by the end of the travel, it turns out we end up with the same term ⓪ we began with; hence, we return to where we started. By doing this travel, we demonstrated where subdominant exponential is present in the complex plane.

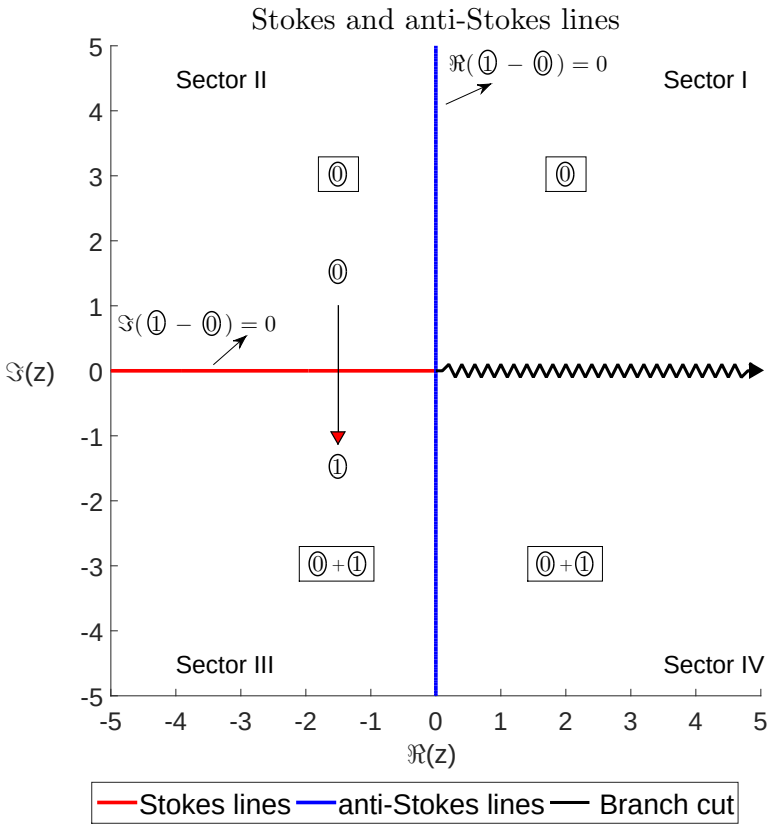


Figure 7.2 Demonstrating Stokes lines and the sudden appearance and disappearance of the exponential terms $\exp(-z/\varepsilon)$ and $\exp(0)$ shown by ① and ⓪, respectively, on the complex plane.There is no inconsistency with having different asymptotic representations on each side of the branch cut. Present exponentials of the associated sectors are illustrated in boxes.

Next, we analyse the remainder differential equation near the turning point and extract the error function smoothing by which the switching on and off occurs across the Stokes lines.

7.5 Error function near the Stokes line

In this section, we will consider the zeroth level remainder of the hyperasymptotics on the vicinity of the Stokes line in detail. In principle, we proceed with the same procedure as that in the previous chapters. Hence, substituting the truncated series (7.32) with the remainder into the CHF equation (7.15) verifies that the zeroth level

remainder is a solution of

$$\varepsilon z\frac{d^2R_{N_0}(z)}{dz^2}+(\varepsilon b-z)\frac{dR_{N_0}(z)}{dz}-aR_{N_0}(z)\sim-\varepsilon^{N_0}\left(z\frac{d^2w_{N_0-1}(z)}{dz^2}+b\frac{dw_{N_0-1}(z)}{dz}\right)$$
$$=\varepsilon^{N_0}\frac{(-1)^{N_0}(a)_{N_0}(a-b+1)_{N_0}}{(N_0-1)!z^{a+N_0}}. \tag{7.57}$$

In order to analyse this differential equation in (7.57), we first re-scale the remainder $R_{N_0}(z)$ according to the homogeneous solution of (7.57). From WKB analysis already know that its homogeneous solution is

$$W_{WKB}(z)=\exp\left(\frac{z}{\varepsilon}\right). \tag{7.58}$$

Through the method of reduction of orders by considering the solution (7.58), let us first suppose that the remainder is in the below form

$$R_{N_0}(z)=K(z)W_{WKB}(z). \tag{7.59}$$

Taking the first and second derivatives of (7.59) and substituting them back into the remainder differential equation (7.57), we find

$$\varepsilon zW_{WKB}(z)\frac{d^2K(z)}{dz^2}+\varepsilon\left(bW_{WKB}(z)+2z\frac{dW_{WKB}(z)}{dz}\right)\frac{dK(z)}{dz}-zW_{WKB}(z)\frac{dK(z)}{dz}$$
$$=\frac{(-\varepsilon)^{N_0}(a)_{N_0}(a-b+1)_{N_0}}{(N_0-1)!z^{a+N_0}}. \tag{7.60}$$

Solving this will enable us to furnish a differential equation which only involves derivatives of $K(z)$ function leading to

$$\varepsilon z\frac{d^2K(z)}{dz^2}+(\varepsilon b+z)\frac{dK(z)}{dz}=\varepsilon^{N_0}\frac{(-1)^{N_0}(a)_{N_0}(a-b+1)_{N_0}}{(N_0-1)!\exp\left(\frac{z}{\varepsilon}\right)z^{a+N_0}}. \tag{7.61}$$

To extract the error smoothing near the Stokes line, it is appropriate to use the polar coordinates, whence we set $|z| = \rho$ and vary θ for ρ fixed by means of

$$z = \rho e^{i\theta}. \tag{7.62}$$

Using the chain rule employed in (2.27) of §2.5 and upon applying (7.62) to (7.61) and then performing Stirling's formula for approximation of the gamma functions, (7.61) transforms into

$$-\frac{\varepsilon e^{-i\theta}}{\rho}\frac{d^2K(\rho,\theta)}{d\theta^2} + \left(\frac{\varepsilon i e^{-i\theta}}{\rho} - \frac{\varepsilon b i e^{-i\theta}}{\rho} - i\right)\frac{dK(\rho,\theta)}{d\theta} \sim C\frac{\rho^{a-b+1/2}}{\varepsilon^{2a-b+1/2}}\exp(-ai\theta)\exp\left[\left(i(\pi-\theta)-1-e^{i\theta}\right)\frac{\rho}{\varepsilon}\right], \tag{7.63}$$

in which the constants a, b and π are absorbed into C. The RHS of (7.63) is exponentially small everywhere but it is maximal at π, as $\varepsilon \to 0$, which is the Stokes line. In order to see the subtle effects of the remainder in the vicinity of the Stokes line, we re-scale θ by setting

$$\theta = \pi + \zeta(\varepsilon)\widehat{\theta}, \tag{7.64}$$

where $|\zeta(\varepsilon)| \ll 1$; the actual scaling will be determined shortly. Rewriting the equation (7.63) in terms of $\widehat{\theta}$ by considering the chain rule allows us to have

$$\frac{\varepsilon e^{-i\zeta\widehat{\theta}}}{\rho\zeta^2}\frac{d^2K(\widehat{\theta})}{d\widehat{\theta}^2} + \left(\frac{-\varepsilon i e^{-i\zeta\widehat{\theta}}}{\rho\zeta} + \frac{\varepsilon b i e^{-i\zeta\widehat{\theta}}}{\rho\zeta} - \frac{i}{\zeta}\right)\frac{dK(\widehat{\theta})}{d\widehat{\theta}} \sim c_2\exp\left(-\frac{\zeta^2\widehat{\theta}^2\rho}{2\varepsilon}\right), \tag{7.65}$$

in which c_2 corresponds to constant terms. This suggests that the exact scaling should be $\zeta = \sqrt{\varepsilon}$, whereby its substitution into (7.65) yields at the leading order $\zeta \to 0$

$$-i\frac{dK(\widehat{\theta})}{d\widehat{\theta}} \sim c_2\exp\left(-\frac{\zeta^2\widehat{\theta}^2\rho}{2\varepsilon}\right). \tag{7.66}$$

It remains for us to recover the error function. Hence, upon direct integration we obtain

$$K(\widehat{\theta}) \sim c_2 i \frac{\sqrt{2\pi}}{2\sqrt{\rho}} \text{erf}\left(\frac{\sqrt{2\rho}}{2}\widehat{\theta}\right). \tag{7.67}$$

The typical error function is expressed as a consequence of the re-scaling in (7.64). In particular, this means the error estimate is approximated in terms of an error function whereby the switching on and off occurs for the subdominant terms. Back-substitution of $K(\widehat{\theta})$ into (7.59) gives

$$\begin{aligned} R_{N_0}(\widehat{\theta}) &= K(\widehat{\theta}) W_{WKB}(\widehat{\theta}) \\ &\sim c_2 i \frac{\sqrt{2\pi}}{2\sqrt{\rho}} \exp\left(-\frac{\rho}{\varepsilon}\right) \text{erf}\left(\frac{\sqrt{2\rho}}{2}\widehat{\theta}\right). \end{aligned} \tag{7.68}$$

Because the point of truncation has been selected optimally, we see that the remainder is exponentially small everywhere by $\exp(-\rho/\varepsilon)$ but maximal at the Stokes line, i.e. $\widehat{\theta} = 0$. Next, we aim to perform the level one hyperasymptotic investigation for the CHF and minimise the relevant error estimate considering the truncation points as variables and discuss its behaviour throughout the upcoming sections.

7.6 First level of hyperasymptotics

We first re-scale the zeroth level truncated remainder according to the RHS of (7.57) and expand the re-scaled new function of the differential equation. Suppose the remainder expression, whose solution is sought, takes the following form

$$R_{N_0}(z) = \varepsilon^{N_0+1} \frac{(-1)^{N_0}(a)_{N_0}(a-b+1)_{N_0}}{(N_0-1)!} \frac{Q(z)}{z^{a+N_0}}. \tag{7.69}$$

Here, $Q(z)$, which will be determined shortly, is an unknown function of z. Taking the first and second derivatives of (7.69) and applying them to (7.57) provide a new

differential equation in which $Q(z)$ is a solution of

$$\varepsilon^2 z\frac{d^2Q(z)}{dz^2}-\varepsilon\left(2\nu_0+z\right)\frac{dQ(z)}{dz}+\left(\frac{\nu_0^2}{z}+\nu_0\right)Q(z)\sim 1, \tag{7.70}$$

where ν_0 is defined by $\nu_0 \sim N_0\varepsilon$ with a large parameter N_0. We proceed with the usual approach of the perturbation theory in order to obtain the asymptotic series solution. Let us assume that the series solution of (7.70), in powers of ε, is in the form of

$$Q(z)\sim\sum_{n=0}^{\infty}\varepsilon^n Q_n(z). \tag{7.71}$$

Since the series expression of $Q(z)$ satisfies the differential equation (7.70), we substitute it directly into (7.70) which governs the terms of the expansion given in (7.71). After substitution, we obtain the following at $\mathrm{O}(1)$ and $\mathrm{O}(\varepsilon^{n+2})$, respectively

$$Q_0(z)=\frac{z}{\nu_0\left(\nu_0+z\right)}, \tag{7.72}$$

$$zQ_n(z)''-\left(2\nu_0+z\right)Q_{n+1}(z)'+\left(\frac{\nu_0^2}{z}+\nu_0\right)Q_{n+2}(z)\sim 0 \qquad \text{for } n\geq 1. \tag{7.73}$$

The crucial observation drawn from (7.72) is that there is a singularity at the leading order term, $Q_0(z)$, at $z=-\nu_0$. Meanwhile, the recurrence relation tells us that the late-order term $Q_{n+2}(z)$ of the expansion can be determined based on the first and second derivatives of the previous terms $Q_{n+1}(z)$ and $Q_n(z)$, respectively. This means that the power of the singularity increases at each level by adding 1 to the power of the singularity of the previous term. Let us assume that the solution for terms in the recurrence relationship given by (7.73) is

$$Q_n(z)\sim\frac{(-1)^n\Gamma(n+\gamma)}{u_1(z)^{n+\gamma}}\left(A_0(z)+\frac{1}{n}A_1(z)+\frac{1}{n^2}A_2(z)+\ldots\right), \quad \text{as } n\to\infty, \tag{7.74}$$

in which γ is a constant and $u_1(z)$ and $A_i(z)$ are to be discussed. Determination of the singulant, $-u_1(z)$, plays a crucial role; therefore, upon substituting this ansatz expression (7.74) into (7.73), we obtain that the singulant satisfies the following in

the limit as $n \to \infty$

$$\left(\frac{du_1(z)}{dz} - \frac{\nu_0}{z} - 1\right)\left(z\frac{du_1(z)}{dz} - \nu_0\right) = 0. \tag{7.75}$$

Solving (7.75) through direct integration gives

$$u_1^1(z) = \nu_0 \ln(z) + z + C_1 \quad \text{and} \quad u_1^2(z) = \nu_0 \ln(z) + C_2, \tag{7.76}$$

where C_1 and C_2 are constants of the integration to be derived by the singularity. Although the late order solution of (7.73) is not complete yet, as we already know that the general term must contain the singularity of the leading order term, $u_1^1(z)$ and $u_1^2(z)$ have to vanish at $-\nu_0$. Therefore, solving the singulants subject to $u_1^{1,2}(-\nu_0) = 0$ produces

$$C_1 = -\nu_0 \ln(-\nu_0) + \nu_0 \quad \text{and} \quad C_2 = -\nu_0 \ln(-\nu_0). \tag{7.77}$$

Thus, $u_1^1(z)$ and $u_1^2(z)$ of the singulants are fully determined as

$$u_1^1(z) = \nu_0 \ln(z) + z - \nu_0 \ln(-\nu_0) + \nu_0 \quad \text{and} \quad u_1^2(z) = \nu_0 \ln(z) - \nu_0 \ln(-\nu_0), \tag{7.78}$$

whereby they have a logarithmic singularity at $z = 0$; whence, there is a branch cut. With these $u_1^1(z)$ and $u_1^2(z)$, substituting the ansatz (7.74) into (7.73) evaluates at $\mathrm{O}(n)$

$$A_{0_{u_1^1}}(z) = \exp\left(-\frac{\nu_0}{z}\right) \quad \text{and} \quad A_{0_{u_1^2}}(z) = \exp\left(\frac{\nu_0}{z}\right), \tag{7.79}$$

according to $u_1^1(z)$ and $u_1^2(z)$, respectively. Hence, determination of the ansatz is completed with calculations of A_0s, which are independent of n, giving

$$Q_n(z) \sim \frac{(-1)^n \Gamma(n+\gamma)}{(\nu_0 \ln(z) + z - \nu_0 \ln(-\nu_0) + \nu_0)^{n+\gamma}} \exp\left(-\frac{\nu_0}{z}\right)\left(1 + \mathrm{O}\left(n^{-1}\right)\right) \quad \text{as} \ \ n \to \infty, \tag{7.80}$$

and

$$Q_n(z) \sim \frac{(-1)^n \Gamma(n+\gamma)}{(\nu_0 \ln(z) - \nu_0 \ln(-\nu_0))^{n+\gamma}} \exp\left(\frac{\nu_0}{z}\right) \left(1 + \mathrm{O}\left(n^{-1}\right)\right) \quad \text{as} \quad n \to \infty, \quad (7.81)$$

in which they are derived in order with respect to $u_1^1(z)$ and $u_1^2(z)$. Having successfully obtained the asymptotic representation of $Q(z)$ in powers of ε with two different singulants, we can now truncate the series (7.71). Truncating the series after $N_1 \gg 1$ terms leads to

$$Q(z) \sim \sum_{n=0}^{N_1-1} \varepsilon^n Q_n(z) + \mathscr{R}_{N_1}(z), \quad (7.82)$$

where $\mathscr{R}_{N_1}$ is a remainder of the series and $\mathscr{R}_{N_1} = \mathrm{O}(\varepsilon^{N_1})$. Since (7.82) must satisfy (7.70), substitution of the expansion plus the remainder term provides that the first level remainder is a solution of following differential equation

$$\begin{aligned} \mathscr{L}\left(\mathscr{R}_{N_1}(z);\varepsilon\right) &\sim \varepsilon^{N_1} \left(\frac{\nu_0^2}{z} + \nu_0\right) Q_{N_1}(z) - \varepsilon^{N_1+1} z \frac{d^2 Q_{N_1-1}(z)}{dz^2} \\ &\sim \varepsilon^{N_1} \left(\frac{\nu_0^2}{z} + \nu_0\right) Q_{N_1}(z), \end{aligned} \quad (7.83)$$

for ε small and N_1 large, where $\mathscr{L}$ is defined by

$$\mathscr{L}\left(\mathscr{R}_{N_1}(z);\varepsilon\right) = \varepsilon^2 z \frac{d^2 \mathscr{R}_{N_1}(z)}{dz^2} - \varepsilon\left(2\nu_0 + z\right) \frac{d\mathscr{R}_{N_1}(z)}{dz} + \left(\frac{\nu_0^2}{z} + \nu_0\right) \mathscr{R}_{N_1}(z).$$

7.6.1 Truncation

Before evaluating the remainder of (7.82) by arbitrary truncation points, we first establish the optimal value of the truncation point for the series solutions that appears when the successive late-order terms have the same magnitude. By this way, we can compare the results of the arbitrary and optimal truncations. We begin the optimisation process by comparing the ratio of the late-order terms in light of (2.9) of §2,

which leads that the series start to grow eventually when

$$N_1 \sim \frac{\left|u_1^{1,2}(z)\right|}{\varepsilon}, \tag{7.84}$$

with respect to $u_1^1(z)$ and $u_1^2(z)$ as given in (7.78). We observe that the first level truncation points are small at the point of singularity $z=-\nu_0$. Hence, in order to proceed further, we assume hereafter that $z \neq -\nu_0$. By back-substitution of (7.82) and (7.69) into (7.32), a truncated series of the first level after N_0 plus N_1 terms is found

$$W(z) \sim \sum_{n=0}^{N_0-1} (-1)^n \varepsilon^n \frac{(a)_n (a-b+1)_n}{z^{a+n} n!} + (-1)^{N_0} \varepsilon^{N_0+1} \frac{(a)_{N_0} (a-b+1)_{N_0}}{(N_0-1)! z^{a+N_0}} \sum_{n=0}^{N_1-1} \varepsilon^n Q_n(z) + (-1)^{N_0} \varepsilon^{N_0+1} \frac{(a)_{N_0} (a-b+1)_{N_0}}{(N_0-1)! z^{a+N_0}} \mathscr{R}_{N_1}(z). \tag{7.85}$$

In comparison with the zeroth level expansion (7.32), since N_1 more terms are added into the expansion, we obtain a higher accuracy with the first level expansion than with the zeroth level expansion of hyperasymptotics. Herein, we define the first level of the truncation error in (7.85) by

$$\begin{aligned} E_{N_1}(z) :&= (-1)^{N_0} \varepsilon^{N_0+N_1+1} \frac{(a)_{N_0} (a-b+1)_{N_0}}{(N_0-1)! z^{a+N_0}} \mathscr{R}_{N_1}(z) \\ &= (-1)^{N_0} \varepsilon^{N_0+N_1+1} \frac{(a)_{N_0} (a-b+1)_{N_0}}{(N_0-1)! z^{a+N_0}} Q_{N_1}(z). \end{aligned} \tag{7.86}$$

Whilst calculating the order of error, we utilise the Stirling's approximation for factorial terms, that gives

$$E_{N_1}(z) \sim \frac{\sqrt{2\pi}(-1)^{N_0+N_1} \varepsilon^{N_0+N_1+1}}{(a-1)^{a-\frac{1}{2}} (a-b)^{a-b+\frac{1}{2}}} \frac{N_0^{N_0+2a-b+\frac{1}{2}} N_1^{N_1+\gamma-\frac{1}{2}}}{z^{a+N_0} \exp(N_0+N_1+\gamma)} \frac{\exp\left(\mp \dfrac{\varepsilon N_0}{z}\right)}{\left(u_1^{1,2}(z)\right)^{N_1+\gamma}}. \tag{7.87}$$

In order to observe the anticipated improvement obtained by the hyperasymptotics, we plot the magnitude of the error (7.87). In Figure 7.3, we compare the error of

the expansion with various truncation points, not only with the optimal one. From the plots we notice that, as expected, the relative error of hyperasymptotics reduces at each level. However, increasing N_0 decreases the error far better than the value of the error obtained by the successive optimal truncations. For instance, truncating the zeroth level of the expansion just 20 terms later than the optimal truncation point reduces the magnitude of the error approximately by 10^{-22} compared to the error of the optimal truncations, which is apparent from the plots.

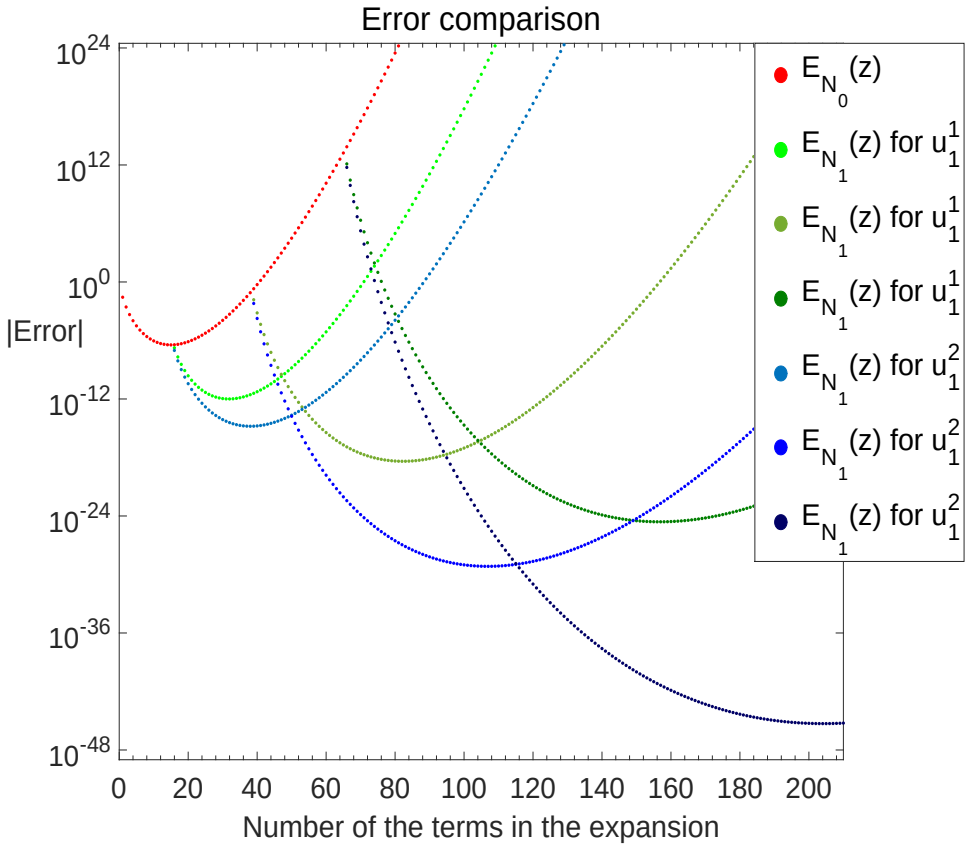


Figure 7.3 Comparison of the error estimates in (7.33) and (7.86) at two levels. It is plotted according to $u_1^1(z)$ and $u_1^2(z)$, respectively, for $z = 1.5i$, and for arbitrarily chosen $a = 1/2$, $b = 1/3$ while $\varepsilon = 0.1$. Green dots correspond to the error estimate occurring according to $u_1^1(z)$ while blue dots correspond to the error estimate occurring according to $u_1^2(z)$ for optimal truncation point and various truncation points. Increasing the level zero truncation point decreases the error.

The next step is, therefore, to minimise the first level error (7.87) with respect to ν_0

and ν_1 by differentiation. In doing this, we find that

$$\frac{dE_{N_1}(z)}{d\nu_0} \sim -\frac{C_1}{\varepsilon}\frac{(-1)^{\frac{\nu_0}{\varepsilon}+\frac{\nu_1}{\varepsilon}}\,\nu_0^{\frac{\nu_0}{\varepsilon}+2a-b+\frac{1}{2}}\nu_1^{\frac{\nu_1}{\varepsilon}+\gamma-\frac{1}{2}}\exp\left(\frac{-\nu_0}{z}\right)\ln\left(\frac{-z}{\nu_0}\right)}{z^{a+\frac{\nu_0}{\varepsilon}}\exp\left(\frac{\nu_0}{\varepsilon}+\frac{\nu_1}{\varepsilon}+\gamma\right)\left(\nu_0\ln\left(\frac{-z}{\nu_0}\right)+z+\nu_0\right)^{\frac{\nu_1}{\varepsilon}+\gamma}}\left[1+\frac{\nu_1}{\nu_0\ln\left(\frac{-z}{\nu_0}\right)+z+\nu_0}\right],$$

$$\frac{dE_{N_1}(z)}{d\nu_1} \sim \frac{C_1}{\varepsilon}\frac{(-1)^{\frac{\nu_0}{\varepsilon}+\frac{\nu_1}{\varepsilon}}\,\nu_0^{\frac{\nu_0}{\varepsilon}+2a-b+\frac{1}{2}}\nu_1^{\frac{\nu_1}{\varepsilon}+\gamma-\frac{1}{2}}\exp\left(\frac{-\nu_0}{z}\right)}{z^{a+\frac{\nu_0}{\varepsilon}}\exp\left(\frac{\nu_0}{\varepsilon}+\frac{\nu_1}{\varepsilon}+\gamma\right)\left(\nu_0\ln\left(\frac{-z}{\nu_0}\right)+z+\nu_0\right)^{\frac{\nu_1}{\varepsilon}+\gamma}}\ln\left[\frac{-\nu_1}{\nu_0\ln\left(\frac{-z}{\nu_0}\right)+z+\nu_0}\right], \tag{7.88}$$

where ν_1 is defined by $\nu_1 \sim N_1\varepsilon$ and C_1 is the constant of the derivatives defined as

$$C_1 = \frac{\sqrt{2\pi}}{\varepsilon^{2a-b+\gamma}(a-1)^{a-\frac{1}{2}}(a-b)^{a-b+\frac{1}{2}}}.$$

If we equate each derivative in (7.88) to zero, we find that the first level of error takes its minimum value at

$$\nu_1 \sim \left|\nu_0\ln\left(-\frac{z}{\nu_0}\right)+z+\nu_0\right|, \tag{7.89}$$

when z is not equal to $-\nu_0$, which is the singular point of the expansion. By minimising this error estimate, we have obtained ν_1 in terms of ν_0. This means that the error (7.87) is determined as a function of ν_0 and z. Thence, we plot the magnitude of the error taking into account (7.89) as well as increasing both truncation points N_0 and N_1 together in order to capture the convergence. Before doing so, we first recognise the actual truncations N_0 and N_1 as

$$N_0 \sim \frac{|z|}{\varepsilon} \quad \text{and} \quad N_1 \sim \frac{\left|\nu_0\ln\left(-\frac{z}{\nu_0}\right)+z+\nu_0\right|}{\varepsilon}. \tag{7.90}$$

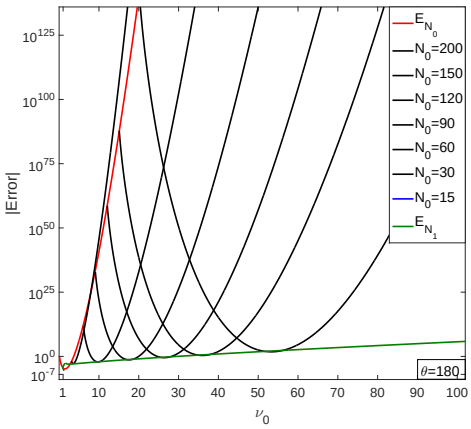
In Figure 7.4, the improvement of hyperasymptotics is shown clearly by black curves if the number of the terms is varied. The green lines of Figure 7.4, which pass through the least points of black curves, represent the relative error when (7.89)

comes to play. The figures of Figure 7.4 show the agreement between the plots. Another observation that can be made from the figures is that as θ decreases, the relative error reduces faster. Getting close to the singularity at $-\nu_0$, we recognise that the speed of the error gets slower and almost stops. The blue curves show the optimally truncated error in the first level; if z equals to $-\nu_0$, we see that the blue curve disappears at Figure 7.4a, as discussed earlier the first level truncation point N_1 is not large at that point. Equivalently, this behaviour of the estimate and its direction are demonstrated near and away from the singularities by its contour plot in Figure 7.5 and Figure 7.6. In order to monitor the θ-dependence, in Figure 7.7a and in Figure 7.7b, we plot the magnitude of the first level error (7.87) according to different values of θ. The plots show that increasing both N_0 and N_1 together reduces the relative error. In considering these figures, we observe that if N_0 and N_1 are fixed, and θ is reduced, the error estimate decreases faster. With this idea, Figure 7.8 is plotted, in which we fix N_1 and decrease θ, and observe that this reduces the magnitude of the error as well.

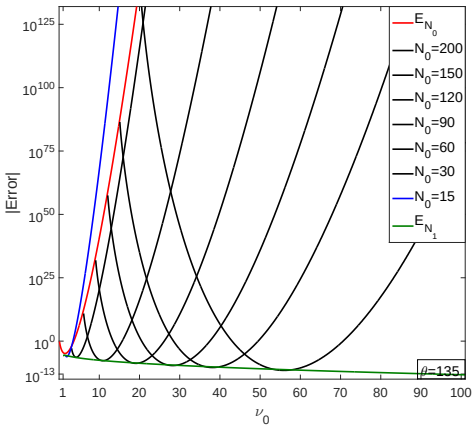
Thus, we conclude that hyperasymptotic error gets exponentially smaller when the truncation point is varied, and its speed further depends upon the phase of z. By having all these figures and comparing them with each other, a very good agreement between each is obtained.

7.6.2 Error analysis and θ dependence

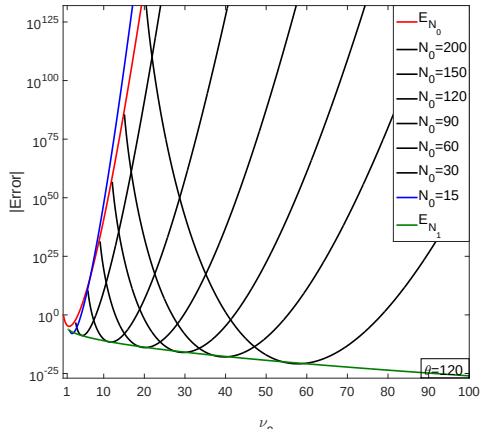
In order to attain a complete agreement between the error estimate and the figures in Figure 7.4 and Figure 7.5, we will inspect the error analytically. Having established the late-order terms in two levels and studied asymptotic behaviours of the first level error (7.87) of the expansion (7.85), we found out that the relative error depends on the phase of the asymptotic expansion. In Figure 7.4, Figure 7.5, Figure 7.7, and more clearly in Figure 7.8, we observe that if the phase of the expansion reduces, the error gets exponentially smaller. However, in Figure 7.4a and Figure 7.5a, as we in-



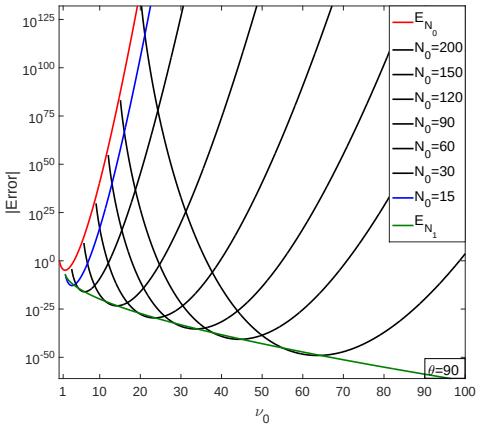
(a) $\theta = \pi$



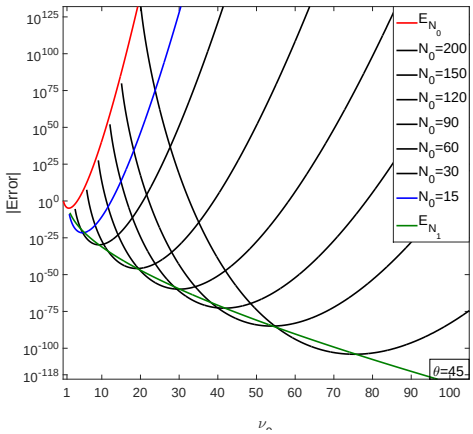
(b) $\theta = \frac{3\pi}{4}$



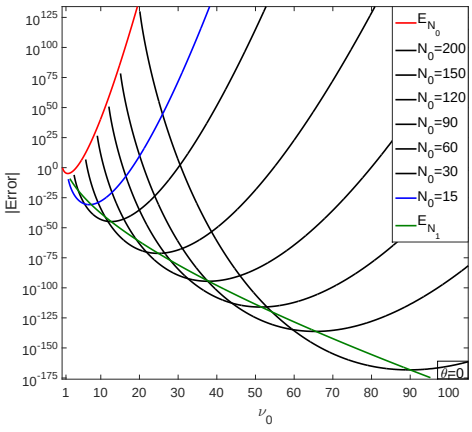
(c) $\theta = \frac{2\pi}{3}$



(d) $\theta = \frac{\pi}{2}$

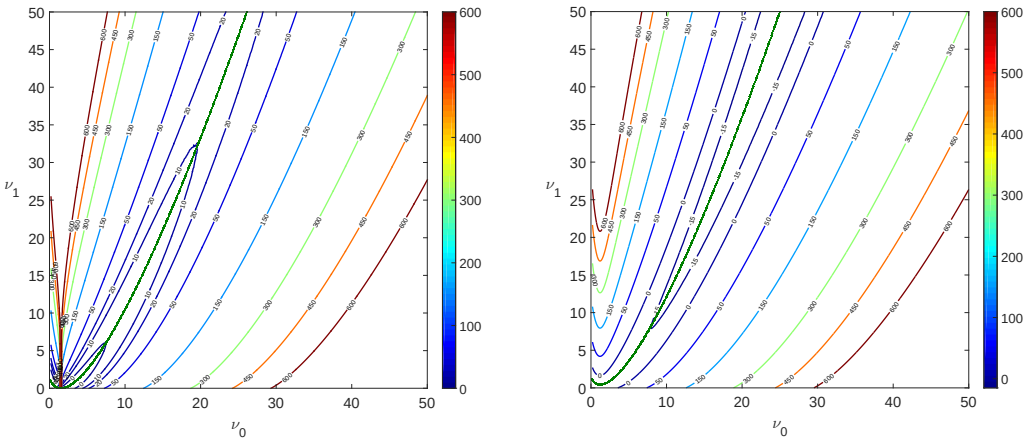


(e) $\theta = \frac{\pi}{4}$

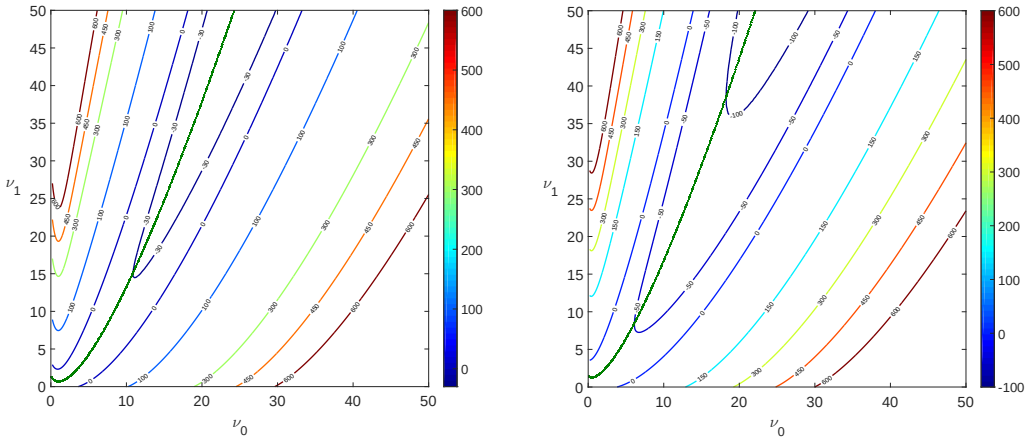


(f) $\theta = 0$

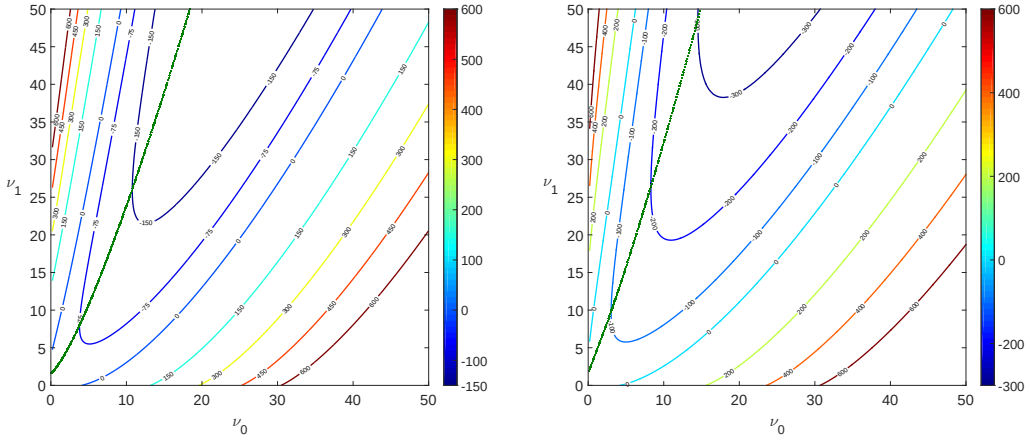
Figure 7.4 Behaviour of the error estimates in (7.33) and in (7.86) according to $u_1^1(z)$, for $|z| = 1.5$ when $\theta = \arg(z) = \pi, 3\pi/4, 2\pi/3, \pi/2, \pi/4, 0$, respectively, for arbitrarily chosen $a = 1/2$, $b = 1/3$ while $\varepsilon = 0.1$. Increasing the level zero truncation point reduces the error, and this bevaiour also depends on θ. Away from the Stokes line the error reduces faster. First level optimal error shown in blue does not occur in Figure 7.4a at the Stokes line. Green lines are plotted if the error is written as a function of ν_0 by employing (7.89).



(a) $\theta = \pi$ (b) $\theta = \frac{3\pi}{4}$

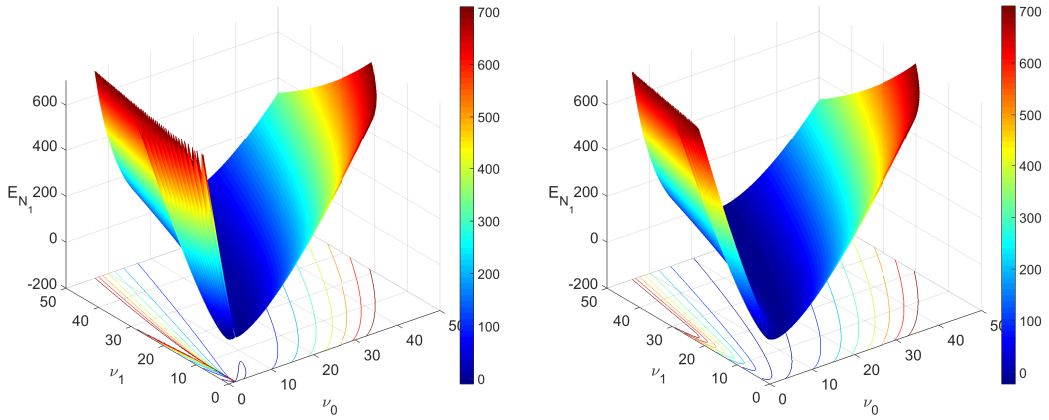


(c) $\theta = \frac{2\pi}{3}$ (d) $\theta = \frac{\pi}{2}$

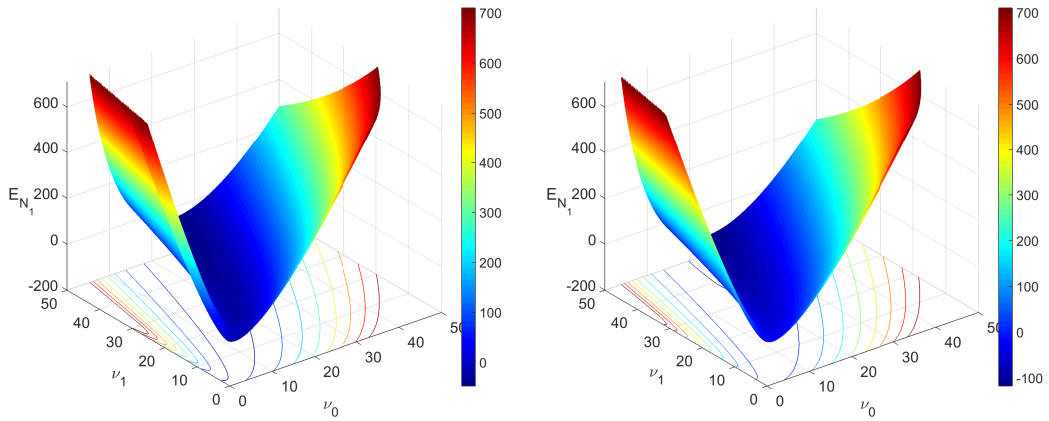


(e) $\theta = \frac{\pi}{4}$ (f) $\theta = 0$

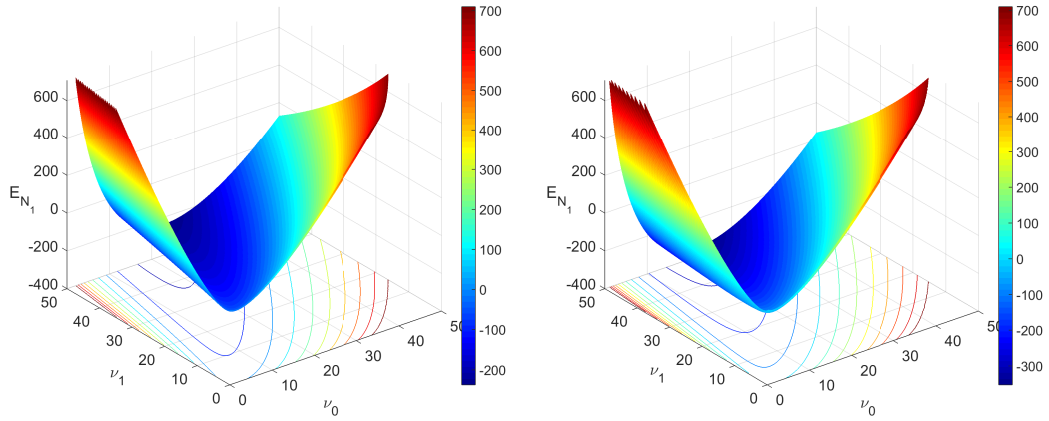
Figure 7.5 Contour plot of the error estimate (7.86) in the ν_0, ν_1 plane according to $u_1^1(z)$, for $|z| = 1.5$ when $\theta = \arg(z) = \pi, 3\pi/4, 2\pi/3, \pi/2, \pi/4, 0$, respectively, for arbitrarily chosen $a = 1/2$, $b = 1/3$ while $\varepsilon = 0.1$. This plot illustrates the behaviour of the decreasing error near and away from the singularity. Green dots are equivelent to the green lines of previous Figure 7.4, and it is a contour plot of (7.89).



(a) $\theta = \pi$ (b) $\theta = \frac{3\pi}{4}$

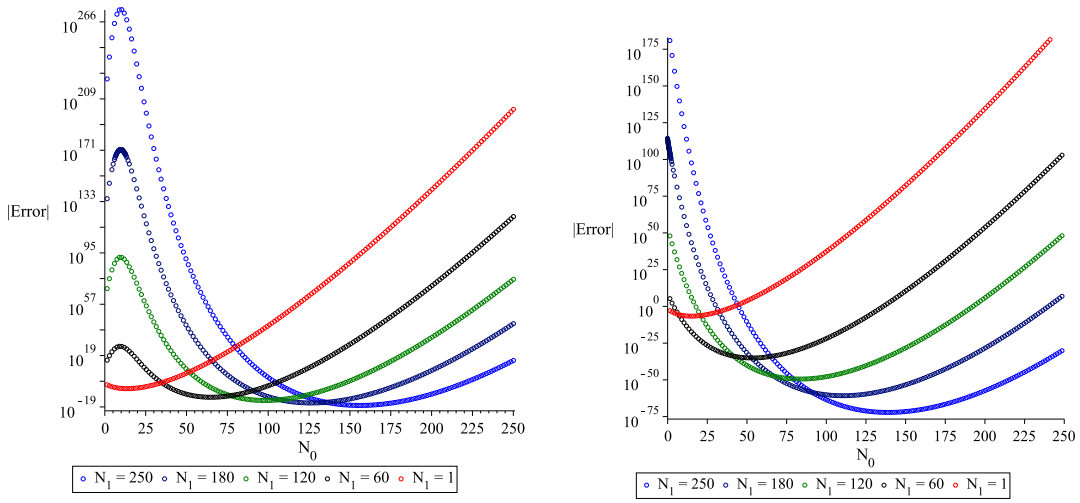


(c) $\theta = \frac{2\pi}{3}$ (d) $\theta = \frac{\pi}{2}$



(e) $\theta = \frac{\pi}{4}$ (f) $\theta = 0$

Figure 7.6 3-D contour plot of the error in (7.86) plotted according to $u_1^1(z)$, for $|z| = 1.5$ when $\theta = \arg(z) = \pi, 3\pi/4, 2\pi/3, \pi/2, \pi/4, 0$, respectively, for arbitrarily chosen $a = 1/2$, $b = 1/3$ while $\varepsilon = 0.1$. It is the 3-D version of Figure 7.5 showing the behaviour of the estimate near and away the Stokes lines. Behaviour of the estimate depends on both truncation points and θ.



(a) $\theta = \dfrac{2\pi}{3}$ (b) $\theta = \dfrac{\pi}{4}$

Figure 7.7 Error estimate in (7.86) plotted according to $u_1^1(z)$, for $|z| = 1.5$ when $\theta = \arg(z) = 2\pi/3$ and $\theta = \pi/4$, respectively, for arbitrarily chosen $a = 1/2$, $b = 1/3$ while $\varepsilon = 0.1$. Red, black, green, navy blue and blue dots correspond to the error estimate while N_0 and N_1 increase at the same time where N_1 is chosen to be $1, 60, 120, 180, 250$ in order to see the agreement. While both N_0 and N_1 increase, the error decreases.

crease $\theta = \arg(z)$ and approach the singularity of the expansion, the error increases rather than stopping near its singularity; which is contrary to what happened in Figure 4.4f, Figure 4.5f and Figure 4.6f of §4. Thence, we will investigate the error estimate (7.87) according to $u_1^1(z)$, especially to identify the behaviour in vicinity of the singularity. First, let us re-arrange and write down the estimate in terms of ν_0 and ν_1

$$E_{N_1}(z) \sim \frac{\sqrt{2\pi}(-1)^{\frac{\nu_0+\nu_1}{\varepsilon}}}{(a-1)^{a-\frac{1}{2}}(a-b)^{a-b+\frac{1}{2}}} \left(\frac{\nu_0}{ze}\right)^{\frac{\nu_0}{\varepsilon}} \left(\frac{\nu_1}{u_1^1(z)e}\right)^{\frac{\nu_1}{\varepsilon}+\gamma} \frac{\nu_0^{2a-b+\frac{1}{2}}}{\nu_1^{\frac{1}{2}} z^a \varepsilon^{2a-b+\gamma}} \exp\left(-\frac{\nu_0}{z}\right), \tag{7.91}$$

where $u_1^1(z)$ and its relationship with the truncation point N_1 of the first level is derived in (7.84) and (7.89). As we are interested in studying the magnitude of the error, we observe that employing the relation given by (7.89) cancels $u_1^1(z)$ and ν_1

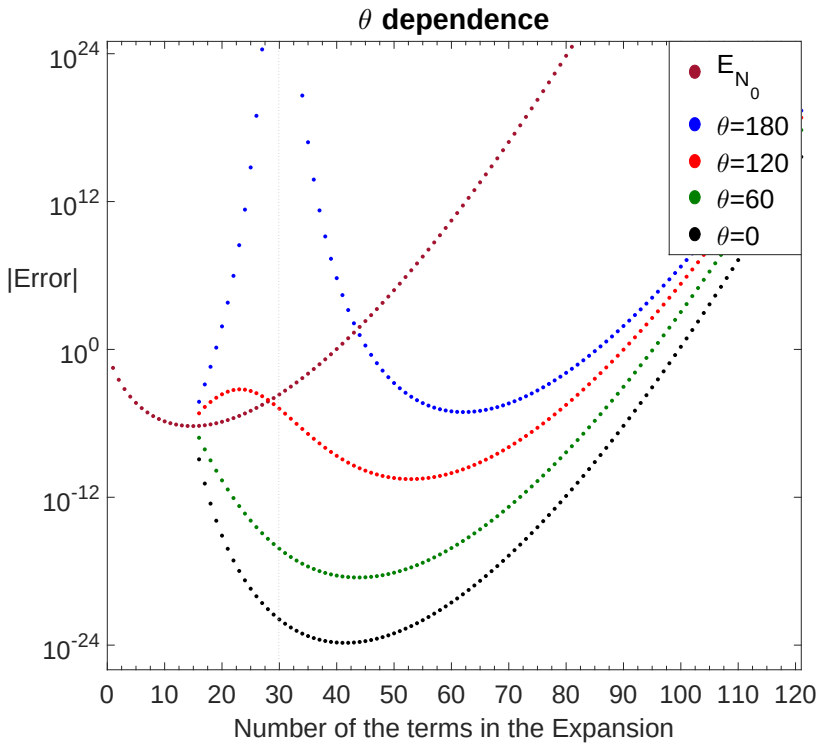


Figure 7.8 First and second level error estimates in (7.33) and in (7.86) according to $u_1^1(z)$, for $|z| = 1.5$ and for $a = 1/2$, $b = 1/3$ while $\varepsilon = 0.1$ with fixed $N_1 = 50$. Black, green,red and blue dots correspond to the error estimate while N_0 and θ both increase at the same time. Here $\theta = \arg(z)$ is picked to be $0, 60, 120$, and 180, respectively. While θ decreases, the error reduces. $\theta = 180$ at 30 corresponds the singularity of the first level in which the expansion breaks down.

terms of the expansion out when its magnitude at the same order. In doing this, we observe that the controlling factor of the error estimate is of the following form

$$E_{N_1}(z) \sim \left(\frac{\nu_0}{ze}\right)^{\frac{\nu_0}{\varepsilon}} \frac{\exp\left(-\dfrac{\nu_0}{z}\right)}{\exp\left(\dfrac{\nu_1}{\varepsilon}\right)}, \tag{7.92}$$

for both ν_0 and ν_1 are sufficiently large. As before, we assume that $z = r\exp(i\theta)$ in order to investigate the error estimate in terms of $ph(z)$. Substitution of this with ν_1 given in (7.89) into (7.92) shows that the forcing factor of the estimate in terms of θ and ν_0 turns out to be

$$E_{N_1}(z) \sim \left(\frac{\nu_0}{r\exp(i\theta+1)}\right)^{\frac{\nu_0}{\varepsilon}} \frac{\exp\left(-\dfrac{\nu_0}{r\exp(i\theta)}\right)}{\exp\left(\dfrac{\left|\nu_0 \ln\left(-\frac{r\exp(i\theta)}{\nu_0}\right)+\nu_0+r\exp(i\theta)\right|}{\varepsilon}\right)}. \quad (7.93)$$

We first evaluate it for $\theta = \pi$ so that the observed increment of Figure 7.4a can be computed. Hence, it is

$$E_{N_1}(z) \sim \left(\frac{\nu_0}{re}\right)^{\frac{\nu_0}{\varepsilon}} \frac{\exp\left(\dfrac{\nu_0}{re}\right)}{\exp\left(\dfrac{|\nu_0\ln(r)-\nu_0\ln(\nu_0)+\nu_0-r|}{\varepsilon}\right)}. \quad (7.94)$$

When ν_0 is sufficiently large, it takes the form of

$$E_{N_1}(z) \sim \exp\left(\frac{\nu_0}{r}-\frac{r}{\varepsilon}\right). \quad (7.95)$$

As we can easily see for large ν_0, this increases near the singularity for $\theta = \pi$, although we used the same method, i.e. the factorial-over-a-power method, in both exponential integral and CHF in order to derive the late order terms of the expansions. As the corresponding A_0 terms of this method are determined uniquely, we find out in both problems that while one for exponential integral is obtained as a constant, the one corresponding to the CHF is obtained as an exponential function of ν_0 given in (7.79). Therefore, compared to §4 or other chapters, the exponential term of CHF, i.e. (7.79), increases the error estimate for π.

Likewise, when the phase of the expansion is 0, the controlling factor (7.92) becomes

$$E_{N_1}(z) \sim \left(\frac{\nu_0}{re}\right)^{\frac{\nu_0}{\varepsilon}} \frac{\exp\left(-\dfrac{\nu_0}{r}\right)}{\exp\left(\dfrac{|\nu_0\ln(-r)-\nu_0\ln(\nu_0)+\nu_0+r|}{\varepsilon}\right)}. \quad (7.96)$$

For large enough ν_0, it is

$$E_{N_1}(z) \sim \exp\left(-\frac{\nu_0}{r} + \frac{r}{\varepsilon}\right), \tag{7.97}$$

which gets exponentially smaller. Hence, we conclude that the speed of the corresponding error estimate depends on the phase of the expansion as well as the ν_0 term, while decreasing. As we approach the singularities by its argument, the speed almost stops or increases. In fact, this corresponds to the Stokes lines, in particular when we move away from the Stokes lines the speed of the decreasing behaviour increases, and on the Stokes lines it stops or increases slowly. Hence, in the next section, we will address the first level Stokes lines.

In summary, increasing the level zero truncation point arbitrarily decreases the first level error estimate. Having written out the estimate as a function of ν_0 by minimisation, we found that the error is reduced faster as ν_0 is increased in theory.

7.6.3 Stokes lines and their form near singularity

In this subsection, we will determine the first level Stokes and anti-Stokes lines originating from the singularities, as well as studying their asymptotic behaviour near the singularities. Hence, we will first consider the singulant that we already derived via the leading order term in (7.78). After having the Stokes lines, in order to see its behaviour, we will inspect the singulant in the neighbourhood of the singularity at $-\nu_0$. To observe these lines, we begin via introducing the polar coordinates by defining

$$z = re^{i\theta}. \tag{7.98}$$

Before beginning this procedure of investigation note that, since the analysis is same for both singulants $u_1^1(z)$ and $u_1^2(z)$ and we already shown the procedure several times in previous chapters, we will only inspect the Stokes (and anti-Stokes) lines for the

singulant $u_1^1(z)$. Moreover, through the local analysis near the turning point, we see that the associated Stokes lines of $u_1^2(z)$ are indeed inactive. For brevity, we do not repeat the similar calculation; refer to §5.3.5 for details. Performing this convenient substitution (7.98) in (7.78) of the singulant gives

$$-u_1^1(z) = -\left(r\cos(\theta) + \nu_0 + \nu_0 \ln\left(\frac{r}{\nu_0}\right)\right) - i\left(r\sin(\theta) + \nu_0(\theta+\pi)\right). \tag{7.99}$$

Relevant Stokes lines, then, emerge when

$$r\sin(\theta) + \nu_0(\theta+\pi) = 0 \quad \text{and} \quad -\left(r\cos(\theta) + \nu_0 + \nu_0 \ln\left(\frac{r}{\nu_0}\right)\right) > 0. \tag{7.100}$$

Hence $\theta = -\pi$ is the solution satisfying the equation (7.100), which is where Stokes lines and the switching of the subdominant exponentials occur. Similarly, inspecting the real part of (7.99) shows us where the anti-Stokes lines lie at when θ satisfies

$$r\cos(\theta) + \nu_0 + \nu_0 \ln\left(\frac{r}{\nu_0}\right) = 0. \tag{7.101}$$

The Stokes and anti-Stokes lines are determined via the singulant; in order to visualise them and their behaviour, it is appropriate to plot them. In Figure 7.9a, red lines show the Stokes lines, whereas dotted lines show the anti-Stokes lines of the first level of hyperasymptotics as discussed in §7.4. Since the only crossing point of the Stokes lines is the turning point, we illustrate the inactive HOSL straightaway using the HOSL recipe given in (5.93). However, HOSL will be addressed in the next chapter in detail. As a similar travel is already done in Figure 4.8 of §4, this part will be kept brief. Travelling in a clockwise direction demonstrates the appearance and disappearance of the exponential terms across the Stokes lines in the figure, and how it gets back to where it started. We remark that, because the level one expansion is produced by the multiplication of the level zero expansion, whenever the level one exponential is turned on, the level zero exponential turns on; hence, ⊖ also demonstrates both the zeroth and first level subdominant exponentials.

To identify the behaviour of the Stokes lines near the singularity, we transform z by setting

$$z = -\nu_0 + \rho, \tag{7.102}$$

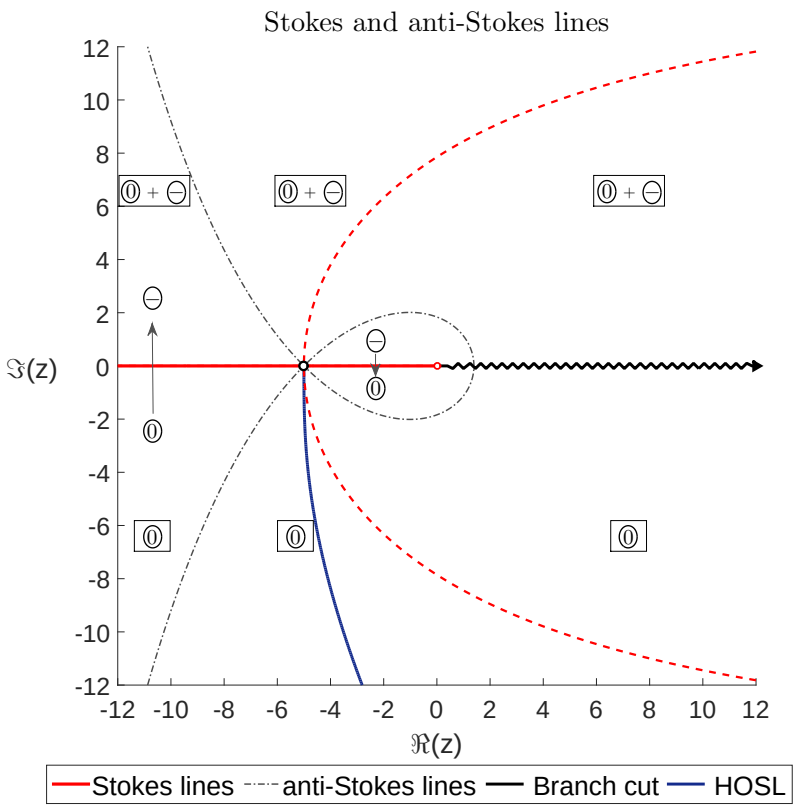
in which the small parameter ρ is $-1 \leq \rho < 1$. Substituting this into the singulant and employing the log function properties for small ρ, we see that the singulant in vicinity of the singularity turns out to be

$$u_1^1(z) = \frac{\rho^2}{2\nu_0}. \tag{7.103}$$

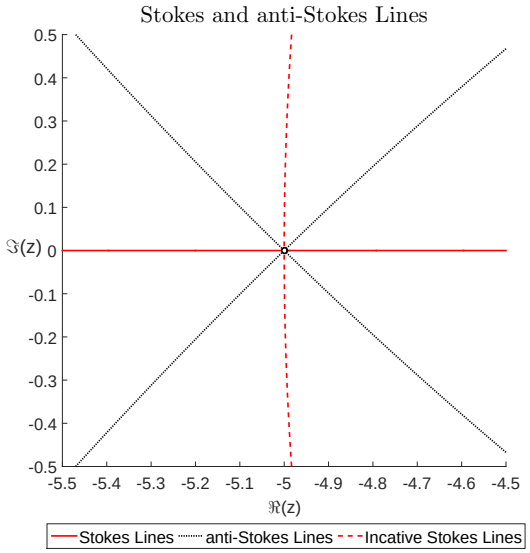
This corresponds to the error function discussed earlier, so that it behaves like an error function near the turning point, the shape of the Stokes and the anti-Stokes lines is known if the singulants are in the form of (7.103). Without loss of generality, we proceed via the assumption that $\rho = \exp\left(i\widetilde{\theta}\right)$ in which $\widetilde{\theta}$ is the phase of ρ. Putting this scaling back into (7.103), we find that the Stokes lines near the singularity lie along 0 and π, and anti-Stokes lines lie along $\pi/4$, $3\pi/4$, $5\pi/4$, $7\pi/4$ under consideration of the Stokes lines definitions. Hence, the Stokes and anti-Stokes lines near the singularity are shown in Figure 7.9b, which is exactly the same as the previous plots of the singulants obtained in previous chapters, such as in §3 and §4.

7.7 Conclusions and comparisons

We have calculated the asymptotic solution of the confluent hypergeometric function (7.3) by the transforming $z_1 = z/\varepsilon$ via hyperasymptotics, rather than performing the Taylor series expansion method of Olde Daalhuis [45]. By doing this fast scaling, we examined the CHF for small ε. In order to study the behaviour of the remainders of the expansions and their exponential smallness, the series of the re-scaled CHF were truncated, and therefore obtained recurrence relations. Based on the investigations of the recurrence relationships at each level, we determined the corresponding late-order terms of the CHF.



(a)



(b)

Figure 7.9 Demonstration of the Stokes lines plotted according to singulant $u_1^1(z)$ for arbitrarily chosen $v_0 = 5$. Active Stokes lines are plotted by $\Im(u_1^1(z)) = \Im(0)$ while $\Re(u_1^1(z)) > \Re(0)$. Inactive Stokes lines are plotted by $\Im(u_1^1(z)) = \Im(0)$ while $\Re(u_1^1(z)) < \Re(0)$. Anti-Stokes lines are represented by black doted lines, given by $\Re(u_1^1(z)) = \Re(0)$. Inactive HOSL is shown in blue. Figure 7.9b is a closer view of the Stokes lines in red and anti-Stokes lines in grey plotted near the singularity.

Combining the zeroth (7.32) and the first level (7.82) remainders of hyperasymptotics in (7.86) we examined the relevant error estimate, rather than only one truncation point at each level, as a function of ν_1, ν_0 and θ, which had not been considered prior to this study in our knowledge. Through this, we have observed that as the number of the terms is increased in the expansion just with two levels of hyperasymptotics, the error estimate decreases. We demonstrated this improvement in Figure 7.3. This is a distinct conclusion of our study compared to previous studies, which is summarised in Figure 7.3, Figure 7.7a, Figure 7.7b. We have also obtained a very good agreement between all plots and asymptotic results. As it was sufficient to achieve this result with just two levels of hyperasymptotics, we did not carry out the process of re-expansion in hyperasymptotics.

Having the late order terms and remainder differential equations, we have located the Stokes and anti-Stokes lines of the CHF (7.15) by examining the behaviour of the singulants near the singularities. In this way we described the remainder in terms of the error function in the vicinity of the Stokes lines, and showed the smoothing of the error function. Switching behaviours of the subdominat exponentials occurs across the Stokes lines were illustrated and demonstrated in Figure 7.2 and in Figure 7.9a. We have verified the method of constructing an approximate solution of a CHF, which contains a small ε, with exponential accuracy through the WKB method, which is in order ε. Upon finding the solutions of the CHF using leading-order-term analysis and the WKB approach, we derived that the remainders are exponentially small everywhere except near the Stokes lines. Moreover, we found out that the level zero turning point is not a turning point in level one, and they occurred in the log function of the singulants in the succeeding level. Hence, they generated the logarithmic branch cuts in the succeeding level.

We have successfully completed the asymptotic analysis of the CHF and observed that the present findings support the findings of §§4, 5 and 6 from which we con-

cluded the diminishing of the error of the hyperasymptotic expansion via considering truncation points as variables. Furthermore, by analysing the remainder solely at two levels, we established that the decreasing behaviour depends on θ. For instance, comparing the θ-dependence both §§4 and 7, we observed that in this chapter, as we reduce the value of θ, the speed of the relative error increases; however, in §4, θ-dependence of the relative error is the opposite. This difference happens only due to the opposite sign of the singularities. Therefore, we comment that as we approach the Stokes lines the speed decreases, and at the Stokes line it takes its slowest speed. Comparing the results of exponential integral, error function and Airy function with the CHF, we showed a satisfactory agreement.

Chapter 8

Higher-order Stokes phenomenon

8.1 Introduction

In the preceding chapters, the methodology of exponential asymptotics was demonstrated and interpreted through various differential equations from which the Stokes phenomenon emerged. The purpose of this chapter is to describe the features of a higher-order Stokes phenomenon using the exponential asymptotics by addressing a second order differential equation in which it occurs. As we analyse the equation, we will address the properties of HOSL and the Stokes lines. The actual process of exploring the higher-order Stokes phenomenon will be similar to that in the previous chapters. Besides, in this chapter, we will inspect the existing intersection points of the Stokes lines.

HOSL may appear when there are more than two asymptotic expansions of the equations. As elucidated earlier, the usual Stokes lines emerge from turning points. However, HOSL emerges from regular points. In particular, according to Olde Daalhuis [60] three or more Stokes lines cross each other, the intersection point of these lines termed as a Stokes crossing point (SCP) by Howls et al. [39]. The difference between these two phenomenon is that, Stokes lines themselves may switch on or off across the HOSL, however the usual Stokes phenomena impacts the switching

on and off of the exponentially small terms across the Stokes lines. Hence, while there is a SCP, ignoring the HOSL may draw an incorrect conclusion in terms of the asymptotic representation, which is the key motivation behind HOSL analysis. Higher-order Stokes phenomenon has the same application areas as the Stokes phenomenon.

Since detailed explanation of the process is already described throughout the thesis, we will now provide a brief layout of the chapter. This chapter will proceed by first introducing the equation to be considered. We will derive the leading order term and a recurrence relation of the equation. By performing the relation, we will obtain the general term of the expansion and truncate it after the optimal number of terms, whereupon we will identify the Stokes and anti-Stokes lines and their crossing points. Thereafter, higher order stokes phenomenon will be demonstrated in §8.4. Then, as before, we will go to the next stage of the multi-level asymptotics: we will firstly rescale the truncated remainder, then expand the scale of the remainder, obtain its asymptotic series solution, and finally truncate it. In order to ensure consistency with the asymptotic solution, we will solve the inhomogeneous remainder differential equation by the WKB approach in §8.5.2. In §8.5.3, we will discuss the associated first level ordinary Stokes and HOSL lines. Lastly, we will end the chapter with discussion in §8.6.

8.2 Model differential equation

In this section, we will consider the asymptotic behaviour of a differential equation in which the nature of the higher-order Stokes phenomenon, with its importance in exponential asymptotics, will be exposed. The existence of a HOSL will be interpreted with the second order differential equation addressed by Olde Daalhuis in [60] satisfying $w(z;u)$ such that

$$\frac{d^2w(z)}{dz^2} + u^2z^2w(z) = \exp\left(iu\left(\frac{z^2}{2} - 4z\right)\right), \tag{8.1}$$

in which u is a large positive parameter and the equation has a double turning point at $z=0$. In order to discuss this equation in the context of a small parameter ε rather than the large parameter u, we first rescale u by $u=1/\varepsilon$ with no loss of generality, which produces the new differential equation equivalent to (8.1) as below:

$$\frac{d^2w(z)}{dz^2}+\frac{z^2}{\varepsilon^2}w(z)=\exp\left(\frac{i}{\varepsilon}\left(\frac{z^2}{2}-4z\right)\right), \tag{8.2}$$

in which $0<\varepsilon\ll 1$. Structurally, this is in the same nature as the second order differential equations of earlier examples obtained in level one, such as (5.65), whence we have two complementary functions and one particular integral. As it will be clearer later in the analysis, associated Stokes lines of this equation intersect each other at regular points which give birth to the HOSL. However, the only crossing points of the earlier examples so far in the thesis were the turning points of the expansions from which solely Stokes lines occur. Moreover, in order to complete the HOSL analysis in the early examples, we needed to go to the first level at least, but in the present example, level zero provides the HOSL inspection with its exponential RHS. To continue, in order to present and provide an explanation regarding the HOSL, we need to analyse the particular solution of the inhomogeneous second order differential equation by exponential asymptotics. Motivated by the RHS of the differential equation (8.2), we first re-scale $w(z)$ by means of

$$w(z)=\varepsilon^2\exp\left(\frac{i}{\varepsilon}\left(\frac{z^2}{2}-4z\right)\right)v(z), \tag{8.3}$$

where $v(z)$ will be discussed. Substitution of (8.3) into (8.2) provides us a singular differential equation involving $v(z)$ such that

$$\varepsilon^2\frac{d^2v(z)}{dz^2}+2i(z-4)\varepsilon\frac{dv(z)}{dz}+\left(8(z-2)+i\varepsilon\right)v(z)=1, \tag{8.4}$$

which is in the desired nature; therefore, we can use the methods in hyperasymptotics. Particularly, in the next two subsections, firstly asymptotic series solution of

(8.4) will be derived, and then it will be truncated optimally.

8.2.1 Asymptotic expansion

As in the usual perturbation method, let us assume that the naive expansion of the differential equation (8.4) in powers of ε is

$$v(z) \sim \sum_{n=0}^{\infty} \varepsilon^n v_n(z). \tag{8.5}$$

Because the expansion (8.5) must solve the differential equation (8.4), a direct substitution of it into (8.4) provides

$$\begin{aligned} \sum_{n=0}^{\infty} \varepsilon^{n+2} \left(\frac{d^2 v_n(z)}{dz^2} + 2i(z-4)\frac{dv_{n+1}(z)}{dz} + 8(z-2)v_{n+2} + iv_{n+1}(z) \right) \\ + \varepsilon \left(2i(z-4)\frac{dv_0(z)}{dz} + 8(z-2)v_1 + iv_0(z) \right) + 8(z-2)v_0(z) = 1. \end{aligned} \tag{8.6}$$

Balancing terms at like powers of ε brings the leading order relation along with a differential recursion expression such that

$$\text{at } \mathrm{O}(1), \qquad v_0(z) = \frac{1}{8(z-2)}, \tag{8.7}$$

$$\text{at } \mathrm{O}(\varepsilon), \qquad 2i(z-4)\frac{dv_0(z)}{dz} + 8(z-2)v_1(z) + iv_0(z) = 0, \tag{8.8}$$

$$\text{at } \mathrm{O}\left(\varepsilon^{n+2}\right), \ \frac{d^2 v_n(z)}{dz^2} + 2i(z-4)\frac{dv_{n+1}(z)}{dz} + 8(z-2)v_{n+2}(z) + iv_{n+1}(z) = 0. \tag{8.9}$$

The leading order term (8.7) comes immediately from (8.6). Performing it in (8.8) generates the next term

$$\begin{aligned} v_1(z) &= \frac{i(z-6)}{64(z-2)^3} \\ &= \frac{i}{64(z-2)^2} - \frac{i}{16(z-2)^3}. \end{aligned} \tag{8.10}$$

We find that the leading-order term $v_0(z)$ and the succeeding term $v_1(z)$ are associated with the singularity at $z = 2$; in fact, this will be considered while studying the

asymptotic behaviour of the late-order terms $v_n(z)$ in (8.5) and determining its representation. Additionally, by successively performing the recurrence relation given in (8.9), we observe that each $v_n(z)$ term of the expansion has a singularity at 2 with an order of $2n+1$ so that the strength of the singularity grows at each order as more terms are added into the expansion. These can also be seen easily from the first two terms determined above, i.e., $v_{0,1}(z)$ in (8.7), (8.10). In order to establish the Stokes lines and study the asymptotic structure of the expansion exponentially, the crucial step is to obtain $v_n(z)$ of the expansion. Because its exact representation cannot be established directly for all n by an application of the recurrence relation in a certain form, we will derive the late order terms through the factorial-over-a-power divergence technique. Hence, let the late order term of the asymptotic expansion in (8.5) be in the nature of

$$v_n(z) \sim \frac{\Gamma(n+\gamma)}{f(z)^{n+\gamma}} \left(\sum_{k=0}^{\infty} \frac{1}{n^k} A_k(z) \right), \tag{8.11}$$

where γ is a constant, A_k and f are independent of n but could be functions of z and ε for large n; they are unknown, but will be determined soon. After inserting (8.11) into the recursive relationship in (8.9), the leading-order relation at $\mathrm{O}(n^2)$ can be written down as $n \to \infty$

$$\left(\left(\frac{df(z)}{dz} \right)^2 - 2i(z-4)\frac{df(z)}{dz} + 8(z-2) \right) \frac{A_0(z)}{f^2} = 0, \tag{8.12}$$

where $A_0(z) \neq 0$ as discussed earlier in the thesis, whence this (8.12) is equivalent to

$$\left(\frac{df(z)}{dz} - 2i(z-2) \right) \left(\frac{df(z)}{dz} + 4i \right) = 0, \tag{8.13}$$

which implies

$$f_1(z) = i(z-2)^2 + k_1 \qquad \text{and} \qquad f_2(z) = -4iz + k_2, \tag{8.14}$$

where $k_{1,2}$ will be derived shortly. At $\mathrm{O}(n)$, we have

$$\frac{A_0(z)}{f^2(z)}\Big(\big(f'(z)\big)^2-2i(z-4)f'(z)+8(z-2)\Big) + \frac{(2i(z-4)-2f'(z))A_0'(z)+(i-f''(z))A_0(z)}{f(z)}=0. \tag{8.15}$$

As it is known from (8.12), the first part of (8.15) is equal to zero; hence, the second part must satisfy

$$2i(z-4)A_0'(z)-2f'(z)A_0'(z)+iA_0(z)-f''(z)A_0(z)=0. \tag{8.16}$$

Solving this differential equation by furnishing $f_{1,2}$ (8.14) produces the leading order term of the summation in (8.11) as

$$A_0(z)=\frac{C_1}{\sqrt{z}}, \tag{8.17}$$

wherein C_1 is an integration constant. Next, to establish the representation of the late-order terms, we must furnish the singularities and turning points of the differential equations in the denominators of the late order terms. From the leading-order terms (8.7) and (8.10), we know that at $z=2$ there exists a singularity for an odd power of the singulant $f(z)$ with the order of $2n+1$. Evaluation of the singulant at this point enables us to derive the unknown constant k_1 and γ such that

$$f_1(2)=0 \implies k_1=0 \quad \text{while} \quad \gamma=\frac{1}{2}. \tag{8.18}$$

On the other hand, due to having a double turning point at $z=0$ and its appearance in the later order term of the particular solutions, which also could be seen by the relation of $1/\sqrt{z}$ whose power increases in each further term evaluated, both singulants are equal to each other at the double turning point, yielding

$$f_1(0)=f_2(0) \implies k_2=4i \quad \text{while} \quad \gamma=\frac{1}{2}, \tag{8.19}$$

so that the related exponentials cancel each other out; for a full discussion see [60], in which the homogeneous solutions of the expansion is discussed by the Hankel

function. Hence, the "power" functions $f_1(z)$ and $f_2(z)$ of the factorial-over-a-power method has been completely determined as

$$f_1(z) = i(z-2)^2 \qquad \text{and} \qquad f_2(z) = -4i(z-1). \tag{8.20}$$

Combining these $f_1(z)$, $f_2(z)$ and $A_0(z)$ with (8.11) completes the derivation of the late term; in fact, the late term is equivalent to the asymptotic solution of (8.4), which is introduced in (8.5). Via back substitution of $v(z)$, we can see that $w(z)$ in (8.3) produces the asymptotic solution of (8.1) which will be of the form

$$\begin{aligned} w(z) &= \varepsilon^2 \exp\left(\frac{i}{\varepsilon}\left(\frac{z^2}{2}-4z\right)\right) v(z) \\ &\sim C_1 \frac{\exp\left(\frac{i}{\varepsilon}\left(\frac{z^2}{2}-4z\right)\right)}{\sqrt{z}} \sum_{n=0}^{\infty} \varepsilon^{n+2} \frac{\Gamma(n+\frac{1}{2})}{f_{1,2}(z)^{n+\frac{1}{2}}}. \end{aligned} \tag{8.21}$$

Thus, we have been able to establish the late order term of the expansion by factorial-over-a-power technique. It is pertinent to point out that at $z = 2$, although the expansion is divergent for the relevant singulant $f_1(z)$, it is not for $f_2(z)$. Next, we can truncate the expansion.

8.2.2 Truncating optimally and the remainder

Having known that the form of the particular solution of (8.1) takes the approximation in (8.21), we can now truncate the asymptotic series solution of $w(z)$. In doing this, we can study the asymptotic behaviour of its tail and identify the location of the Stokes lines and higher-order Stokes structure. For this purpose, an algebraic series solution of $w(z)$ primarily will be truncated in the place where it takes its least value. It is worth briefly commenting that due to the relation introduced in (8.3), truncating $v(z)$ is equivalent to truncating $w(z)$. In particular, truncation of (8.21) after N_0 terms yields

$$w(z) = \exp\left(\frac{i}{\varepsilon}\left(\frac{z^2}{2} - 4z\right)\right)\left[\sum_{n=0}^{N_0} \varepsilon^{n+2} \frac{\Gamma(n+\frac{1}{2})}{f_{1,2}(z)^{n+\frac{1}{2}}} \frac{C_1}{\sqrt{z}} + R_{N_0}(z)\right] \tag{8.22}$$

$$= \exp\left(\frac{i}{\varepsilon}\left(\frac{z^2}{2} - 4z\right)\right) \sum_{n=0}^{N_0} \varepsilon^{n+2} \frac{\Gamma(n+\frac{1}{2})}{f_{1,2}(z)^{n+\frac{1}{2}}} \frac{C_1}{\sqrt{z}} + \mathscr{R}_{N_0}(z), \tag{8.23}$$

where $R_{N_0}(z)$ and $\mathscr{R}_{N_0}(z)$ are the remainders of $v(z)$ and $w(z)$, respectively. Moreover, we can introduce the truncation error of the zeroth level as

$$\mathscr{E}_{N_0}(z) := \exp\left(\frac{i}{\varepsilon}\left(\frac{z^2}{2} - 4z\right)\right) E_{N_0}(z), \tag{8.24}$$

where $\mathscr{E}_{N_0}(z)$ is the first neglected term of the asymptotic expression of $w(z)$, while $E_{N_0}(z)$ of (8.24) is equivalently the first neglected term of $v(z)$, which is observable from the squarebracket in (8.22) after the truncation. Considering the general terms of the expansion in (8.23) for $f_1(z)$ and $f_2(z)$ separately, and minimising with respect to n, the optimal truncation points appear at

$$N_0 \sim \frac{\left|f_{1,2}(z)\right|}{\varepsilon}, \tag{8.25}$$

by which we extract the exponential dependence. Motivated by the form of the expansion, the relative error estimates, with respect to $f_1(z)$ and $f_2(z)$ separately, after employing the truncation points (8.25) with Stirling's formula in the truncated expansion (8.23), at the leading order reveal

$$\mathscr{E}_{(N_0,f_1(z))} \sim C_1 \varepsilon^2 e^2 \frac{\sqrt{2\pi e}}{\sqrt{z}} \frac{1}{\sqrt{i(z-2)^2}} \exp\left(\frac{i}{\varepsilon}\left(-\frac{z^2}{2} - 4\right)\right), \tag{8.26}$$

$$\mathscr{E}_{(N_0,f_2(z))} \sim C_1 \varepsilon^2 e^2 \frac{\sqrt{2\pi e}}{\sqrt{z}} \frac{1}{\sqrt{-4i(z-1)}} \exp\left(\frac{i}{\varepsilon}\left(\frac{z^2}{2} - 4\right)\right). \tag{8.27}$$

Here, all distinct associated exponential asymptotic behaviours of the expansion (8.21) including the RHS of the original equation (8.2) are identified by

$$\lambda_1 = i\left(\frac{z^2}{2} - 4z\right) \quad \lambda_2 = i\left(-\frac{z^2}{2} - 4\right) \quad \lambda_3 = i\left(\frac{z^2}{2} - 4\right), \tag{8.28}$$

in which λ_i are the powers of the exponential terms, i.e. $\exp(\lambda_i/\varepsilon)$ for $i = 1,2,3$.

Having completely derived the exponential terms of the expansion in (8.28), we are now ready to locate the Stokes and HOSL lines of (8.1) from these expressions. These will be considered in the next two following sections.

8.3 Stokes phenomenon

Let us first begin considering the presence of the Stokes and anti-Stokes lines of $w(z)$ in (8.1) via these three exponential terms. As already discussed in earlier, all the Stokes lines can be presented via calculating

$$\Im(\lambda_i) - \Im\left(\lambda_j\right) = 0 \quad \text{while} \quad \Re(\lambda_i) - \Re\left(\lambda_j\right) > 0, \tag{8.29}$$

and all the anti-Stokes lines present via calculating

$$\Re(\lambda_i) - \Re\left(\lambda_j\right) = 0, \tag{8.30}$$

where $i, j = 1,2$ and 3 such that $i \neq j$. Therefore, we will first evaluate the relevant subtractions of $\lambda_i - \lambda_j$

$$\lambda_1 - \lambda_2 = i(z-2)^2, \tag{8.31}$$

$$\lambda_1 - \lambda_3 = 4i(1-z), \tag{8.32}$$

$$\lambda_2 - \lambda_3 = -i(z)^2, \tag{8.33}$$

which correspond to combinations of the singulants derived in (8.20); thence, deriving the Stokes phenomenon of $w(z)$ is equivalent to locating the Stokes phenomenon of $v(z)$. Assuming $z = x + iy$ and performing this transformation in (8.29), we obtain the Stokes lines according to (8.31) such that

$$(x-2)^2 - y^2 = 0 \quad \text{while} \quad 2(x-2)y > 0. \tag{8.34}$$

Likewise, the Stokes lines arise based on (8.32) and (8.33), respectively, when they fulfil the conditions

$$4(1-x)=0 \quad \text{while} \quad y>0, \tag{8.35}$$

$$y^2-x^2=0 \quad \text{while} \quad xy>0. \tag{8.36}$$

By the definition of the singulants, we know that at the turning points $z=0$ and $z=2$, Stokes lines cross each other, in particular for (8.33) and (8.31), respectively. However, in this case, as we have the third exponential in comparison with the previous chapters, we see that the Stokes lines cross at $z=1+i$ and $z=1-i$, which are the SCPs [39] and can be for instance evaluated by equating (8.33) and (8.31). They will be demonstrated in Figure 8.2. Similarly, all the anti-Stokes lines of $w(z)$ with respect to (8.31), (8.32) and (8.33) in order occur when

$$y=0, \quad xy=0 \quad \text{and} \quad (x-2)y=0. \tag{8.37}$$

After the Stokes and anti-Stokes lines of the zeroth level is located, we have sufficient information to plot them. Although we find SCPs from which the HOSL emerges, in order to see the inconsistency with the outcomes upon making a complete circuit in the complex plane if the HOSL is ignored; we plot these in Figure 8.1. The figure demonstrates that if we start to travel on the LHS of the thunderbolt, with the assumption of ① being present, we complete the travel with ①+③ when we return the same sector; this is the inconsistency occurring due to the existence of the HOSL. We kept this part brief as the detailed explanation of the travel will be made in the upcoming section. In §8.4, as well as addressing the HOSL, its behaviour will be illustrated with care.

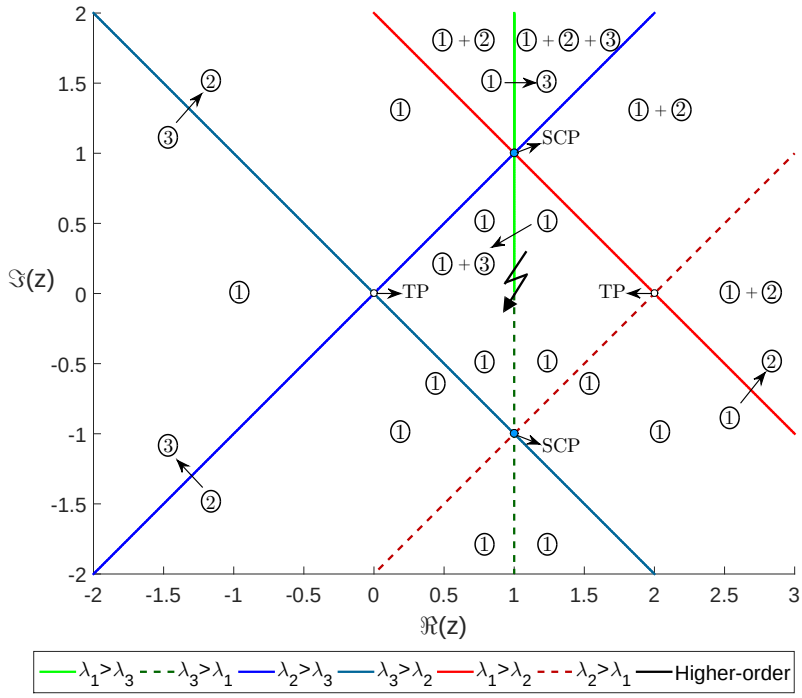


Figure 8.1 Red, blue and green lines show the Stokes lines while the dashed lines show the inactive-Stokes lines. White dots at $z = 0$ and $z = 2$ are the turning points (TP), and blue dots at $z = 1 \pm i$ are the Stokes crossing points (SCP) of $w(z)$. ①, ② and ③ correspond to the exponential terms with powers λ_1, λ_2 and λ_3 in (8.28) respectively. Completing a circuit around the SCP leads to a contradiction next to green line indicating that ① and ①+③ are both present in the same region. Thunderbolt represents the inconsistency if the HOSL is not taken into consideration.

8.4 Higher-order Stokes phenomenon

Knowing the exponential terms of (8.1), we can now focus on the higher-order Stokes phenomenon in this section. As mentioned earlier, the condition of the HOSL is to have at least three exponentials which we already derived in §8.2.2. With the presence of these exponentials, we can observe that an active Stokes line will change its behaviour across the HOSL. According to [39, 56, 60], a HOSL takes place when

$$\Im\left(\ln\left(\lambda_1-\lambda_2\right)\right)=\Im\left(\ln\left(\lambda_1-\lambda_3\right)\right) \text{ while } \Re\left(\ln\left(\lambda_1-\lambda_2\right)\right)>\Re\left(\ln\left(\lambda_1-\lambda_3\right)\right), \tag{8.38}$$

which can equivalently be written as

$$\frac{\lambda_1(z)-\lambda_2(z)}{\lambda_1(z)-\lambda_3(z)}\in\mathbb{R}. \tag{8.39}$$

This implies it occurs when

$$\frac{(z-2)^2}{4(1-z)}\in\mathbb{R}. \tag{8.40}$$

which corresponds to a circle $|z-1|=1$ in the complex z-plane shown in Figure 8.2. Let us reveal the circle by the definition of HOSL. Influenced by the figure and the SCPs, suppose $z=1+re^{i\theta}$ and insert it into the function of (8.40) such that

$$\frac{(re^{i\theta}-1)^2}{-4re^{i\theta}}=R, \tag{8.41}$$

in which $R>0$ corresponds to a real value since we are interested in purely real values of (8.40). The equation can then be rewritten as

$$-\frac{re^{i\theta}}{4}+\frac{1}{2}-\frac{e^{-i\theta}}{4r}=R, \tag{8.42}$$

by Euler's formula, the imaginary part of the above turns out to satisfy

$$r^2=1, \tag{8.43}$$

whence, by the definition of z given earlier, this reads that it is a circle centring at 1 whose radius is 1 as in Figure 8.2. The higher-order anti-Stokes line (anti-HOSL) [62] is similarly present when they fulfil the condition

$$\Re\left(\ln\left(\lambda_1-\lambda_2\right)\right)=\Re\left(\ln\left(\lambda_1-\lambda_3\right)\right), \tag{8.44}$$

which implies

$$\Re\left(\ln\left(\frac{(z-2)^2}{4(1-z)}\right)\right)=0. \tag{8.45}$$

This creates the black teardrop-like shape in the Figure 8.3, in which anti-Stokes and anti-HOSL lines are illustrated without any consideration of the Stokes lines. As already explained, anti-Stokes lines help us identify which exponentials are dominant in which region of the complex plane. By the same token, the tear-drop shaped figure shows the dominance of the associated exponentials $|\lambda_1-\lambda_2|$ and $|\lambda_1-\lambda_3|$ across the black shape, [57]. As we did earlier, we have sufficient information to see the behaviour of the Stokes and HOSL lines when we travel in the z-plane and are able to test whether we come back to where we start. In Figure 8.2, these lines are plotted and SCPs are shown by blue dots appearing at $z=1\pm i$, and related exponential terms of λ_1, λ_2 and λ_3 are represented by ①, ② and ③, respectively. The sign $>$ means that the left side switches the right side on; for instance in $\lambda_1>\lambda_2$, λ_1 switches λ_2 on as we cross the corresponding Stokes line, i.e., red line. We may assume any combination of λ_1, λ_2 and λ_3 are present in any region of the complex plane and travel through the plane in a counter-clockwise or clockwise direction.

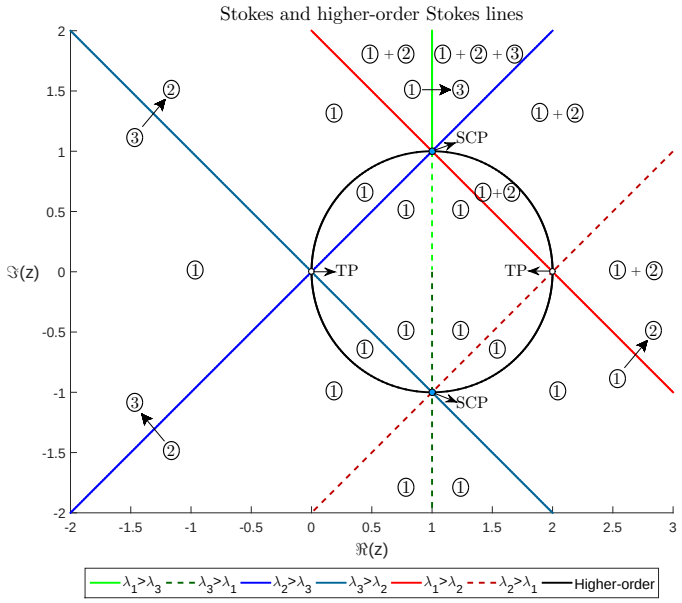
To start, suppose ① is present in the second quadrant below the blue line on the LHS of the dashed green line in Figure 8.2a. Moving upward and crossing the blue line in a clockwise direction has no effect for ① since it is irrelevant for ①. Likewise the HOSL circle also has no effect on the switching on and off. Next, we cross the red line in which ① turns ② on; thence, ① and ② are present. Moving through the first quadrant by crossing the light green line ③ is switched on, and therefore ①, ②, ③ are present. Likewise, as we cross the blue line, since the Stokes line is active there, ③ is switched off, so that ① and ② are present. Across the HOSL circle, as before, nothing happens, and so in the region between the HOSL and red line ① and ② are present. Crossing the red line, because it is active, ② is turned off so that ① becomes the only term present on the RHS of the green dashed line in the circle. Although the light green line is active on the positive imaginary axes, due to the effect

of the HOSL, active Stokes line between both SCPs become inactive. Therefore, as the dashed green line is crossed, nothing happens. We finish the travel with the same assumption we started with; particularly, we return to where we started with the same solution. Moreover, if the travel is continued around the complex plane, we see that the picture is self consistent. In order to have a contradictory example, we illustrate Figure 8.2b in which we assumed ① and ② are present next to the green line in the first quadrant and then travelled in a counter-clockwise direction. Upon having done a similar travel around the plane, we observed contradictions in the third and fourth quadrants that as represented by thunderbolts. Hence, this plot does not provide a consistent solution of the expansion as it does not come back to the original assumption we began with. Note that Olde Daalhuis in [60] has the same plot (Fig. 2) as Figure 8.2a.

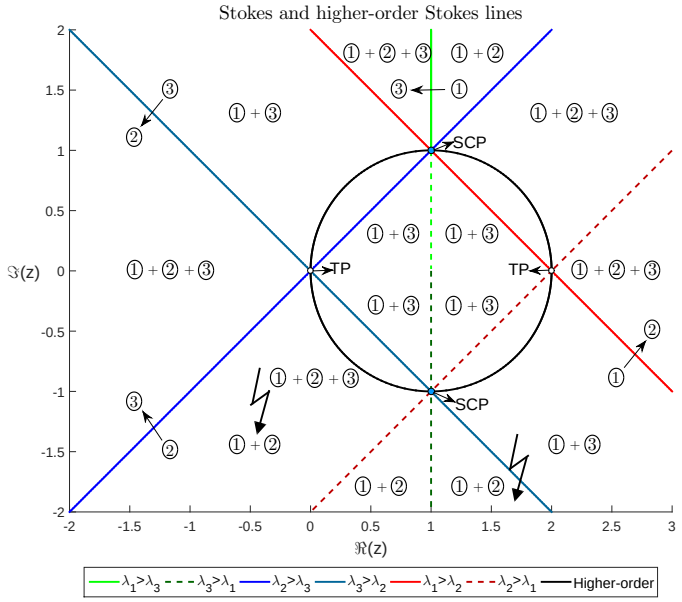
Having discussed the zeroth level Stokes and HOSL lines, we can move to the next natural step: evaluation of the truncated remainder. In the forthcoming section, we will rescale the remainder prior to expansion and truncation.

8.5 First level of hyperasymptotics

In this section, we will inspect the resultant remainder of level zero in hyperasymptotics. As before, after generating the remainder differential equation, the first step is to rescale the remainder based on its RHS. The second step is to expand and derive the leading order term by which we find the singular points of the expansion. Application of the factorial-over-a-power method under the consideration of the singularities enables us to determine the late order terms. Then the natural step is to truncate the series so that subdominant exponentials can be established. In order to be consistent with the exponentials, we also employ the WKB approach from which the exponential terms of the expansion arise explicitly. In §8.5.3, we will conduct the Stokes and HOSL analysis of the first level.



(a)



(b)

Figure 8.2 Red, blue and green lines show the regular Stokes lines while the black circle demonstrates the HOSL. Dashed lines correspond to the inactive Stokes lines. Blue points where the HOSL and Stokes lines are crossed at $z = 1 \pm i$ are the SCPs, and TPs are marked with the white dots at $z = 0$ and $z = 2$. ①, ② and ③ represent the exponentials whose powers are λ_1, λ_2 and λ_3 respectively. Due to the SCP, active Stokes line in green is terminated and so it leads to consistency after the complete travel unlike Figure 8.1. Figure (a) illustrates the consistency whereas Figure (b) shows the inconsistency. Figure (a) is similar to the 'Fig. 2' of Olde Daalhuis in [60].

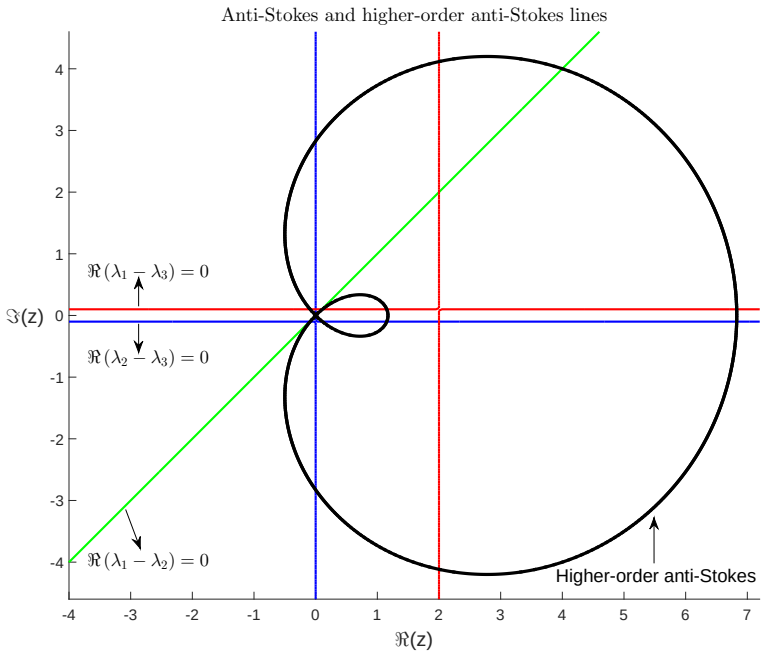


Figure 8.3 Red, blue and green lines show the anti-Stokes lines while the black lines show the higher order anti-Stokes lines of $w(z)$ whose shape like a "teardrop", plotted when $|\lambda_1-\lambda_2|=|\lambda_1-\lambda_3|$. Across the anti-Stokes lines, exponentials only change their form (subdominant to dominant), but they do not impact the switching on and off.

8.5.1 Evaluating the remainder

Substituting the truncated expansion in (8.5) into its original differential equation (8.4) leaves a differential equation containing R_{N_0}

$$\begin{aligned}\mathscr{L}\left(R_{N_0}(z);\varepsilon\right) &= 8(z-2)\varepsilon^{N_0}v_{N_0}(z)-\varepsilon^{N_0+1}v''_{N_0-1}(z)\\ &\sim 8(z-2)\varepsilon^{N_0}v_{N_0}(z),\end{aligned} \tag{8.46}$$

for N_0 large and in the limit as ε goes to zero. Herein, the operator $\mathscr{L}$ is defined by

$$\mathscr{L}\left(R_{N_0}(z);\varepsilon\right)=\varepsilon^2R''_{N_0}(z)+2i(z-4)\varepsilon R'_{N_0}(z)+\left(8(z-2)+i\varepsilon\right)R_{N_0}(z). \tag{8.47}$$

We rescale $R_{N_0}(z)$ according to the RHS of (8.46) such that

$$R_{N_0}(z) = 8(z-2)\varepsilon^{N_0} v_{N_0}(z) Q(z), \tag{8.48}$$

in which $Q(z)$ will be addressed as follows. Since the general term of the expansion is determined in terms of the singulants $f_1(z)$ and $f_2(z)$ derived in (8.20), without loss of generality we continue the analysis of the expansion in the first level with the singulant $f_1(z)$. Next, substitution of (8.48) into the remainder differential equation (8.46) generates the singular differential equation for $Q(z)$ as

$$\begin{aligned}
&\varepsilon^2 Q''(z) + \varepsilon\left(2i(z-4) - \frac{4\nu_0}{z-2} - \frac{\varepsilon}{z}\right) Q'(z) \\
&+ \left(8(z-2) - \frac{4i(z-4)\nu_0}{z-2} + \frac{4\nu_0^2}{(z-2)^2} + \frac{3\varepsilon^2}{4z^2} + \frac{2\varepsilon\nu_0}{z(z-2)} + \frac{4i\varepsilon}{z}\right) Q(z) \sim 1,
\end{aligned} \tag{8.49}$$

where ν_0 represents εN_0 for convenience. As usual, expanding $Q(z)$ formally into powers of ε yields

$$Q(z) \sim \sum_{n=0}^{\infty} \varepsilon^n Q_n(z), \tag{8.50}$$

and substituting the series solution straightforwardly in the differential equation, after some computation, gives

$$\begin{aligned}
&\sum_{n=0}^{\infty} \varepsilon^{n+2} \left[\begin{array}{c} Q_n'' + \left(2i(z-4) - \dfrac{4\nu_0}{z-2}\right) Q_{n+1}' - \dfrac{1}{z} Q_n' \\ + \left(8(z-2) - \dfrac{4i(z-4)\nu_0}{z-2} + \dfrac{4\nu_0^2}{(z-2)^2}\right) Q_{n+2} + \dfrac{3}{4z^2} Q_n + \left(\dfrac{2\nu_0}{z(z-2)} + \dfrac{4i}{z}\right) Q_{n+1} \end{array} \right] \\
&+\varepsilon \left[\left(2i(z-4) - \frac{4\nu_0}{z-2}\right) Q_0' + \left(8(z-2) - \frac{4i(z-4)\nu_0}{z-2} + \frac{4\nu_0^2}{(z-2)^2}\right) Q_1 + \left(\frac{2\nu_0}{z(z-2)} + \frac{4i}{z}\right) Q_0 \right] \\
&\qquad + \left(8(z-2) - \frac{4i(z-4)\nu_0}{z-2} + \frac{4\nu_0^2}{(z-2)^2}\right) Q_0 \sim 1.
\end{aligned} \tag{8.51}$$

As it is already clear by the expression above, like powers of ε gives at the leading order $\mathrm{O}(1)$

$$Q_0(z) = \frac{(z-2)^2}{8(z-2)^3 - 4i(z-4)(z-2)\nu_0 + 4\nu_0^2}, \tag{8.52}$$

whereby the leading order term contains 3 singularities at

$$z_1 = 2 + \frac{i\nu_0}{2}, \quad z_2 = 2 - i\sqrt{i\nu_0} \quad \text{and} \quad z_3 = 2 + i\sqrt{i\nu_0}, \tag{8.53}$$

which must be present at the late order terms. Likewise, the differential recursive relation is derived from (8.51) at $\mathrm{O}(\varepsilon^{n+2})$ as

$$\begin{aligned} Q_n''(z) + \left(2i(z-4) - \frac{4\nu_0}{z-2}\right) Q_{n+1}'(z) - \frac{1}{z} Q_n'(z) + \frac{3}{4z^2} Q_n(z) + \left(\frac{2\nu_0}{z(z-2)} + \frac{4i}{z}\right) Q_{n+1}(z) \\ + \left(8(z-2) - \frac{4i(z-4)\nu_0}{z-2} + \frac{4\nu_0^2}{(z-2)^2}\right) Q_{n+2}(z) = 0. \end{aligned} \tag{8.54}$$

Since the repeated use of the recursive relation from the leading order term does not provide the general term in a formula, we assume that the late order term is in the nature of a factorial-over-a-power and its denominator secures the singularities obtained in (8.53), that is,

$$Q_n(z) = \frac{\Gamma(n+\gamma_1)}{u(z)^{n+\gamma_1}} \sum_{k=0}^{\infty} \frac{B_k(z)}{n^k}, \tag{8.55}$$

in which $u(z), B_k(z)$ and γ_1 are defined as before, and will be discussed. Employing this ansatz in the recurrence relation yields at order n^2

$$\left[\left(u'(z)\right)^2 - \left(2i(z-4) - \frac{4\nu_0}{z-2}\right) u'(z) + 8(z-2) - \frac{4i(z-4)\nu_0}{z-2} + \frac{4\nu_0^2}{(z-2)^2}\right] \frac{B_0(z)}{u(z)^2} \sim 0, \tag{8.56}$$

and at order n

$$\begin{aligned} &\left[\left(u'(z)\right)^2 - \left(2i(z-4) - \frac{4\nu_0}{z-2}\right) u'(z) + 8(z-2) - \frac{4i(z-4)\nu_0}{z-2} + \frac{4\nu_0^2}{(z-2)^2}\right] \frac{B_1(z)}{u(z)^2} \\ &+ \left(\frac{1}{z}u'(z) - u''(z) + \frac{2\nu_0}{z(z-2)} + \frac{4i}{z}\right) B_0(z) - \left(2u'(z) - 2i(z-4) + \frac{4\nu_0}{z-2}\right) B_0'(z) \sim 0. \end{aligned} \tag{8.57}$$

As explained earlier, $B_0(z)$ cannot equal to 0 in (8.56). Thus, this leaves us with the function in the squarebracket

$$\big(u'(z)\big)^2-\left(2i(z-4)-\frac{4\nu_0}{z-2}\right)u'(z)+8(z-2)-\frac{4i(z-4)\nu_0}{z-2}+\frac{4\nu_0^2}{(z-2)^2}\sim 0, \tag{8.58}$$

which, equivalently, may be reorganised as follows

$$\left(u'(z)-\frac{2}{z-2}\left(i(z-2)^2-\nu_0\right)\right)\left(u'(z)+\frac{2}{z-2}\left(2i(z-2)+\nu_0\right)\right)\sim 0. \tag{8.59}$$

Solving each of the above parentheses separately by direct integration, we obtain the level one singulants

$$u_1(z)=iz^2-4iz-2\nu_0\ln(z-2)+c_1, \tag{8.60}$$

$$u_2(z)=-4iz-2\nu_0\ln(z-2)+c_2, \tag{8.61}$$

wherein c_1 and c_2 are the constants of the integration and they are to be derived from the singularities. Upon substitution of these singularities into $u_1(z)$ and $u_2(z)$, the singulants with the relevant constants are completely determined as

$$u_1(z)=\begin{cases} i(z-2)^2+2\nu_0\ln\left(\dfrac{i\nu_0}{2(z-2)}\right)+\dfrac{i\nu_0^2}{4} & \text{when} \quad z_1=2+\dfrac{i\nu_0}{2}, \\ i(z-2)^2+2\nu_0\ln\left(-\dfrac{i\sqrt{i\nu_0}}{z-2}\right)-\nu_0 & \text{when} \quad z_2=2-i\sqrt{i\nu_0}, \\ i(z-2)^2+2\nu_0\ln\left(\dfrac{i\sqrt{i\nu_0}}{z-2}\right)-\nu_0 & \text{when} \quad z_3=2+i\sqrt{i\nu_0}, \end{cases} \tag{8.62}$$

and

$$u_2(z)=\begin{cases} 4i(2-z)+2\nu_0\ln\left(\dfrac{i\nu_0}{2(z-2)}\right)-2\nu_0 & \text{when} \quad z_1=2+\dfrac{i\nu_0}{2}, \\ 4i(2-z)+2\nu_0\ln\left(-\dfrac{i\sqrt{i\nu_0}}{z-2}\right)+4\sqrt{i\nu_0} & \text{when} \quad z_2=2-i\sqrt{i\nu_0}, \\ 4i(2-z)+2\nu_0\ln\left(\dfrac{i\sqrt{i\nu_0}}{z-2}\right)-4\sqrt{i\nu_0} & \text{when} \quad z_3=2+i\sqrt{i\nu_0}. \end{cases} \tag{8.63}$$

All singulants obtained above have a logarithmic branch cut at $z=2$, which in fact happens due to the presence of a singularity at this point in the zeroth level. In light of these singulants, we can now obtain the leading order term, $B_0(z)$, of the

summation in the ansatz (8.55). Particularly, the first part of (8.57) is already equal to zero by the definition of the singulants from (8.56), and therefore we have

$$\left(-u''(z)+\frac{1}{z}u'(z)+\frac{2\nu_0}{z(z-2)}+\frac{4i}{z}\right)B_0(z)=\left(2u'(z)-2i(z-4)+\frac{4\nu_0}{z-2}\right)B_0'(z). \tag{8.64}$$

Solving (8.64) separately with respect to $u_1(z)$ and $u_2(z)$ in (8.60) and (8.61) gives

$$B_0(z)=C_3\left(\frac{z}{z-2}\right)^{\frac{i\nu_0}{4}}\exp\left(\frac{i\nu_0}{2(z-2)}\right), \quad \text{for} \quad u_1(z), \tag{8.65}$$

$$B_0(z)=C_4\left(\frac{z-2}{z}\right)^{\frac{i\nu_0}{4}}\exp\left(\frac{i\nu_0}{2(z-2)}\right), \quad \text{for} \quad u_2(z). \tag{8.66}$$

wherein C_3 and C_4 are the integration constants. Thence, the general terms of the expansion for large n has been obtained via the ansatz (8.55), by means of

$$Q_n(z)\sim C_3\frac{\Gamma(n+\gamma_1)}{u_1^{n+\gamma_1}}\left(\frac{z}{z-2}\right)^{\frac{i\nu_0}{4}}\exp\left(\frac{i\nu_0}{2(z-2)}\right), \tag{8.67}$$

and

$$Q_n(z)\sim C_4\frac{\Gamma(n+\gamma_1)}{u_2^{n+\gamma_1}}\left(\frac{z-2}{z}\right)^{\frac{i\nu_0}{4}}\exp\left(\frac{i\nu_0}{2(z-2)}\right). \tag{8.68}$$

As we have fully determined the general terms, we next truncate the series solution (8.55) after N_1 terms,

$$Q(z)=\sum_{n=0}^{N_1-1}\varepsilon^n Q_n(z)+\mathscr{R}_{N_1}(z), \tag{8.69}$$

where $\mathscr{R}_{N_1}$ is the remainder of the first level of the expansion whereupon we may define the error estimate of $Q(z)$ as

$$E_{N_1}(z):=\varepsilon^{N_1}Q_{N_1}(z). \tag{8.70}$$

By back substitution of this truncated summation in (8.22) via (8.48), the first level truncation error estimate of $w(z)$ can be further introduced,

$$\mathscr{E}_{N_1}(z) := \varepsilon^{N_0+N_1+2} \exp\left(\frac{i}{\varepsilon}\left(\frac{z^2}{2}-4z\right)\right) 8(z-2)v_{N_0}(z)Q_{N_1}(z), \tag{8.71}$$

where $\mathscr{E}_{N_1}(z)$ corresponds to the first neglected term of $w(z)$ in (8.21) for the first level. Since we are interested in truncating the expansion in a point where its magnitude takes its minimum value, using one of the optimisation techniques as detailed throughout the thesis, for instance in (2.9) of §2, enables us to have the optimal truncation points at

$$N_1(z) \sim \frac{\left|u_{1,2}(z)\right|}{\varepsilon}, \tag{8.72}$$

where $\nu_1 \sim \varepsilon N_1$ and ν_1 is a function of $\nu_0 \sim \varepsilon N_1$. Next, we can employ the technique we developed. Having derived the asymptotic series solution of the expansion and its error estimate in the first level, we can now plot the level one estimate (8.71). We first keep the level zero truncation point as a free parameter and increase it arbitrarily and inspect the behaviour of the error. Although both blue and black lines are derived from the first level error, blue shows the error by optimal truncation, whereas black shows the error by arbitrary truncation in Figure 8.4. It is clear from the figure that increasing the level zero truncation point arbitrarily decreases the error estimate. On the other hand, having derived the truncation point of the first level in (8.72), which is a function of ν_0, enables us to write the first level estimate in terms of ν_0 as addressed earlier in the thesis. From what we have just discussed, we infer that increasing ν_0 in the sense of (8.72) should reduce the error. Thence, in light of this idea, we have plotted the error whereupon the green line demonstrates the diminution of the level one estimate. Moreover, as it is written out by the first level optimal truncation point $\nu_1(\nu_0)$, while diminishing, it crosses the minimum values of the first level errors, namely blue and black lines. These findings support the findings of previous chapters.

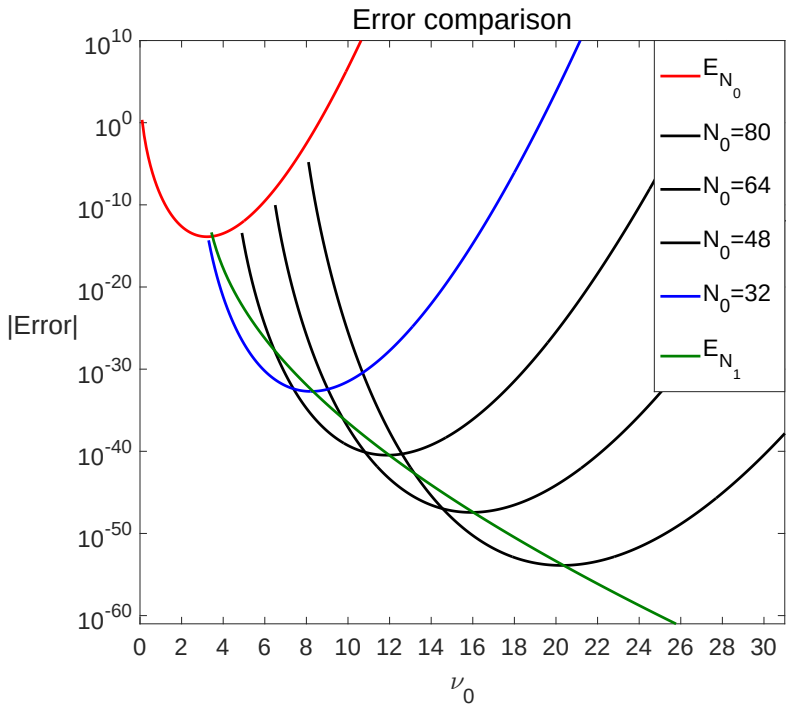


Figure 8.4 First level error estimate of $w(z)$ in (8.71) based on $f_1(z)$ in (8.20) and the last $u_1(z)$ of (8.62) for randomly selected $z = 0.2\sqrt{2} - i0.2\sqrt{2}$ and $\varepsilon = 0.1$. While red and blue lines illustrate the zeroth in (8.24) and optimally truncated first level estimates, black lines show that increasing the level zero truncation point arbitrarily decreases the error exponentially. The green line demonstrates the behaviour of the first level estimate as a function of ν_0.

In the upcoming section, before doing the investigation of the Stokes structure, we will perform the WKB analysis so that the exponential terms of the expansion will arise directly without the need of employing Stirling's approximation, and at the same time we will illustrate the strength of the agreement between both methods.

8.5.2 WKB approach

Let us suppose the WKB approximate solution of $Q(z)$ is

$$Q(z) = \exp\left[\frac{1}{\delta}\sum_{n=0}^{\infty}\delta^n S_n(z)\right], \qquad \delta \to 0, \tag{8.73}$$

wherein δ is a function of ε. Having already used the WKB method in §7, we know the derivative of the exponential in (8.73). Therefore, a straightforward substitution of the derivative by making use of (7.38) into (8.49) gives for the homogeneous part such that

$$\begin{aligned}\frac{\varepsilon^2}{\delta^2}\left[(S_0')^2+2\delta S_0'S_1'+2\delta^2S_0'S_2'+\delta^2(S_1')^2+2\delta^3S_1'S_2'+\ldots\right]+\frac{\varepsilon^2}{\delta}S_0''+\varepsilon^2S_1''+\varepsilon^2\delta S_2''+\ldots\\ +\left(2i(z-4)-\frac{4\nu_0}{z-2}\right)\left(\frac{\varepsilon}{\delta}S_0'+\varepsilon S_1'+\varepsilon\delta S_2'\right)-\frac{\varepsilon^2}{\delta z}S_0'-\frac{\varepsilon^2}{z}S_1'-\frac{\varepsilon^2\delta}{z}S_2'-\ldots\\ +8(z-2)-\frac{4i(z-4)\nu_0}{z-2}+\frac{4\nu_0^2}{(z-2)^2}+\frac{3\varepsilon^2}{4z^2}+\frac{2\varepsilon\nu_0}{z(z-2)}+\frac{4i\varepsilon}{z}\sim 0.\end{aligned}\tag{8.74}$$

Leading order analysis suggests that $\delta=\varepsilon$; then after back substitution of this into the above, we are left with the following at order $\mathrm{O}(1)$

$$(S_0')^2+\left(2i(z-4)-\frac{4\nu_0}{z-2}\right)S_0'+8(z-2)-\frac{4i(z-4)\nu_0}{z-2}+\frac{4\nu_0^2}{(z-2)^2}=0,\tag{8.75}$$

and at order $\mathrm{O}(\varepsilon)$

$$2S_0'S_1'+S_0''+\left(2i(z-4)-\frac{4\nu_0}{z-2}\right)S_1'-\frac{S_0'}{z}+\frac{2\nu_0}{z(z-2)}+\frac{4i}{z}=0.\tag{8.76}$$

Observe that (8.75) is exactly the same as the equation of the singulant in (8.58). Hence, it will produce the same outcomes. After some computations, solving (8.75) we evaluate that

$$S_0(z)=-i(z-2)^2+2\nu_0\ln(z-2)+C_5,\tag{8.77}$$

$$S_0(z)=4iz+2\nu_0\ln(z-2)+C_6,\tag{8.78}$$

where C_5 and C_6 are constants to be determined based on the singular points of the leading order term in (8.53). However, as the leading order term has already been determined in (8.52), $S_0(z)$s must satisfy its singularities; henceforth, the constants C_5 and C_6 must be derived. To avoid redundancy we are leaving these calculations

out. However, refer to the previous section for details. Note here that these above $S_0(z)$s and the singulants $u_{1,2}(z)$s in (8.60) and (8.61) have the opposite signs. To proceed, employing these $S_0(z)$ of (8.77) and (8.78) respectively in (8.76) enabled us to have

$$S_1(z) = \frac{i\nu_0}{4}\ln\left(\frac{z}{z-2}\right) - \frac{i\nu_0}{2(z-2)} + C_7, \tag{8.79}$$

$$S_1(z) = -\frac{i\nu_0}{4}\ln\left(\frac{z}{z-2}\right) + \frac{i\nu_0}{2(z-2)} + C_8, \tag{8.80}$$

where C_7 and C_8 are unknown constants. As they suffice to attain the leading WKB solution in the limit as $\varepsilon \to 0$, the homogeneous solution of (8.49) occurs as

$$\begin{aligned} Q_{hom}(z) \sim C_9 \left(\frac{z}{z-2}\right)^{\frac{i\nu_0}{4}} \exp\left(\frac{-iz^2+4iz+2\nu_0\ln(z-2)+C_1}{\varepsilon} - \frac{i\nu_0}{2(z-2)}\right) \\ + C_{10}\left(\frac{z-2}{z}\right)^{\frac{i\nu_0}{4}} \exp\left(\frac{4iz+2\nu_0\ln(z-2)+C_2}{\varepsilon} + \frac{i\nu_0}{2(z-2)}\right), \end{aligned} \tag{8.81}$$

in which C_9 and C_{10} represent the combinations of all the constants in the relevant late order terms but $S_0(z)$s; particularly, C_1 and C_2 are the constants as they were derived in the singulants (8.60) and (8.61).

Thence, we have obtained the WKB solutions of the first level differential equation from which we obtained the exponential terms of the expansion explicitly. We have observed that the negative powers of the exponentials are same as the singulants found via the application of the factorial-over-a-power. Now, we will discuss the Stokes and HOSL of the first level of hyperasymptotics.

8.5.3 Stokes and higher-order Stokes phenomenon

As remarked earlier, knowing the singulants $u_i(z)$ or equivalently the exponential terms $\exp(-u_i(z)/\varepsilon)$ of the expansion, enables use to locate the Stokes and anti-Stokes lines. Across the Stokes lines, if the relevant Stokes line is active, the sub-

dominant exponential term switches on by the dominant one. In what follows, we will first discuss the Stokes and then the HOSL analysis based on the singulants.

Stokes and anti-Stokes lines

As there are six singulants from the three existing singular points, we will begin our investigation using only two without the loss of generality. We first select $u_1(z)$ and $u_2(z)$ determined by the singularity z_1. Before locating the Stokes lines, let us analyse the first level differential equation locally near the turning point to unpick its behaviour. Hence, we rescale z as $z = 2 - i\nu_0/2 + \delta\zeta$ where $|\delta| \ll 1$ is the small new parameter. Employing this into (8.49) enables us to have

$$\frac{\varepsilon^2}{\delta^2}Q''(\zeta) - \frac{\varepsilon\nu_0}{\delta}Q'(\zeta) + 8\delta\zeta Q(\zeta) \sim 1, \tag{8.82}$$

for small delta. Once δ is balanced by ε, (8.82) turns out to be

$$-\delta Q'(\zeta) + 8\delta\zeta Q(\zeta) \sim 1, \ \text{ where } \ \varepsilon = \delta^2, \tag{8.83}$$

$$Q''(\zeta) - \nu_0 Q'(\zeta) \sim 1, \ \text{ where } \ \varepsilon = \delta. \tag{8.84}$$

Since (8.83) is in the form of an error function differential equation, it behaves like an error function near the singularity. However, because (8.84) does not involve ζ unlike to (8.83), it does not generate a divergent series, and therefore the associated Stokes line is inactive. This has been detailed in previous chapters such as in §4.7. By the same token, when we conduct the local analysis for the corresponding singulants, we find

$$u_1(2 - i\nu_0/2 + \delta\zeta) \sim \delta\zeta(2i - \nu_0), \qquad u_2(2 - i\nu_0/2 + \delta\zeta) \sim -4\delta^2\zeta^2/4, \tag{8.85}$$

in which u_2 corresponds to an erf function. When the same analysis is performed for $u_{1,2}$ subject to $z_{2,3}$, it turns out that u_1 for $z_{2,3}$ and u_2 for z_1 behave as the error function and the active Stokes lines appear from them. Figure 8.5 demonstrates the

Stokes lines of the first level. As it can be seen from the figures, due to the presence of the preceding level turning point at $z = 2$, there is a logarithmic branch cut in the present level singulants. Once we travel in Figure 8.5a and Figure 8.5b, we return where we started, since the only active Stokes lines are red and blue lines, respectively, in the figures.

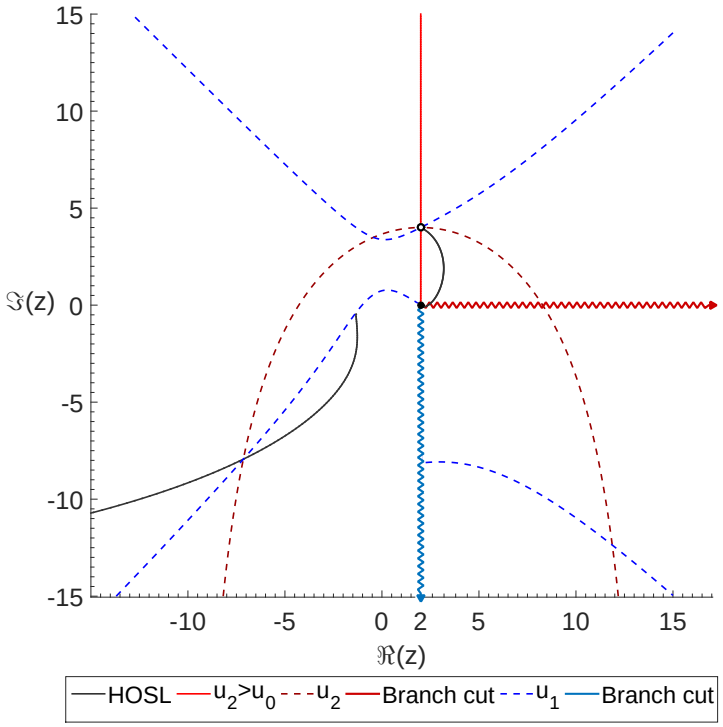
We next select $u_1(z)$ determined by the singularity z_2 in (8.62) and $u_2(z)$ determined by z_1 in (8.63). We set the polar coordinates $z = 2 + re^{i\theta}$ for simplicity. Substitution of the coordinates into the singulants yields

$$u_1(\theta;r) = -r^2\sin(2\theta) + 2\nu_0 \ln\left(\frac{\sqrt{\nu_0}}{r}\right) - \nu_0 + i\left(r^2\cos(2\theta) + 2\nu_0\left(\frac{3\pi}{4} \pm \pi - \theta\right)\right), \tag{8.86}$$

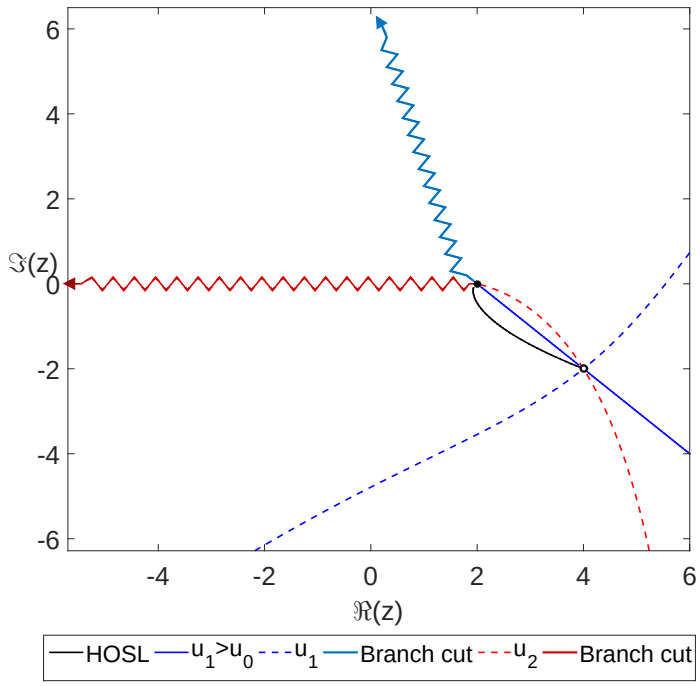
$$u_2(\theta;r) = 4r\sin(\theta) + 2\nu_0 \ln\left(\frac{\nu_0}{2r}\right) - 2\nu_0 + i\left(2\nu_0\left(\frac{\pi}{2} - \theta\right) - 4r\cos(\theta)\right). \tag{8.87}$$

We can now evaluate the Stokes and anti-Stokes lines of (8.49) via $u_1(z)$, $u_2(z)$ and its RHS (e.g. u_0). As discussed in the beginning of this chapter, for $u_1(z)$ and the RHS, the Stokes line lies along $\theta = -\pi/4$ by (8.86) whose real part is positive for any r and ν_0, unless r and ν_0 are infinitesimally close to each other and $r = \sqrt{\nu_0}$; in fact, this corresponds to the singular point of $u_1(z)$ at this phase where the expansion breaks down. Likewise from (8.30), after computation, we observe that the anti-Stokes lines arise when (8.86) is purely imaginary. By the same token, we may carry out the same analysis for $u_2(z)$ and its RHS, whereupon the relevant Stokes line occurs when $\theta = \pi/2$ and anti-Stokes lines appear whenever the real part of (8.87) vanishes. Similar analyses between $u_1(z)$ and $u_2(z)$ may be done. These will be illustrated in Figure 8.6.

Performing $z = 2 - i\sqrt{i\nu_0} + \delta\zeta$ in the singulant fro analysing the local behaviour, we are left with



(a) For the turning point z_1



(b) For the turning point z_2

Figure 8.5 An illustration of Stokes lines of $u_{1,2}$ and u_0, the RHS of (8.49), for $v_0 = 8$ subject to the turning points z_1 and z_2, respectively. While dashed lines are the inactive Stokes lines, the zigzags are the branch cuts of the associated colours. Black lines are the inactive HOSL crossing in the turning points.

$$u_1(2 - i\sqrt{i\nu_0} + \delta\zeta) \sim 2i\delta^2\zeta^2, \qquad \text{as } \delta \to 0, \tag{8.88}$$

whereupon setting the polar coordinates to observe the Stokes (and anti-Stokes) lines of the singulant establishes that active Stokes lines occur at $3\pi/4$ and $7\pi/4$ while the inactive ones occur at $\pi/4$ and $5\pi/4$. Likewise, the associated anti-Stokes lines near the singular point lie along 0, $\pi/2$, π and $3\pi/2$. Hence, these behaviours can be seen from Figure 8.6 near the singularity marked by the white-dot on the blue line. Similar analysis for $u_2(z)$ is already done in (8.85), and $u_2(z)$ has identical behaviour near the turning point on the red line.

As it is discussed in §8.4, a HOSL [39] lies when

$$\frac{u_0 - u_1(z)}{u_0 - u_2(z)} \in \mathbb{R}, \tag{8.89}$$

whereby $u_0 := 0$ is the exponential power of RHS of (8.49), i.e. $e^0 = 1$. In Figure 8.6, black curves represent the HOSL, which cross the turning points of both singulants. By the existence of the branch cut at $z = 2$ for $u_1(z)$ and $u_2(z)$, the HOSL has the branch cut emerging from the same point as they are located in its numerator and denominator. However, although the SCPs of the Stokes lines were supposed to be the white dots on green lines in the figure, they cross each other at different points, when we consider the two singulants in the first level obtained by two different turning points. Hence, the behaviour of the HOSL in the first level is not clear. We further plot Figure 8.7 for the singulants subject to z_1 for two different values of $\nu_0 = 6$ and $\nu_0 = 30$. Increasing the values of ν_0 effects the place of the crossing points of the Stokes lines. Even though the only SCPs were supposed to be $z = 2$, for the former we received four crossing points. When we increase ν_0, we demonstrated that the three of the crossing points were not actual crossing points as the HOSL does not cross them. Therefore, based on these findings, what happens to the HOSL when we go to the higher levels of hyperasymptotics is yet to be elucidated.

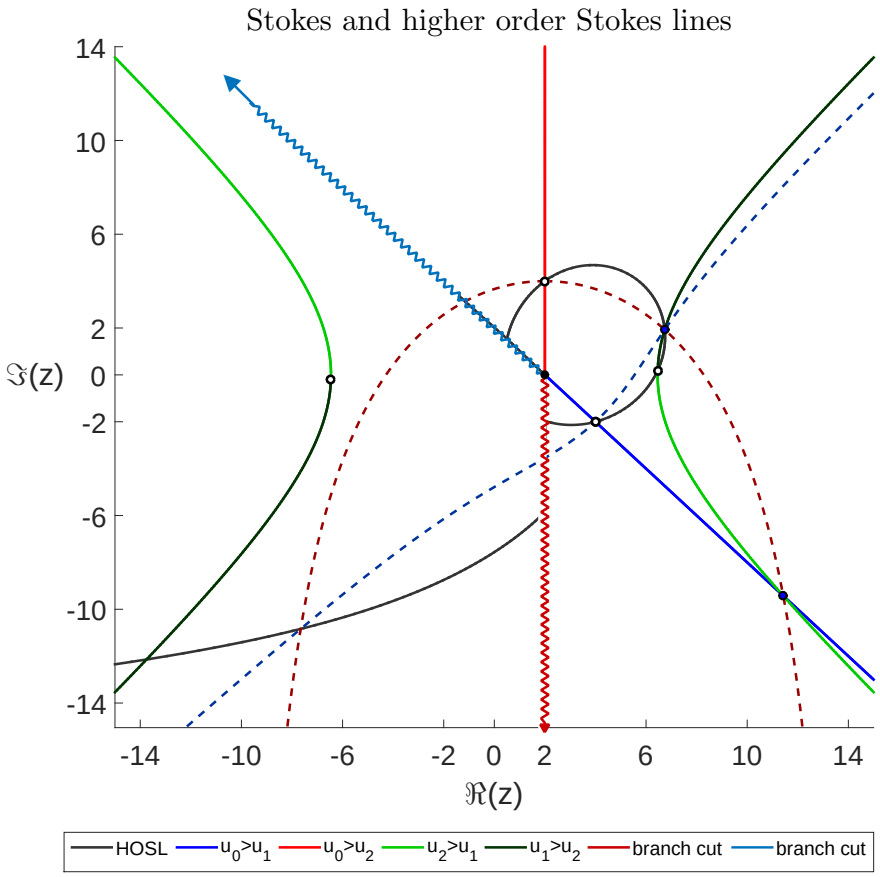
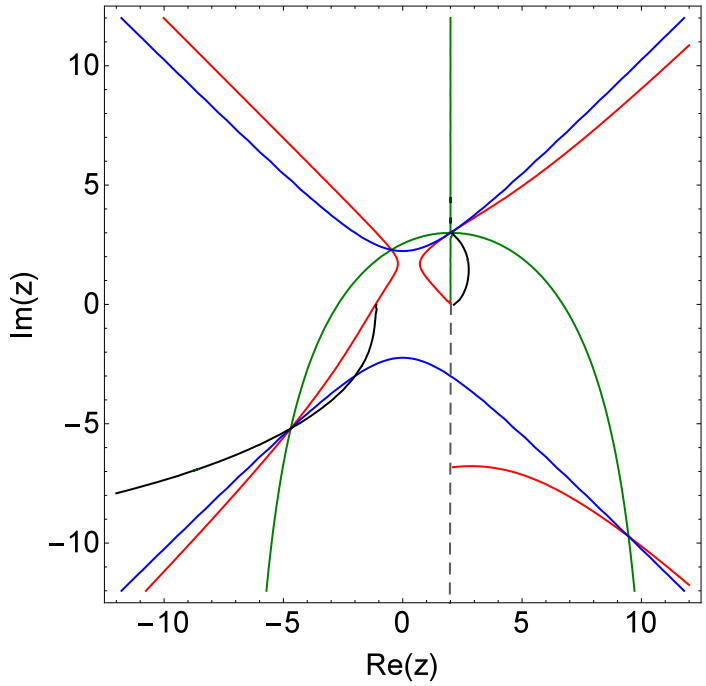


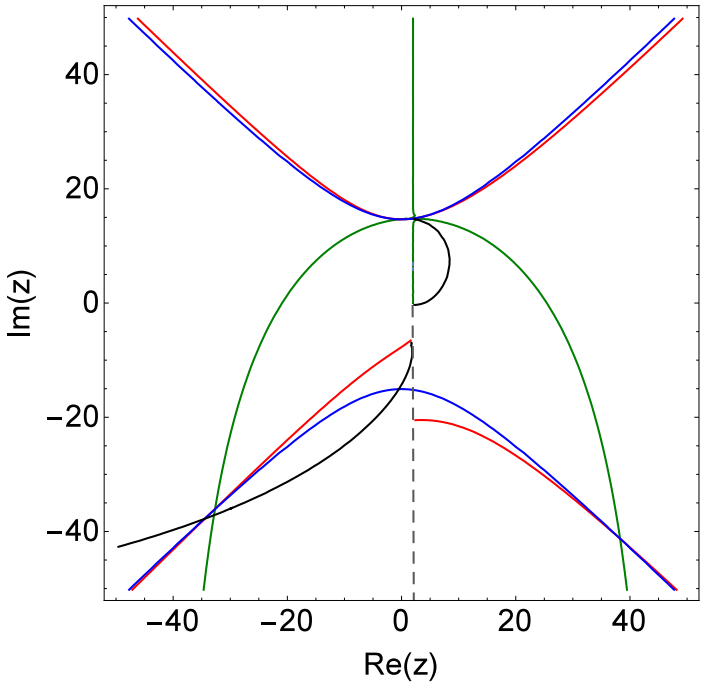
Figure 8.6 Stokes and HOSL of u_1 for z_2 in (8.62) and u_2 for z_1 in (8.63) arbitrarily selected $\nu_0 = 8$. $2+4i$ and $4-2i$ correspond the singular point of u_1 and u_2 while $6.46 \pm 0.19i$ are the singular point of $u_1 - u_2$. $z = 2$ represents the zeroth level turning point from which there appear logarithmic branch cuts in the first level.

8.6 Discussion

In this chapter, we have investigated the inhomogeneous differential equation given in (8.1) by means of a higher order Stokes phenomenon in two levels. Upon expansion and truncation, we explicitly derived the singulants by the turning points. The usual Stokes analysis enabled us to locate the active, inactive and anti-Stokes lines. However, unlike the previous chapters, since we have three exponentials in the present case and they crossed each other at the SCPs, we observed a HOSL. We found that a HOSL corresponds to a circle passing from turning points and the



(a) $\nu_0 = 6$



(b) $\nu_0 = 30$

Figure 8.7 Stokes and HOSL lines of (8.49) based on $u_1(z)$ and $u_2(z)$ defined subject to z_1 with its RHS in which ν_0 is selected 6 and 30, respectively. Red, green, blue show the putative Stokes lines emerging by $u_1(z)$ and RHS, $u_2(z)$ and RHS, and $u_1(z)$ and $u_2(z)$ while black shows the HOSL. Dashed line illustrates the branch cut at $z = 2$. Increasing ν_0 changes the place of the crossing points besides the turning point.

SCPs, and we noticed that the active Stokes line (green in Figure 8.2) is inactivated in a regular point (SCP) although it was not a turning point; particularly, when the Stokes line crosses a turning point, it changes its behaviour.

In the first level of hyperasymptotics, the resultant remainder differential equation is expanded and the singulants are derived subject to singular points by both the factorial-over-a-power method and the WKB approach. Based on these singulants, first level Stokes and HOSL lines are discussed. Depending on the values of the truncation points, some Stokes lines cross each other at regular points rather than at the turning points and SCPs. Increasing the values of the truncation point changes both the behaviour of the figures and the place of the crossing points. Hence, the HOSL analysis needs more investigation. What happens to the HOSL when the higher level of hyperasymptotics taken into consideration is still an unanswered question. On the other hand, upon truncation of the first level expansion and writing out the level one error estimate in terms of the level zero truncation point, we obtained that the error decreases as the zeroth level truncation point in the first level is increased. Moreover, the level zero turning point is not a turning point of level one, and it generates a branch cut in the first level as those in the preceding chapters. Therefore, the present chapter supports the findings of the earlier chapters.

Chapter 9

Conclusion

In this study, we have introduced the multi-level asymptotics or hyperasymptotics in the sense of this thesis by using the techniques in exponential asymptotics and applied it to several singular equations from §§2-8. In each of these equations, the form of the late order terms as well as their behaviours have been derived and investigated carefully in the vicinity of the singularities, since they cause their asymptotic series solution to diverge. In these equations after the expansions, if it is not explicit, we first demonstrated that the form of the late order terms were obtained by applying the factorial over-a-power method. Each asymptotic series solutions in the thesis are truncated and shown that if the truncation points are selected at a point where the series take their absolute minimum value, the truncated remainders appeared to be exponentially small as discussed by Berry et al [43] and Chapman et al [30]. Examination of the remainders enabled us to derive exponential accuracy so that studying the behaviours of the remainders exponentially increased the accuracy in consecutive levels in hyperasymptotics. In previous studies, to obtain the most accurate solution in hyperasymptotics, one needed to use the Borel summation of the factorial terms by their integral representation and analyse the sum by truncating the series optimally [43] or use the integral representation [75] or integrals with saddles [33]. A detailed comparison with that of Berry and Howls [33] was conducted in §4.11. In our approach, we keep truncating the resultant remainder of the series optimally in

each level without using the terminants and analyse them straightaway. Moreover, our contribution to the subject suggests that just two levels of hyperasymptotics decrease the error estimate. This is established by writing the first level error estimate in terms of a function of level zero truncation point. Although, in practice, it is not easy to increase the number of the terms as much as we want, in theory, we have shown the reduction in the error estimates. As we move away from the Stokes lines by the phase, the speed of the error increases, and it takes its slowest speed at the Stokes lines in each level for each differential equation. Furthermore, the original singularities of the differential equations are not singular points in the higher levels. In fact, they generated logarithmic branch cuts in the succeeding levels.

9.1 Review

In §2, we first addressed the methodology of the exponential asymptotics via the introductory example from which the required features of the technique emerged. Then, in §3, we discussed the usual form of the differential equation arising from the first order differential equations in the first and higher levels of the hyperasymptotics and derived the connection formula between the pre-factor of the equations and their singulant when expanded. The general form of the first and higher levels resultant differential equations and the associated singulants were generated for the first level ordinary differential equations.

In §4, we have obtained the asymptotic solution of the problem (4.1) with an exponential accuracy by employing the hyperasymptotics in four levels. By this method, the accuracy of the asymptotic solution was increased exponentially at each level. Having systematically investigated each level of the remainder of the hyperasymptotics, we obtained information about the expansion which cannot be extracted using the regular asymptotic techniques. We have observed that the resultant remainders are much more complicated at each successive stage of hyperasymptotics. Partic-

ularly, in comparison with the usual hyperasymptotics, we examined the truncated remainder estimate (4.34), instead of examining only one truncation point, as a function of the truncation points ν_1, ν_0 and the argument θ. In doing this, we have found that as we increase the level zero truncation point arbitrarily in the first level, the error estimate of the expansion decreases. If the first level estimate is minimised with respect to ν_1 and written out as a function of ν_0, the estimate reduces faster when ν_0 and ν_1 are increased. Moreover, the speed of the error depends on θ, whether it is near or further from the Stokes lines; in fact, it took the slowest speed on the Stokes lines and fastest speed away from the lines. To introduce the concept of multi-level asymptotics, we have done two more levels of analysis subsequently. In each of these levels the system produced a new singular differential equation for the remainders. Moreover, we found out that the singular equation of each levels protected the prefactor of the preceding levels in its leading term; for example, see the prefactor of $T(z)$ in (4.90). So, due to the existence of the prefactor of the previous levels, the singularity(ies) of the preceding levels are stored and these prefactors have occurred in the log function of the singulants which generated a logarithmic branch cut in each further stage.

With this information ascertained, we performed level two in hyperasymptotics. Having revealed the second level error estimate, we conducted the error analysis based on ν_0, ν_1 and ν_2. Specifically, increasing the first level truncation point arbitrarily decreases the second level error estimate. However, we further obtained that increasing only the level zero truncation point in the second level even reduces the estimate better than the estimate of the first level obtained by 'optimal' truncation point as demonstrated in Figure 4.11. In fact this is also true for the third level error estimate, see Figure 4.13 and Figure 4.14. As illustrated in Figure 4.14, although the zeroth and first level arbitrary truncation points derive a better error estimate than the error estimate of the third level 'optimal' truncation, the speed of the first level was faster than the zeroth level as it requires less term to achieve an equivalent result.

On the other hand, as seen in Figure 4.11 and Figure 4.13, optimal truncation points increase after the zeroth level. This means that hyperasymptotics method for this particular problem is not finite.

Moreover, in each level we demonstrated the Stokes phenomenon and illustrated the behaviour of the exponentials near and away from the Stokes lines including the Stokes switching. We showed that the switching happens across the Stokes lines smoothly by an error function. We also obtained that the remainders are exponentially small except near the Stokes lines and they grow by the anti-Stokes lines as we examined the remainders with the singularities of the expansion in each level.

We have conducted the analysis of the hyperasymptotics by following the above methods for the error function, Airy function and confluent hypergeometric function in §§5, 6, 7, and each of which supported the general findings of §4. §5 was divided into two sections for the presence of the error function for two different types of differential equations, and indeed both equations further generated similar results to each other. On the other hand, since it was sufficient to achieve the desired result just with two levels of hyperasymptotics, we did not examine the second and third levels in these chapters like we did in §4. For example, in §7, we investigated the confluent hypergeometric function (7.3) via exponential asymptotics, instead of Taylor series expansion utilised in [45], and studied the behaviour of the remainders of the expansions and their exponential smallness. Employing the hyperasymptotic techniques at two levels provided an exponentially minimum error estimate, which was attained by the re-expansion of the remainder functions with truncation. Particularly, upon inspection of the remainders at the leading-order, more information on the expansion was extracted, and by consideration of the error estimate in (7.86) in terms of ν_1, ν_0 and θ, as for the first time in the literature to our knowledge, we decreased the error estimate just with two levels of analysis by increasing the zeroth level truncation freely. Thence, as well as introducing the concept of multi-level asymptotics we

minimised the error estimate, as demonstrated in Figure 7.3.

Examining the later order terms and the singulants in vicinity of the turning points, Stokes analysis of the CHF (7.15) was performed in both levels. We showed the method of constructing approximate solution of a CHF through the WKB method from which the exponential terms emerge explicitly. We also illustrated that the remainders are exponentially small everywhere but the Stokes lines, and observed the switching behaviour of the subdominant series across these lines so that the contribution of the exponential terms are established. These calculations were conducted in each chapter for each level of the expansion such as Figure 4.8a. After inspecting the truncated remainders by rescaling z near the Stokes lines, we showed the jump occurring across these lines, whereby these were described in terms of an usual error function.

Finally, in §8, as well as doing the hyperasymptotic analysis, we addressed the existence of the HOSL. Compared with the previous chapters, here we had the three exponentials in the zeroth level. Doing similar analysis to the prior chapter, we extracted the Stokes lines of the equation. However, due to the crossing of the Stokes lines at the regular point, an active Stokes line was terminated across HOSL. The effect of this line is illustrated by the instructive figures. In level one, as we received extra crossing points besides the turning points and SCPs and their dependency on the level zero truncation point, there were some unresolved issues in the level one HOSL. Hence, the behaviour of the HOSL in level one is still unclear and therefore requires further analysis. On the other hand, truncation of the level one error estimate based on the arbitrary point decreased the error estimate. Moreover, if this is written out as a function of level zero truncation point, by increasing it, the error is reduced exponentially. Similarly, the original singular point of the expansion generated a branch cut in level one, like the early chapters.

Thus, we were able to express the error estimates in terms of the previous level truncation points. Upon consideration of the truncation point(s) as a free variable, instead of an optimal one, and increasing it arbitrarily in the succeeding levels, we have demonstrated that the estimates decrease; in fact, they theoretically converge. This is a unique conclusion of our study compared to previous studies. It may be summarised by Figure 4.13, Figure 4.14 , Figure 7.3, 7.7a, 7.7b. We have also obtained a very good agreement between all the plots and asymptotic results.

9.2 Discussion

A general picture of hyperasymptotics after repeated reexpansions of the remainders appears like a 'staircase', as drawn in four levels such as in Figure 4.13 and Figure 4.14 in §4. Increasing the number of the terms in level zero for the first level error estimate theoretically produces the equivalent result obtained by the repeated optimal truncation in four levels. In practice, a higher number of terms cannot be included, since it causes computational difficulties. However, derivation of the higher level of hyperasymptotics, as is discussed more thoroughly in the thesis, also has computational difficulties. Indeed, especially after level two, the form of the late order terms derived by the factorial-over-a-power method and their associated singulants become increasingly complicated. Although repeated reexpansion requires more work and increasing the number of the terms decreases the error estimates in theory, it is yet to be practical. Furthermore, we note that it is challenging to estimate the general terms of the hyperseries obtained at each level, whence it might not 'converge' to the exact values of the special functions.

We may now address some possible avenues for future work.

9.3 Further work

Although we were able to derive the complete form of the singulant without specifying individual turning points in the second and higher levels of the Stokes lines analysis, there are some loose ends. In particular, the position of the each singularities was not determined separately in §4. Hence, further analysis can be made by inspecting expansion of the higher levels by individual singulants. Further work is required to single out each turning point and to carry out detailed Stokes phenomenon investigation.

We have analytically and theoretically provided the concept of the hyperasymptotics. A numerical analysis of this new method would be great interest for the future work.

Moreover, further analysis could be done regarding the behaviour of the higher order Stokes phenomenon for the higher levels of the hyperasymptotics for second and higher order singular differential equations. Possible research questions include whether the HOSL can make the active Stokes lines itself inactive when there are more than two asymptotic behaviours arising from the same turning points in the higher levels. When there is a HOSL, what happens to that HOSL when we go to the higher level analysis of the hyperasymptotics; does it terminate and is it not active any more or does it generate a different HOSL? A possible project would be to seek the answers to these questions.

Bibliography

[1] JP Boyd. The devil's invention: Asymptotic, superasymptotic and hyperasymptotic series. *Acta Applicandae Mathematicae*, 56(1):1–98, 1999.

[2] RE Meyer. Exponential asymptotics. *SIAM Review*, 22(2):213–224, 1980.

[3] JP Boyd. A hyperasymptotic perturbative method for computing the radiation coefficient for weakly nonlocal solitary waves. *Journal of Computational Physics*, 120(1):15–32, 1995.

[4] RM Terrill. On some exponentially small terms arising in flow through a porous pipe. *The Quarterly Journal of Mechanics and Applied Mathematics*, 26(3):347–354, 1973.

[5] MD Kruskal and H Segur. Asymptotics beyond all orders in a model of crystal growth. *Studies in applied mathematics*, 85(2):129–181, 1991.

[6] CJ Lustri. *Exponential asymptotics in unsteady and three-dimensional flows.* PhD thesis, University of Oxford, 2013.

[7] JB Van den Berg and JR King. Vanishing beyond all orders: Stokes lines in a water-wave model equation. *Nonlinearity*, 23(1):1, 2010.

[8] PH Trinh and SJ Chapman. New gravity–capillary waves at low speeds. Part 1: Linear geometries. *Journal of Fluid Mechanics*, 724:367–391, 2013.

[9] PH Trinh and SJ Chapman. New gravity–capillary waves at low speeds. Part 2: Nonlinear geometries. *Journal of Fluid Mechanics*, 724:392–424, 2013.

[10] SJ Chapman and JM Vanden-Broeck. Exponential asymptotics and gravity waves. *Journal of Fluid Mechanics*, 567(1):299–326, 2006.

[11] CJ Lustri and SJ Chapman. Steady gravity waves due to a submerged source. *Journal of Fluid Mechanics*, 732:660–686, 2013.

[12] JM Vanden-Broeck and SJ Chapman. Exponential asymptotics and capillary waves. *SIAM Journal on Applied Mathematics*, 62(6):1872–1898, 2002.

[13] L Piela. *Ideas of quantum chemistry*. Elsevier Science, 2006.

[14] MV Berry and R Lim. Universal transition prefactors derived by superadiabatic renormalization. *Journal of Physics A: Mathematical and General*, 26(18):4737, 1993.

[15] AD Dean, PC Matthews, SM Cox, and JR King. Exponential asymptotics of homoclinic snaking. *Nonlinearity*, 24(12):3323, 2011.

[16] CJ Howls. Exponential asymptotics and boundary-value problems: keeping both sides happy at all orders. In *Proceedings of the Royal Society of London A: Mathematical, Physical and Engineering Sciences*, volume 466, pages 2771–2794. The Royal Society, 2010.

[17] TF Ogilvie. Singular-perturbation problems in ship hydrodynamics. *Advances in Applied Mechanics*, 17(91-186):119, 1977.

[18] SX Chen and TF Ogilvie. Water waves generated by a slowly moving two-dimensional body, part ii. Technical report, University of Michigan, 1982.

[19] PH Trinh and SJ Chapman. Waveless ships in the low speed limit: Results for multi-cornered hulls. *arXiv preprint arXiv:1304.5423*, 2013.

[20] JP Boyd. *Weakly nonlocal solitary waves and beyond-all-orders asymptotics: generalized solitons and hyperasymptotic perturbation theory*. Kluwer Academic Publishers, 1998.

[21] SJ Chapman, CJ Howls, JR King, and AB Olde Daalhuis. Why is a shock not a caustic? The higher-order Stokes phenomenon and smoothed shock formation. *Nonlinearity*, 20(10):2425, 2007.

[22] H Poincaré. Sur les intégrales irrégulières. *Acta mathematica*, 8(1):295–344, 1886.

[23] FWJ Olver, DW Lozier, RF Boisvert, and CW Clark, editors. *NIST Handbook of Mathematical Functions*. Cambridge University Press, New York, NY, 2010. Print companion to [78].

[24] RB Dingle. *Asymptotic expansions: their derivation and interpretation*. Academic Press London, 1973.

[25] MV Berry. Asymptotics, Superasymptotics, Hyperasymptotics. *Asymptotics beyond all orders, NATO ASI series B*, 284:1–14, 1991.

[26] O Costin and S Tanveer. An introduction to exponential asymptotics. *Available as a preprint from http://www. math. ohio-state. edu/tanveer/expasymp4. pdf*, 2004.

[27] AB Olde Daalhuis, SJ Chapman, JR King, JR Ockendon, and RH Tew. Stokes phenomenon and matched asymptotic expansions. *SIAM Journal on Applied Mathematics*, pages 1469–1483, 1995.

[28] AD Dean. *Exponential asymptotics and homoclinic snaking*. PhD thesis, University of Nottingham, 2012.

[29] JD Murray. Asymptotic analysis. *Applied Mathematical Sciences, New York: Springer, 1984*, 1, 1984.

[30] SJ Chapman, JR King, and KL Adams. Exponential asymptotics and Stokes lines in nonlinear ordinary differential equations. *Proceedings of the Royal Society of London. Series A: Mathematical, Physical and Engineering Sciences*, 454(1978):2733–2755, 1998.

[31] KL Adams. *Exponential asymptotics.* PhD thesis, University of Nottingham, 1997.

[32] KL Adams, JR King, and RH Tew. Beyond-all-orders effects in multiple-scales asymptotics: travelling-wave solutions to the Kuramoto-Sivashinsky equation. *Journal of engineering mathematics*, 45(3-4):197–226, 2003.

[33] MV Berry and CJ Howls. Hyperasymptotics for integrals with saddles. *Proceedings of the Royal Society of London. Series A: Mathematical and Physical Sciences*, 434(1892):657–675, 1991.

[34] PH Trinh, SJ Chapman, and JM Vanden-Broeck. Do waveless ships exist? *Bulletin of the American Physical Society*, 54, 2009.

[35] JP Boyd. Hyperasymptotics and the linear boundary layer problem: Why asymptotic series diverge. *SIAM review*, 47(3):553–575, 2005.

[36] MV Berry. Uniform asymptotic smoothing of Stokes's discontinuities. *Proceedings of the Royal Society of London. A. Mathematical and Physical Sciences*, 422(1862):7–21, 1989.

[37] MV Berry and CJ Howls. Infinity interpreted. *Physics World*, 6:35–35, 1993.

[38] GG Stokes. On the discontinuity of arbitrary constants that appear in divergent developments. *Transactions of the Cambridge Philosophical Society*, 10:105, 1864.

[39] CJ Howls, PJ Langman, and AB Olde Daalhuis. On the higher-order Stokes phenomenon. *Proceedings of the Royal Society of London. Series A: Mathematical, Physical and Engineering Sciences*, 460(2048):2285–2303, 2004.

[40] NM Temme. Uniform asymptotic expansions of integrals: a selection of problems. *Journal of Computational and Applied Mathematics*, 65(1):395–417, 1995.

[41] O Costin and MD Kruskal. On optimal truncation of divergent series solutions of nonlinear differential systems. *Proceedings of the Royal Society of London. Series A: Mathematical, Physical and Engineering Sciences*, 455(1985):1931–1956, 1999.

[42] AB Olde Daalhuis and FWJ Olver. On the asymptotic and numerical solution of linear ordinary differential equations. *SIAM review*, 40(3):463–495, 1998.

[43] MV Berry and CJ Howls. Hyperasymptotics. *Proceedings of the Royal Society of London. Series A: Mathematical and Physical Sciences*, 430(1880):653–668, 1990.

[44] AB Olde Daalhuis. Hyperasymptotic solutions of higher order linear differential equations with a singularity of rank one. *Proceedings of the Royal Society of London. Series A: Mathematical, Physical and Engineering Sciences*, 454(1968):1–29, 1998.

[45] AB Olde Daalhuis. Hyperasymptotic expansions of confluent hypergeometric functions. *IMA journal of applied mathematics*, 49(3):203–216, 1992.

[46] CJ Howls. Hyperasymptotics for integrals with finite endpoints. *Proceedings of the Royal Society of London. Series A: Mathematical and Physical Sciences*, 439(1906):373–396, 1992.

[47] AB Olde Daalhuis. Hyperasymptotics and the Stokes's phenomenon. *Proceedings of the Royal Society of Edinburgh: Section A Mathematics*, 123(04):731–743, 1993.

[48] AB Olde Daalhuis. Hyperasymptotic solutions of second-order linear differential equations II. *Methods Appl. Anal*, 2:198–211, 1995.

[49] AB Olde Daalhuis. Exponential asymptotics. *Orthogonal Polynomials and Special Functions*, pages 211–244, 2003.

[50] JR Airey. Lii. The "converging factor" in asymptotic series and the calculation of Bessel, laguerre and other functions. *The London, Edinburgh, and Dublin Philosophical Magazine and Journal of Science*, 24(162):521–552, 1937.

[51] MV Berry. Stokes's phenomenon; smoothing a Victorian discontinuity. *Publications Mathématiques de l'Institut des Hautes Études Scientifiques*, 68(1):211–221, 1988.

[52] J Heading. The Stokes phenomenon and certain nth-order differential equations II. The Stokes phenomenon. In *Mathematical Proceedings of the Cambridge Philosophical Society*, volume 53, pages 419–441. Cambridge Univ Press, 1957.

[53] SJ Chapman. On the non-universality of the error function in the smoothing of Stokes discontinuities. In *Proceedings of the Royal Society of London A: Mathematical, Physical and Engineering Sciences*, volume 452, pages 2225–2230. The Royal Society, 1996.

[54] CJ Lustri, SW McCue, and BJ Binder. Free surface flow past topography: A beyond-all-orders approach. *European Journal of Applied Mathematics*, 23(4):441–467, 2012.

[55] AB Olde Daalhuis. Hyperasymptotics for nonlinear ODEs I. A Riccati equation. *Royal Society of London Proceedings Series A*, 461:2503–2520, 2005.

[56] GL Body, JR King, and RH Tew. Exponential asymptotics of a fifth-order partial differential equation. *European Journal of Applied Mathematics*, 16(05):647–681, 2005.

[57] CJ Howls and AB Olde Daalhuis. Exponentially accurate solution tracking for nonlinear ODEs, the higher order Stokes phenomenon and double transseries resummation. *Nonlinearity*, 25(6):1559, 2012.

[58] SJ Chapman, PH Trinh, and TP Witelski. Exponential asymptotics for thin film rupture. *SIAM Journal on Applied Mathematics*, 73(1):232–253, 2013.

[59] SJ Chapman, JMH Lawry, JR Ockendon, and RH Tew. On the theory of complex rays. *SIAM review*, pages 417–509, 1999.

[60] AB Olde Daalhuis. On higher-order Stokes phenomena of an inhomogeneous linear ordinary differential equation. *Journal of computational and applied mathematics*, 169(1):235–246, 2004.

[61] HL Berk, William McCay Nevins, and KV Roberts. New stokes' line in WKB theory. *Journal of Mathematical Physics*, 23(6):988–1002, 1982.

[62] SJ Chapman and DB Mortimer. Exponential asymptotics and Stokes lines in a partial differential equation. *Proceedings of the Royal Society A: Mathematical, Physical and Engineering Science*, 461(2060):2385–2421, 2005.

[63] FWJ Olver. Exponentially-improved asymptotic solutions of ordinary differential equations i: The confluent hypergeometric function. *SIAM journal on mathematical analysis*, 24(3):756–767, 1993.

[64] MV Berry. Asymptotic dominance by subdominant exponentials. *Proceedings of the Royal Society of London. Series A: Mathematical, Physical and Engineering Sciences*, 460(2049):2629–2636, 2004.

[65] MV Berry. Stokes's phenomenon for superfactorial asymptotic series. *Proceedings of the Royal Society of London. Series A: Mathematical and Physical Sciences*, 435(1894):437–444, 1991.

[66] JR King and SJ Chapman. Asymptotics beyond all orders and Stokes lines in nonlinear differential-difference equations. *European Journal of Applied Mathematics*, 12(4):433–463, 2001.

[67] CM Bender and SA Orszag. *Advanced mathematical methods for scientists and engineers: Asymptotic methods and perturbation theory*, volume 1. Springer Verlag, 1978.

[68] M Abramowitz and IA Stegun. *Handbook of mathematical functions: with formulas, graphs, and mathematical tables*. New York, NY: Dover Publication, 1972.

[69] TM Apostol. *Mathematical analysis*. Addison Wesley Publishing Company, 1974.

[70] MJ Ablowitz and AS Fokas. *Complex Variables: Introduction and Applications*, volume 35, chapter 4, page 222. Cambridge University Press, 2003.

[71] CJ Howls. Hyperasymptotics for multidimensional integrals, exact remainder terms and the global connection problem. *Proceedings of the Royal Society of London. Series A: Mathematical, Physical and Engineering Sciences*, 453(1966):2271–2294, 1997.

[72] GG Stokes. On the discontinuity of arbitrary constants that appear as multipliers of semi-convergent series. *Acta Mathematica*, 26(1):393–397, 1902.

[73] EJ Hinch. *Perturbation methods*. Cambridge University Press, 1991.

[74] FWJ Olver. *Asymtotics and special functions*. 1974.

[75] JGB Byatt-Smith. Formulation and summation of hyperasymptotic expansions obtained from integrals. *European Journal of Applied Mathematics*, 9(02):159–185, 1998.

[76] FWJ Olver. Uniform, exponentially improved, asymptotic expansions for the generalized exponential integral. *SIAM journal on mathematical analysis*, 22(5):1460–1474, 1991.

[77] WP Schleich. E: Airy function. *Quantum Optics in Phase Space*, pages 621–627.

[78] NIST Digital Library of Mathematical Functions. http://dlmf.nist.gov/, Release 1.0.10 of 2015-08-07. Online companion to [23].

[79] MH Holmes. *Introduction to perturbation methods*, volume 20, chapter 4, page 236. Springer Science & Business Media, 2012.

[80] O Vallée and M Soares. *Airy functions and applications to physics*. Imperial College Press, 2004.

[81] RB White. *Asymptotic analysis of differential equations*. Imperial College Press, 2005.

[82] RE Meyer. A simple explanation of the Stokes phenomenon. *SIAM review*, 31(3):435–445, 1989.

[83] AM Ishkhanyan. New analytically integrable models of the two-state problem. *Optics communications*, 176(1):155–161, 2000.

[84] LJ Slater. *Confluent hypergeometric functions*. University Press Cambridge, 1960.

[85] TA Ishkhanyan and AM Ishkhanyan. Expansions of the solutions to the confluent heun equation in terms of the Kummer confluent hypergeometric functions. *arXiv preprint arXiv:1403.1833*, 2014.

[86] LJ El-Jaick and BDB Figueiredo. Confluent heun equations: convergence of solutions in series of coulomb wavefunctions. *Journal of Physics A: Mathematical and Theoretical*, 46(8):085203, 2013.

[87] LU Ancarani and G Gasaneo. Derivatives of any order of the confluent hypergeometric function ${}_1F_1(a, b, z)$ with respect to the parameter a or b. *Journal of Mathematical Physics*, 49, 2008.

[88] AS Kadyrov, I Bray, AM Mukhamedzhanov, and AT Stelbovics. Scattering theory for arbitrary potentials. *Physical Review A*, 72(3):032712, 2005.

[89] H Buchholz. *The confluent hypergeometric function: with special emphasis on its applications*. Springer Science, 1969.

[90] ED Rainville. *Special functions*, volume 442. New York, 1960.

[91] JL López, P Pagola, and EP Sinusía. New series expansions of the function. *Journal of Mathematical Analysis and Applications*, 421(2):982–995, 2015.

[92] NM Temme. *Special functions: An introduction to the classical functions of mathematical physics*. John Wiley & Sons, 2011.

[93] AB Olde Daalhuis. *Confluent hypergeometric functions*. New York: Cambridge University Press, 2010.

[94] AD MacDonald. *Properties of the confluent hypergeometric function*. Research Laboratory of Electronics, Massachusetts Institute of Technology, 1948.